HYDROCONVERSION OF N-HEXANE OVER PLATINUM SUPPORTED ZEOLITE CATALYSTS PREPARED BY SUPERCRITICAL TECHNIQUE

A Thesis
Submitted to the College of Engineering
of Nahrain University in Partial Fulfillment of the
Requirements for the Degree of Doctor of Philosophy
in Chemical Engineering

by
USAMA AKRAM SAED AL-RAWI
(B. Sc. 2000, M. Sc. 2003)

Jumadi Al-A'kher 1429
June 2008

Certification

I certify that the preparation of this thesis entitled **"Hydroconversion of N-Hexane Over Platinum Supported Zeolite Catalysts Prepared by Supercritical Technique"** was prepared by **Usama Akram Saed Al-Rawi** under my supervision at Nahrain University/ College of Engineering in partial fulfillment of the requirements for the degree of **Doctor of Philosophy** in **Chemical Engineering**.

Signature: J. Shanshool

Name: **Prof. Dr. Jabir Shanshool**
(Supervisor)

Date: 19 / 6 /2008

Signature:

Name: **Prof. Dr. Qasim J. Slaiman**
(Head of Department)

Date: 19 / 6 /2008

Certificate

We certify, as an examining committee, that we have read this thesis entitled **"Hydroconversion of N-Hexane Over Platinum Supported Zeolite Catalysts Prepared by Supercritical Technique"**, examined the student **Usama Akram Saed Al-Rawi** in its content and found it meets the standard of thesis for the degree of Doctor of Philosophy in Chemical Engineering.

Signature:
Name: **Prof. Dr. Jabir Shanshool**
(Supervisor)
Date: 19/6/2008

Signature:
Name: **Prof. Dr. Nada B. Nakkash**
(Member)
Date: 17/6/2008

Signature:
Name: **Prof. Dr. Talib B. Kashmoula**
(Member)
Date: 17/6/2008

Signature:
Name: **Assist. Prof. Dr. Cecilia Kh. Haweel**
(Member)
Date: 17/6/2008

Signature:
Name: **Assist. Prof. Dr. Wadood T. Mohammed**
(Member)
Date: 19/6/2008

Signature:
Name: **Prof. Dr. Abbas H. Sulaymon**
(Chairman)
Date: 17/6/2008

Approval of the College of Engineering

Signature:
Name: **Prof. Dr. Muhsin J. Jweeg**
(Dean)
Date: 1/7/2008

Summary

Two types of synthetic crystalline zeolites have been used as supports for noble-metal catalysts, namely HZSM-5 and H-Mordenite with SiO_2/Al_2O_3 ratios of 90 and 40 respectively. The cations, Barium and Strontium zeolite forms were prepared by twice repeated ion-exchange with appropriate chloride solution of 3 normality at pH 7.2 and 50 ^oC. The modified zeolites were dried at 110 ^oC and calcined at 450 ^oC by step wise temperature increase. The ion-exchange by strontium was more effective than by Barium cation. While the ability of H-replacement at HMOR was higher than in case of HZSM-5.

The loading of noble metals on all considered zeolite forms were carried out in supercritical carbon dioxide as solvent. Mono-di- and trimetallic catalysts were prepared with Platinum, Ruthenium and Zirconium as acetylacetonate compounds. Platinum was loaded using $PtMe_2COD$ for Mono metallic loading, whereas this compound are very soluble in supercritical carbon dioxide ($scCO_2$), the other noble metal compounds contains acetylacetonate have low solubility in $scCO_2$, therefore 10% of methanol was added to increase the polarity of $scCO_2$. This relatively modern technique is used in the present work for the first time, to load of noble metals on zeolite catalysts for hydroconversion of hydrocarbons.

The percent metal loading was affected by increasing the pressure, reaching to about 87 % at 300 bar and 100 ^oC. High pressure increases the polarity and density of $scCO_2$ and gives high ability for dissolving the substrate and penetration through the zeolite pores. Temperature increase has a little effect on loading ability and there has been no significant increase of loading values after 24 hr contact time.

Measurement techniques, including X-Ray diffraction, FTIR spectroscopy, BET surface area measurement, Thermal Gravimetric Analysis (TGA) and Transmission Electron Microscopy (TEM) have been used to characterize the noble metal supported ZSM-5 and MOR catalysts, and to show the suitability of $scCO_2$ technique for metal loading. It has been found founds that metal loading in $scCO_2$ results in more uniform and very small nanoparticles metal dispersion with high stability after reduction than those obtained by the conventional impregnation method. It is clearly evident that high loading pressure in $scCO_2$ (i.e. 280-300 bar) causes increase in the amount at metallic phase and higher dispersion. This is resulting in higher surface area and catalytic activity.

The catalytic behavior of the mono-, di-, and trimetalic supported on ZSM-5 and MOR zeolites in the forms, H-Sr- and Ba cations, have been studied for n-Hexane hydroconversion in a fixed bed microreactor unit. The gaseous product was analyzed on-line by Gas Chromatography, while the liquid product was analyzed batch wise in another GC. The catalytic activity of all catalyst types toward n-Hexane isomerization and hydrocracking were investigated as function of time for a temperature range of 250 to 325 ^{o}C, 5 bar pressure and H_2/HC ratio of 3, 6 and 9. While, no or minor cyclic products were deducted with these catalysts.

The catalytic activity of catalysts loaded in Supercritical carbon dioxide is generally higher than that of catalysts prepared by impregnation method, at the same time, the sintering of metals in the later was noticeable.

The small pored ZSM-5 zeolite as a support showed the highest catalytic activity compared to the large pored MOR zeolite. Moreover, Strontium and Barium modified zeolites are more active and selective than H-Forms. The Barium forms were the most efficient type.

Platinum and Zirconium loaded ZSM-5 and MOR catalysts of all forms showed good activity toward the isomerization of n-Hexane. While Ruthenium containing zeolite catalysts revealed significantly lower isomerization activity and a high cracking ability at all operating conditions. High selectivity, more than 90% towards the isomerizing hexanes with good conversion around 80 % of n-Hexane have been achieved at the conditions of 275-300°C and 6-9 H_2/HC ratio with Pt and Zr, mono-and dimetallic by $scCO_2$ loaded on Sr and Ba ZSM-5 and MOR zeolite catalysts.

An attempt has been done to calculate the rate of reactions for isomerization and hydrocracking of n-Hexane for the catalyst types considered in the present work. Activation energy and pre-exponential values were also evaluated.

The rate of isomerization reaction was modeled using adsorption desorption isotherm, taking the surface reaction as a rate limiting step. The parameters of the derived equation were evaluated using statistical method, with a correlation coefficient of 0.9929. This mode gave very accurate results at different temperatures and different hydrogen to hydrocarbon ratios. Furthermore the rate constants were evaluated at different temperatures depending on Arrhenius equation. The error of this model did not exceed 2% in comparison with experimental data.

List of Contents

	Title	Page No.
	Summary	**i**
	List of Contents	**iv**
	Nomenclature	**viii**
	Subscript	**x**
	Superscript	**xi**
	List of Tables	**xii**
	List of Figures	**xiii**
	Chapter One Introduction	
1.1	Platinum Supported Catalyst	**1**
1.2	Supercritical Fluid Technology	**3**
1.3	Aim of This Work	**4**
	Chapter Two Literature Survey	
2.1	Platinum- Alumina Catalysts	**5**
2.1.1	Introduction	**5**
2.1.2	Catalytic Reforming	**7**
2.1.3	Catalytic Isomerization	**11**
2.2	Platinum Zeolite Catalyst	**14**
2.2.1	Introduction	**14**
2.2.2	Structure, Classification and Properties of Zeolites	**17**
2.2.2.1	Mordenite Type Zeolite	**21**
2.2.2.2	ZSM-5 Type	**23**
2.3	Zeolite Applications	**26**
2.4	Zeolite Modifications	**28**
2.4.1	Introduction	**28**
2.4.2	Ion Exchange	**28**
2.5	Methods of Metal Precursor to Supports	**30**

2.6	Characterizations	**31**
2.6.1	Introduction	**31**
2.6.2	Physical Adsorption for Surface Area measurements	**33**
2.6.3	X-Ray Diffraction Crystallinity	**34**
2.6.4	Thermal Analysis	**34**
2.6.5	Infrared Spectroscopy	**36**
2.6.6	Scanning Electron Microscopy	**37**

Chapter Three Super Critical Fluids

3.1	Introduction	**39**
3.2	Properties of SCFs	**40**
3.3	Local Enhancement of density	**42**
3.4	Opportunities for Application of SCFs in Heterogeneous Catalysis	**44**
3.4.1	Elemination of Gasliquid Phase transfer Resistance	**44**
3.4.2	Enhancement of Reaction Rate	**44**
3.4.3	Control of Selectivity	**44**
3.4.4	Enhanced Mass and Heat Transfer	**45**
3.4.5	Catalyst Life Time and Regeneration	**45**
3.4.6	Facilitated Separation	**46**
3.4.6	Process Intensification	**46**
3.4.8	Catalyst Preparation	**47**
3.5	Experimental Laboratory Techniques	**49**
3.6	Loading of Metal on Catalyst	**50**

Chapter Four Experimental Work

4.1	Introduction	**52**
4.2	Chemicals	**53**
4.3	Catalyst Modifications	**54**
4.3.1	Apparatus	**54**
4.3.2	Procedure	**55**
4.4	Metal loading	**56**
4.4.1	Loading of Metal by Supercritical Carbon Dioxide	**56**

4.4.1.1 Apparatus **56**
4.4.1.2 Loading of Noble Metals **58**
4.4.2 Loading of Platinum by Impregnation **61**
4.5 Characterization **61**
4.5.1 FTIR Spectra **61**
4.5.2 Inductively Coupled Plasma Spectroscopy (ICP-MS) **62**
4.5.3 X-Ray Diffraction **62**
4.5.4 Surface Area Measurements **62**
4.5.5 Thermo Gravimetric Analysis (TGA) **63**
4.5.6 Transmission Electron Microscopy (TEM) **64**
4.6 Catalytic Hydroconversion of n-Hexane **66**
4.6.1 Apparatus **66**
4.6.1.1 Liquid Feed System **66**
4.6.1.2 Gas Feed System **66**
4.6.1.3 Reactor **67**
4.6.1.4 Separations of Gas and Liquid **67**
4.6.2 Operating Procedure **70**
4.6.3 Gas Chromatography Analysis **71**
4.6.4 Method of Calculations **72**
4.6.5 Reaction Rate and Activation Energy **73**

Chapter Five Results and Discussion

5.1 Introduction **76**
5.2 Back Ion Exchange of Hydrogen Cation **77**
5.3 Loading of Metal **81**
5.4 Characterization of Samples **86**
5.4.1 FTIR Spectra **86**
5.4.2 X-Ray Diffraction **89**
5.4.3 BET Surface Area **92**
5.4.4 TGA Analysis **95**
5.4.5 TEM Analysis **99**
5.5 Catalytic Activity for Isomerization Reaction **103**

5.5.1 Introduction **103**
5.5.2 Platinum Loaded H-Zeolite **104**
5.5.2.1 Temperature Effect **104**
5.5.2.2 Hydrogen to n-Hexane Ratio **105**
5.5.2.3 Yield **106**
5.5.3 Platinum on Modified Cation Zeolite **117**
5.5.3.1 Temperature Effect **117**
5.5.3.2 Yield **119**
5.5.4 Multi Metal Loaded Zeolite Catalysts **131**
5.6 Rate of Reaction and Activation Energy **148**

Chapter Six Kinetic Modeling

6.1 Introduction **151**
6.2 Kinetic Modeling Based on Adsorption Desorption Isotherm **152**
6.2.1 Introduction **152**
6.2.2 Steps in Catalytic Reaction **153**
6.2.3 Synthesizing A Rate Law, Mechanism, and Rate Limiting Step **154**
6.3 Determine Rate Low Parameter **160**

Chapter Seven Conclusions and Future Work

7.1 Conclusions **168**
7.2 Recommendation **169**

References **170**

Appendices
Appendix A **A-1**
Appendix B **B-1**
Appendix C **C-1**
Appendix D **D-1**

Nomenclature

Symbol	Description	Units
A	Pre-exponential Factor	
A	n-C_6H_{14} in eq. 6-2	
B_2	Hydrogen in eq. 6-2	
BET	Brunauer, Emmett and Teller method	
C	i-C_6H_{14} in eq. 6-2	
Ct	Total Vacant	
Cv	Vacant Site Occupied	
DMB	Diethyl Butane	
E_a	Activation Energy	kJ/mole
EPR	Electron Paramagnetic Resonance	
F_A	Flow Rate of Inlet n-Hexane to The Reactor	mole/s
GC	Gas Chromatography	
HC	Hydrocarbon	
H_2PtCl_6	Chloroplatinic acid hexahydrate	
HRTEM	High Resolution Transmission Electron Microscopy	
ICP	Inductively Coupled Plasma Spectroscopy	
Ke	Equilibrium Reaction Constant	
k_o	Reaction Constant	
k_T	Isothermal Compressibility	
LHSV	Liquid Hour Space Velocity	
M	Metal	

MOR	Mordenite	
MP	Methyl Pentane	
N_A	Concentration of Component A at time t	mole/liter
N_{Ao}	Initial Concentration of Reactant A	mole/liter
NMR	Nuclear Magnetic Resonance	
N_t	Total Moles of The Product Mixtures	mole/liter
P	Pressure	bar
Pc	Critical Pressure	kPa
pH	Acidity Measurement	
Pr	Reduced Pressure	
$Pt(acac)_2$	Platinum acetylacetonate	
$PtMe_2COD$	Dimethyl (1, 5- cyclooctadlene) PlatinumII	
R	Gas Constant	J/mole.K
$Ru(acac)_3$	Ruthenium acetylacetonate	
$-r_A$	Rate of Reaction	mole/g.s
S	Vacant Site	
$scCO_2$	Supercritical Carbon Dioxide	
T	Temperature	K
Tc	Critical Temperature	K
TEM	Transmission Electron Microscopy	
TGA	Thermo Gravimetric Analysis	
Tr	Reduced Temperature	
t	Time	hr
w	Weight of Catalyst Filled in the Reactor	g
X	Conversion	
XRD	X-Ray Diffraction	
y	Mole Fraction	

Z	Valence of Cation	
$Zr(acac)_4$	Zirconium acetylacetonate	
ZSM-5	Zeolite Socony Mobile No. 5	
ε	Correction Factor	
θ	Mole of Species per mole of Elementary Reactant	
ρ	Density	kg/m^3

Subscript

Symbol	Description
A	Reactant A
AA	Adsorption of Reactant A
AB_2	Adsorption of Reactant B_2
A.S	Concentration of A in the Vacant
B_2	Reactant B_2
B_2.S	Concentration of B_2 in the Vacant
c	Critical
C.S	Concentration of C in the Vacant
D	Desorption
DA	Desorption of Reactant A
DC	Desorption of Product C
e	Equilibrium
o	Initial
r	Reduced

SA	Surface Reaction of Reactant A
T	Isothermal
t	Total
v	Vacant

Superscript

Symbol	Description
++	Charge
o	Initial

List of Tables

Table No.	Title	Page
2-1	Examples of Reforming Reaction	10
2-2	Commercially Available Zeolites	19
2-3	Maximum Free Diameter for Zeolites	20
2-4	Zeolite Applications	27
2-5	The general properties or characterization of catalysts and methods of measuring them	32
3-1	Comparison of Magnitudes of Physical Properties of Liquid, Gases and Supercritical Fluids in the near Critical Reagion	40
4-1	List of chemical compound, purity and its supplier	53
4-2	Retention Time for the Reactant and Product Components	72
5-1	Amount of Ion Exchange for Barium and Strontium	78
5-2	Percent of Loading and its Efficiency for Different conditions for HMOR Zeolite type	81
5-3	Platinum Contents in Zeolite Samples Loaded by Supercritical Carbon Dioxide Method	85
5-4	Platinum and Ruthenium Contents in Zeolite Samples Loaded by Supercritical Carbon Dioxide Method (mg of metal/gram of zeolite sample)	85
5-5	Platinum and Zirconium Contents in Zeolite Samples Loaded by Supercritical Carbon Dioxide Method (mg of metal/gram of zeolite sample)	86
5-6	Platinum, Ruthenium and Zirconium Contents in Zeolite Samples Loaded by Supercritical Carbon Dioxide Method (mg of metal/gram of zeolite sample)	86
5-7	BET Surface Area for Zeolite Pt/HMOR at different Temperature and Pressure	94
5-8	BET Surface Area and Pore Volumes for Different Zeolite Loaded with Platinum, Ruthenium and Zirconium	94
5-9	Catalytic Performance of Platinum Loaded by $scCO_2$ on Different Cation Forms ZSM-5 and MOR Zeolites by Hydroconversion of n-Hexane at 300 ^oC, 5 bar 3 H_2/HC Ratio.	120
5-10	Hydroconversion of n-Hexane on Mono-Di and Trimetals Zeolite Catalysts at 300 ^oC and H_2/HC ratio=3	134
5-11	Activation Energy (E_a) in (kJ/mole) and pre-exponential factor (A)in (s^{-1}) for Different Noble Metal Loaded Zeolite Catalysts	149
6-1	Steps in a Catalytic Reaction	153
6-2	The parameters of eq. 5-23 at different temperature and the activation energy with there pre-exponential factor	162

List of Figures

Fig. No.	Title	Page
2-1	Reaction Network for Reforming of C_6 Hydrocarbon	6
2-2	Three Commercial Zeolites with Different Pore Dimensionalities	20
2-3	a and b Skeletal Diagram for Zeolites	20
2-4	**(a)** Mordenite framework viewed along the C-axis, (b) the two-dimensional channels in Mordenite and (c) 6-ring sheet of tetrahedral of Mordenite viewed along the a-axis	22
2-5	Skeletal Diagram of (010) Face of ZSM-5	24
2-6	Channel Structure of ZSM-5	24
3-1	Effect of pressure on density at subcritical ($T_1<T_C$) and supercritical ($T_2>T_C$,$T_3>>T_C$) conditions	42
3-2	Schematic illustration of spatial distribution of molecules for a liquid, supercritical and gaseous system	43
3-3	Sequence of physical and chemical steps occurring in a heterogeneously catalyzed gas/Solid reaction and comparison of such a reaction at subcritical and supercritical conditions	48
3-4	Reactor types suitable for the study of heterogeneously catalyzed reactions at supercritical conditions	49
4-1	The apparatus of ion exchange using Bach wise with reflux conditions	55
4-2	Schematic diagram for metal loading setup	56
4-3	Photo picture for metal loading setup	57
4-4	Photo picture for metal loading setup	57
4-5	Photo picture for Autoclave parts	58
4-6	Micrometric ASAP 2000 device that used to measure BET surface area	63
4-7	Shown is a typical working desk for the mechanical preparation and thinning of the TEM samples	65
4-8	TEM Device in Max Plank Instituite.	65
4-9	Schematic flow diagram for the setup used for reaction	68
4-10	Photo picture for the flow diagram used for reaction	68
4-11	Picture for the reactor that used for reduction and reaction	69
4-12	Separator Designed to separate gas from liquid using iso-propanol dry ice	69
5-1	Ability of Exchange Between Strontium and Hydrogen for Two Different Zeolite	79
5-2	Ability of Exchange Between Barium and Hydrogen for Two Different Zeolite	79
5-3	fluctuation of Ph of the Solution for Strontium Exchange with Hydrogen and addition of NaOH to the Solution	80
5-4	fluctuation of Ph of the Solution for Barium Exchange with Hydrogen and addition of NaOH to the Solution	80
5-5	Efficiency of Loading vs. Pressure and Temperature	83
5-6	Efficiency of Loading vs. Treatment Time for T=80 ^oC and P=280 bar	84

5-7	FTIR Spectra for Original HZSM-5 and HMOR	87
5-8	FTIR Spectra for Original HZSM-5 Before and After Ion Exchange with Ba^{++} and Sr^{++}	88
5-9	FTIR Spectra for Original HMOR Before and After Ion Exchange with Ba^{++} and Sr^{++}	88
5-10	XRD for Original HZSM-5 and for Replaced Hydrogen Ion with Barium and Strontium Ions	90
5-11	XRD for Original HMOR and for Replaced Hydrogen Ion with Barium and Strontium Ions	90
5-12	XRD of HMOR and Pt/HMOR at different temperature and Pressure=300 bar	91
5-13	XRD of HZSM-5 and Different of Metal Loaded at T=80 ^{o}C and P=280 bar	91
5-14	XRD of HMOR and Different of Metal Loaded at T=80 ^{o}C and P=280 bar	92
5-15	BET Surface Area vs. Pressure and Temperature at pt content 0.912 wt%	93
5-16	TGA Thermograph of Pure and Loaded $PtMe_2COD$ on Zeolites at Different Temperature	97
5-17	TGA Thermograph of Pure and Loaded $Pt(acac)_2$ and $Ru(acac)_3$ on Zeolites at Different Temperature	97
5-18	TGA Thermograph of Pure and Loaded $Pt(acac)_2$ and $Zr(acac)_4$ on Zeolites at Different Temperature	98
5-19	TGA Thermograph of Pure and Loaded $Pt(acac)_2$, $Ru(acac)_3$ and $Zr(acac)_4$ on Zeolites at Different Temperature	98
5-20a	TEM Micrograph for pt/HMOR loaded by Impregnation Method	100
5-20b	TEM Micrograph for pt/HMOR loaded by $scCO_2$ at 40°C and P=300bar, t=24hr	100
5-20c	TEM Micrograph for pt/HMOR loaded by $scCO_2$ at 60°C and P=300bar ,t=24 hr	100
5-20d	TEM Micrograph for pt/HMOR loaded by $scCO_2$ at 80°C and P=300bar, t=24 hr	100
5-20e	TEM Micrograph for pt/HMOR loaded by $scCO_2$ at 100°C and P=300bar, t=24hr	100
5-20f	TEM Micrograph for pt/HMOR loaded by $scCO_2$ at 80°C and P=300bar,t=48hr	100
5-21a	TEM Micrograph for Pt loaded Over HZSM-5 by Impregnation Method	101
5-21b	TEM Micrograph for Pt loaded Over HZSM-5 by $scCO_2$	101
5-22a	TEM Micrograph for Pt loaded Over HMOR by Impregnation Method	102
5-22b	TEM Micrograph for Pt loaded Over HMOR by $scCO_2$	102
5-23	Selectivity and Conversion vs.Temperature for Zeolite Pt/HZSM-5 at Pressure 5bar and H/HC=3	108
5-24	Selectivity and Conversion vs.Temperature for Zeolite Pt/HZSM-5 at Pressure 5bar and H/HC=6	108
5-25	Selectivity and Conversion vs.Temperature for Zeolite Pt/HZSM-5	109

	at Pressure 5bar and H/HC=9	
5-26	Selectivity and Conversion vs.Temperature for Zeolite Pt/HMOR at Pressure 5bar and H/HC=3	109
5-27	Selectivity and Conversion vs.Temperature for Zeolite Pt/HMOR at Pressure 5bar and H/HC=6	110
5-28	Selectivity and Conversion vs.Temperature for Zeolite Pt/HMOR at Pressure 5bar and H/HC=9	110
5-29	Selectivity and Conversion vs. H/HC for Zeolites Pt/HZSM-5 and Pt/HMOR at Pressure 5bar and T=250 ^{o}C	111
5-30	Selectivity and Conversion vs. H/HC for Zeolites Pt/HZSM-5 and Pt/HMOR at Pressure 5bar and T=275 ^{o}C	111
5-31	Selectivity and Conversion vs. H/HC for Zeolites Pt/HZSM-5 and Pt/HMOR at Pressure 5bar and T=300 ^{o}C	112
5-32	Selectivity and Conversion vs. H/HC for Zeolites Pt/HZSM-5 and Pt/HMOR at Pressure 5bar and T=325 ^{o}C	112
5-33	Yield of 2MP vs. Temperature for Zeolites Pt/HZSM-5 and Pt/HMOR at Pressure 5bar and H/HC=3	113
5-34	Yield of 2MP vs. Temperature for Zeolites Pt/HZSM-5 and Pt/HMOR at Pressure 5bar and H/HC=6	113
5-35	Yield of 2MP vs. Temperature for Zeolites Pt/HZSM-5 and Pt/HMOR at Pressure 5bar and H/HC=9	114
5-36	Yield of 3MP vs. Temperature for Zeolites Pt/HZSM-5 and Pt/HMOR at Pressure 5bar and H/HC=3	114
5-37	Yield of 3MP vs. Temperature for Zeolites Pt/HZSM-5 and Pt/HMOR at Pressure 5bar and H/HC=6	115
5-38	Yield of 3MP vs. Temperature for Zeolites HZSM-5 and HMOR at Pressure 5bar and H/HC=9	115
5-39	Yield of (C_1-C_5) vs. Temperature for Zeolites Pt/HZSM-5 and Pt/HMOR at Pressure 5bar and H/HC=3	116
5-40	Yield of (C_1-C_5) vs. Temperature for Zeolites Pt/HZSM-5 and Pt/HMOR at Pressure 5bar and H/HC=6	116
5-41	Yield of (C_1-C_5) vs. Temperature for Zeolites HZSM-5 and HMOR at Pressure 5bar and H/HC=9	117
5-42	Selectivity and Conversion vs. Temperature for Zeolite Pt/SrZSM-5 at P=5bar and H/HC=3, 6 and 9	122
5-43	Selectivity and Conversion vs. Temperature for Zeolite Pt/SrMOR at P=5bar and H/HC=3, 6 and 9	122
5-44	Selectivity and Conversion vs. Temperature for Zeolite Pt/BaZSM-5 at P=5bar and H/HC=3, 6 and 9	123
5-45	Selectivity and Conversion vs. Temperature for Zeolite Pt/BaMOR at P=5bar and H/HC=3, 6 and 9	123
5-46	Selectivity and Conversions vs. Temperature at H/HC=3 and P=5bar for Pt on H, Sr and BaZSM-5 Zeolite	124
5-47	Selectivity and Conversions vs. Temperature at H/HC=6 and P=5bar for Pt on H, Sr and BaZSM-5 Zeolite	124
5-48	Selectivity and Conversions vs. Temperature at H/HC=9 and P=5bar for Pt on H, Sr and BaZSM-5 Zeolite	125

5-49	Selectivity and Conversions vs. Temperature at H/HC=3 and P=5bar for Pt on H, Sr and BaMOR Zeolite	125
5-50	Selectivity and Conversions vs. Temperature at H/HC=6 and P=5bar for Pt on H, Sr and BaMOR Zeolite	126
5-51	Selectivity and Conversions vs. Temperature at H/HC=9 and P=5bar for Pt on H, Sr and BaMOR Zeolite	126
5-52	Yield of 2MP vs. Temperature for Zeolite Pt/ZSM-5 for H^+, Sr^{++} and Ba^{++} catios at P=5bar and H/HC=3	127
5-53	Yield of 2MP vs. Temperature for Zeolite Pt/MOR for H^+, Sr^{++} and Ba^{++} catios at P=5bar and H/HC=3	127
5-54	Yield of 3MP vs. Temperature for Zeolite Pt/ZSM-5 for H^+, Sr^{++} and Ba^{++} catios at P=5bar and H/HC=3	128
5-55	Yield of 3MP vs. Temperature for Zeolite Pt/MOR for H^+, Sr^{++} and Ba^{++} catios at P=5bar and H/HC=3	128
5-56	Yield of DMB's vs. Temperature for Zeolite Pt/ZSM-5 for H^+, Sr^{++} and Ba^{++} catios at P=5bar and H/HC=3	129
5-57	Yield of DMB's vs. Temperature for Zeolite Pt/MOR for H^+, Sr^{++} and Ba^{++} catios at P=5bar and H/HC=3	129
5-58	Yield of (C1-C5) vs. Temperature for Zeolite Pt/ZSM-5 for H^+, Sr^{++} and Ba^{++} catios at P=5bar and H/HC=3	130
5-59	Yield of (C1-C5) vs. Temperature for Zeolite Pt/MOR for H^+, Sr^{++} and Ba^{++} catios at P=5bar and H/HC=3	130
5-60	Selectivity and Conversion vs. Temperature for Zeolite PtRu/HZSM-5 at P=5bar and H/HC=3, 6 and 9	135
5-61	Selectivity and Conversion vs. Temperature for Zeolite PtRu/HMOR at P=5bar and H/HC=3, 6 and 9	135
5-62	Selectivity and Conversion vs. Temperature for Zeolite PtRu/SrZSM-5 at P=5bar and H/HC=3, 6 and 9	136
5-63	Selectivity and Conversion vs. Temperature for Zeolite PtRu/BaZSM-5 at P=5bar and H/HC=3, 6 and 9	136
5-64	Selectivity and Conversion vs. Temperature for Zeolite PtRu/SrMOR at P=5bar and H/HC=3, 6 and 9	137
5-65	Selectivity and Conversion vs. Temperature for Zeolite PtRu/BaMOR at P=5bar and H/HC=3, 6 and 9	137
5-66	Selectivity and Conversion vs. Temperature for Zeolite PtZr/HZSM-5 at P=5bar and H/HC=3, 6 and 9	138
5-67	Selectivity and Conversion vs. Temperature for Zeolite PtZr/HMOR at P=5bar and H/HC=3, 6 and 9	138
5-68	Selectivity and Conversion vs. Temperature for Zeolite PtZr/SrZSM-5 at P=5bar and H/HC=3, 6 and 9	139
5-69	Selectivity and Conversion vs. Temperature for Zeolite PtZr/BaZSM-5 at P=5bar and H/HC=3, 6 and 9	139
5-70	Selectivity and Conversion vs. Temperature for Zeolite PtZr/SrMOR at P=5bar and H/HC=3, 6 and 9	140
5-71	Selectivity and Conversion vs. Temperature for Zeolite PtZr/BaMOR at P=5bar and H/HC=3, 6 and 9	140

5-72	Selectivity of MP's vs. Temperature at H/HC=3 and P=5bar for Four Zeolite Pt/HZSM-5, Pt/HMOR and Bimetal with Zr Metal	141
5-73	Selectivity of DMB's vs. Temperature for Zeolite Pt/HZSM-5 and PtZr/HZSM-5 at P=5bar and H/HC=3	141
5-74	Selectivity and Conversion vs. Temperature for Zeolite PtRuZr/HZSM-5 at P=5bar and H/HC=3, 6 and 9	142
5-75	Selectivity and Conversion vs. Temperature for Zeolite PtRuZr/HMOR at P=5bar and H/HC=3, 6 and 9	142
5-76	Selectivity and Conversion vs. Temperature for Zeolite PtRuZr/SrZSM-5 at P=5bar and H/HC=3, 6 and 9	143
5-77	Selectivity and Conversion vs. Temperature for Zeolite PtRuZr/BaZSM-5 at P=5bar and H/HC=3, 6 and 9	143
5-78	Selectivity and Conversion vs. Temperature for Zeolite PtRuZr/SrMOR at P=5bar and H/HC=3, 6 and 9	144
5-79	Selectivity and Conversion vs. Temperature for Zeolite PtRuZr/BaMOR at P=5bar and H/HC=3, 6 and 9	144
5-80	Selectivity and Conversions vs. Temperature at H/HC=3 and P=5bar for Four Zeolite Pt, PtRu, PtZr and PtRuZr Over HZSM-5	145
5-81	Selectivity and Conversions vs. Temperature at H/HC=6 and P=5bar for Four Zeolite Pt, PtRu, PtZr and PtRuZr Over HZSM-5	145
5-82	Selectivity and Conversions vs. Temperature at H/HC=9 and P=5bar for Four Zeolite Pt, PtRu, PtZr and PtRuZr Over HZSM-5	146
5-83	Selectivity and Conversions vs. Temperature at H/HC=3 and P=5bar for Four Zeolite Pt, PtRu, PtZr and PtRuZr Over HMOR	146
5-84	Selectivity and Conversions vs. Temperature at H/HC=6 and P=5bar for Four Zeolite Pt, PtRu, PtZr and PtRuZr Over HMOR	147
5-85	Selectivity and Conversions vs. Temperature at H/HC=9 and P=5bar for Four Zeolite Pt, PtRu, PtZr and PtRuZr Over HMOR	147
5-86	$Ln(-r_A)$ vs. 1/T for all modification and loading for Zeolite ZSM-5 at 5 bar	150
5-87	$Ln(-r_A)$ vs. 1/T for all modification and loading for Zeolite MOR at 5 bar	150
6-1	Experimental and Modeled Rate of Reaction vs, Conversion for Isomerization of n-Hexane Using Pt/HZSM-5 at 5 bar total Pressure and H/HC=3	163
6-2	Experimental and Modeled Rate of Reaction vs, Conversion for Isomerization of n-Hexane Using Pt/HMOR at 5 bar total Pressure and H/HC=3	163
6-3	Experimental and Modeled Rate of Reaction vs, Conversion for Isomerization of n-Hexane Using PtRu/HZSM-5 at 5 bar total Pressure and H/HC=3	164
6-4	Experimental and Modeled Rate of Reaction vs, Conversion for Isomerization of n-Hexane Using PtRu/HMOR at 5 bar total Pressure and H/HC=3	164
6-5	Experimental and Modeled Rate of Reaction vs, Conversion for Isomerization of n-Hexane Using PtZr/HZSM-5 at 5 bar total Pressure and H/HC=3	165

6-6	Experimental and Modeled Rate of Reaction vs, Conversion for Isomerization of n-Hexane Using PtZr/HMOR at 5 bar total Pressure and H/HC=3	165
6-7	Experimental and Modeled Rate of Reaction vs, Conversion for Isomerization of n-Hexane Using Pt/SrZSM-5 at 5 bar total Pressure and H/HC=3	166
6-8	Experimental and Modeled Rate of Reaction vs, Conversion for Isomerization of n-Hexane Using Pt/BaZSM-5 at 5 bar total Pressure and H/HC=3	166
6-9	Experimental and Modeled Rate of Reaction vs, Conversion for Isomerization of n-Hexane Using Pt/HZSM-5 at 5 bar total Pressure and H/HC=6	167
6-10	Experimental and Modeled Rate of Reaction vs, Conversion for Isomerization of n-Hexane Using Pt/HZSM-5 at 5 bar total Pressure and H/HC=9	167

Chapter One
Introduction

1.1 Platinum Supported Catalysts

The petroleum refinery includes many unit operations and unit processes. The first unit operation in a refinery is the continuous distillation of the crude oil being refined. The overhead liquid fraction is called naphtha and will become a major component of the refinery's gasoline (Petrol) product after it is further processed through a catalytic hydrodesulfurizer to remove sulfur containing hydrocarbons and a catalytic reformer to reform its hydrocarbon molecules into more complex molecules with a higher octane rating value. The naphtha is a mixture of many very different hydrocarbon compounds. It has an initial boiling point of about 35 °C and a final boiling point of about 200 °C. Naphtha contains paraffins, naphthenes (cyclic paraffins) and aromatic hydrocarbons ranging from those containing 4 carbon atoms to those containing about 10 or 11 carbon atoms [1].

The aim of catalytic reforming is to increase the quality of gasoline, as measured by the research octane number (RON), by converting molecules with a relatively low RON (linear and cyclic alkanes) into molecules with a relatively high RON (branched alkanes, aromatics) [2].

Catalytic reforming reactions proceed on bifunctional catalysts with two types of active sites. The supported metal catalyst (such as platinum) for hydrogenation and dehydrogenation reaction, and the active sites on the surface of the support (e.g. activated alumina) such as the acid sites for the isomerisation, cracking and cyclization reactions. The Pt/Al_2O_3 as a

bifunctional reforming catalyst have been used since the 1950's in the oil industry [3].

Isomerization of normal C_5/C_6 paraffines, which is the major component of the petroleum fraction boiling below 70 ^oC, is of considerable practical and scientific interest to enhance the octane number of gasoline pool using bifunctional catalysts also [4]. The catalyst should be able to convert the feedstocks at the lowest temperature as possible in order to favor higher yield of dibranched hexane. Therefore, the catalyst should exhibit strong acidic properties. The current industrial catalyst falls into two categories: (i) metal halide catalysts, which are active at low temperature, but are very sensitive to water, require continuous addition of a chloride compound, and generate corrosive HCl, (ii) zeolite catalysts, which are much more stable but at the expense of isomer yield since they operate at higher temperature [5].

Active components for hydrogenation-dehydrogenation are normally noble metals such as Platinum, Palladium, Tin, Ruthenium, Gallium, Tungsten, Iridium and Rhenium. The bi or multimetalic compounds are usually introduced to the pores of zeolites and reduced to their elemental form with hydrogen under selective condition toward aromatic hydrocarbons. Thus the metal is finely distributed probably mainly atomically in the pores of the zeolite lattice [3].

Several factors are also incorporated in the study of zeolite catalysts which makes it a very interesting type. Their specific properties such as ion exchange ability, high exchange capability, crystalline structure with regular pores of molecular size, quantity of cations and active sites, and the silica to alumina ratio. These properties provide a metal loaded zeolite system which has promise as catalyst in petroleum refining and in petrochemicals [6].

The degree of the improvement of catalytic properties and characterization depend on several factors such as, amount of interchanged

metals, size of metallic ions, surface area increasing, acidity modifications and thermal stability under operation conditions. On the other hand, the conditions and methods of catalyst preparation, owing to the changes in the nature of interaction of catalyst components are; dispersion, pore structure and other factors. All these parameters, independently or simultaneously can influence the rate of production for a given case [7].

In heterogeneous catalytic processes one usually considers three major performance characteristics: activity, selectivity toward one or several products, and stability of operation, that is, low catalyst aging [8].

1.2 Supercritical Fluid Technology

Supported metal nanocomposites have unique electronic, optical, electrooptical, and catalytic properties that are directly related to the specific concentration, size, and distribution of the metal particles within their host environment. There are several ways to synthesize supported nanoparticles, including impregnation, sol-gel processing, or microemulsion generation using organic stabilizing agents. However, control over particle size, distribution, and metal concentration in the composite is challenging [9].

The supercritical fluid was utilized as a processing medium to incorporate metal nanoparticales into different substrates. A supercritical fluid (SC) is a fluid that has been heated and compressed above its critical temperature and pressure. The thermophysical properties of a SC are intermediate between those of a gas and a liquid and can be adjusted by slight changes in temperature and/ or pressure. Among the supercritical fluids, supercritical carbon dioxide ($scCO_2$) (T_C=31.1^{o}C, P_C=71.8bar) is particularly attractive for a wide variety of applications because it is chemically inert, nontoxic, environmentally acceptable and leaves no residue in the treated

medium. Such properties have been exploited in the development of novel processes for the synthesis of nanostructured materials [10].

There are few investigations concerning metal loading on supports in super critical fluids, while no work was presented on loading of noble metals on zeolites in SC.

1.3 Aim of This Work

The aim of the present project can be summarized as follows:

1- Modifying and synthetic ZSM-5 and Mordenite zeolite by exchanging H-form by to Barium and Strontium cations at constant conditions with different periods of salt solution treatment.

2- Platinum loading over zeolite using the supercritical carbon dioxide technique, by using sufficient metal compounds that could be soluble in CO_2 at supercritical conditions.

3- Loading other noble metals such as Zirconium and Ruthenium promoted with Platinum in $scCO_2$ to form bi and trimetalic loading.

4- Investigating the characteristic performance of the noble metal/zeolite catalysts such as; surface properties, thermal analysis, metal content and catalysts crstallinity by X-Ray diffraction and other related techniques.

5- Studying the effect of metal loading and zeolite modification on catalyst activity and selectivity towards n-Hexane isomerization, at different Hydrogen to Hydrocarbon ratios and different temperatures.

6- Developing a mathematical model to describe the rate of reaction of isomerization of normal hexane, and estimating all parameters corresponding to this model.

Chapter Two
Literature Survey

2.1 Platinum- Alumina Catalysts

2.1.1 Introduction

The platinum-alumina catalyst system belongs to the class of catalysts known as bifunctional types [11]. These catalysts consist of two principal components; a metal **(**Pt**)** dispersed on an acidic support (Al_2O_3). Platinum is well known to be highly active as a catalyst for hydrogenation and dehydrogenation reactions. The role of the support is to accelerate acid-catalyzed reactions for isomerization and cyclization. Because the support alone possesses activity and may interact synergistically with the metal component, the activity and selectivity of bifunctional catalysts is often much different from that of the catalysts possessing purely metallic properties [12].

Reforming and isomerization can be considered as significant processes, which are carried out on bifunctional catalysts [13].

Reforming is a process in which a low-octane straight-run gasoline or naphtha is treated to improve the octane number and thus, improve ignition performance. The treatment takes place under specifically controlled conditions. Upgrading gasoline quality is achieved by an increase in octane number. The increase is caused by the reduction in molecular sizes mainly by the conversion of normal paraffins to iso-paraffins aromatics, and olefins, along with the conversion of naphthenes to aromatics [14].

The bifunctional nature of the catalyst was first demonstrated by Weisz by using a mixed bed of silica alumina for the acid component and Pt/SiO_2 for dehydrogenation [15].

Bifunctionality takes place on Pt/Al_2O_3 by dehydrogenation of the alkane on the platinum sites to produce the corresponding alkene which migrate to the acidic sites of the alumina to undergo skelated rearrangement or ring closure or ring enlargement through a carbonium ion mechanism, yielding an isomer of the original alkene or cycloalkane. This then migrates back to the metal where it can be rehydrogenated to the corresponding iso-or cyclo-alkanes [16].

Mills and co-workers [13] proposed that, the two functions of the reforming reactions interact through olefins, which are the key intermediates in the reaction network, as shown in the mechanism in Fig. 2-1.

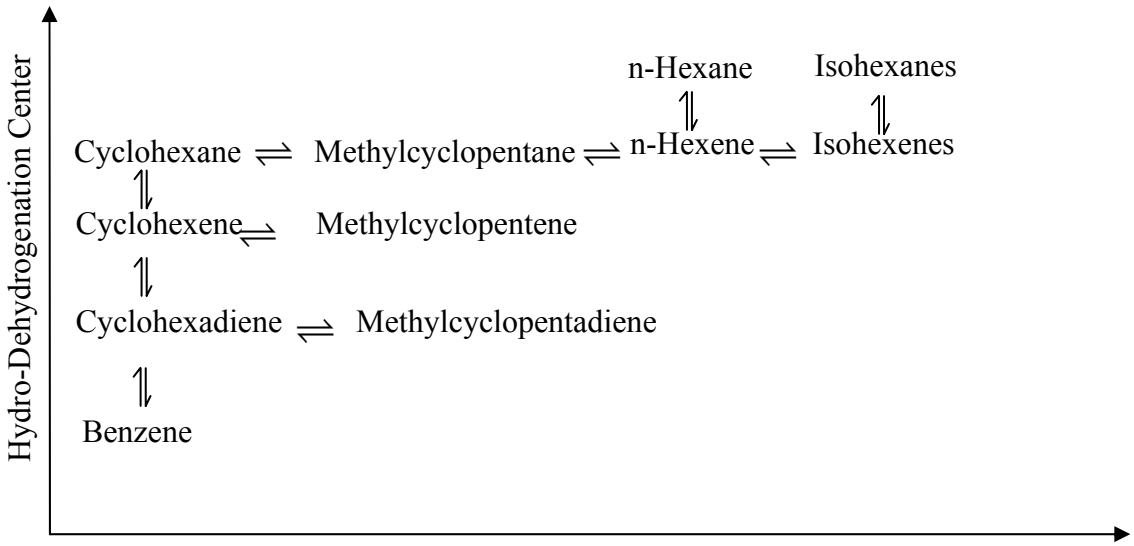

Figure 2-1: Reaction Network for Reforming of C_6 Hydrocarbon [13]

The vertical reaction paths in previous figure takes place the hydrogenation-dehydrogenation centers of the catalyst and the horizontal reaction paths on the acidic centers. According to above mechanism, the conversion of n-hexane to benzene, for example first, involves dehydrogenation on the metal to give straight-chain hexene**.** The hexene migrates to a neighboring acid center; where it is protonated to give a secondary carbonium ion which can react to form methylcyclopentane, which can react further to form cyclohexene and then benzene as shown in Fig. 2-1.

Another metal such as Rhenium, Iridium, and Gallium can be introduced with Pt on the alumina carrier. In this case the catalyst said to be bimetallic or trimetallic catalyst. The main advantage of these catalysts is a reduced rate of coke formation and increased stability rather than an increased aromatization activity [4].

2.1.2 Catalytic Reforming

Catalytic reforming is one of the major conversion processes in the petroleum refinery. The most important chemical reactions are the conversion of paraffins and naphthenes to aromatics. Its product, catalytic reformate, is the chief source of high octane components for motor gasoline and aromatics for the petrochemical industry [17].

The heart of the reforming process is the catalyst, thus most of the major improvement in the process efficiency have been due to the development of improved catalysts.

The development of catalytic reforming since its beginning in the 1940 has been a story of catalyst development [12]. The original process used molybdenum-oxide supported on alumina catalyst in fixed bed reactors with very short cycle times between regenerations to burn off deposited carbon. Later in the 1950 this catalyst was used in fluid bed process with continuous regeneration to decrease the cycle times and increases the catalyst activity [18].

Platinum-alumina catalyst (Platforming process) was first introduced by UOP (Universal Oil Products) in 1948, when it was discovered that platinum is more stable and active than catalysts previously used. This catalyst made it possible to provide the higher reformer severities needed to meet the increasing motor gasoline octane requirements [19].

The Pt/Al_2O_3 catalyst contains metal sites-namely platinum (0.3-0.6 wt% Pt) that promote hydrogenation-dehydrogenation reactions, and acid sites associated with the alumina base that promote carbonium ion type reaction. Either sites may act alone for a given reaction or one site may form intermediates needed for the reaction on the other site [13].

A second generation of the reforming catalysts began roughly in the late sixties with introduction of bimetallic catalysts such as platinum-rhenium and platinum-iridium supported on an acidic alumina. These new catalysts maintain their activity at lower hydrogen pressure, also allows an increased cyclization of paraffins to aromatics [20, 21].

In 1969 Chevron research announced its rhenium promoted Pt/Al_2O_3 reforming catalyst which contains rhenium in addition to the platinum. The effect of rhenium is to lower the rate at which carbon is deposited and hence the temperature may be raised more slowly**,** which the catalyst life is thereby prolonged [22].

To meet the great demands on the platformer. UOP produced the continuous platforming technique with continuous regeneration that offer maximum yields of reformate of a high octane [19].

The term "reforming reaction" actually encompasses a complex network of reactions. Among the overwhelming number of reactions, the main reactions are naphthene dehydrogenation, naphthene isomerization, dehydrocyclization, paraffin isomerization, and hydrocracking [14, 23]. Examples of each of these reactions are given in Table 2-1.

These reactions occur to varying degrees, and the extent to which each takes place depends upon the nature of the catalyst, the composition of the naphtha feed, and conditions of operation.

The heat of reactions are the most important thermodynamic data. Some, such as dehydrogenation of paraffins, are mildly endothermic. Others,

such as the dehydrogenation of naphthenes or the dehydrocyclization of paraffins, are highly endothermic; for this reason, platinum reforming consists of several fixed bed adiabatic reactors in series with reheating in between to supply the heat of reaction. On the other hand, hydroisomerization reactions are very slightly exothermic [8].

Coke formation in bifunctional reforming catalyst is the main cause of deactivation. The catalyst deactivation is relatively slow and is being suppressed as compared with reforming reactions [8].

In the field of platinum-alumina catalyst and its promoted types, there are many studies that show the influence of preparation conditions on the properties of the catalysts. **Mills and co-workers [24]** studied the effect of Pt concentration on cyclohexane dehydrogenation to benzene at 343 C^o and on naphtha reforming at commercial conditions. About 0.3-0.4 wt% of Pt content was observed for cyclohexane dehydrogenation.

Sinfelt et al. [25] examined the effect of Pt content on n-heptane isomerization, n-heptane dehydrocyclization and methylcyclohexane dehydrogenation. They concluded that over the range of 0.1 to 0.5 wt% Pt the rate of isomerization was constant, while the rate of the methylcyclohexane dehydrogenation was proportional to Pt content and the rate of cyclization increased by 75 to 100% due to increasing the Pt content at both 471 and 526°C. **Hettinger et al. [26]** found that n-heptane dehydrocyclohexane rate increased as Pt content was raised to 0.1 and methycyclohexane dehydrogenation activity increased up to 0.6 wt% Pt.

Christoffel et al. [27] studied the dehydrocyclization of n-hexane in the temperature range 400-500°C on a commercial Pt/Al_2O_3 catalyst. They concluded from product distributions that at least four different reaction paths for the aromatization are possible, 5-and 6-membered ring closure and cyclization of cis-2-hexane and 1,5-hexadiene.

The acidic component of the Pt/Al_2O_3 reforming catalyst is normally associated with the alumina base and in particular with the 0.3-1.5 wt % chloride deposited on the alumina base during platinum impregnation. Catalyst acidity usually controls the overall activity of the reforming catalyst [4].

***Table 2-1*:** Examples of Reforming Reaction [23]

Reaction Type	ΔH kJ/mol.
1- Naphthene Dehydrogenation 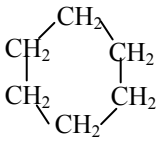 $\xrightleftharpoons[\text{Catalyst}]{\Delta}$ 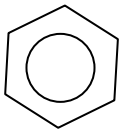 $+ 3H_2$ Very Fast Cyclohexane Benzene	+221
2- Naphthane Isomerization 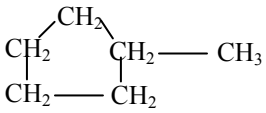 $\xrightleftharpoons[\text{Catalyst}]{\Delta}$ 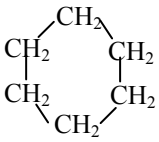 Fast Methylcyclopentane Cyclohexane	-15
3-Dehydrocyclization $CH_3(CH_2)_4CH_3$ $\xrightleftharpoons[\text{Catalyst}]{\Delta}$ 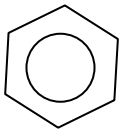 $+4H_2$ Slow Normal Hexane Benzene	+266
4-Paraffin Isomerization $CH_3(CH_2)_4CH_3$ $\xrightleftharpoons[\text{Catalyst}]{\Delta}$ $CH_3\text{-}\overset{\overset{\displaystyle CH_3}{\vert}}{C}H\text{-}CH_2\text{-}CH_2\text{-}CH_3$ Fast Normal Hexane 2-Methylpentane	~5
5-Hydrocracking $CH_3(CH_2)_7CH_3 + H_2$ $\xrightleftharpoons[\text{Catalyst}]{\Delta}$ $CH_3(CH_2)_2CH_3 + CH_3(CH_2)_3CH_3$ Slow Nonane Butane Pentane	-2.3

2.1.3 Catalytic Isomerization

Isomerization of normal paraffin over dual function catalysts is becoming increasingly important in gasoline pool production [28]. These catalysts consist of an active hydrogenation dehydrogenation component (transition metal or metal oxides), supported on an active acidic support. Platinum is considered as the most suitable metallic component for isomerization catalysts [29].

It is generally accepted that catalytic isomerization of saturated hydrocarbons proceeds through a carbonium ion intermediate which once formed can isomerize by intra-molecular rearrangement. The principle and widely accepted scheme starts with the formation of olefins from paraffins at the metallic centers and the formation of carbonium ions from these olefins at acidic centers [30, 31, 32]. The carbonium ions may undergo rearrangement and splitting according to certain rules of carbonium ion behaviour.

It is proposed generally that isomerization proceeds in three stages [33, 34, 35]. Adsorption of an n-paraffin molecule on a the metal site followed by dehydrogenation into an n-olefin; desorption of the n-olefin from the dehydrogenation sites and diffusion to a skeletal rearranging sites, which convert the n-olefine into an iso-olefine via a carbonium ion mechanism and desorption of the iso-olefine from the skeletal rearranging sites where it is finally hydrogenated into an iso-paraffin molecule. The mechanism can be represented schematically as follows:

$$n-Paraffine \overset{Pt}{\rightleftharpoons} n-Olefin \overset{Al_2O_3}{\rightleftharpoons} i-Olefin \overset{Pt}{\rightleftharpoons} i-Paraffin \qquad (2\text{-}1)$$

Further substantiation of a carbonium ion mechanism is provided by the lower molecular weight hydrocarbons formbed by hydrocracking during the isomerization of hydrocarbon, the main products are propane and butanes which occur at the center of the molecules [35, 36, 37].

An alkane isomerization mechanism on supported noble metals can be countered in three typical situations depending on the acid strength of the carrier. For a catalyst of very strong acidity, isomerization occurs on acid sites, the role of the metal being limit the coke formation and the deactivation of acid sites, but for catalysts of very low acidity, isomerization occurs on metal sites which depend on the size of crystallites and for catalysts of average acidity such as Pt/SiO_2, isomerization occurs through the conventional bifunctional mechanism [38, 39, 40].

Haensel and Donaldson [41] and **Sinfelt and Rohrer [42]** studied the heptane isomerization reaction on Pt/Al_2O_3 catalyst. All found that 70-95% of the C_7 isomers were 2 and 3 methylhexane while the remainder is dimethylpentane.

The effect of hydrogen pressure on n-heptane isomerization was studied by **Rohrer et al [43]**. Isomerization rate increased with pressure from 1 atmosphere up to 5-6 atmospheres due to hydrogenation of hydrogen deficient residues on the active sites. Increasing hydrogen pressure caused a slight decrease in isomerization due to competition with heptane for active sites.

El-Kady et al. [38] studied the isomerization activity and selectivity of the prepared catalyst containing 0.3-0.8 wt% Pt supported on silica - alumina. At temperature range 300- 425°C and a pressure 60 atm, they found that the catalyst containing 0.4% platinum is the best active and selective catalyst for n-heptane isomerization. They concluded that increase of Pt content on the catalyst decrease the number of the isomerization sites and increasing the olefin content which led to side reactions such as cracking.

Joseph and Raynor [44] studied paraffin isomerization at low temperature by reaction of a Pt/Al_2O_3 catalyst with various chlorinating agents such as hydrogen chloride, thionyl chloride, sulfuryl chloride and sulfur monochloride. They found that catalyst activity increased when Pt/Al_2O_3 was treated with hydrogen chloride prior to sulfur chloride treatment. These chlorinated platinum alumina catalysts are capable of isomerizing butane, pentane and hexane to near their equilibrium isomer distributions at temperatures below 176 ^oC.

Orkin [45] studied the isomerization reaction of C_{11} to C_{14} normal paraffins on fluorided platinum alumina catalyst in a continuous flow bench reactor under hydrogen pressure. They found that reducing total hydrogen pressure from 1000 to 50 psig increased the isomerization conversion from 37 to 88%**.** At 300 psig, a 5% fluoride catalyst was more active than either 10% fluoride or the fluoride-free catalyst.

Choudhary [46] carried out the isomerization of n-pentane to iso-pentanes over platinum on fluorinated alumina. Aconstant conversion (52-53%) was observed for one year operation.

Choudhary and Doraiswamy [47] have applied the group screening method for the selection of the best catalysts among 46 solid catalysts for the isomerization of n-butene to isobutene. Fluorinated eta (n) alumina containing 1% F was found to be the best catalyst with highest activity 33.5%, Conversion of n-butene to isobutene and a good selectivity (87.1% for isobutene).

Burch [48] studied the isomerization of n-hexane to branched chain isomers over a range of nickel on silica- alumina catalysts containing between 5 and 16 wt% nickel, and found that a 7% Ni catalyst has a high activity and selectivity for isomerization which is comparable to a commerical platinum catalyst under the same condition.

Shanshool and co-workers [49] studied the isomerization of n-hexane on both prepared and commerical Pt/Al_2O_3 as well as commercial $Pt\text{-}Re/Al_2O_3$. They studied the effects of chlorinated hydrocarbon addition (methylene chloride, trichloroethylene (TCE), chloroform and carbon tetrachloride) in the liquid feed on the activity. They concluded that chloroform show a most favorable chlorinating agent and they indicate that upon chlorination the isomerization selectivity increased and the cyclization selectivity decreased.

Gerberich et al. [50] studied the isomerization of cyclopropane to propylene over alumina containing 0-6% fluorine. The catalytic test was carried out at 127 °C**.** The maximum isomerization rate occurs at 1.2% F and is about 5000 times that found for fluorine free alumina. At higher fluorine content, the rate constant decreased moderately to a value which was about 30% that at the maximum. The activation energy decreased sharply from 29 kcal/mole for pure alumina to a minimum of 13 kcal/rnole. It is gradually increased to 16-18 kcal/mole for higher fluorine content.

2.2 Platinum Zeolite Catalyst

2.2.1 Introduction

The term "Zeolite" is said to have its origin in the two greek words Zeo and Lithos, which mean "to boil" and "stone". The phenomena of melting and boiling at the same time are termed intumescence [51]. Furthermore, Boron Cronstedt described the first zeolite mineral (Stilbite) in Sweden in 1756 [52].

Sand et. al. [53], reported that adsorption characteristics of chabazite were attributed to tiny pores (< $5A^o$ in diameter) that allowed small molecules to enter but excluded larger ones; hence, the term "molecular sieve".

Barrer, [54], classified zeolite minerals into three classes depending on the size of the molecule absorbability: rapidly, slowly, or not appreciably at

room temperature or above. In 1948, he synthesized small port Mordenite at high temperature and pressure heralded the era of synthetic zeolites.

However, zeolite did not find any significant commercial use until synthetic zeolite was made and developed (large, minerable deposits of natural zeolites were not discovered until the late 1950).

From 1949 through the early 1950s, the commercially significant zeolites A, X, and Y were discovered by **Milton and Breck** [55] at the Linde Air Laboratories. These zeolites were synthesized from readily available raw materials at much lower temperature and pressure than used earlier.

Hegedus et. al. [56], said that in the later of 1950s, that catalytic reactions can take place inside these structures, and the level of research activity into zeolite synthesis, structure, and properties changed from one of slow continual progress to intense pursuit.

In 1953, Linde type A zeolite became the first synthetic zeolite to be commercialized as an adsorbent to remove oxygen impurity from argon at a Union Carbide plant [55]. Synthetic zeolites were introduced by Union Carbide as a new class of industrial adsorbents in 1954 and as hydrocarbon conversion catalysts in 1959. New zeolites and new uses appeared steadily through the 1960s. An explosion of new zeolites structures and composition occurred in the 1980s and 1990s and zeolites now serve the petroleum refining, petrochemical, and chemical process industries as selective catalysts, adsorbents, and ion exchangers [57].

Zeolites have a uniform pore structure determined by the crystal structure with known pore diameters (channels) between 3 and 10 A^o. The channels may be circular or elliptical, tubular or containing periodic cavities and straight or zigzag. If the counterions are located within the channels they can be exchanged and hence the catalytic capacity of the zeolite may be enhanced. Apertures consisting of a ring of oxygen atoms of connected

tetrahedral limit access to the channels. There may be 4, 5, 6, 8, 10 or 12 oxygen atoms in the ring. This regular structure of the pores with their aperture in the atomic scale enables the zeolite to work as a molecular sieve and hence zeolites can have high selectivity's as catalysts for certain reactions. The pore size and structure of zeolites may affect the selectivity of a reaction in one or more of three ways [58]:

1. Reactant selectivity: The pore size can hinder certain reactants from reaching the interior of the zeolite. This occurs when the aperture size is smaller than the molecule i.e. only sufficiently small molecules can reach the active sites. Hence the term “molecular sieve” is justified. An example where reactant selectivity is important is in reforming processes of high-octane gasoline [59].
2. Product selectivity: Products larger than the aperture size cannot diffuse out from the zeolite. Therefore these larger molecules will not be formed or they will be converted to smaller molecules or to carbonaceous deposits within the pore. Unfortunately this may deactivate the zeolite due to pore blockage. An example of a reaction where product selectivity is important is the alkylation of toluene over H-ZSM-5 [60].
3. Restricted transition state selectivity: This third form of shape selectivity causes less undesirable side reactions or hinders larger intermediates that would be formed in other environments, to escape from the pore. Only those intermediates that can fit in the pore can be formed. However, in practice it is difficult to distinguish restricted transition state selectivity from product selectivity. An example of a reaction where restricted transition state selectivity is the methanol to olefine process (MTG) which uses an H-ZSM-5 catalyst [61].

2.2.2 Structure, Classification and Properties of Zeolites

2.2.2.1 General

Zeolites synthesized or formed in nature are aluminosilicates of group I and II elements.It has the chemical formula $M_{2/n}O.\ Al_2O_3\ .x\ SiO_2\ .y\ H_2O$, where the charge-balancing non-framework cation M has valence n, x is 2 or more, and y is the moles of water in the voids. The Al and Si tetrahedral atoms, or T-atoms, form three-dimensional (3D) framework of AlO_4 and SiO_4 tetrahedral linked together by shared oxygen ions. Although SiO_4 tetrahedral is charge balanced, an AlO_4 tetrahedral has a negative charge balanced by a positive charge on M. Furthermore, examples of compositional ranges of important zeolites is illustrated by Table 2-2 [62].

The zeolite framework contains channels and interconnected voids, which are occupied by cations and water molecules. Generally the cations are mobile and can be replaced by exchange with other cations, which modify the pore diameter. Inter crystalline water can be removed, some times reversibly [57].

The catalytic activity of zeolite is attributed to acidic sites, i.e. to electron acceptors known as Lewis centers (L) and to proton donors accepted as Bronsted (B) sites. Both Bronsted and Lewis acid sites are found in zeolites. The former are protons attached to lattice oxygen atoms, while the latter can be the charge-compensating cations or trigonal aluminum atoms at oxygen – deficient sizes or at cation positions [63].

The crystal structure of a zeolite is defined by the specific order in which a network of tetrahedral units is linked together. In A, X, and Y zeolites, four- and six-membered rings are joined together and they form cubic octahedron referred to as a sodalite unit. Oxygen bridges between the six-membered rings, forming a hexagonal prism (zeolite X and Y) which connects these sodalite units. These arrangements leave in the framework

cages with 8 (zeolite A) or 12 (zeolite X, Y) oxygen membered windows which determine the pore structure. In the mordenite framework, TO_4 tetrahedrals are arranged to form five -membered rings, these are joined to form five chains and the chains are linked to form the crystal [64].

Zeolites are chemically differentiated by SiO_2/Al_2O_3 ratio in their anionic framework. The quantity SiO_2/Al_2O_3 considerably determines the structure and properties of zeolites (the acid resistance and thermal stability of zeolites increase as the SiO_2/Al_2O_3 ratio increases). Its values range between 2 to ∞ therefore, in the A-type zeolite SiO_2/Al_2O_3 is close to 1; in the X type zeolite, it varies from 1 to 1.5; for Y, it is 1.5 to 3.0, and in synthetic mordenite it reaches 10 [58]. On the other hand, zeolite is commonly lumped into three classes depending on the number of tetrahedral and maximum free diameter zeolites are illustrated in Table 2-3 [56]:

Another classification of zeolites depends on the pore dimensionalities, which are different from type to type of zeolites. Zeolite may have a one, two, or three dimensional pore structures. Type A has three intersection channels running through the structure; ZSM–5 has two intersecting channels-one straight and the other sinusoidal; and mordenite has a single channel system, resembling a pack of soda straws [65, 66].

***Table 2-2*:** Commercially Available Zeolites [62]

Zeolite	***Pore size*** Å	***Composition***	
		Si/Al	***Cation***
Faujasite:			
X	7.4	1 - 1.5	Na
Y	7.4	1.5 - 3	Na
US-Y	7.4	> 3	H
A	3	1.0	K, Na
A	4	1.0	Na
A	4.5	1.0	Ca, Na
Chabazite	4	4	*N*
Clinoptilolite	4x5	5.5	*N*
Erionite	3.8	4	*N*
Ferrierite	5.5x4.8	5 - 10	H
L type	6	3 – 3.5	K
Mazzite	5.8	3.4	Na, H
Mordenite	6x7	5.5	*N *
Mordenite	6x7	5 - 6	Na
Mordenite	6x7	5 - 10	H
Offretite	5.8	4	K, H
Phillipsite	3	2	*N *
Silicalite	5.5	∞	H
ZSM-5	5.5	10 - 500	H
where *N* = Mineral Zeolite; Cation variable and usually Na, K, Ca, Mg.			

***Table 2-3*:** Maximum Free Diameter for Zeolites [56]

Pore size	***No. of tetrahedral***	***Max. Free Diameter (Å)***	***Example (e.g.)***
Small	6 - 8	4.3	A and Erionite
Medium	10	5.5	ZSM-5
Large	12	7	Mordenite & Faujasite

Figures.2-2 and 2-3a and b illustrate an example of pore structure for different types of zeolites [62].

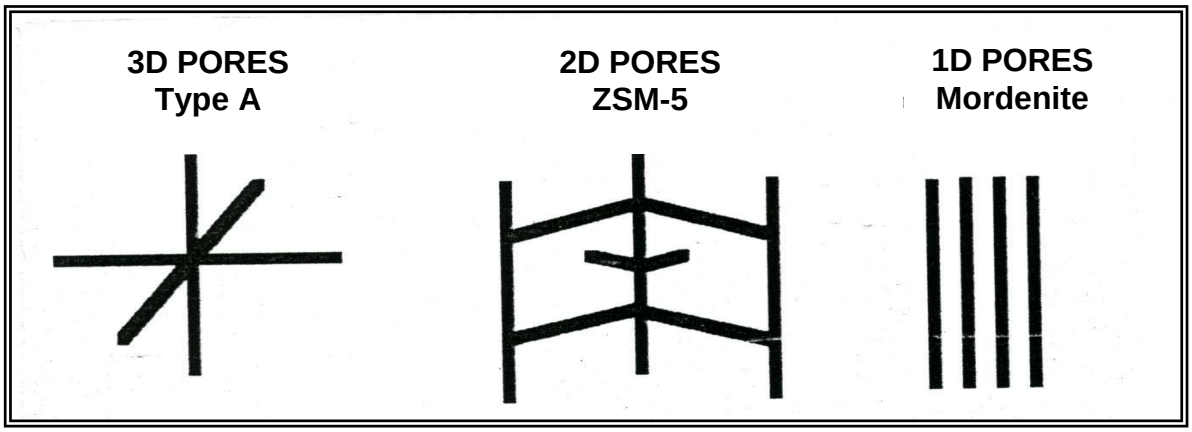

***Figure 2-2*:** Three Commercial Zeolites with Different Pore Dimensionalities.

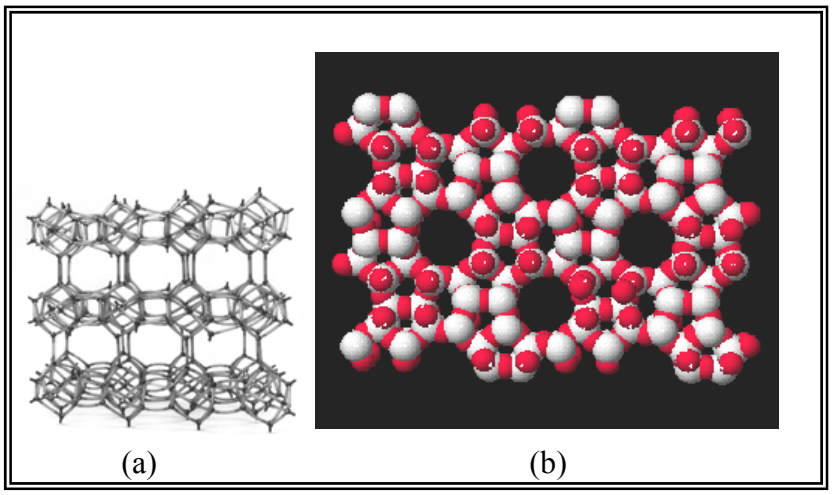

***Figure 2-3*:** a and b Skeletal Diagram for Zeolites

2.2.2.2 Mordenite Type Zeolite

Mordenite is a natural and synthetic zeolite with an idealized composition (Na_8 AL_8 Si_{40} O_{96} $.24H_2O$). Its structure is orthorhombic with unit cell parameter a=1.81, b=2.05, and c=0.75 nm [67]. It is one of the high silica rich zeolite minerals with SiO_2/Al_2O_3 ratio of about 10. The narrow range of SiO_2/Al_2O_3 ratio suggests that the aluminum atoms be distributed in an orderly manner in the lattice.

Its structure consists of chains of tetrahedral cross-linked by the sharing of oxygen atoms. Each tetrahedron belongs to one or more five member rings in the framework. The high thermal stability of mordenite is probably a result of the presence of the large number of five member rings that are energetically favored. The framework structure of mordenite was determined by **Meier et al. [68]**, it can be reconstructed either from a combination of 5-1 secondary building units (consisting of one single 5-ring with an attached tetrahedron) or from an assembly of single 6-rings sheets linked through single 4-rings. The aluminosilicate skeleton so generated exhibits a pore system consisting of parallel linear channels with 12 or 8 ring apertures. Four non-equivalent crystallographic types of tetrahedral can be distinguished: T_1 and T_2 in the 6-rings sheets and T_3 and T_4 located in the 4-rings as shown in figure 2-4 [69].

Zeolites are structurally classified according to the openness of their framework as measured by their water sorption capacity; mordenite has a water sorption capacity of 0.27-0.33 $cm^3$of H_2O/cm^3 of zeolite, and the pore structure of mordenite consisting of parallel tubes has an approximately elliptical cross section with a major and minor diameter of 6.95 and 5.81 A^o, respectively [68].

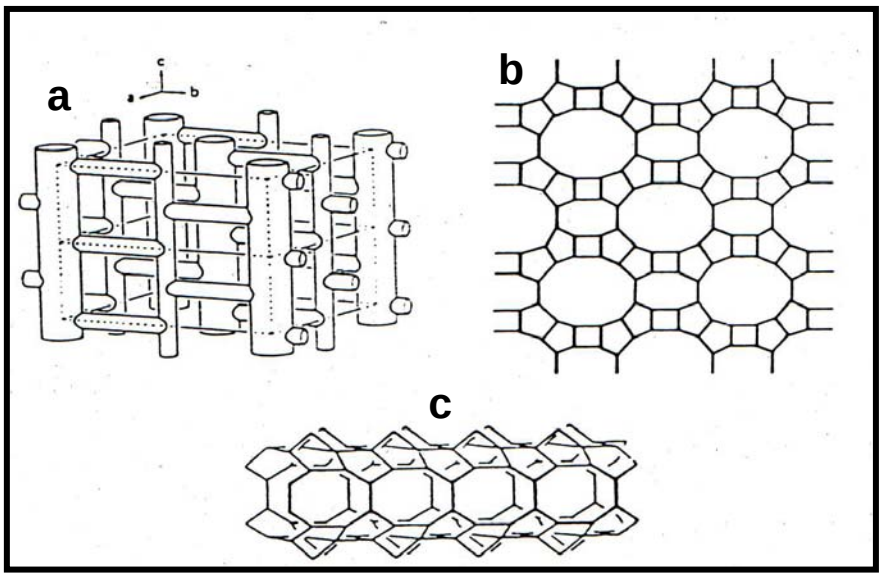

***Figure (2-4)*: (a)** Mordenite framework viewed along the C-axis, (b) the two-dimensional channels in Mordenite and (c) 6-ring sheet of tetrahedral of Mordenite viewed along the a-axis [69]

Mordenite can exist in two forms distinguishable by their absorption properties, "large port" and "small port" which cannot be distinguished by X–ray diffraction. The natural mineral form is of the small pore type because the pore system is partially blocked by amorphous impurities or cations resulting in an effective diameter of about $4A^{o}$. The synthesized form of mordenite exhibits the absorption properties characteristic of its structure and is capable of absorbing molecules such as benzene and cyclohexane [70].

Mordenite, a high silica zeolite, is increasingly being used as a molecular sieve in the adsorptive separation of gas-liquid mixtures involving acidic components. It also finds extensive application as a catalyst for various industrially important reactions such as hydrocracking, hydroisomerization, alkylation, reforming, and cracking [71].

The sodium form of mordenite readily adsorbs materials such as water, CO_2, SO_2, and other hydrocarbons of bigger molecular diameter are physically excluded from them. When the sodium is replaced by hydrogen,

the effective pore diameter of the mordenite molecular sieve increases and it adsorbs o-xylene, cumene etc. Furthermore, mordenite type zeolite molecular sieves are preferred for use in highly acidic or basic environments and at comparatively higher temperatures [72].

In general, mordenite is very acidic material and shows excellent stability and catalytic activity in many reactions. Research on mordenite has progressed slowly due to its one dimensional pore system, which is readily blocked by carbonaceous residues in hydrocarbon conversion systems. Therefore, the use of mordenite has been restricted to selected applications [73].

2.2.2.3 ZSM-5 Type

The discovery of ZSM-5 (Zeolite Socony Mobile-5) zeolite in 1972 by Mobile Oil Corporation, added a new class of shape selective catalysts with unique channel structure [74].

ZSM-5 is hydrophobic and organophilic and selectively adsorbs organic molecules in the presence of water, unlike aluminosilicate zeolites which are hydrophilic [75].

The framework of ZSM-5 contains a novel configuration of linked tetrahedral as shown in Fig. 2-5-A and consists of eight membered rings. These ZSM-5 units join through edge to form chain as shown in Fig. 2-5-B. The chain can be connected to form sheets and the linking of sheets leads to a three dimension framework structure. This channel system can be classified as one parallel, straight channel which runs parallel to the direction (010) and which has an elliptical cross section of 5.1 x 5.8 Å and second system of sinusoidal, or zigzag channels which in plane (100) perpendicular to the straight channels, and which has a nearly circular cross section of 5.4 x 5.6 Å as shown in Fig. 2-5-C [76].

Two types of channels, straight (elliptical) and sinusoidal (circular) are formed by the 10 membered rings of oxygen atoms. Channels have an effective diameter between small pore zeolite, e.g. type A, erionite zeolite, and large pore zeolite, e.g. faujasite, mordenite. ZSM-5 crystallizes in the idealized or the rhombic system with lattice constants a = 20.1, b = 19.9, and c = 13.4, as shown in Fig. 2-6 [76].

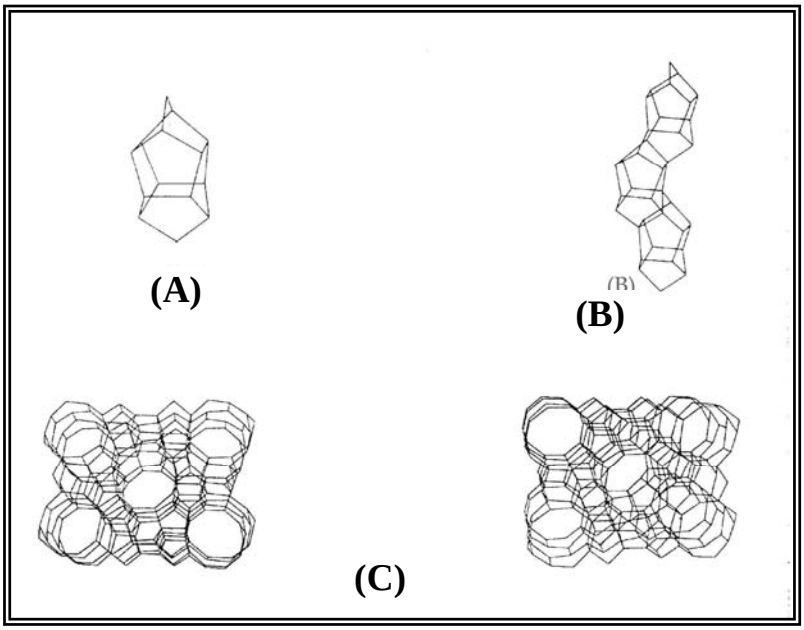

Figure 2-5: Skeletal Diagram of (010) Face of ZSM-5 [76]

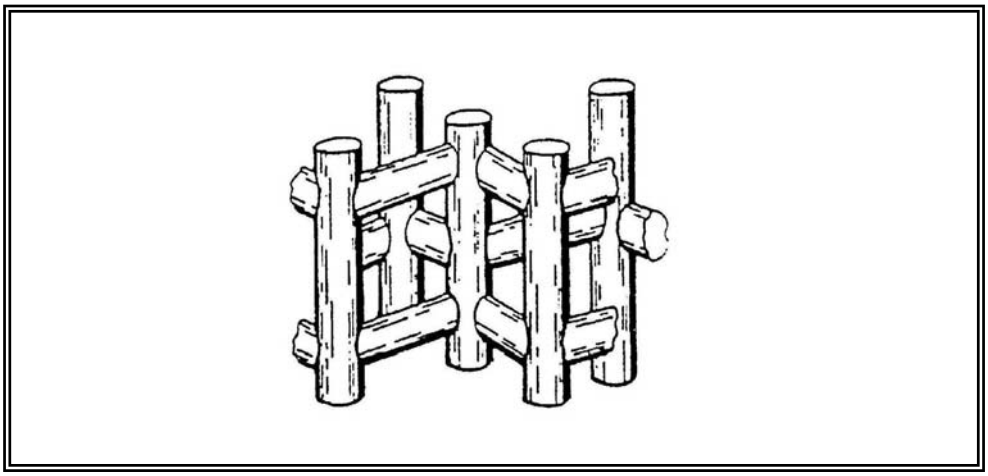

Figure 2-6: Channel Structure of ZSM-5 [76].

ZSM-5 composition can be identified in terms of mole ratio of oxides as follows:

$$0.9 \pm 0.2\ M_{2/n}O : Al_2O_3 : 5 - 100\ SiO_2 : Z\ H_2O$$

where M is selected from the group consisting of a mixture of a alkali metal cation, especially sodium, and tetra-alkyl-ammonium cation, the alkyl groups of which preferably contains 2-5 carbon atoms, n is the valence of cation, Z is from 0 - 40.

ZSM-5 zeolite catalysts have made possible the development of commercially significant petroleum and chemical processes. At room temperature ZSM-5 readily sorbs linear and monomethyl substituted paraffins as well as and rejects the larger molecules such as 2, 2-dimethyl butane and o-xylene [77].

Many properties of ZSM-5 vary with composition that is with its SiO_2/Al_2O_3 ratio, e.g. of such composition-dependent properties: ion exchange capacity, hydrophobicity, and catalytic activity. These properties vary linearly with aluminum content. Other properties, such as, X-ray pattern, pore size, and volume, framework structure are independent of SiO_2/Al_2O_3 ratio [78].

ZSM-5, as a catalyst, show a variety of unusual properties such as, distillate dewaxing, ethylbenzene synthesis, xylene isomerization, toluene disproportionation and conversion of methanol to MTBE [75].

2.3 Zeolite Applications

Zeolites also find industrial applications in many areas other than catalysis e.g., ion exchange, gas separation, drying of gases and detergent formulation [57]. In general, zeolites economy importance and there main applications are given in Table 2-4 [58].

Applications in separation and purification processes often use the ability of zeolites and other molecular sieves to exclude molecules too large to enter the pores and admit smaller ones. Similarly, shape-selective catalysis takes advantage of the ability of the pores to favor the admission of smaller reaction product molecules, or the restriction of the size of transition-state complexes inside the micropores of the zeolite [59].

As far as catalysis is concerned, zeolites are crystalline materials that share the following six properties that make them attractive as heterogeneous catalysts [60]:

1- Well –defined crystalline structure.

2- High internal surface areas (> 600 m^2/g).

3- Uniform pores with one or more discrete sizes.

4- Good thermal stability.

5- Ability to sorbs and concentrate hydrocarbons.

6- Highly acidic sites when ion is exchanged with protons.

***Table 2-4*:** Zeolite Applications [58]

***A - Zeolites as Catalysts*:**
In the hydroisomerization of n- to iso-alkanes for motor gasoline upgrading, (Pt - or Pd - containing H- zeolite).
In the catalytic cracking of crude oil distillate for fuel manufacture.
In the manufacture of fuels. Conversion of methanol into hydrocarbons.
In hydrocracking, conversion of crude oil fractions in petrol in the presence of hydrogen to lower fractions.
B - Zeolites as Adsorption Agents
Water removal from gases, air, and liquid circulates and in double- glazing.
Adsorption of carbon dioxide, hydrogen sulfide, and marcaptans from gases.
C - Zeolites for the Separation of Materials (Molecular Sieves):
Manufacture of oxygen – enriched air.
Separation of n- and iso- alkanes.
Separation of Xylol isomers.
D - Zeolites as Ion Exchangers:
Clinoptilolite used for the removal of ammonium from wastewater.
Zeolite A is used in detergents for the deposite of calcium and magnesium ions from the washing liquid.

2.4 Zeolite Modifications

2.4.1 Introduction

Modification of zeolites is more attractive at present time. High attention as a method of regulation of their catalytic and sieve properties as well as a way to design bifunctional catalysts. Most reactions conducted on zeolites are to enhance the acid catalytic sites [76].

The modification of a zeolite can affect a large variety of its structure, chemical and physical properties; so, different catalytic properties can be obtained- depending on the technique of preparation. Typical- modifications to zeolite catalysts include ion exchange and dealumination by extraction of alumina with acids [77, 78].

2.4.2 Ion Exchange

The cation exchange property of zeolite minerals was first observed 100 years ago. The case of cation exchange in zeolites and other minerals and their three-dimension framework structures, so they do not undergo any appreciable dimensional change with ion exchange, leading to an early interest in ion exchange materials for use as water softening agents [79].

Cation exchange in zeolite is accompanied by dramatic alteration of stability, selectivity and catalytic activity and other important physical properties. Most synthetic zeolites are crystallized in the monovalent alkali metal form and have little or no catalytic activity. For so called-acid catalyzed reactions in the alkanes isomerization process, the sodium form of the zeolite is inactive as a support for the palladium or platinum [80].

The rate and the degree of cation exchange depend on th following factors [77].

1- The nature of the cation species, its size, and charge.

2- The exchange conditions, temperature, concentration, time.

3- Any previous treatment of zeolite (thermal or chemical).

4- The locations of the cations in the zeolite structure

5- The structural properties of the zeolite and its silica to alumina molar ratio.

The capability of zeolites of exchanging the cation used in the synthesis (mainly sodium) with other cations is very important. The sodium forms in the zeolite can be replaced by different cations namely, mono valent cations such as K^+, Cs^+, Ag^+, NH_4^+; divalent cation such as Ca^{2+}, Sr^{2+}, Hg^{2+},Ba^{2+}, and trivalent or higher valence cations such as La^{3+},Ce^{3+}, $Th^{3+,}$ Ta^{4+} [81].

Depending on the zeolite type and the cations required, there are several techniques, which can be used, such as exchanging from the sodium to ammonium form, conversion to a divalent or trivalent cation form, especially rare earth salt, and exchanging with transition metal ion. Calcination or reduction must follow such conversion [82].

Gray and Cobb [77] studied the hydroisomerization and hydrocracking of normal pentane over various mordenite catalysts. They showed that the extent of sodium ion exchange possible followed the order NH_4^{1+} > Ba^{2+}> Sr^{2+}>Ca^{2+}>Mg^{2+}>La^{3+} and the maximum catalytic activities for H-MOR, Ca-MOR and La-MOR occurred at calcinations temperatures of 510, 525, and 400 ^oC receptively.

Chester [83] indicated, netutralization of the acid sites generated during the preparation of pt/NaY reduces both activity and aromatization selectivity for n-Hexane dehydrocyclization. Replacement of Na^+ with Li^+ or K^+ has only minor effects, but replacement with Ca^{++} or Mg^{++} increases acidic cracking.

Shanshool, et al. [84] Prepared different types of decationized and multi-valent ions (such as calcium, magnesium and aluminum) from the sodium form of three types of zeolites (Y, X, and Iraqi zeolite A). Raouf used multistage ion exchange technique at different conditions which gave samples with 40-97% exchanged sodium, by one to three stages of ion-exchange.

Montes et al. [85] found that the cracking of n-hexane on Na-H-mordenite increases slowly with increasing the percent of exchange of cation for Na^+, but after 90 % exchange, they found a sharp increase in activity. The same behavior was also observed in Na-H-Y when different degrees of Na^+ were exchanged.

2.5 Methods of Metal Precursor to Supports

Realization of the importance of catalyst preparation to the activity, selectivity and life of a catalyst has led to increasing interest in the scientific basis of different preparation methods [86].

The common supports for platinum catalyst are alumina, silica, silica-alumina, charcoal and zeolite. The metal is introduced to the support, usually from aqueous solution or suspension, by process such as impregnation, adsorption, co-precipitation and ion exchange followed by drying and calcination at suitable temperature and finally reduction with hydrogen. During calcination and reduction the degree of metal dispersion is maximized [87].

So that, the objectives of calcination are to obtain [88]:

a) A well-determined structure for the active agents or supports.

b) The parallel adjustment of the texture with respect to surface and pore volume

c) A good mechanical resistance if it does not already exist.

d) The creation of a generally macroporous texture through decomposition and volatilization of substances previously added to the solid at the moment of its shaping (binder).

e) Modifications of texture through sintering small crystals or particles will turn in to bigger ones.

However, there are many factors influence catalysts preparation, such as solution concentration, contact time, washing, temperature and method of reduction [89, 90].

2.6 Characterizations

2.6.1 Introduction

Characterization of the catalysts is an predominate step in catalyst study and at every stage of the catalyst development. Critical parameters are measured not only to check the effectiveness of each operation but also to provide specifications for future products. Characterization might be studied or controlled in terms of support properties, metal dispersion and location and surface morphology [23, 91].

The quality of any catalyst is determined by a number of factors, such as activity, selectivity for certain product, and stability. These parameters are themselves functions of pretreatment conditions of the catalyst preparation and reaction conditions. The interpretation of catalytic performance through the mechanism of catalytic action depends on a study of the intrinsic chemical and physical characteristics of the solid and recognition of correlations between some of these characteristics and catalytic performance [1, 88].

The main characteristic in the selecting the support are thermal and chemical stability, mechanical strength, total area**,** pore structure, and acidity. Other methods which are essential for characterization of the supported metal

catalysts are related to metal dispersion and location on the support. Table 2-5 offered the general physico-chemical properties of catalysts and methods of measuring them [93].

Table 2-5: The general properties and characterization of catalysts and methods of measuring them [1]

Properties	***Measurement Methods***
1-Composition of chemical elements	Standard chemical analysis X-ray fluorescence Emission spectrometry Atomic adsorption Flame spectrometry Neutronic activation
2. Nature and structure of the catalytic chemical species	X-ray diffraction Electron diffraction Nuclear magnetic resonance (NMR) Electron paramagnetic resonance (EPR) Infrared and Raman spectroscopy Visible and ultraviolet spectroscopy Magnetic methods Thermogravimetric analysis Differential thermal analysis Mösshauer spectroscopy
3.The texture of the catalyst: Texture of the support (porosity, specific surface, pore distribution) State of the dispersed active agents.	BET methods Porosimetry Chemisorption X-ray diffraction Electron microscopy Scanning electron microscopy Magnetic methods Chemical methods Electron microprobe analyzer
4. The quality of the active surface .	Chemisorption kinetics Flash desorption Heats of adsorption Color doping EPR, infrared spectroscopy
5. Electronic properties	EPR Conductivity, semi-conductivity Electron extraction work functions

2.6.2 Physical Adsorption for Surface Area measurements

In practice, the method most used for determining specific surface area is the BET method (Brunauer, Emmett and Teller) based on the physical adsorption of an inert gas at constant temperature, usually nitrogen at the temperature of liquid nitrogen. The principle of measurement consists in determining the point when a mono-molecular layer of gas covers the surface of the catalyst [94].

Namba et al [95] performed dealumination of NaZSM-5 zeolites by treatment with gaseous $SiCL_4$. Aluminum is eliminated as gaseous $AlCl_3$ and the zeolite structure is not destroyed as the BET surface area is not significantly affected by the $SiCl_4$ treatment.

Ciapetta [96] stated that the catalyst used in dehydrogenation of butane to butadiene have an activities that are directly proportional to the total surface area of the catalyst. He also stated that catalytic cracking of gas oil, conversion increases as the surface area of the catalyst increases.

Ghosh and Kydd [97] have observed that fluorination of alumina decreases its specific surface area. These decreases depend on the fluorine content and fluorination process. They showed that aluminum fluoride was formed during fluorination which has a lower surface area and this causes large decrease in surface area of the catalyst.

Ali [98] mentioned that in catalytic refining process such hydrodesulfurization and reforming, catalyst activity declines with on stream time due to coke deposit on the catalyst which causes surface area and pore volume reduction. The equilibrium coked catalyst in residue hydrodesulfurization had surface area only about one-third of the original fresh catalyst.

2.6.3 X-Ray Diffraction Crystallinity

X-ray diffraction used for the determination of zeolite crystallinity. The individual zeolites being crystalline solids, have characteristic X-ray diffraction patterns, which are used to identify the zeolite and provide an indication of its purity.

Scherzer [99] used X-ray diffraction to study the crystallinity of zeolite Y, which was dealuminated by combining acid leaching (HCl) and hydrothermal treatment. A series of dealuminated faujasite-type zeolites was obtained with SiO_2/Al_2O_2 ratio less than 100. The zeolites obtained by this procedure have good crystallinity and high thermal stability.

Halasz and co-workers [100] investigated the changes in the Y zeolite component of cracking catalysts during their active life. They investigated the SiO_2/Al_2O_2 ratio as function of temperature and duration of hydrothermal treatment and concluded that this ratio affects the product quality.

Tan et al. [101] prepared ZSM-5 zeolite which used as support for platinum in the hydrogen-deuterium reaction. X-ray diffraction was used to determine the crystal structure of the prepared zeolite, which indicated a good crystallinty. **Ward [102]** checked the stability of zeolite Y lattice by X-ray diffraction studies. These showed that up to 800°C only minor changes in X-ray pattern occurred, indicating little loss of lattice structure**.**

2.6.4 Thermal Analysis

The thermal stability is defined as the ability of a substance to maintain its properties as nearly unchanged as possible on heating. From a practical point of view, thermal stability need to be considered in terms of the environment to be imposed on the material and the functions it has to perform. The

thermobalance is a useful technique for studying the ability of a catalyst maintain its mass under a variety of conditions [103].

The thermal analysis technique of thermogravimetry (TGA) is used to determine changes in sample weight, which may result from chemical or physical transformations, as a function of temperature [104, 105].

Tolovski and co-workers [106] studied the effect of SiO_2/Al_2O_2 ratio on the thermal stability and phase transitions of Na and H forms of silica-rich mordenites which dealuminated by leaching with HCl. The data obtained by X-ray analysis, TGA, DTA, electron microscopy have shown the highest thermal stability for mordenite with SiO_2/Al_2O_2=18.

Shanshool and AL-Sammerrai [107] studied the evaluation and thermal stabilities of some platinum/alumina catalysts, which are commonly used in reforming processes. Data obtained from thermo-ana1ytica1 investigation in a differential scanning calorimeter and thermogravimetrically under atmospheres of N_2 and O_2 provided useful information on thermal stabilities properties of these catalysts which are usually subjected to elevated temperatures during reforming and conversion processes.

Bremer et al. [108] studied the thermal stabilities and properties of cation exchanged Y zeolites. They showed that, the thermal stability of modified zeolites depends not only on the SiO_2/Al_2O_2 molar ratio, but also on cation type and the degree of exchange. The differences in the thermal stabilities arise from specific interactions between the cation and zeolite framework.

Shanshool, et al. [84] studied by thermal gravimetric analysis and differential thermal analysis the thermal behavior of zeolite Y, X, and Iraqi zeolite type A. These zeolites were exchanged with ammonium and magnesium and fluorinated zeolites. They indicated that all zeolites are thermally stable in temperature range from 20° C to 1100 ^oC.

2.6.5 Infrared Spectroscopy

The infrared technique is one of the most widely used in surface chemistry of solids and catalysis to determiner the surface structure and acidity.

From amorphous silica only one OH stretching band, at approximately 3740cm^{-1}, is observed and it is assigned to the Si-OH group terminating polymer chains. In addition to this terminal Si-OH group, other bands are observed in zeolites 3650 and 3540 cm^{-1}, the number and frequency of vibration depending upon zeolite structure, pretreatment and composition [81].

The spectra can be grouped into two classes in zeolites

i) Those due to internal vibrations of tetrahedron which is the primary unit of structure and which are not sensitive to other variations.

ii) Vibrations which may be related to the linkages between tetrahedral.

Class (ii) vibrations are sensitive to the overall structure and joining of the individual tetrahedra in secondary structural units, as well their existence in the large pore openings [79].

Kustov and co-workers [109] studied IR spectroscopy of the lowis acid centers that are formed upon dehydroxylation of decationized zeolites type Y, ZSM-5, and mordenite. As a test for a protonic acid centers, they used molecular hydrogen, and showed that upon dehydroxylation, the zeolites are partially dealuminated. So that, three types of lewis acid centers are presences: tricoordinated lattice ions of silicon and aluminum and centers related to extra lattice aluminum. The ratio between these centers will depend on the type and composition of the zeolite and also on the treating temperature.

Bolton and Bujalski [110] concluded during cracking of hexane on (HY) zeolite, that the gradual deactivation of the Catalyst is accompanied by the progressive removal of OH groups. The reaction caused the removal of first, the 3640cm^{-1} band and subsequently the 3540cm^{-1} band. **Tsuneje et al. [111]** studied the migration of barium in to ZSM-5 zeolite, and measured by IR spectra of hydroxyl groups of' ZSM-5 and $BaCO_3$-mixed ZSM-5 before and after calcining. The spectrum of ZSM-5 was characterized by-well defined peak at 3650cm^{-1} assigned to an acidic bridged OH of Si(OH)Al, which is supposed to be an essential chemical formula of strong acid sites.

Tempere and Dela [112] studied some dicationized forms of A type zeolite using IR spectrum. They showed, by thermal treatment under vacuum between 220-350°C, NH_4A zeolite undergoes structural modifications associated with the appearance of IR band at 3710, 3670 and 3620cm^{-1}. These extensively decationized samples are reactive in catalyzing the isomerization of 1-butene in to cis-and trans-2-butene.

2.6.6 Scanning Electron Microscopy

Scanning electron microscopy is extremely powerful technique for obtaining information on the morphology and structural characteristics of catalysts. There are some advantages in this technique, which are: great depth of focus, the possibility of direct observation of external form of real objects, and the ability to switch over a wide range of magnification, so as to zoom down to fine detail on some part identified in position on the whole object [113]. This technique has been used to follow changes in particle structure and morphology of platinum catalyst as a result of treatments involving different atmospheres and temperatures. **Smith and co-workers [114]** examined by electron microscopy model catalysts consisting of platinum on alumina

support. It was found that, the particle size distributions and particle sintering depends on treatment temperature, atmosphere, and metal loading.

Tzou and Sachtler [115] studied the formation and growth mechanism of Pt particles in Y zeolites, using SEM, H_2 chemisorption and temperature programed methods. It was found that the initial calcination temperature Tc largely controls the type Pt particle. At low Tc (360°C) all Pt ions are located in the supercages and small Pt particles after reduction. At medium Tc (450°C) some Pt ions migrate to sodalite cages. At very high (550°C) large Pt aggregates are formed on the zeolite.

Baker et al. [116] observed a nucleation and growth of carbon deposits on nickel during the catalyzed decomposition of acetylene in dynamic experiments in the scanning electron microscopy for studying a catalyst poisoning and changes in catalytic, activity due to particle agglomeration.

Aiello et al. [117] studied the influence of various sodium salts on the crystlization of zeolite Nu-10 type in the presence of tetraethylenepentamine. Size and morphology of zeolite crystals were showed by SEM. They found that the addition of sodium chloride appears a limited influence on the length of zeolite crystals.

Giannetto and co-worker [118] studied the preparation of pentasil-type zeolites by using SEM. Three samples of zeolites were prepared, using tripropylamine sample (A), tetrapropylammonium bromide sample (B) and tetrabutylammonium bromide sample (C). They showed that the morphology of the zeolite crystal of samples (A) and (C) have crystallite structures constituted by regular parallelepipeds of about (4 μm) while that of sample (C) by spherical and spheroidal grains formed by aggregates of small needle-shaped crystallites (1 μm).

Chapter Three
Super Critical Fluids

3.1 Introduction

Impetus for the utilization of supercritical fluids (SCFs) as media for chemical reactions originates from their unique solvent properties which have been convincingly applied and are now well-established in separation technology [119, 120]. This technology takes advantage of the unusual properties of SCFs in the region near the critical point (Tr~ 1-1.1 and Pr~1-2)[121], where densities are a significant fraction of the liquid density. At these conditions, the fluid exists as a single phase, possessing favorable properties of both a liquid and a gas. The density is sufficient to afford substantial dissolution power, but the diffusivity of solutes in SCFs is higher than in liquids, and the viscosity is lower, enhancing mass transfer. Supercritical fluids also have unique properties in the sense that compounds which are insoluble in a fluid at ambient conditions can become soluble in the fluid at supercritical conditions [122], or conversely, compounds which are soluble at ambient conditions can become less soluble at supercritical conditions [123]. It has been recognized for some time that the same properties that are advantages for separation (extraction, chromatography, etc) offer even more opportunities in terms of tuning reactions [124, 125]. Conducting chemical reactions at supercritical conditions affords opportunities to tune the reaction environment (solvent properties), to eliminate transport limitations on reaction rates, and to integrate reaction and product separation.

3.2 Properties of SCFs

A fluid is termed supercritical when its temperature exceeds the critical temperature (Tc). At this point the two fluid phases, liquid and vapor, become indistinguishable. Figure 3-1 illustrates the different domains in a phase diagram. Many of the physical properties of a supercritical fluid are intermediate between those of a liquid and a gas [126]. This holds true for properties of fluids which are decisive for mass and heat transfer (diffusivity, viscosity, thermal conductivity, heat capacity). At the critical point the isothermal compressibility of any pure fluid.

$$k_T = \frac{1}{\rho}\left(\frac{\partial \rho}{\partial P}\right)_T \tag{3-1}$$

Where ρ is density, is infinite and is very large under conditions usually met in practical applications of SCFs. Table 3-1 provides a rough comparison of the magnitude of some of these properties for liquids, gases, and supercritical fluids in the near critical region.

Table 3-1: Comparison of Magnitudes of Physical Properties of Liquid, Gases and Supercritical Fluids in the near Critical Reagion [119].

Physical quantity	***Gas (ambient)***	***Supercritical fluid (T_C, P_C)***	***Liquid (ambient)***
Density (kg/m^3)	0.6-2	200-500	600-1600
Dynamic viscosity (mPa.s)	0.01-0.3	0.01-0.03	0.2-3
Kinematic viscosity (10^6 m^2/s)	5-500	0.02-0.1	0.1-5
Diffusion coefficient (10^6 m^2/s)	10-40	0.07	0.0002-0.002

As emerges from Table 3-1 diffusivity and viscosity of a supercritical fluid are more gaslike in the supercritical region, whereas

density is comparable to liquid. Consequently a reaction which is diffusion-controlled in the liquid phase can be enhanced by conducting it at supercritical conditions, due to higher diffusivity and elimination of gas/fluid and fluid/fluid interphases. The unique property of an SCF is its pressure-dependent density, which can be continuously adjusted from that of a vapor to that of a liquid. This is illustrated by the isotherms T_2 and T_3 in Figure 3-1. Note that particularly in the region about the critical point large changes in fluid density and related properties such as materials solubility[127, 128], are observed with small changes in pressure. These characteristics of SCFs provide the opportunity to engineer, the reaction environment by manipulating temperature and pressure. In many applications of SCFs dilute mixtures (solvent, reactant(s), product(s)) are important. All known applications of SCFs involve mixtures, where the solute is generally much less volatile and of higher molecular weight than the solvent. Such mixtures are termed attractive mixtures [129]. Dilute attractive mixtures are characterized by large and negative solute partial molar volumes and enthalpies near the solvent's critical point and over an appreciable range of supercritical pressures.

In addition to their promising physicochemical properties, SCFs may also provide very favorable qualities with regard to ecology and economy: the ideal SCF for industrial applications is nontoxic, environmentally benign, nonflammable and available in high purity at low cost; it is gaseous under ambient conditions and has moderate critical conditions to facilitate process design. It is very convenient that there are SCFs that meet all or most these criteria in addition to their very interesting "supercritical" features [130].

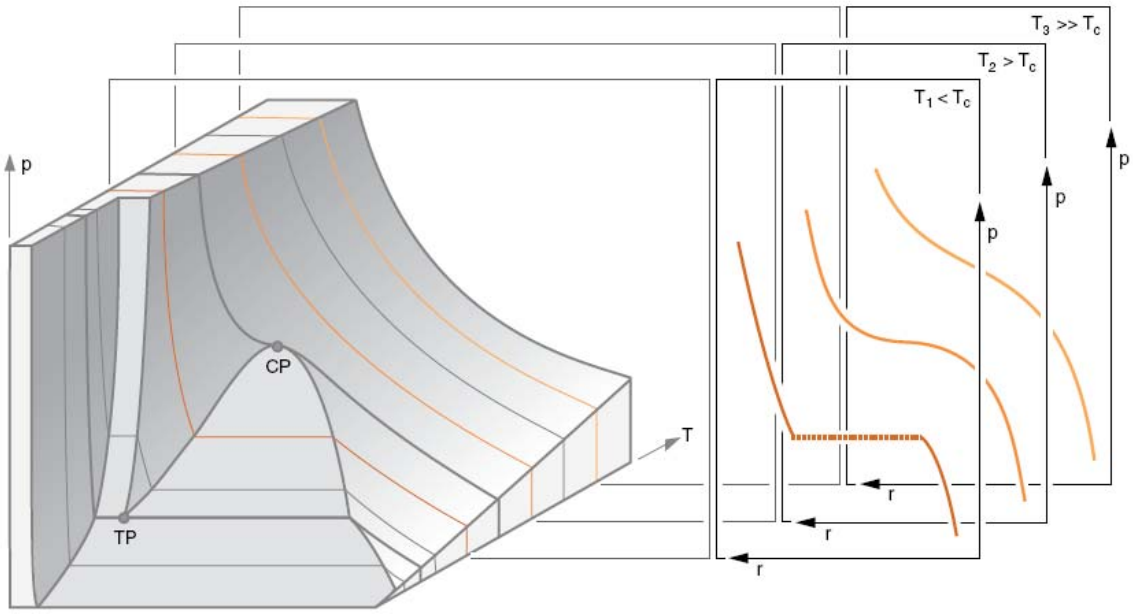

Figure 3-1: Effect of pressure on density at subcritical ($T_1<T_C$) and supercritical ($T_2>T_C$,$T_3>>T_C$) conditions, isotherm T_1 illustrates the discontinuity in the density vs. pressure function at subcritical conditions due to the phase change. Isotherms T_2 and T_3 typify the continuous from gas-like to liquid- like densities with increasing pressure. Note that the effect of pressure on density for a SCF, in terms of change in density with a small variation in pressure, is more pronounced near the critical point [127].

3.3 Local Enhancement of density

The high compressibility in SCFs and the gas-like behavior with regard to surface tension allows attractive forces to move molecules into energetically favorable locations. The resulting non-uniform spatial distribution of solvent and cosolvent molecules about solute molecules, as schematically illustrated in Figure 3-2, gives rise to interesting solvent effects not ordinarily found in liquid mixtures. This phenomenon, which has been termed local density enhancement [131], clustering [132], or molecular charisma [133], can affect the rates and selectivity's of chemical reactions through both physical and chemical mechanisms [134].

Local anisotropy phenomena also may occur at supercritical fluid-solid interfaces as a consequence of different interaction strength (adsorption enthalpy) of solute (reactant), solvent, and cosolvent, with the solid surface and clustering phenomena in the bulk phase near its critical point. Fundamental knowledge of these interactions is important to understand the mechanism of solid catalyzed reactions. Unfortunately, there appears to be no fundamental work dealing with this aspect crucial for understanding catalytic surface reactions in solute solvent (reactant solvent) systems.

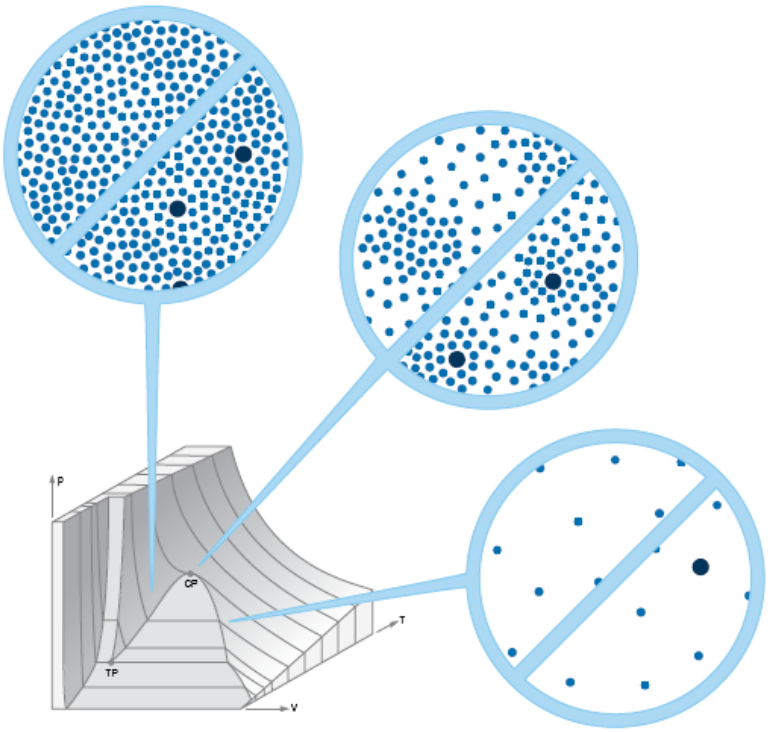

***Figure 3-2*:** Schematic illustration of spatial distribution of molecules for a liquid, supercritical and gaseous system. The upper left part of the circles show a pure fluid; the lower right part also involves a volatile solute. Whereas liquid and gaseous systems show a uniform spatial distribution of molecules, the large isothermal compressibility of SCFs allows attractive forces to move molecules into energetically favorable locations at low cost of free energy and thus leads to density fluctuations and clustering phenomena. The range of those density fluctuations is often comparable to the wavelength of visible light. Note that the extent of clusters for the SCF is shown in reduced scale for reasons of clearness [131].

3.4 Opportunities for Application of SCFs in Heterogeneous Catalysis

3.4.1 Elemination of Gasliquid Phase transfer Resistance

The most obvious opportunity for the use of SCFs in heterogeneous catalysis is the elimination of gas/liquid phase transfer resistances in reactions involving three phases under subcritical conditions (see Fig. 3-3). This together with lowered external fluid film diffusion resistances resulting from lower viscosity of SCFs may significantly accelerate the reaction, since diffusion of the gaseous reactant to the catalyst surface often represents the rate limiting step in three-phase reactions [135].

3.4.2 Enhancement of Reaction Rate

The effect of pressure on reaction rates in the supercritical region can be assigned to the kinetic pressure effect, enhanced mass- and heat transfer as well as occasional higher reactant solubilities. Since all these influences on the reaction rate strongly depend on pressure, temperature and the fluid itself, reaction rates can be tuned by corresponding adjustments in the reaction conditions. [135].

3.4.3 Control of Selectivity

The rate and equilibrium of a given reaction can be tuned in SCFs by altering pressure and temperature and/or adding a corresponding cosolvent. For a network of parallel or competing reactions, the different reactions may be influenced in a different way and degree by these alterations in the reaction conditions. Consequently such tuning of the reaction conditions may favor one of the reactions over the others, offering some potential to enhance the selectivity to the desired product. However, this method of controlling

selectivity is rather demanding, because the activation and reaction volumes of the various reactions as well as the influence of the components on the phase behavior of the system need to be known [135].

Further possibilities for the control of selectivity are linked with tuning of solute solvent interactions through change of local density, and clustering. Furthermore the use of cosolvents which through specific interactions (usually hydrogen bonds) with a transition state or a product can alter both rates [136] and product distributions [137].

3.4.4 Enhanced Mass and Heat Transfer

Fluids exhibit high diffusivities and very low kinematics viscosities in the supercritical region, resulting in high mass and heat transfer rates. Consequently, working in the supercritical region may accelerate mass transfer controlled liquid reactions and lead to better heat removal in highly exothermic gas-phase reactions, where careful temperature control is essential for selectivity and product stability. In either case, transport properties of SCFs are very favorable for conducting chemical reactions [135].

3.4.5 Catalyst Life Time and Regeneration

Supercritical fluids exhibit considerably higher solubility's for heavy organics which may act as catalyst blocking agents and thereby deactivate catalysts and promote coking. This deactivation may be suppressed by changing working conditions from gas phase to dense supercritical medium [138, 139]. Furthermore enhanced diffusivity can accelerate the transfer of poisons from the internal and external catalyst surface. Regeneration of catalysts deactivated by coking can be accomplished by extracting the carbonaceous deposits from the catalyst surface.

3.4.6 Facilitated Separation

The pressure tenability of the solubility of solutes near the critical point may allow the easy precipitation of the product, if it is less soluble than the reactants. This is used to advantage in the polymerization of ethylene, where polymers will fall out of the supercritical solution when they reach a certain molecular weight, corresponding to the solubility limit. In an equilibrium-limited reaction, this continuous removal of the product would enhance conversion. Conversely, a slight release in pressure after the reactor will precipitate unused reactant(s), allowing their re introduction into the feed (reactant recycling). The same strategy is also applicable for separating product(s) from solvent(s) [135].

3.4.7 Process Intensification

Higher reaction rates and facile product separation allow the construction of continuous reactors, considerably smaller than required for conventionally operated continuous reactors of equal performance [140]. This opportunity provides interesting advantages concerning process safety and space requirement of chemical plants [141, 142].

3.4.8 Catalyst Preparation

Supercritical fluids provide unique opportunities in the preparation of catalytic materials and supports. Proper use of SCFs allows to tailor and optimize the morphology of a catalyst.

In the preparation of aerogels [143] via the solution solgel route, supercritical drying is imperative. If the liquid (solvent) entrapped in the tenuous sol-gel network is directly evaporated, the structure of the gel is severely damaged due to the acting capillary pressure when the liquid recedes into the sol-gel body. This capillary stress can be circumvented either by transferring the entrapped solvent from the liquid to the supercritical state or by replacing the solvent typically with supercritical CO2, thus eliminating any liquid-vapor interface inside the sol-gel-product during solvent extraction. The sol-gel method combined with ensuing supercritical drying provides unique opportunities for the preparation of mixed oxides and metal/metal oxide catalysts [143, 144].

Another interesting opportunity for the use of SCFs in catalyst preparation is the possible control of the particle size and morphology of catalytic materials due to the highly adjustable properties in the supercritical region with small changes in temperature or pressure [135].

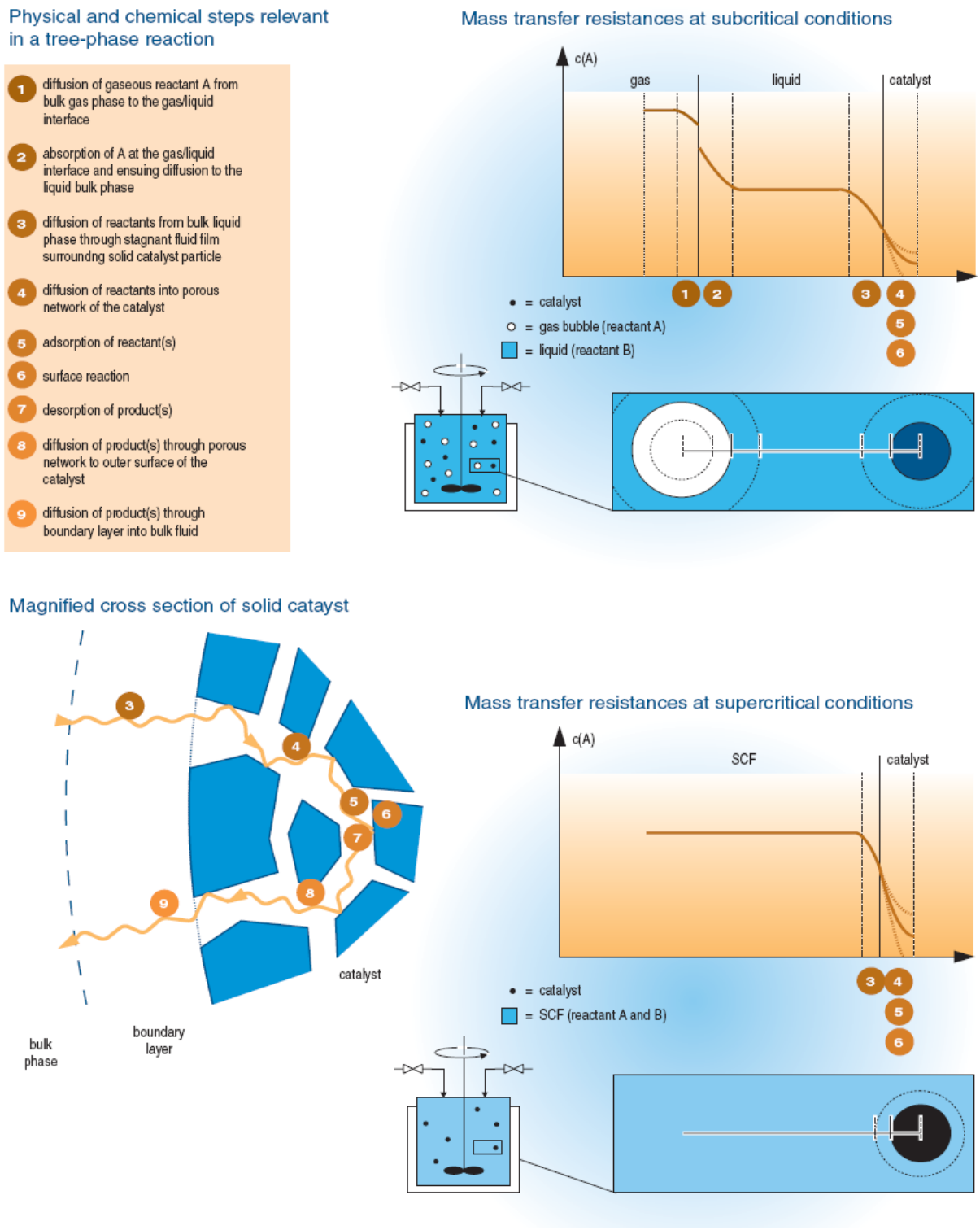

Figure 3-3: Sequence of physical and chemical steps occurring in a heterogeneously catalyzed gas/Solid reaction and comparison of such a reaction at subcritical and supercritical conditions [135].

3-5 Experimental Laboratory Techniques

Typically, reactions using SCFs are performed at elevated pressure (up to 400 bar) and temperatures up to 600˚C [135]. The use of such conditions is demanding on the experimental equipment used [130]. Furthermore, the potential danger of these conditions should never be ignored and full safety precautions should be made for all experiments.

For heterogeneous catalytic reactions two principle reactor types are suitable, batch reactors (autoclaves) or continuous flow reactors. The advantages and disadvantages of the two reactor types are well known in heterogeneous catalysis and also apply to the use of SCFs. For industrial applications, however, the extremely good mass and heat transfer properties of SCFs render tubular fixed-bed reactors ideal for heterogeneously catalyzed reactions, both on grounds of safety (low reactor volume) and costs. Fig. 3-4 schematically shows the reactor types most frequently used for heterogeneous catalytic reactions at supercritical conditions.

In contrast to homogeneous reactions, monitoring of heterogeneously catalyzed reaction systems is impaired by the presence of the suspended solid catalyst particles, necessitating a more complex design of the analytical system [135].

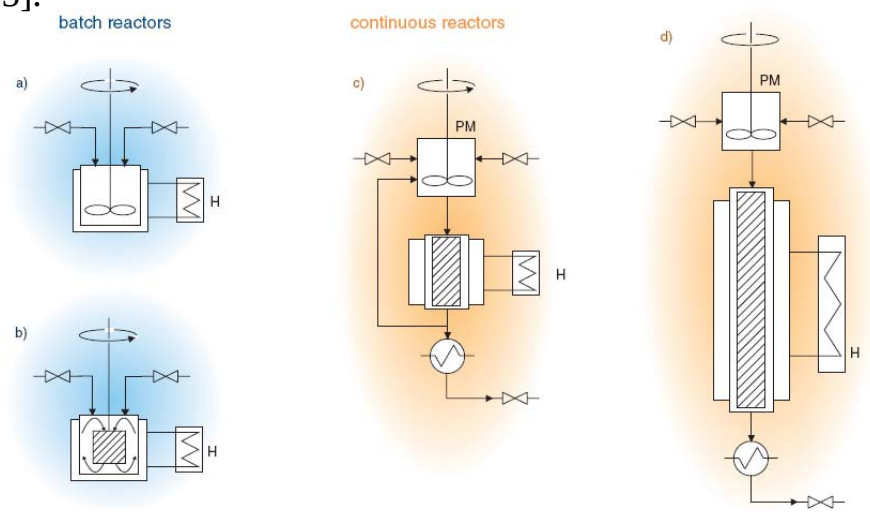

Figure 3-4: Reactor types suitable for the study of heterogeneously catalyzed reactions at supercritical conditions. a) stirred autoclave, b) stirred autoclave with internal recycle, c) differential (gradientless reactor, and d) continuous flow reactor. PM: premixing chamber; H: heat exchanger [135]

3.6 Loading of Metal on Catalyst

There are little publications concerning the loading of metals using supercritical fluids, which are used as catalysts.

The old methods that used for metal loading have some difficulties with the availability, perturbation of the support surface structure, non-uniform distribution of the particles and particles aggregate formation [145]. These methods are, wet impregnation method [146], synthetic insertion [147], co-assemble [148], and surface sol-gel modification method [149].

The potential use of supercritical carbon dioxide is an attractive much interest as a sustainable and "green" medium for material synthesis. As metioned before it can be handled easily because it is non toxic, non flammable and inexpensive. The unique properties of $scCO_2$ combine the advantages of liquid phase and gas phase process. The tunable density of $scCO_2$ can be controlled to match that of the liquid phase, which enables the medium to dissolve the metal precursor. On the other hand, low viscosity, high diffusivity and zero surface tension which are closer to the gas phase [146].

Y. Zhang et. all. [150], used supercritical carbon dioxide for platinum loading on a wide variety of substrates, including carbon aerogel, carbon black, silica aerogel, silica, γ-alumina and Nafion. The platinum compounds that he used was dimethyl(1, 5-cyclooctadiene)platinum(II) ($PtMe_2COD$) at 80 ^oC and 27.6 MPa. for 24 hr. The resulting dispersion was characterized with different devices and he showed that particle size ranging from 1.2 to 6.4 nm and a narrow particle size distribution.

Carel D. Saquing et. all. [151], also used $PtMe_2(COD)$ for platinum compounds, "using of this complex metal compounds depends on its solubility in supercritical carbon dioxide", also he used the same conditions

for metal loading but for Pt loading as high as 40% and the resulting precursor was reduced with nitrogen in different temperatures from 300K to 1000K. The particle size as small as 1 nm were achieved, he concluded that it is possible to control the dispersion of Pt particles through the strength of the interaction between metal precursor and the substrate, metal loading and reduction temperature.

A. Bayrakceken et. al. [152], concluded that, if we need loading of 10% Pt, this leads to dispersion as high as 70%, with particle size as small as 1 nm. Moreover, metal loading as high as 70% could be obtained without increasing the particle size dramatically, about ~3nm. He used the same Platinum compound as above, and used also $Pt(acac)_2$ with $Ru(acac)_3$ for bimetallic loading and 10% of methanol to increase the polarity of CO_2. The key difference between this work and those adopted by other workers are the type of precursor and the reduction method, because they used hydrogen for reduction of metal.

Y. Zhang et.all in 2005 [153], studied the effect of ruthenium dispersion using two complex compounds namely $Ru(acac)_3$ and $Ru(cod)(tmhd)_2$ on carbon aerogels. They found that very fast adsorption of metal and the adsorption isotherms follow the Langmuir model. The average size of Ru loading obtained under different conditions ranged from 1.7 to 3.8 nm once complete decomposition of the precursor has been achieved, and the mean size of ruthenium particles increased with increasing the reduction temperature.

Chapter Four
Experimental Work

4.1 Introduction

Preparation, characterization and catalytic activity of noble metal supported zeolites were investigated in the present work. Two types of zeolites, ZSM-5 and Mordinat, both in hydrogen form.

The experimental work was done in laboratories of ITMC/TC RWTH Technical University Aachen, Germany.

The hydrogen ions were replaced by two cationic forms, Strontium and Barium ions.

Supercritical fluid technology was used for loading of metal to zeolite at high pressures and suitable temperatures using carbon dioxide as supercritical fluid. Zeolite-supported platinum catalysts were prepared using Dimethyl (1, 5- cyclooctadiene) Platinum ($PtMe_2COD$) as a metalic complex organic compounds, which are soluble in $scCO_2$.

The resultant catalysts were tested for n-hexane hydroconversion reaction. In order to investigate this phenomenon, additional supported catalysts were prepared such as a bimetallic zeolite using Ruthenium and Zirconium complex compounds, in addition to Platinum complex. The Ru and Zr compounds that used are Ru(acetylacetonate)$_2$ and Zr(acetylacetonate)$_4$ in presence with Pt(acetylacetonate)$_2$ all these noble- metal compounds are soluble in $scCO_2$.

Characterization of the catalysts were studied with FTIR, Thermogravometric Analysis (TGA), Surface Area Measurement, Transmission Electron Microscopy (TEM), X-ray diffraction (XRD) and Inductivity Coupled Plasma Spectroscopy (ICP-MS).

Catalytic activity studies were carried out using fixed bed reactor for hydroconversion of n-hexane. The product gas was separated and analyzed online by gaschromatography. While liquid product was analyzed batch wise in another gaschromatography.

4.2 Chemicals

n-Hexane supplied from Fisher Scientific International company was used as raw material for isomerization activity tests, with purity of 99.8% and density 0.659 g/cm^3.

Two types of zeolite, H-ZSM-5 with Si/Al ratio 90 and H-Mordenite with Si/Al ratio 40 were purchased from Sued-Chemie company, Germany in palletized form (1.5mm d*2-3mm L). Other chemicals and metal compounds used are listed in Table 4-1:

Table 4-1: List of Chemical Compounds, Purity and its Supplier

Compounds	***Purity%***	***Supplier***
Strontium Chloride	99	Fluka
Barium Chloride	99	Fluka
Sodium Hydroxide	99.2	Fluka
Siliver Nitrate	1N/L	Fluka
Dimethyl (1,5- cyclooctadlene) PlatinumII	99	Strem Chemical
Platinum acetylacetonate	99	Strem Chemical
Ruthenium acetylacetonate	99	Strem Chemical
Zirconium acetylacetonate	99	Strem Chemical
Methanol	99.8	ALDRICH
Hydrogen	99.9	ITMC Lab. line
Nitrogen	99.99	ITMC Lab. line
Chloroplatinic acid hexahydrate	99% with 38-40% Pt	Strem Chemical
Argon	99	BASF
Carbon Dioxide	99	BASF

4.3 Catalyst Modifications

4.3.1 Apparatus

The H-form of ZSM-5 and Mordenite zeolite were modified by exchanging H^+ cation with Barium and Strontium cations.

The apparatus for ion exchange were shown in figure 4-1 which consists of the following parts:

1- Hot Plate Magnetic stirrer manufactured by IKA Labortechnik in Germany.

2- Motor Stirrer, multi speed manufactured by IKA-Werk fitted directly to the round bottom flask with glass road and impeller to prevent cracking of zeolite pallets.

3- Digital pH meter manufactured by HANNA with temperature thermocouple placed inside the flask in touch with solution, to get constant temperature.

4- Digital Thermocouple manufactured by Greisinger Electronic inserted inside the flask to read the temperature of the solution.

5- Round Bottom Flask with five necks.

6- Condenser.

7- NaOH container.

8- Controller connected with magnetic stirrer to keep constant temperature of oil bath.

9- Bath of silicon oil

Figure 4-1b: The apparatus of ion exchange using Bach Wise

4.3.2 Procedure

The Hydrogen form of zeolite types H-ZSM-5 and H-MOR were used as support for all catalysts. The hydrogen ion was exchanged by Barium or Strontium cation.

The operating procedure for ion exchange was carried out using a series of hot batch wise treatment as shown in figure 4-1. Thus 50 g of each zeolites were slurred in an aqueous solution of barium chloride (3N). Thus, 183.21 g of $BaCl_2.2H_2O$ in 500 ml distilled water with stirring for 2hr and 50 ^oC. In case of strontium chloride, 199.96 g of $SrCl_2.6H_2O$ was used in 500 ml distilled water for each batch. This procedure was repeated two times with fresh solution in order to get good ion exchange. The pH of the solution was held constant at about 7.2 for all samples. The exchanged zeolites had been filtered off and washed many times with deionized water to be free of chlorine ions, dried at 110 ^oC over night and calcinaed in a furnace at temperature 450 ^oC for temperature ramp 1^oC per minute, then the samples was held at this temperature for 4 hr.

4.4 Metal loading

4.4.1 Loading of Metals by Supercritical Carbon Dioxide

4.4.1.1 Apparatus

The experiments were done using two different types of autoclaves, the first one for applying a wide range of pressure (150-300 bar), temperature (40-100 ^{o}C) and time (12- 48 hr) for platinum dispersion and with different percent of loading. This autoclave was manufactured in mechanical workshop RWTH Aachen with 10 ml volume, maximum pressure 400 bar and maximum temperature 120 ^{o}C. The autoclave was designed from stainless steel and was fitted with two sapphire windows (Luftsite PN 400), thermocouple inserted inside the autoclave and digital manometer for accurate pressure reading.

Schematic diagram of the setup and photo pictures for detailed process used for metal dispersion, small and larger autoclaves are given in Figs 4-2, 4-3 and 4-4 respectively.

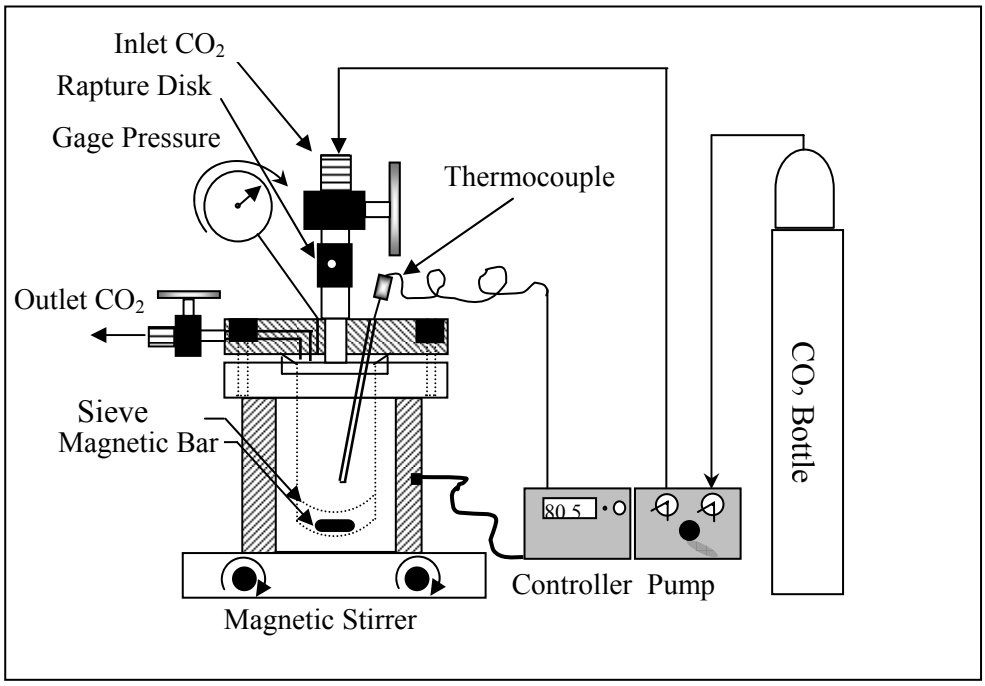

Figure 4-2: Schematic diagram for metal loading setup

Figure 4-3: Photo picture for metal loading setup, 1- Body of autoclave, 2-digital manometer, 3- thermocouple, 4- magnetic stirrer

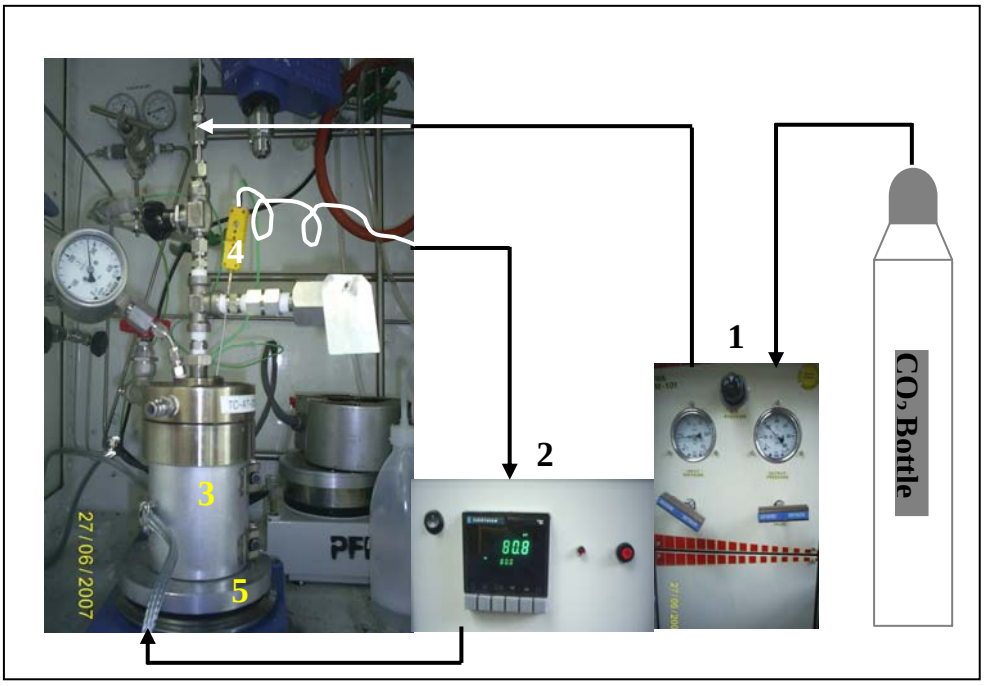

Figure 4-4: Photo picture for metal loading setup, 1- HPLC pump, 2- Controller, 3- heater shell, 4- thermocouple, 5- magnetic stirrer

The other type of autoclave with 100 ml capacity vessel was designed and manufactured in mechanical work shop in RWTH Aachen (Max. P= 350bar and Max. T=350°C) and made of stainless steel. It was fitted with K-type thermocouple assembly (Greisinger Electronic), a pressure transducer (WIKA type up to 400 bar), a vent line, a rupture disk assembly (Brilon, Max. P=312 bar and Max. T=80 °C), and sieve to separate solid pellets from magnetic stirrer as shown in Fig. 4-5 below.

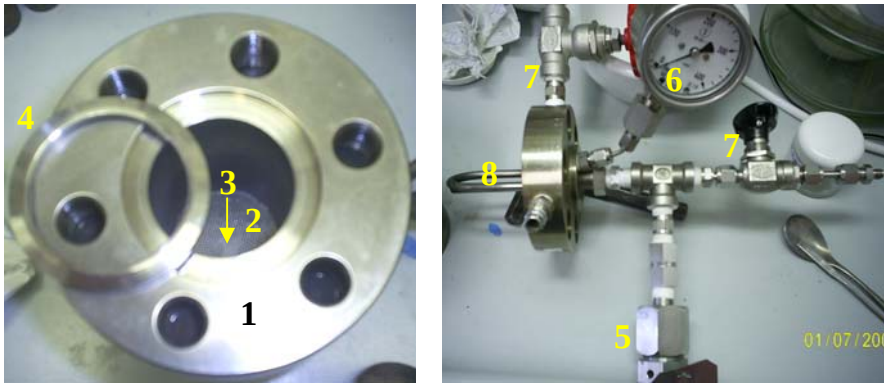

Figure 4-5: Photo picture for Autoclave parts, 1- body of autoclave, 2- sieve, 3- magnetic bar, 4- ring for closing, 5- rapture disk, 6- gage pressure, 7- inlet and outlet vents, 8- hole of thermocouple to the center of autoclave

4.4.1.2 Loading of Noble Metals

Dimethyl (1, 5-cyclooctadiene) Platinum(II) ($PtMe_2COD$) was used, due to its solubility in supercritical carbon dioxide. For each run, a certain amount of organometallic precursor $PtMe_2COD$, and a certain amount of substrate were placed into the vessel; for loading of 0.3 wt% of Pt on zeolite, 8 g zeolite and 41 mg of $PtMe_2COD$ were introduced to the autoclave under Argon.

The vessel was sealed and filled with a certain amount of CO_2 gas to a pressure of 80 bar then heated to a temperature of 80 °C by a heater shell

(JEKA 100w) and controlled with very sensitive controller (error ± 0.5 ^{o}C). After the temperature inside the autoclave reach 80 ^{o}C, the autoclave was pressurized with CO_2 to 275 bar using high syringe pump (HPLC NBA, PW-101) and kept at these conditions for 24 hr. During this process, all precursor added to the vessel was dissolved in $scCO_2$ or adsorbed into the zeolite support.

The Vessel was then depressurized slowly (5 bar/min) through a restrictor into the atmosphere. After the vessel had cooled, the precursor/ substrate composite were removed. The amount of precursor adsorbed was determined by the weight change of the substrate using analytical balance (Sartorius CP 324 S) accurate to ± 0.1 mg. and with ICP-MS device to see the error between measurements.

The substrate was dried under vacuum at room temperature for 15 minute and then placed in the reactor tube as shown in figure 4-11. The impregnated organometallic precursor was reduced thermally at 400 ^{o}C in presence of hydrogen and nitrogen flow mixture in a 50:50 volumetric ratio at 100 ml/min flow rate and kept at these conditions for 6 hr.

In addition to the single metal loading above, the bi and trimetal loading were tested. The platinum and ruthenium compounds used here should be have the same solubility in $scCO_2$, therefore Platinum (II) (acetylacetonate) and Ruthenium (III)(acetylacetonate) were used for platinum- ruthenium dispersion respectively.

The apparatus shown in figures 4-2, and 4-4 were used. Therefore for the loading process 0.3 wt% of platinum and ruthenium precursor were prepared for all zeolite samples. Thus 8 g of zeolite catalyst with 48.4 mg $Pt(acac)_2$, 94 mg $Ru(acac)_3$ and 10% methanol were filled into the autoclave under argon. Methanol was used to increase the polarity of CO_2 because the $Pt(acac)_2$ and $Ru(acac)_3$ compounds have low solubility in $scCO_2$. The

autoclave was then sealed good and pressurized with CO_2 to a suitable pressure and heated up to a temperature 80 ^oC then the autoclave was also pressurized to a pressure 275 bar and kept with stirring for 24 hr.

After the time was done the autoclave was depressurized slowly and carefully at 5 bar/min, until atmospheric pressure. The autoclave was in cooled in water or ice to the ambient temperature; then the autoclave was opened and toke the zeolite sample to the reduction step. The same apparatus shown in figure 4-11 was used for metal reduction with equal volum of hydrogen and nitrogen flow mixture.

The other bimetal catalyst, Platinum (II)(acetylacetonate) and Zirconium(IV) acetylacetonate were used for Pt-Zr dispersion over all the zeolite samples.

The apparatus shown in Fig. 4-5 was used for dispersion using the same procedure used in last section, where 48.4 mg of $Pt(acac)_2$ and 128.29mg of $Zr(acac)_4$ was add to 8 gram of zeolite samples under argon (Zirconium compounds was very sensitive to air)with 10 % of methanol and the autoclave was sealed and heated to 80 ^oC after pressurizing to 80 bar. When the autoclave was reaching the equilibrium at 80^oC and known pressure, the CO_2 was pumped to 275 bar and kept at these conditions for 24 hr.

The autoclave was depressurized and cooled to ambient temperature. The zeolite samples were collected and hydrogenated. The catalyst samples were stored in desiccators, for characterization and activity test.

In case of trimetal loading, the same procedure was used with addition of the three organic components, in form of Platinum, Ruthenium and Zirconium acetylacetonate with the same percent of dispersion of three metals (0.3 wt% for each).

4.4.2 Loading of Platinum by Impregnation

Two types of zeolites were used namely HZSM-5 and HMOR as support for platinum, to produce 0.3 wt % of Platinum on the supports by impregnation. Were, 125 mg of H_2PtCl_6 and 8 g of each zeolitie. The zeolite sample was put in a conical flask with 20ml distilled water followed by addition of H_2PtCl_6. Since, the Hexachloro Platinic acid is easy soluble in water producing a yellow to orange solution. The closed flask content then mixed mechanically by stirrer as shown in figure 4-1 to prevent cracking of zeolite pallets. The samples were kept at room temperature for 24 hr. It was observed that after about five hour of mixing, the color of solution was disappeared, indicating that the most quantity of platinum complex was impregnated.

The loaded zeolite sample was filtered off and washed carefully with distilled water and then dried in an oven for 24 hr at 110 ^{o}C. The calcinations of catalyst samples was carried out in the reactor, shown in figure 4-11 at a temperature of 260 ^{o}C for 3 hr under dry air flow of 100 ml/min. The reduction of catalyst samples were also done in the reactor immediately after the calcinations by hydrogen at 350 ^{o}C for about 3.30 hr.

4.5 Characterization

4.5.1 FTIR spectra

This device was used to observe Brounested and Lewis acid of original and prepared catalysts by FTIR device type Shematzo. Those 2 mg of catalyst sample was mixed with 300 mg KBr as indicator in a crucible, and mixed carefully. A suitable quantity of the mixture was taken and pressed to 50 bar by a press under vacuum. At a retention time of about 1.62 min. The acidity of the catalysts was estimated from the peak of spectra.

4.5.2 Inductively Coupled Plasma Spectroscopy (ICP-MS)

Platinum, Ruthenium and Zirconium content in all zeolite samples was analyzed in the Institute of Fuel Chemistry and Physicochemical Process Engineering (IBC RWTH- Aachen) using ICP/OES, Perkin-Elmer, Optima 3300XL with AS 91 auto sampler.

Samples of supported metal were digested with 5ml of HNO_3 and 5ml HCl in a hot black tube at 95 ^oC for 4hr. After being kept at room temperature overnight, 2 ml of HF was added to the sample solutions and digested at 95 ^oC for 2 hr. The resulting solution was analyzed to get the metal content of zeolite samples.

4.5.3 X-Ray Diffraction

XRD spectra of the sample were recorded using Siemens D5000 with a moving phase sensitive detector using Cu-Kα radiation (44 kV, 35 mA) over 2θ range of 5°-55° with step 1° at residence time 5s at each point. The data have been smoothed to increase the signal-to-noise ratio. X-Ray diffraction patterns are used to identify the catalyst crystallinity and its purity.

4.5.4 Surface Area Measurements

The pore size distribution and BET surface area were determined by adsorption and desorption data of liquid nitrogen acquired on a Micromeritics ASAP 2000 apparatus. The samples were evacuated under vacuum of $5*10^{-3}$ torr at 350 °C for 15 h. Specific total surface areas were calculated using equation 4-1, whereas specific total pore volumes were evaluated from N_2 uptake at a relative pressure (P/Po) of N2 equal to 0.99. Figure (4-6) show the device that used for surface area measurements.

Figure 4-6: Micrometric ASAP 2000 device that used to measure BET surface area

$$\text{BET surface area } (m^2/g) = \frac{Digital\ Reading\ (see\ the\ picture)}{Sample\ Weight\ (\approx 50mg)} \qquad (4\text{-}1)$$

4.5.5 Thermo Gravimetric Analysis (TGA)

Thermogravimetric analyses were carried out with a Shemazu TGA-50 apparatus. Curves were recorded simultaneously by placing the sample (<20mg) in an aluminum crucible and heating up at a rate of 10 ^{o}C/min under flowing of nitrogen (50 mL/min). The maximum temperature that reached was 580 ^{o}C and no holding time with all samples. Then the device was cool down to 50 ^{o}C to start new analyses.

4.5.6 Transmission Electron Microscopy (TEM)

The materials, which are intended to be investigated by transmission electron microscopy (TEM), have to be prepared in such a way that electron transparent areas are present in the final TEM sample.

The first step in the TEM preparation is a mechanical treatment of the materials, like sawing, ultra-sonic grinding or punching to give the sample a circular form with a diameter of approximately 3 mm. To prepare cross-sectional specimens of, e.g., grain boundaries or heterophase interfaces, the formation of sandwiches of the film/substrate material is a common procedure, which is later on glued inside a ceramic or metallic tube. After sawing the tube in small disks, each disk is mechanically grinded to a thickness of 100 mm to 150 mm. In most cases, the grinding is followed by a dimpling process until the specimen thickness reaches 10 mm to 50 mm in the thinnest regions. The final thinning procedure is performed by Ar+ ion bombardment with ion energies in the range of 100eV to 6 keV. Within this preparation step the ion-thinning parameters, such as the glancing angle or the ion-beam energy are varied to obtain an optimal TEM specimen quality. An in-situ observation of the ion-thinning is possible since all ion-thinning machines are equipped with light microscopes and video cameras.

In Figures 4-7 and 4-8, a part of the TEM specimen preparation laboratory is presented. Figure 4-7 shows a typical working desk for the mechanical preparation and thinning of the samples. Figure 4-8 shows TEM device that used for analysis the specimen.

Apart from the already described methods, pure metals are prepared by electro-polishing. In special cases, also Tripod grinding and cutting using an ultra-microatome is used for some materials.

Readily prepared TEM samples can finally carbon coated to increase its electrical conductivity. An additional plasma cleaning process can remove eventually occurring impurities on the specimen surfaces.

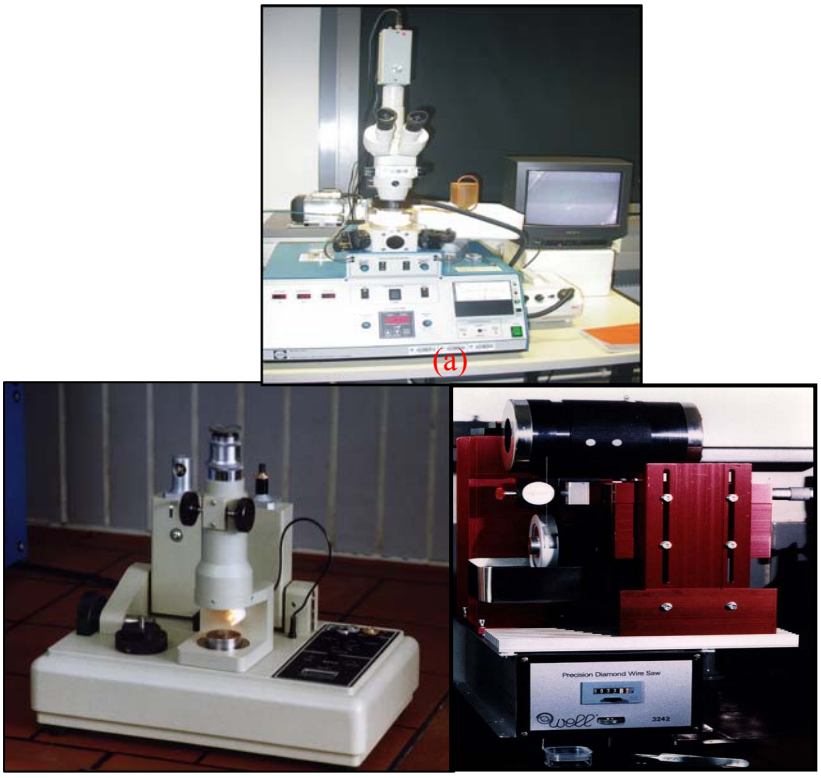

(b) (c)

Figure 4-7: A typical working desk for the mechanical preparation and thinning of the TEM samples. Each desk is equipped with a (a) grinding/polishing machine, (b) a dimpler, (c) and a wire-saw.

Figure 4-8: TEM Device in Max Plank Institute.

4.6 Catalytic Hydroconversion of n-Hexane

4.6.1 Apparatus

Catalytic activity studies were carried out in a conventional continuous-flow, micro-catalytic reactor unit manufactured by mechanical workshop in ITMC, RWTH Aachen/Germany

The equipment consists of four identical unit scales. The first one is for feed section (gas and liquid), the second one is for reactor section, the third one is for control section, and the last one for separation of gas liquid mixture and connecting to GC online. Schematic and photo picture for the flow diagram was shown in figures 4-9 and 4-10 respectively.

4.6.1.1 Liquid Feed System

The first unit has a feed pump system manufactured by (Gilson HPLC) Germany. The pump has a capacity of 1 liter and can deliver feed at rates from 0.1 to 12 ml/min, The pump is digitally controlled with a precision of three decimal digits. The capacity of feed tank is 2 liter and connected directly to the pump. The liquid was heated up to a temperature 150 ^{o}C before entering the reactor using high efficiency microstructure evaporator.

4.6.1.2 Gas Feed System

Gases feed to the unit includes hydrogen in one line and both nitrogen and air in the other line. The hydrogen gas was delivered using mass flow controller, types (Brooks 5850 E) and it was controlled by voltage. The calibration was done using water bubbling as shown in appendix C-1.

The air line was passed to the drier (Schumacher 7180) contains molecular sieve (4A) and oil removal filter because the air was pressurized at 7 bar and some oil droplet was coming with flow. The using of air only for

regeneration of Zeolite after each experiment to insure the carbon deposit was removed form zeolite.

The nitrogen line was connected with air line using three way valve and the flow of nitrogen and air was controlled by mass flow controller, type of (El-Flow). The calibration of the controller was made with different voltage as shown in appendix C-2. Nitrogen was used as diluents for reduction of metal compounds with hydrogen.

One way valves were connected to hydrogen and nitrogen air lines, while the two lines were connected together to the three way connection.

4.6.1.3 Reactor

A Stainless steel reactor was designed in mechanical workshop in RWTH Aachen/Germany as show in figure 4-11. The dimensions were 20 mm inside diameter, 50 mm outside diameter and 15 cm length, which was charged for each experiment with 7 gram of Zeolite samples and placed in the middle zone. While the upper and lower zones were filled with glass balls and separated from catalyst zone, bottom and top by sieves. The reactor feed was rotated around the outer surface from up to down and connected from the bottom of reactor and the exit stream was taken from the top of the reactor.

The reactor was placed inside an oven, which was constructed with an air ventilation also in the mechanical workshop of RWTH Aachen. The temperature was controlled automatically with PI controller using two thermocouples, one inserted to the center of Zeolite and the other one was placed on the center of the oven.

4.6.1.4 Separations of Gas and Liquid

The gases exit from the reactor was cooled by a heat exchanger with cooled water and separated using separator as shown in figure 4-12. The gas stream connected online to GC and the liquid sample was separated and injected in to other GC.

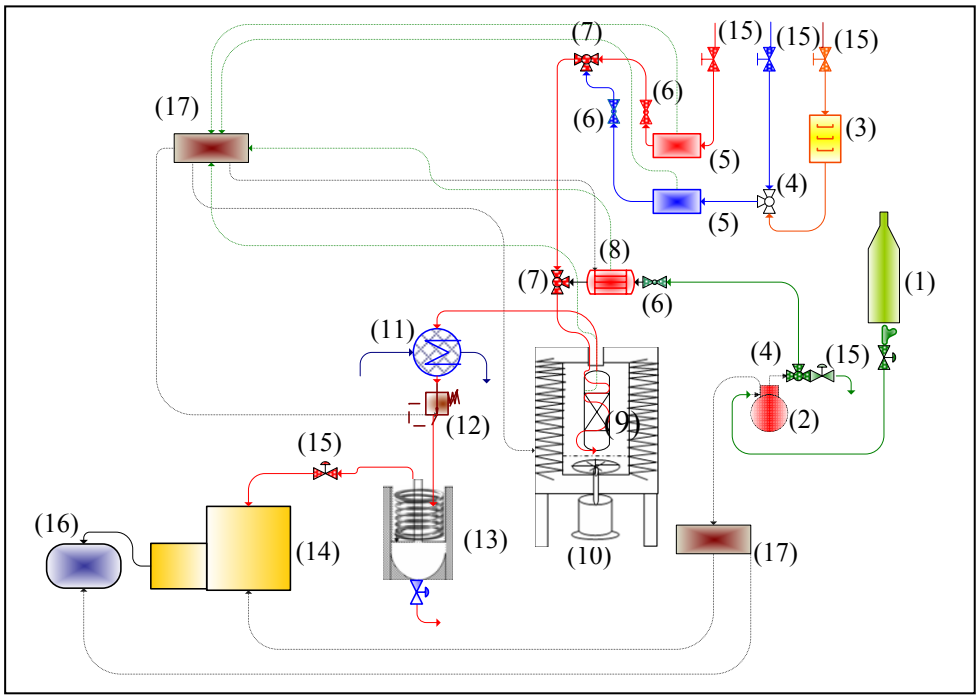

Figure 4-9: Schematic Flow Diagram of Catalytic Experimant Rig, **1**- feeding tank, **2**- dosing pump, **3**- dryer, **4**- three way valve, **5**- mass flow meter for gases, **6**- one way valve, **7**-three way connection, **8**- evaporator, **9**- reactor, **10**-oven, **11**- heat exchanger, **12**- back pressure regulator, **13**- separator, **14**- GC, **15**- manual valve, **16**-PC, **17**- Control and power supply box

Figure 4-10: Photo Picture for the Flow Diagram of Catalytic Study Rig**,**

Figure 4-11: Picture for the reactor that used for reduction and reaction, 1- Hollow beam represents inner diameter of reactor, 2- upper sieve, 3- feed from down, 4- upper cover for reactor, 5- hole for thermocouple to the center, 6- down sieve.

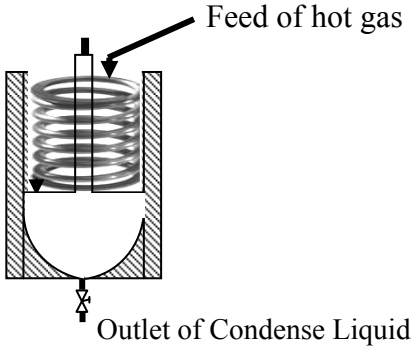

Figure 4-12: Gas-Liquid Separator Designed to separate gas from liquid using iso-propanol dry ice

4.6.2 Operating Procedure

The Pt over cataions H, Ba, Sr for the two zeolite sample (ZSM-5 and MOR) loaded by super critical CO_2 were tested for isomerization of n-hexane and compared with platinum loaded by impregnation method. Furthermore Pt-Ru, Pt-Zr, and Pt-Ru-Zr over the same cations were used for the test of reaction.

The samples were originally extruded (1.5mmd*2-3mmL), filled into the reactor and activated for one hour at temperature 350 C^o just before runs in flow of hydrogen, 100ml/min. 8g of each catalyst type was used in each run.

n-Hexane feed was charged to the pump from a reservoir. Feed was pumped under pressure and passed through one way valve to microstructure evaporator to heated up of n-hexane to about 150 C^o. Outlet from the evaporator was mixed with hydrogen before the reactor inlet then passed through the catalyst bed from the bottom of reactor.

The product was cooled with heat exchanger using cooled water (inlet temperature 5 C^o) then passed through digital back pressure regulator manufactured by (Burkert 8624-2) maximum operating pressure 28 bar. The product gas entered to the separator that filled with iso-propanol dry ice (T = -98 C^o). The uncondensed gas product connected online to GC, while condensed liquid samples was collected and analyzed with another GC.

A pre test period of about half hour was used before each run to adjust the feed rate and temperature to the desired values. The catalyst samples have been tested under a wide range of operating temperature 250-325 C^o. Hydrogen total pressure was kept constant at 5 bar, liquid hour space velocity (LHSV) equal to 1.76 hr^{-1} and hydrogen to hydrocarbon ratio (H_2/HC) were taken 3, 6 and 9 moles.

4.6.3 Gas Chromatographic Analysis

Two gas chromatography was used to analyze the product mixture, one for gas phase that is enable to condense it and the second one was used for liquid product. For gas mixture, GC was programmed to make analysis for 20 min retention time because no peak was appeared after this time and also the GC should be cooled before starting the next experiment. Siemens model with 50 m length capillary column (PLOT-FS-AL 203/KCL 2004) was used and connected to a computer to carry out the analysis on-line. The temperature was programmed at 60-200 ^{o}C in a rate of 8°C/min and 1 bar nitrogen pressure with auto sample injection of 100 μl on each run with hydrogen as carrier gas. GC was calibrated using known compounds mixture as shown in table 4-2.

The second GC (Siemens) was programmed to start at a temperature of 30 ^{o}C and still 15 min at this temperature then increased to 250 ^{o}C at a rate of 5°C/min. A column of 50m length, packed with PONA was used to separate the products. The volume of sample injected to the GC was 0.14 μl, Helium gas was used as carrier gas. The GC was connected to computer and printer to evaluate the area percent directly. Before making injection, GC was calibrated using reference components that appeared in the product and mixed together, and then the retention time was recorded as shown in table 4-2

Table 4-2: Retention Time for the Reactant and Product Components

Gas Phase Product		***Liquid Phase Product***	
Component	***Retentions Time(min)***	***Components***	***Retentions Time (min)***
Methane	2.905	Propane	4.59
Ethane	3.283	Iso-Butane	4.77
Ethylene	4.862	n-Butane	4.94
Propane	7.765	2MB	5.54
Iso-Butane	9.437	n-Pentane	5.88
Butene	10.008	2.2DMB	6.49
n-Butane	13.233	2.3DMB	7.23
Iso-Pentane	15.637	2MP	7.35
n-Pentane	16.252	3MP	7.81
2.2DMB	20.081	n-Hexane	8.42
2.3DMB	20.112	Methylecyclopentane	9.66
2MP	20.315	Benzene	11.33
3MP	20.499	Toluene	11.60
n-Hexane	21.33	Ethyl benzene	19.18
Methylecyclopentane	27.245	M+P-Xylene	23.77
Benzene	32.75	O-Xylene	24.70

4.6.4 Method of Calculations

Conversion and selectivity were calculated after each run using defined equations in the literature. The percentage conversion of n-hexane to products was calculated by equation 4-2.

$$Conversion = (1 - \frac{N_A}{N_{A_o}}) * 100 \qquad (4\text{-}2)$$

where N_{Ao}=initial moles of reactant A

N_A=moles of component A at time t

The selectivity of reaction product defined as the moles of the product i divided by all moles of the product as in equation 4-3

$$\%\,Selectivity = \frac{N_i}{N_{Ao} - N_A} * 100 \qquad (4\text{-}3)$$

where N_i=total moles of the product i.

The percentage yields either 2- and 3-methylpentane and cracked fraction was calculated by using equation 4-4.

$$\%Yield = \frac{N_i}{N_{Ao}} * 100 \tag{4-4}$$

The experimental and calculated data were presented in appendix A

4.6.5 Reaction Rate and Activation Energy

Rate of reaction was calculated using design equation of tubular reactor as in equation 4-5.

$$w = F_{A_o} . \int_0^x \frac{dx}{-r_A} \tag{4-5}$$

where w=weight of catalyst filled in the reactor

F_{Ao}=flow rate of inlet n-hexane to the reactor

$-r_A$=rate of reaction

Rearranging equation 4-5 to get $-r_A$

$$-r_A = \frac{F_{A_o} . X}{w} \tag{4-6}$$

The integration of reaction rate was taken as on increment because they calculated in small rang of time. Equation 4-6 used for calculation of reaction rate in units mole/g.hr. The rate of overall and isomerization reaction were presented in appendix B.

Arrhenius equation gives the reaction rate k as function of temperature as in equation 4-7

$$k = A . \exp\left(\frac{-E_a}{R.T}\right) \tag{4-7}$$

where k=rate constant of reaction at temperature T

A=Pre-exponential Factor

E_a=activation energy

R=gas constant

T=temperature of reaction

The rate of reaction is directly proportional with surface coverage θ_n [154].

$$-r_A = k_o \theta_n \tag{4-8}$$

Substitute equation 4-8 in equation 4-7 gives.

$$-r_A = A.\exp\left(\frac{-E}{R.T}\right) \tag{4-9}$$

This equation used if small temperature range and nearly higher pressure was applied to the reaction. Equation 4-9 can be simplified by taking ln to each side.

$$Ln\,(-r_A) = Ln\,(A) - \left(\frac{E}{R.T}\right) \tag{4-10}$$

Activation energy was calculated by plotting $Ln\,(-r_A)$ vs. 1/T, the slop indicate E/R and Intercept give $Ln\,(A)$.

Chapter Five
Results and Discussion

5.1 Introduction

Two types of zeolite were chosen as a support for noble metals, Platinum, Ruthenium and Zirconium to prepare bifunctional catalysts for isomerization of n-Hexane. The H-form of these zeolites, namly ZSM-5 and Mordenite were modified by Ion-exchange technique with Barium Chloride and Strontium Chloride solutions to produce the corresponding Barium- and Strontium cationic forms. The purpose of such modification was to get improved surface characterization and suitable activity towards isomerization reactions of low hydrocarbons.

The metal loading on the zeolite support was carried out by the conventional impregnation method and by the relatively new technique using supercritical carbon dioxide as solvent. It is trusty to study the different parameters affecting the metal loading in $scCO_2$, such as temperature, pressure, co-solvent and time of treatment.

Characterization of the catalyst is a predominate step in the catalytic studies, to investigate the relevant aspects of catalyst structure, surface properties and activity. Characterization of metal loaded zeolite catalysts were studied by FTIR spectra, X-Ray diffraction, Surface Area Measurement, Thermogravimetric Analysis (TGA) and Transmission Electron Microscopy (TEM).

The catalytic behavior of the prepared metal/Zeolite catalysts were studied in the isomerization of n-Hexane. It was worthy to investigate the

performance of metal loading by $scCO_2$ technique on the activity of zeolite supported catalysts toward the isomerization reactions. Therefore, search was done for different conditions, such as bimetallic loading, temperature and H_2/HC ratio on the selectivity of branched Hexane isomers for upgrading octane number of motor gasoline.

5.2 Back Ion Exchange of Hydrogen Cation

Extrudes of the initial Zeolites HZSM-5 and HMOR (1.5mmd, 2*3mmL) were exchanged with two different cations, strontium and barium. The exchange technique used in this study was batch wise treatment under constant temperature with stirring for two hours. The procedure was repeated with fresh solution to ensure high ion-exchange.

Figures 5-1 and 5-2 show the effect of treatment time on the cation content in the Zeolite. The percent of cation exchanging with time was measured by ICP.MS. The hydrogen content should be measured by MAS-NMR, but the samples were very sensitive to air, therefore they gave unaccurate value of hydrogen content, and required additional time to prepare the samples under argon.

As it is expected, the percent of exchange for strontium and barium was increased with treatment time. This increase was not linear and differs according to the cation solution used and the type of Zeolite. After 3 hr of treatment the exchange still increased slowly and very small for barium but decreased for strontium, indicating that Sr cation arrived a constant level in which there is no further increase in the replacement of cations. This indicates that the ion exchange reaction reached an equilibrium in which there is no further replacement occurs, because of the diffusion difficulties of the exchanged ions into the Zeolite structure.

The highest percentage of ion-exchange was achieved with strontium and for the large-pored zeolite Mordenite as shown in table 5-1. While, the degradation was shown after 3hr of treatment for both types. The replacement of hydrogen ion by Barium was noticeable less than in case of strontium ion for both zeolite types. Here, also, the ion-exchange for Mordenite is higher than for ZSM-5 zeolite, as shown in table 5-1.

The pH of the solution was decreased directly when the cation solution was added to the Zeolite samples as show in figures 5-3 and 5-4, due to formation of HCl by ion exchange. Therefore 0.1 N solution of NaOH was added, when the pH of the solution decreases. The addition of NaOH enhances the ability of ion exchange that appears when strontium cation was exchanged with hydrogen. While for barium the addition of NaOH was done after 1/2 hr, because the lowering of pH was very slow and depending on the formation of HCl.

Table 5-1: Amount of Ion Exchange for Barium and Strontium

Sample	Time (hr)	mg/g zeolite
BaZSM-5	1	0.02
	2	0.05
	3	0.12
	4	0.19
BaMOR	1	0.02
	2	0.9
	3	1.12
	4	1.23
SrZSM-5	1	2.45
	2	3.99
	3	4.06
	4	3.01
SrMOR	1	5.21
	2	22.96
	3	24.21
	4	16.24

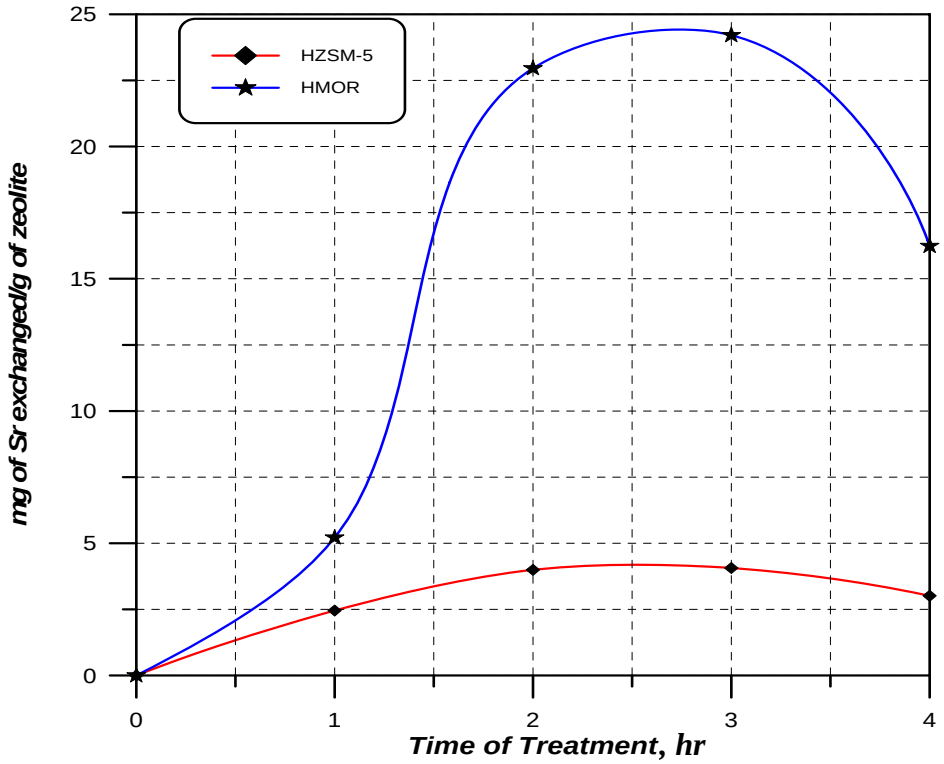

Figure 5-1: Ability of Exchange Between Strontium and Hydrogen for Two Different Zeolite

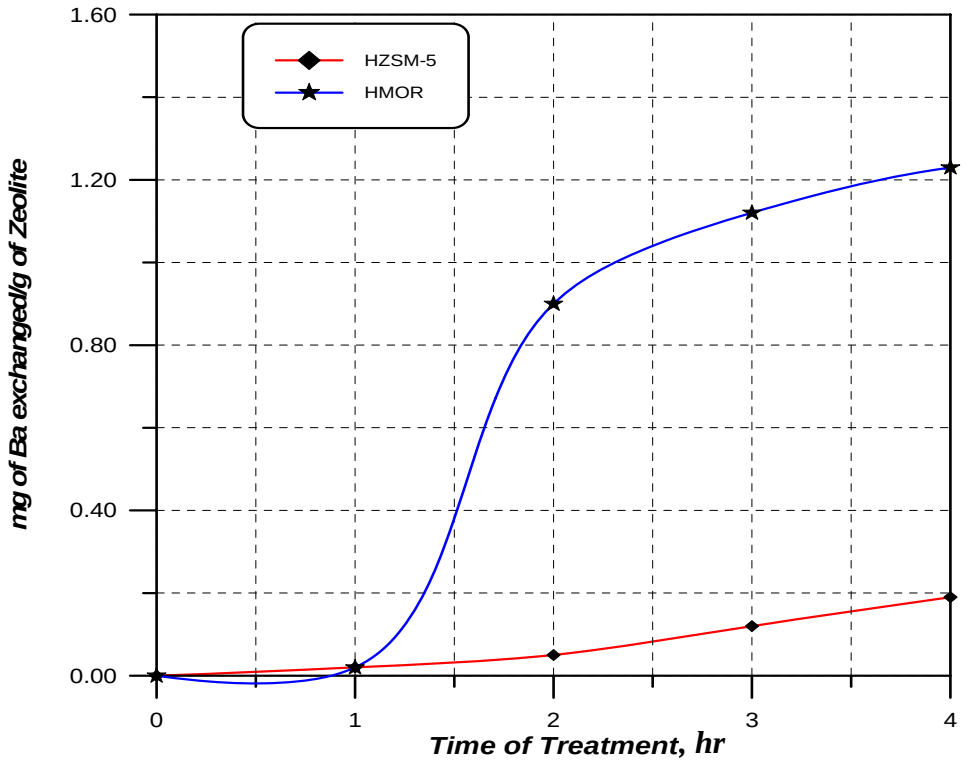

Figure 5-2: Ability of Exchange Between Barium and Hydrogen for Two Different Zeolite

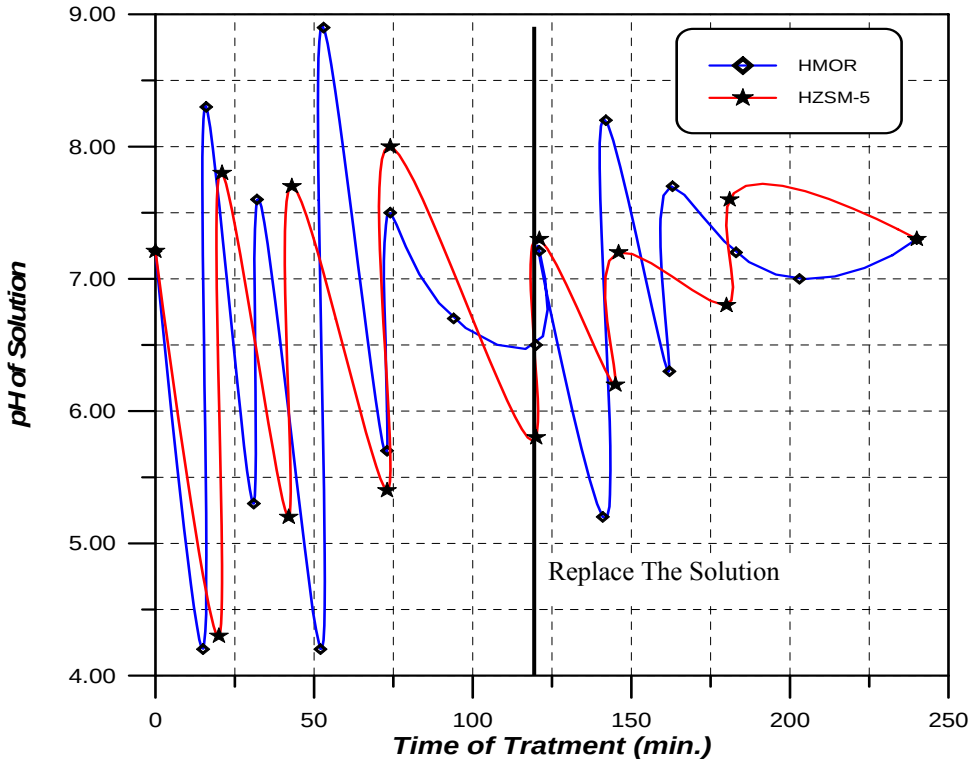

Figure 5-3: Fluctuation of pH of the Solution for Strontium Exchange with Hydrogen, at addition of NaOH to the Solution

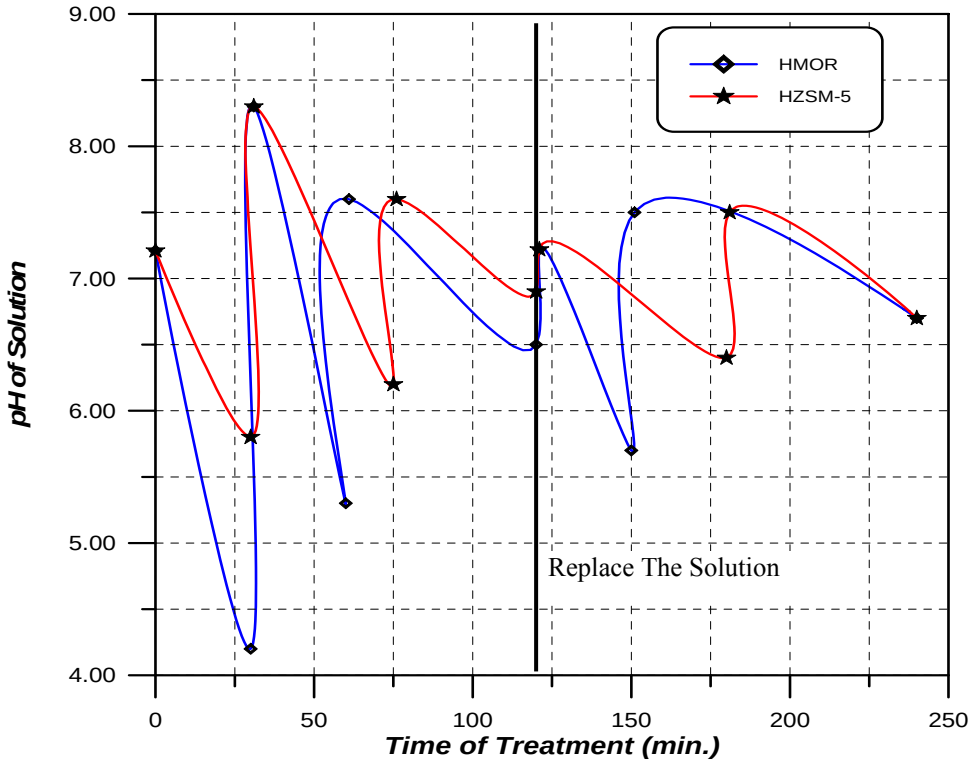

Figure 5-4: Fluctuation of pH of the Solution for Barium Exchange with Hydrogen at addition of NaOH to the Solution

5.3 Loading of Metal

The loading of platinum particles in supercritical fluid CO_2 was different from than by impregnation concerning percent of loading and surface area. The impregnation resulted in about complete loading of platinum compound. While, the loading in $scCO_2$ gave higher surface area. Further more, using supercritical CO_2 for metal dispersion on the zeolite gave nano particle that loaded on surface of inside diameter of pore volume, also it's depended on pressure of supercritical fluid.

Table 5-2 shows the percent of loading and efficiency at different conditions, where the efficiency of loading was calculated from equation 5-1.

$$Efficiency\ (\%) = \frac{wt.of\ \ Metal\ add - wt.of\ \ Metal\ \text{detected by}\ ICP}{wt.of\ \ Metal\ add} * 100 \qquad (5\text{-}1)$$

Table 5-2: Percent of Loading of platinum and its Efficiency for Different conditions for HMOR Zeolite type

T (^{o} C)	P (bar)	t (hr)	wt% of Loading	Efficiency %
40	153	24	1.01	66.14
40	194	24	1.039	68.85
40	250	24	1.205	64.37
40	300	24	0.715	81.81
60	150	24	0.656	44.84
60	200	24	0.853	53.21
60	250	24	1.061	72.63
60	300	24	2.789	73.41
80	169	24	1.632	63.68
80	200	24	1.127	67.65
80	250	24	1.186	89.11
80	300	24	0.596	66.08
80	280	12	0.932	45.65
80	280	48	0.921	91.03
100	169	24	0.912	64.78
100	200	24	0.621	69.97
100	250	24	0.754	86.87
100	300	24	0.961	87.38

The data in table 5-2 show, that the loading efficiency was affected by pressure rather than by temperature as shown in figure 5-5, the platinum was loaded over zeolite Mordinet only because this zeolite have one dimensional structure in addition to the cost of platinum component. The amount of platinum component that used in each experiment had low different in weight with the other one due to the difficulties of weighting 8 mg of platinum component under Argon in addition to use of very accurate balance. Thus the data in table 5-2 shows fluctuations of loading percent in some experiments like T=60 ^{o}C and P=300 bar but this effect was neglected if the comparison was made by efficiency percent.

Figure 5-5 shows the effect of temperature and pressure on percent of loading, where the increasing of loading was affected by increasing of pressure due to the increasing of polarity and density of CO_2 which increases the ability for dissolving of platinum component and to penetrate through the pours. The effect of pressure was clearly shown after p=250 bar on the dark regions, where the percent of loading was reached to 87.38% at pressure 300 bar.

The increasing of temperature has a little effect on the loading until temperature 100 C. It could conclude that higher temperature is necessary to get high loading values of platinum on zeolite support together with the increasing of pressure to suitable value.

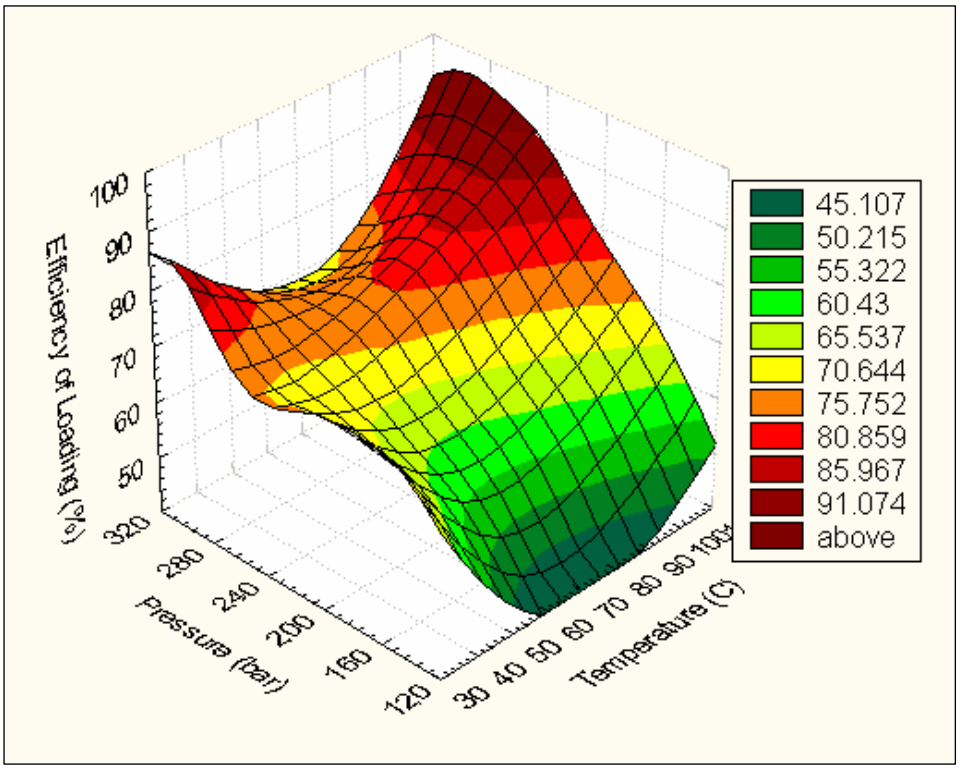

Figure 5-5: Effect of Temperature and Pressure on the Efficiency of Loading in $scCO_2$ for Zeolite Pt/HMOR

Figure 5-6 shows the effect of time on percent of loading at temperature, 80 ^{o}C and pressure 280 bar. These conditions were considered as standard for all experiments, since such conditions were used for working in super critical carbon dioxide [150, 151, 152, 153]. The efficiency is increased with time due to the fact that the loading is depended on contact time of precursor with Zeolite. Figure 5-6 shows clearly that at 24 hr contact time resulted in high loading efficiency. By further increase of time, until 48 hr gave in low more loading values. Therefore, contact time 24hr is considered to be suitable for the process.

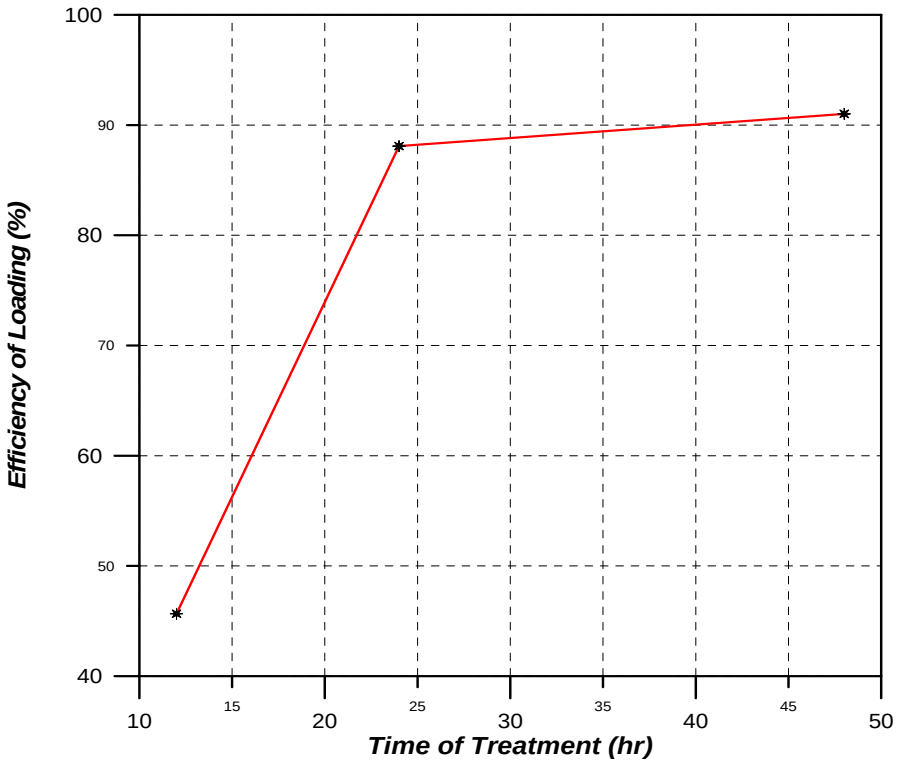

Figure 5-6: Efficiency of Loading of Platinum Over HMOR vs. Treatment Time for T=80 ^{o}C and P=280 bar

Table 5-3 summarized the results of loading of platinum on ZSM-5 and Mordenite zeolites containing of different cations. The percentage platinum loaded on all these types was 0.210 to 0.268 by weight, which are in the range of platinum required for isomerization reactions of paraffinic hydrocarbons. This observation leads to the fact, that the zeolite types (ZSM-5 and MOR) as well as the cation types (H^{+}, Ba^{++} and Sr^{++}) have no consedrable effect on Platinum loading on these supports in super critical carbon dioxide.

Table 5-3: Platinum Contents in Zeolite Samples Loaded by Supercritical Carbon Dioxide Method

Zeolite Sample	**mg Pt/g zeolite**	**wt % Pt**
Pt/HZSM-5	2.68	0.268
Pt/HMOR	2.64	0.263
Pt/BaZSM-5	2.78	0.277
Pt/ BaMOR	2.17	0.216
Pt/SrZSM-5	2.11	0.210
Pt/SrMOR	2.22	0.222

The loading of bimetals, Platinum-Ruthenium, Platinum-Zirconium and trimetals, Platinum-Ruthenium-Zirconium on all considered zeolite types was carried out also in supercritical carbon dioxide at similar conditions as in platinum alone. While the results are illustrated in tables 5-4, 5-5 and 5-6 respectively.

The weight percent loading of the bimetals and trimetals on the different zeolite types used is seemed to be similar. The little variation in these values could be attributed to the variation of weight of original noble-metal used. Further more, the weight percent of noble metal supported on both ZSM-5 and Mordenite of different cations are within the range of commercial catalysts of these types

Table5-4: Platinum and Ruthenium Contents in Zeolite Samples Loaded by Supercritical Carbon Dioxide Method (mg metal/gram zeolite) at T=80 ^{o}C and P=280 bar

Zeolite Sample	**mg Pt/g**	**mg Ru/g**	**wt % Pt**	**wt % Ru**
Pt-Ru/HZSM-5	2.36	2.92	0.235	0.291
Pt-Ru /HMOR	2.53	2.79	0.252	0.278
Pt-Ru /BaZSM-5	2.23	2.68	0.222	0.268
Pt-Ru / BaMOR	2.51	2.77	0.250	0.276
Pt-Ru /SrZSM-5	2.57	2.55	0.257	0.254
Pt-Ru /SrMOR	2.61	2.82	0.260	0.281

Table 5-5: Platinum and Zirconium Contents in Zeolite Samples Loaded by Supercritical Carbon Dioxide Method (mg metal/gram zeolite) at T=80 ^{o}C and P=280 bar

Zeolite Sample	**mg Pt/g**	**mg Zr/g**	**wt % Pt**	**wt % Zr**
Pt-Zr/HZSM-5	2.48	2.11	0.247	0.220
Pt-Zr /HMOR	2.87	2.59	0.286	0.258
Pt-Zr /BaZSM-5	1.99	2.89	0.201	0.288
Pt-Zr / BaMOR	2.07	3.02	0.206	0.301
Pt-Zr /SrZSM-5	2.59	2.95	0.258	0.294
Pt-Zr /SrMOR	2.61	2.98	0.260	0.297

Table 5-6: Platinum, Ruthenium and Zirconium Contents in Zeolite Samples Loaded by Supercritical Carbon Dioxide Method (mg metal/gram zeolite) at T=80 ^{o}C and P=280 bar

Zeolite Sample	**mg Pt/g**	**mg Ru/g**	**mg Zr/g**	**wt % Pt**	**wt % Ru**	**wt % Zr**
PtRuZr/HZSM-5	2.21	2.34	2.09	0.221	0.233	0.209
PtRuZr /HMOR	2.60	2.80	2.94	0.259	0.279	0.293
PtRuZr /BaZSM-5	2.17	2.76	2.77	0.217	0.275	0.276
PtRuZr / BaMOR	2.24	2.54	2.91	0.223	0.253	0.290
PtRuZr /SrZSM-5	2.78	2.89	2.85	0.277	0.288	0.288
PtRuZr /SrMOR	2.81	2.92	2.94	0.280	0.291	0.293

The results for bimetals and trimetals loading show better Platinum content in comparison with Ruthenium and Zirconium, because the platinum component (Pt-acetylactonate) used for these experiments was different from that used for Pt alone (Pt-dimethyl, 1, 5-cyclooctadiene) and has low solubility in supercritical carbon dioxide.

5.4 Catalysts Characterization

5.4.1 FTIR Spectra.

The infrared spectroscopy lattice vibration spectra in the 400-4000 cm^{-1} of original and prepared samples show the bands resulting from a typical siliceous material, with a main band at 1080 cm^{-1} together with a shoulder at 1227 cm^{-1}, due to a symmetric Si-O-Si stretching mode. There is also a

weaker band at 800 cm^{-1} due to Si-O-Si symmetric stretching modes and a strong band at 585.8 cm^{-1}, due to rocking Si-O-Si (as shown in figure 5-7). It is worthy noted that the incorporation of aluminum cases a decrease in intensity of the component assigned to the Si-(OH) stretching mode at 950 cm^{-1}[27]. This result is understandable with the post synthesis incorporation of aluminum.

The O-H stretching was illustrated in region 3000-3700 cm^{-1}. Spectra are shown in figure 5-7 for the original H-ZSM-5 and HMOR. The intensity of the band at 3444.2 cm^{-1} for HZSM-5 and 3448.6 cm^{-1} for HMOR, which is characteristic of Brønsted acid protons.

Figures 5-8 and 5-9 show IR-Spectra for the exchanged H^+ cation Barium and strontium cations. Thus, spectra of all BaZSM-5, BaMOR, SrZSM-5 and SrMOR still present the main features of the original H-form of corresponding zeolite structure. Therefore the infrared spectroscopy results to the conclusion, that the H-Ba-and SrZSM-5 and MOR zeolite have similar surface characteristics and structure before and after the ion exchange operation.

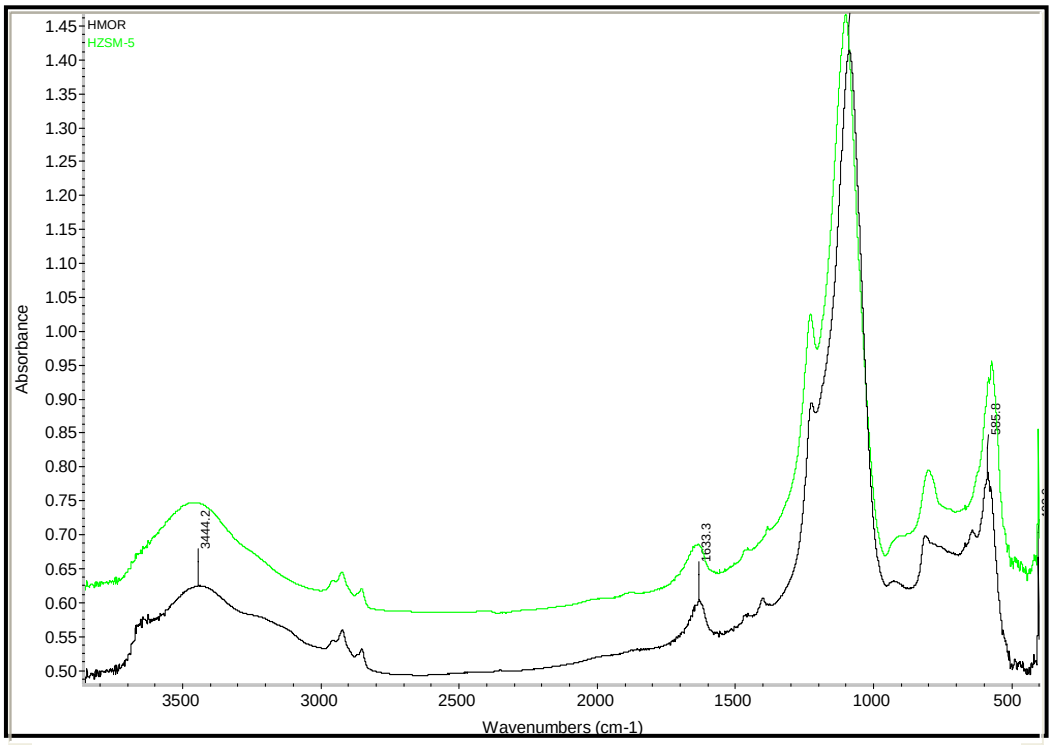

Figure 5-7: FTIR Spectra for Original HZSM-5 and HMOR

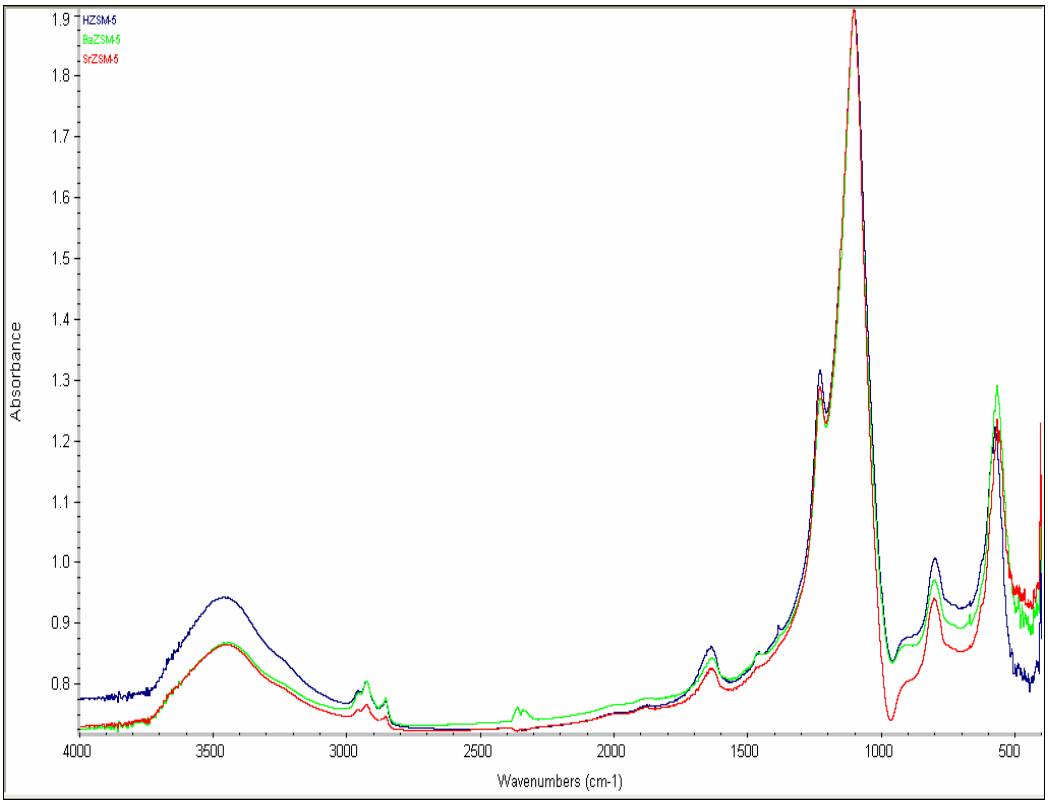

Figure 5-8: FTIR Spectra for Original HZSM-5 before and After Ion Exchange with Ba^{++} and Sr^{++}

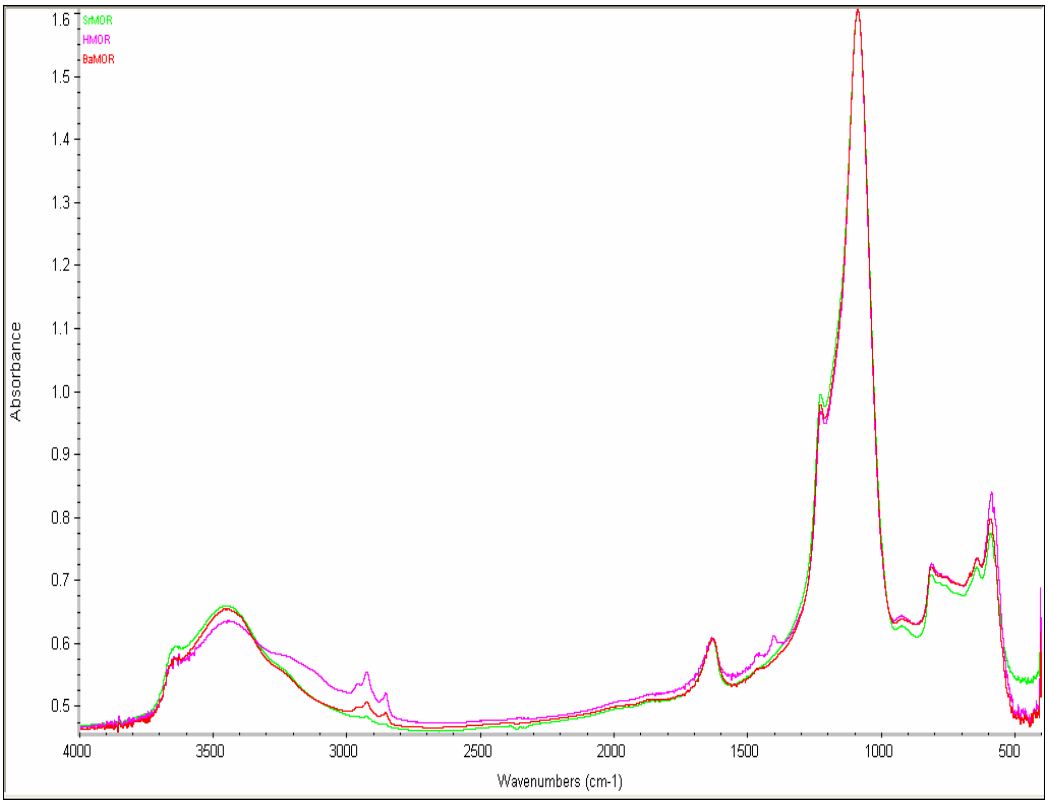

Figure 5-9: FTIR Spectra for Original HMOR Before and After Ion Exchange with Ba^{++} and Sr^{++}

5.4.2 X-Ray Diffraction

X-Ray diffraction was used to study the effect of the modifications processes on the crystallinity and frame work structure of Zeolite. Figures 5-10 to 5-13 show the XRD patterns of selected Zeolite types HZSM-5, HMOR, Barium and Strontium forms and with different metal loaded catalysts.

Figures 5-10 and 5-11, show XRD that taken after ion exchange of hydrogen cation with barium and strontium cations and calcanation process. The presence of these two ions to the zeolites had no change of the structure and crystallinity of zeolites.

Figure 5-12, shows the effect of loading of platinum by supercritical CO_2 at different temperatures and at constant pressure on the structure of H-Mordenite Zeolite. The shape and crystals of all samples were still the same without any change due to different percent of loading because the loading with $scCO_2$ was used and gave small platinum particles size that should be appeared at $2\theta=40$ [33], The original Zeolite contains more peaks in addition to the small crystal size cased to unclearly detection of the peak of metals.

Figures 5-13 and 5-14, show the XRD of Zeolite loaded with different metals, platinum, ruthenium and zirconium. The same behavior was observed for ruthenium and zirconium as discussed above for platinum; there is no effect due to loading and reduction of all Zeolite samples. Furthermore, the particles were very small and unable to detect by XRD because there peaks was mixed with original Zeolite peaks.

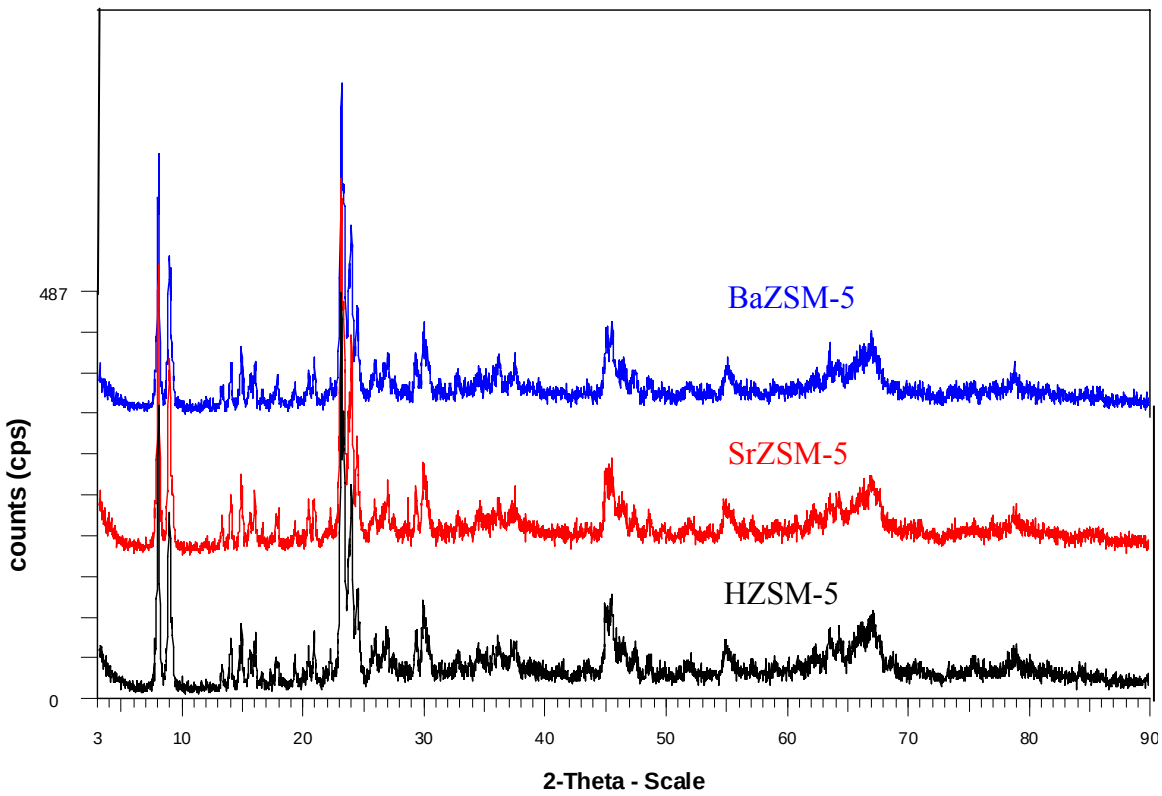

Figure 5-10: XRD for Original HZSM-5 and for Replaced Hydrogen Ion with Barium and Strontium Ions

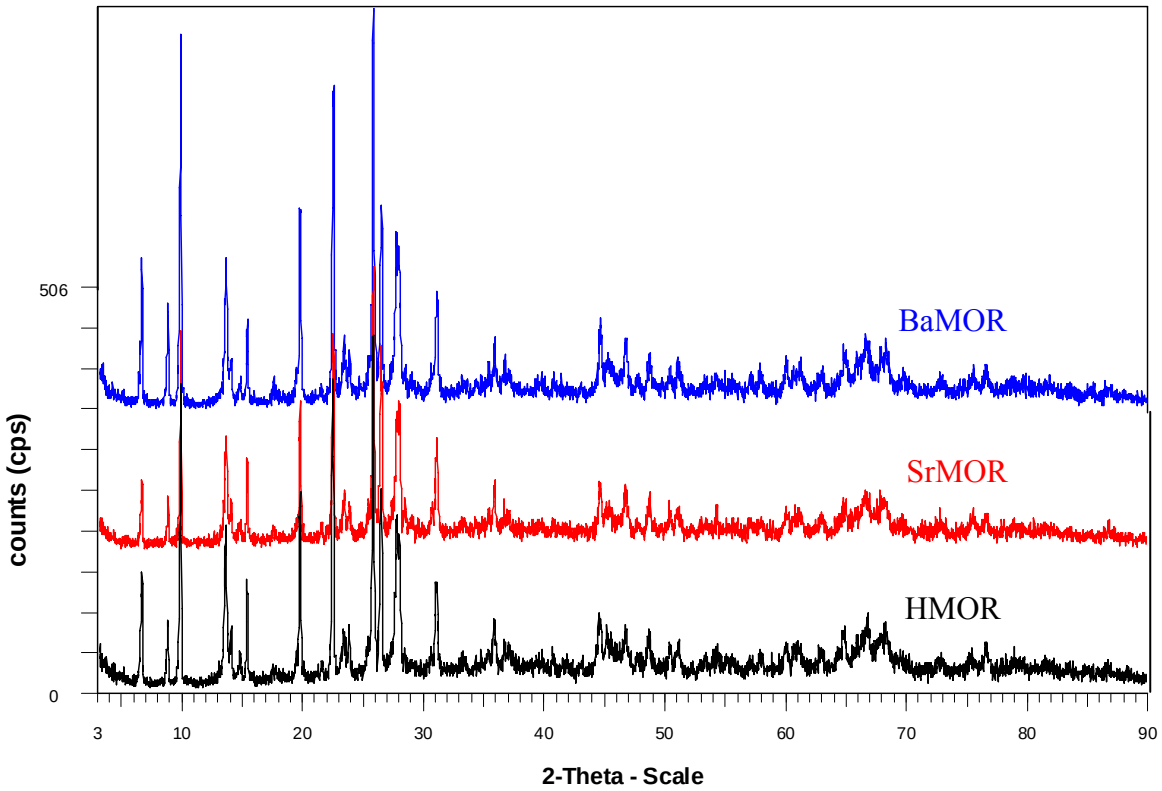

Figure 5-11: XRD for Original HMOR and for Replaced Hydrogen Ion with Barium and Strontium Ions

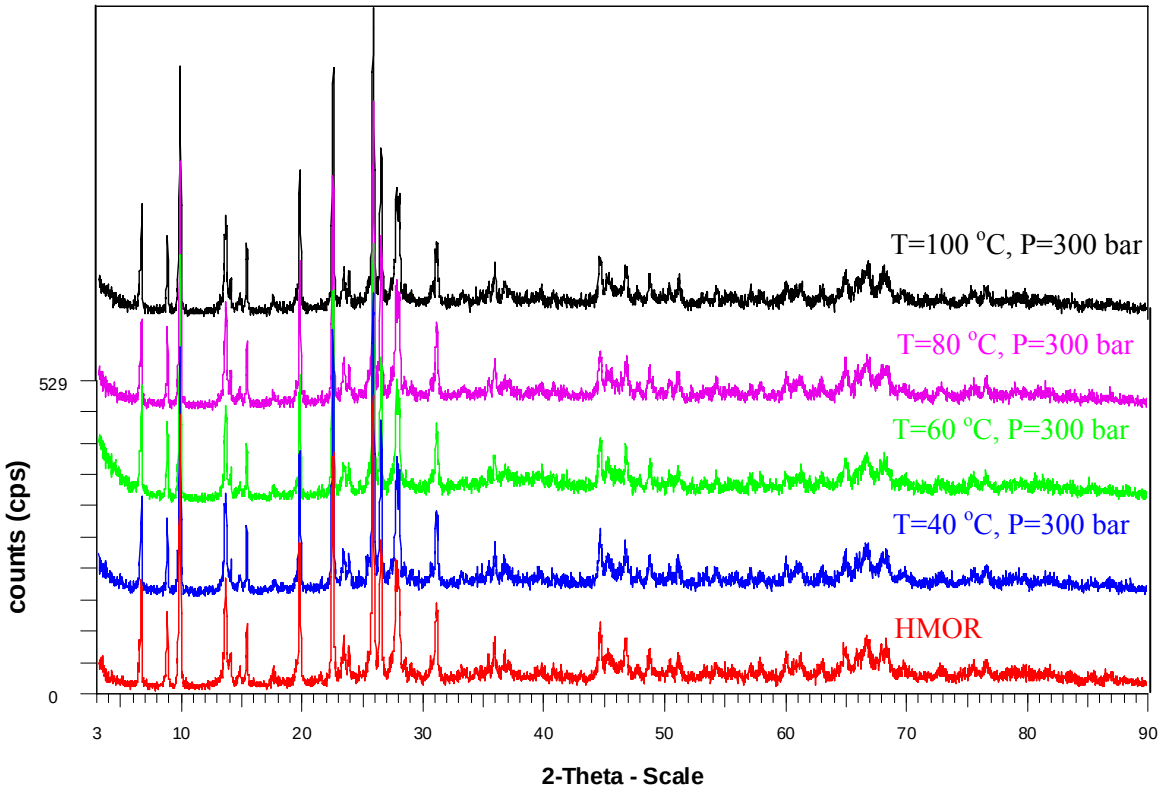

Figure 5-12: XRD of HMOR and Pt/HMOR Loaded by $scCO_2$ at different temperature, Pressure=300 bar

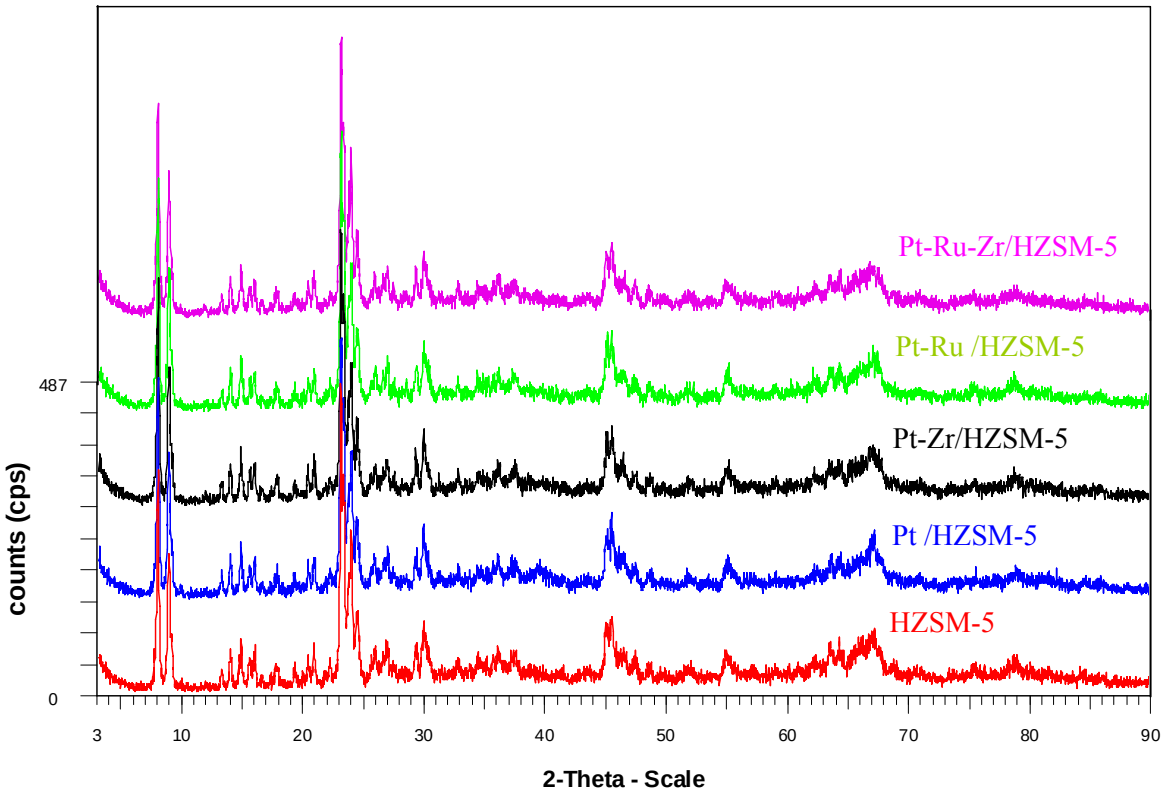

Figure 5-13: XRD of HZSM-5 and Different of Metal Loaded at T=80 °C and P=280 bar

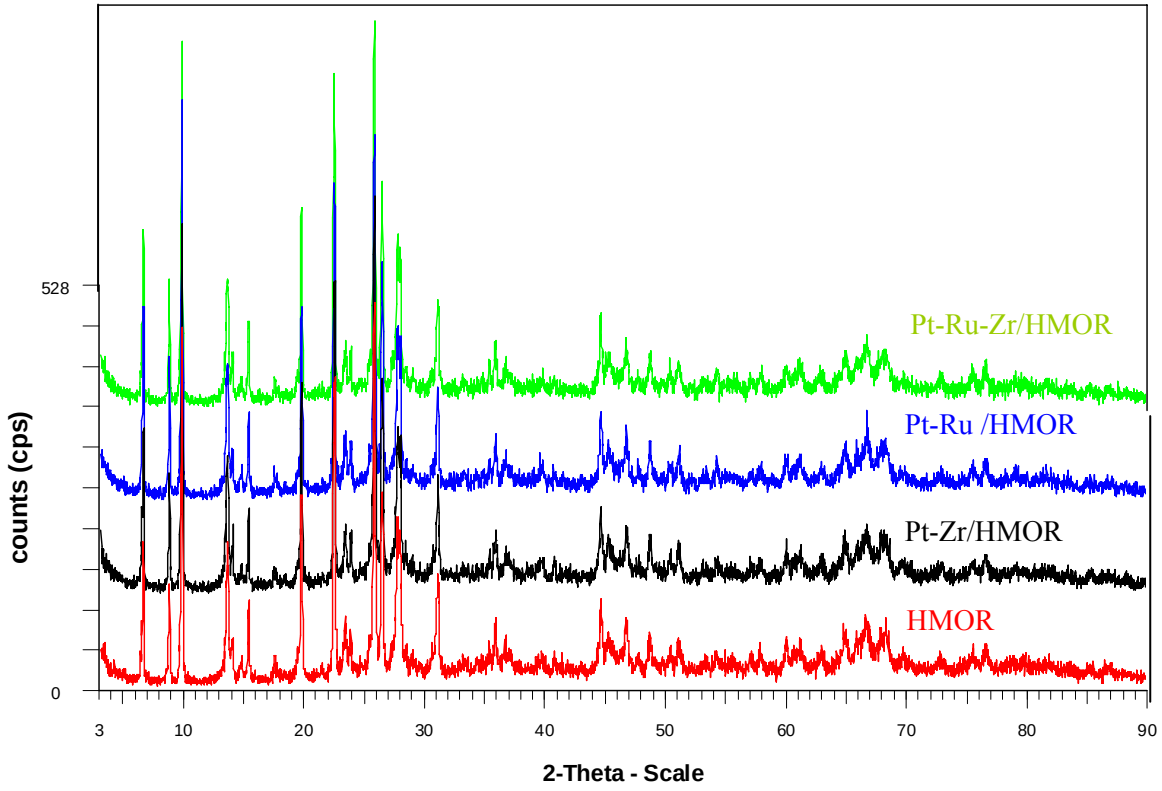

Figure 5-14: XRD of HMOR and Different of Metal Loaded at T=80 ^{o}C and P=280 bar

5.4.3 BET Surface Area

Surface area of prepared platinum zeolite catalysts were determined by nitrogen physisorption, BET method. The data for surface area and other surface properties were taken directly by software that interfaced with the device.

The BET surface area was strongly depended on the noble metal content of Zeolite, produced by impregnation method, while the metal loading by supercritical CO_2 show different sense. Here the mouth of pore volume was still opened in spite of loading with different platinum content.

Figure 5-15, show the effect of pressure on BET surface area. The results shows when pressure increase, the BET surface area will increase and reach maximum at T=100 ^{o}C and P=300 bar. It is worthy noted that the BET

surface area depends on the size and quantity of platinum loaded. For high pressure of CO_2 gave very small nanoparticle that was disturb on the surface of pores, therefore the pore mouth remains opened and not affected by deposition of metals. The effect of temperature on BET surface area was small. As shown in figure 5-15, there is no effect of temperature until 100 ^{o}C, while the surface area was increased when pressure increased. The facts that taken from figure 5-15 are the same as that taken from figure 5-5 for the effect of pressure and temperature. Thus, for good metal loading and large surface area it should be take on the considerations the increasing of pressure instead of temperature.

The results of surface properties for original, modified and noble metal loaded zeolite at different pressure and temperatures are listed in tables 5-7 and 5-8.

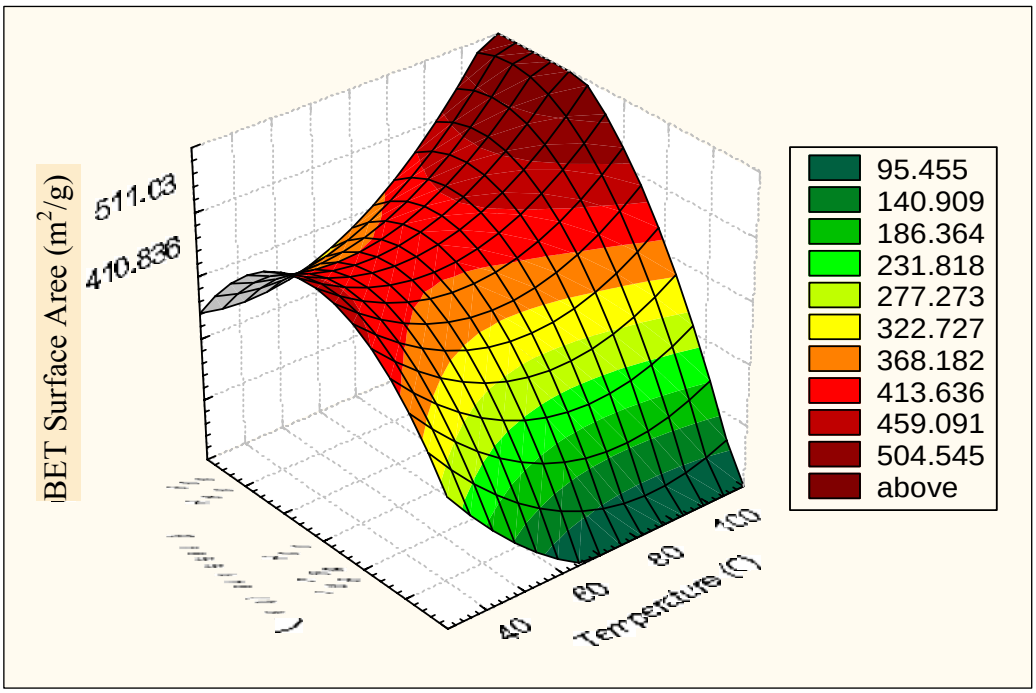

Figure 5-15: Effect of Temperature and Pressure on BET Surface Area for Pt/HMOR at pt content 0.912 wt%

Table 5-7: BET Surface Area for Zeolite Pt/HMOR at different Temperatures and Pressures and different Pt content

Pt content (wt%)	Temperature (^oC)	Pressure (bar)	Time (hr)	Surface Area (m^2/g)
0	---	----	---	**539.2112**
1.01	40	153	24	362.96
1.039	40	194	24	330.948
1.205	40	250	24	393.863
0.715	40	300	24	358.527
0.656	60	150	24	379.745
0.853	60	200	24	362.421
1.061	60	250	24	386.261
2.789	60	300	24	385.118
1.632	80	169	24	378.097
1.127	80	200	24	322.556
1.186	80	250	24	391.317
0.596	80	300	24	397.426
0.921	80	280	48	410.836
0.932	80	280	12	430.573
0.912	100	169	24	352.313
0.621	100	200	24	312.034
0.754	100	250	24	403.761
0.961	100	300	24	511.03

Table 5-8: BET Surface Area and Pore Volumes for Different Zeolite catalysts Loaded with Platinum, Ruthenium and Zirconium

Sample name	BET surface area (m^2/g)	Area of pours (m^2/g)	Pore volume (cm^3/g)	Volume of pores (cm^3/g)	Pore size (A)
HMOR	539.2112	117.5630	0.157485	0.266646	90.725
BaMOR	337.14	---	---	---	---
SrMOR	360.9	---	---	---	---
Pt/BaMOR	385.1929	105.8914	0.146832	0.245997	92.924
Pt-Zr/HMOR	421.8425	121.1862	0.157428	0.254891	84.132
Pt-Ru/HMOR	421.7972	122.6878	0.158174	0.255646	83.348
PtRuZr/HMOR	417.1341	120.1847	0.156292	0.251766	83.793
HZSM-5	403.7416	195.3045	0.076035	0.512954	105.057
BaZSM-5	355.325	---	----	---	--
SrZSM-5	309.927	---	---	---	---
Pt/HZSM-5	338.3526	206.4149	0.078006	0.525849	101.901
Pt-Zr/HZSM-5	348.1686	223.4837	0.76816	0.515548	92.275
Pt-Ru/HZSM-5	348.2464	222.2813	0.076962	0.529515	95.287
PtRuZr/HZSM-5	341.4123	212.8502	0.77294	0.515294	96.837

5.4.4 TGA Analysis

Thermogravimetric analysis, which is a precise measurement of the weight change of a solid as it is heated at a controlled rate, was carried out to investigate the decomposition of the precursors and to determine the appropriate weight reduction temperature range. TGA of pure $PtMe_2COD$, $Pt(acac)_2$, $Ru(acac)_3$ and $Zr(acac)_4$ and for Pt, PtRu, PtZr and PtRuZr loaded to HZSM-5 and HMOR were carried out over the range of 30-580 ^oC.

TGA trace of original $PtMe_2COD$ and there loaded zeolites are shown in Fig. 5-16. The starting temperature of weight loss for pure $PtMe_2COD$ was about 100 ^oC. While the temperature of the end of the rapid process was around 180 ^oC. This behavior indicates that the precursor does not decompose to elemental platinum, but instead it vaporize. The weight losses was 92.468 wt%, and the expected weight content of platinum not more than 58 wt%.

The decomposition of pt loaded to HZSM-5 and HMOR show that weight losses started at around 80 ^oC and stopped at 400 ^oC for Pt/HMOR and 500 ^oC for Pt/HZSM-5. The decomposition at 80 ^oC indicated to the removal of moisture from the samples. While by further temperature increase until the end of the process, the decomposition of Pt precursor was taken place, as shown in figure 5-16. The total weight losses were 7.410 wt% and 5.585 wt % for Pt/HZSM-5 and Pt/HMOR respectively.

The TGA analysis were done to other types of precursor, namely $Pt(acac)_2$, $Ru(acac)_3$ and $Zr(acac)_4$. The results were shown in Figs. 5-17, 5-18 and 5-19 respectively. The decomposition of $Pt(acac)_3$ was started at around 180 ^oC and hardly decomposed and vaporized at around 270 ^oC (96.227 %). The decomposition of $Ru(acac)_3$ was started at about 190 ^oC and vaporized at 300 ^oC, the weight losses of decomposition was 93.448%. On the other hand, the decomposition of PtRu/HZSM-5 and PtRu/HMOR were started at around 100 ^oC, while the moisture was completely removed at around 180 ^oC as

shown in figure 5-17. The total weight losses of water removed was 2.390% and 2.216 % for PtRu/HZSM-5 and PtRu/HMOR respectively. The decomposition of precursor was clearly observed at about 180 ^{o}C and stopped at 260 ^{o}C. The amount decomposion were 2.216% for PtRu/HZSM-5 and 3.109% for PtRu/HMOR.

Figure 5-18 shows the decomposition of $Pt(acac)_2$ and $Zr(acac)_4$ compounds. The decomposition of $Zr(acac)_4$ was started at around 150 ^{o}C and decomposed to elemental zirconium gradually until they reach 400 ^{o}C. The weight losses were measured as 78.12 %. Thus, the decomposition of precursor was nearly to the theoretical value (75%). Above 400 the zirconium started to evaporate slowly and completely at 750°C. TGA for Pt and Zr loaded to HZSM-5 and HMOR show that the decomposition started at around 80 ^{o}C and finished at 500 ^{o}C. The total weight losses were measured as 5.44 % and 6.31 for PtZr/HZSM-5 and PtZr/HMOR respectively.

Figure 5-19 shows the decomposition of $Pt(acac)_2$, $Ru(acac)_3$ and $Zr(acac)_4$ and Pt, Ru and Zr loaded to HZSM-5 and HMOR. The decomposition of PtRuZr/HMOR shows higher rate than for PtRuZr/HZSM-5, because the metal loading to HMOR was than to HZSM-5 as discussed in section of loading. The weight losses was measured as 9.715 % and 5.45 % for PtRuZr/HMOR and PtRuZr/HZSM-5 respectively.

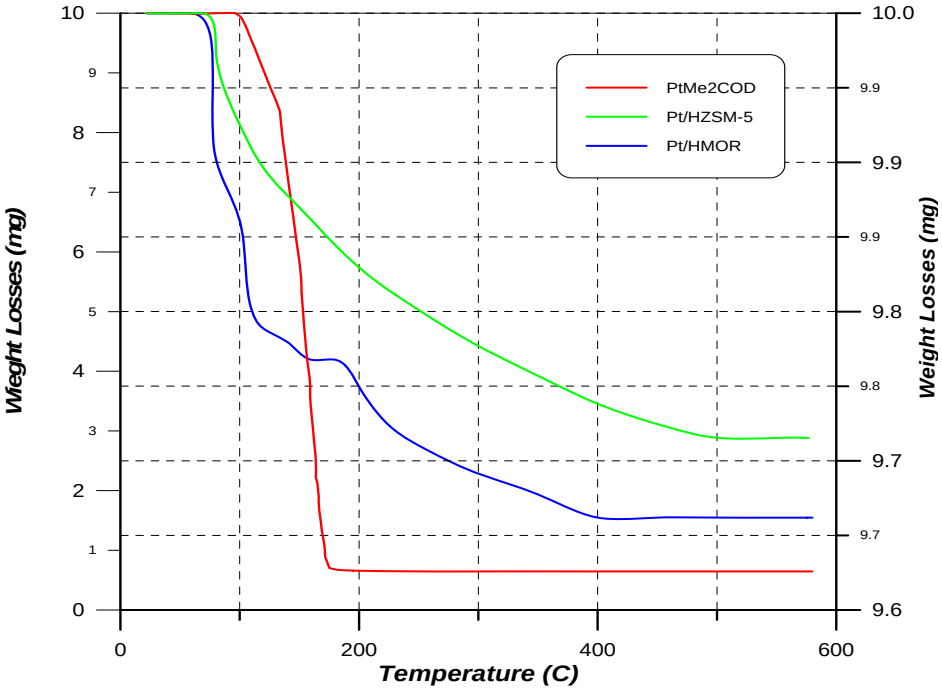

Figure 5-16: TGA Thermograph of Pure and Loaded $PtMe_2COD$ on Zeolites at Different Temperature

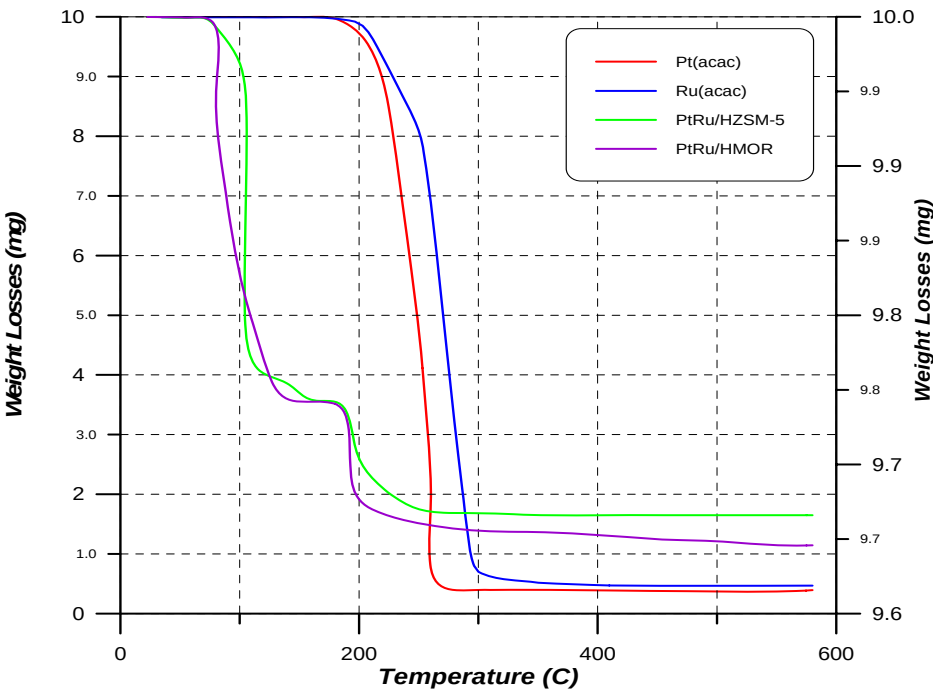

Figure 5-17: TGA Thermograph of Pure and Loaded $Pt(acac)_2$ and $Ru(acac)_3$ on Zeolites at Different Temperature

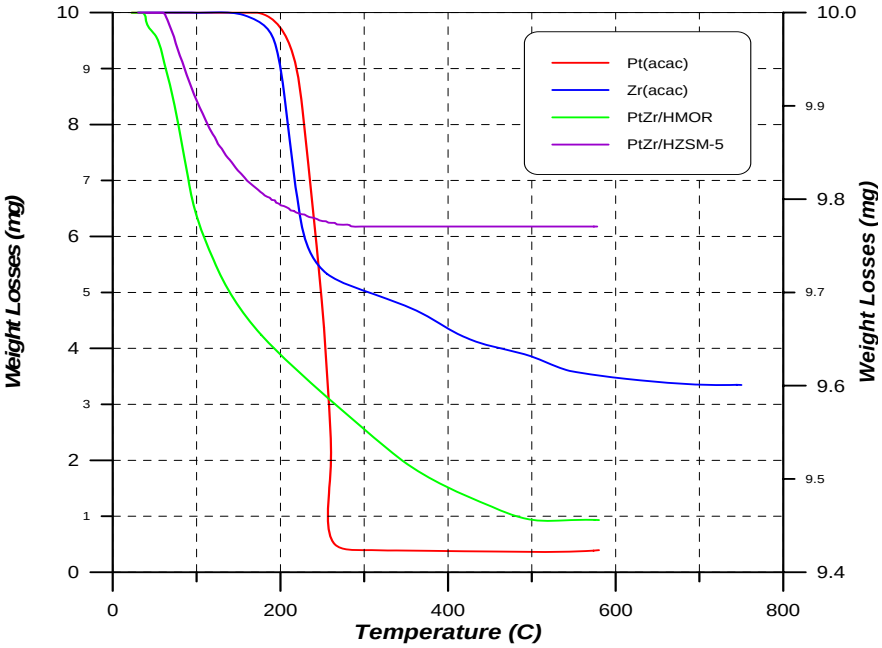

Figure 5-18: TGA Thermograph of Pure and Loaded $Pt(acac)_2$ and $Zr(acac)_4$ on Zeolites at Different Temperature

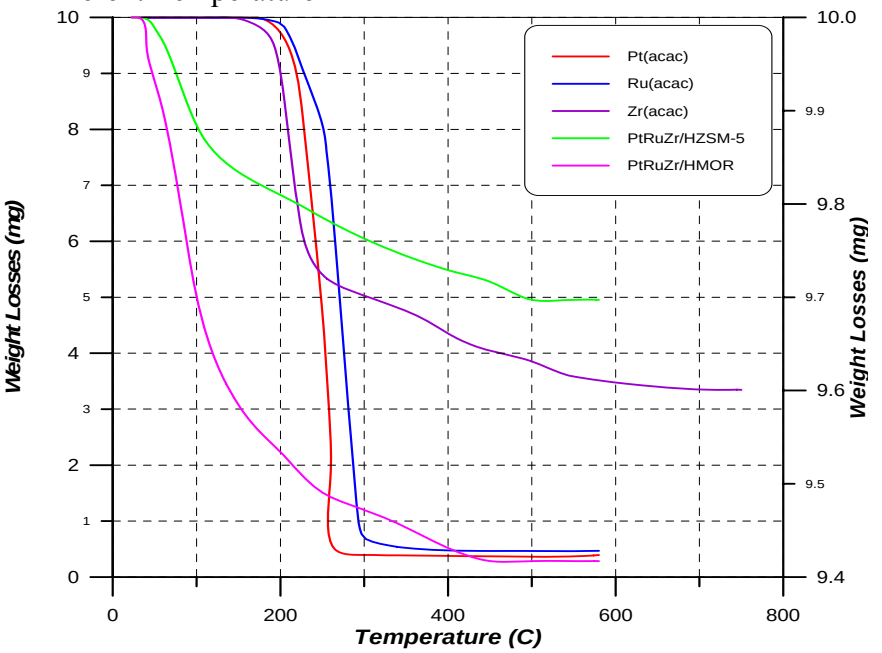

Figure 5-19: TGA Thermograph of Pure and Loaded $Pt(acac)_2$, $Ru(acac)_3$ and $Zr(acac)_4$ on Zeolites at Different Temperature

5.4.5 TEM Analysis

The morphology of the supported metal nanocomposites was characterized by Transmission Electron Microscopy (TEM). Figures 5-20a, to f, show the effect of pressure and temperature on the distributions of platinum nanoparticle. These figures were taken at pressure 300 bar and different temperatures. This condition was chosen due to there similarity to thus used for higher percent of loading, as discussed previously in section 5-3. These figures indicate the complement of the conclusions for the best conditions for loading.

The platinum was dispersed on the zeolite as shown by light reflection. It was very small nanoparticle and has highly dispersion where there is no space between particles. The mean size of these particles was detected between 0.9 to 1.2nm. The error in particle size is probably due to the reflection of light. Figure 5-20a shows the micrograph of platinum loaded by impregnation method. The mean size was detected as 6.78 nm and the picture shows the aggregation of the particles together to form big particles as shown by light reflection.

Figures 5-21 a and b and figures 5-22a and b, show the micrograph that taken by High Resolution TEM (HRTEM). They give a comparison between the platinum loaded by impregnation and those by $scCO_2$ method. The aggregation of platinum particles and non-uniform distribution of particles was detected as for platinum loaded by impregnation method for each graph. The mean size of platinum particles was 8.847 and 6.893 nm for Pt/HZSM-5 and Pt/HMOR respectively. The distribution of particles in addition to formation of nanoparticles are approximately equal size and equal distance that can be obtained by loading with $scCO_2$ as shown in figures 5-21b and 5-22b. The mean size of the platinum nanoparticles was 1.377 and 1.837 nm for zeolite Pt/HZSM-5 and Pt/HMOR respectively.

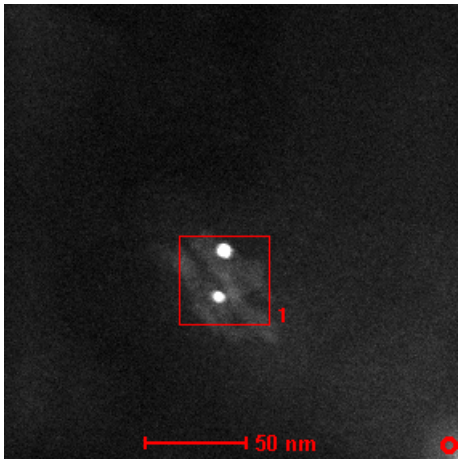

Figure 5-20a:TEM Micrograph for pt/HMOR loaded by Impregnation Method

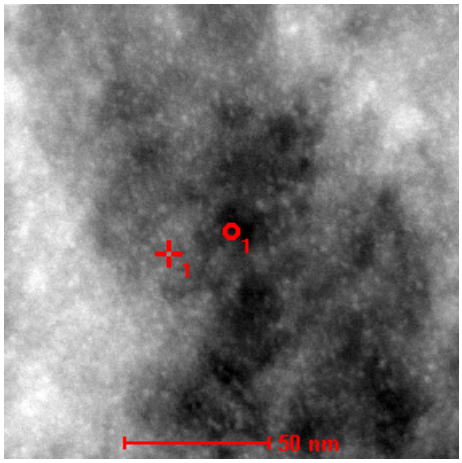

Figure 5-20b:TEM Micrograph for pt/HMOR loaded by $scCO_2$ at 40°C and P=300bar, t=24hr

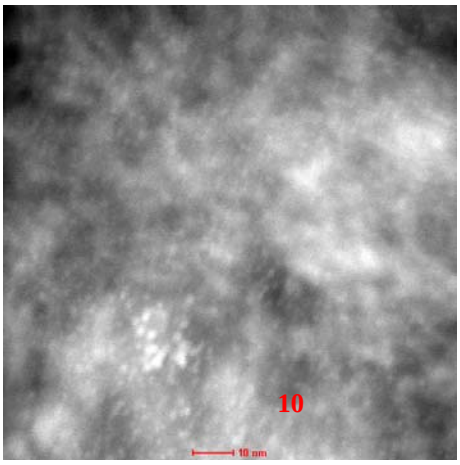

Figure 5-20c:TEM Micrograph for pt/HMOR loaded by $scCO_2$ at 60°C and P=300bar ,t=24 hr

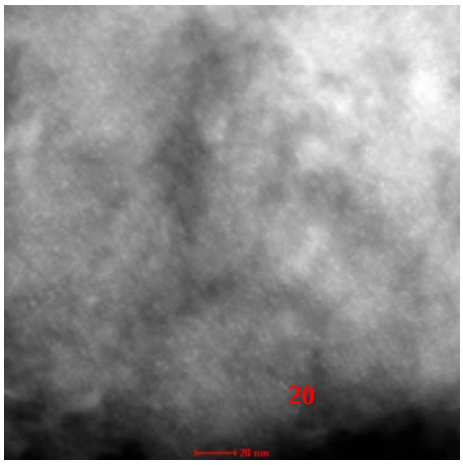

Figure 5-20d:TEM Micrograph for pt/HMOR loaded by $scCO_2$ at 80°C and P=300bar, t=24 hr

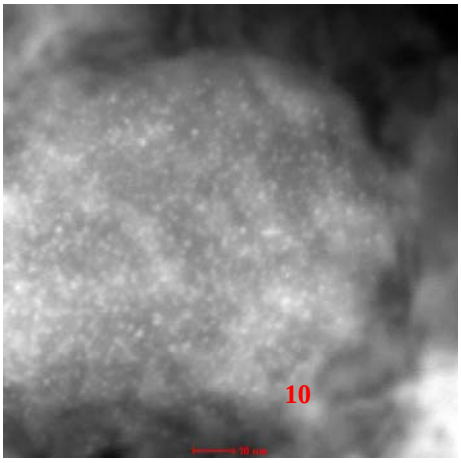

Figure 5-20e:TEM Micrograph for pt/HMOR loaded by $scCO_2$ at 100°C and P=300bar, t=24hr

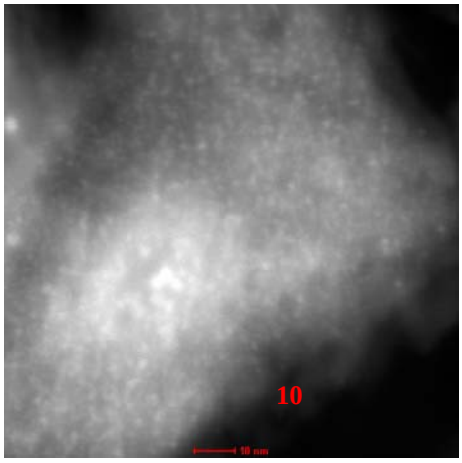

Figure 5-20f:TEM Micrograph for pt/HMOR loaded by $scCO_2$ at 80°C and P=280bar,t=48hr

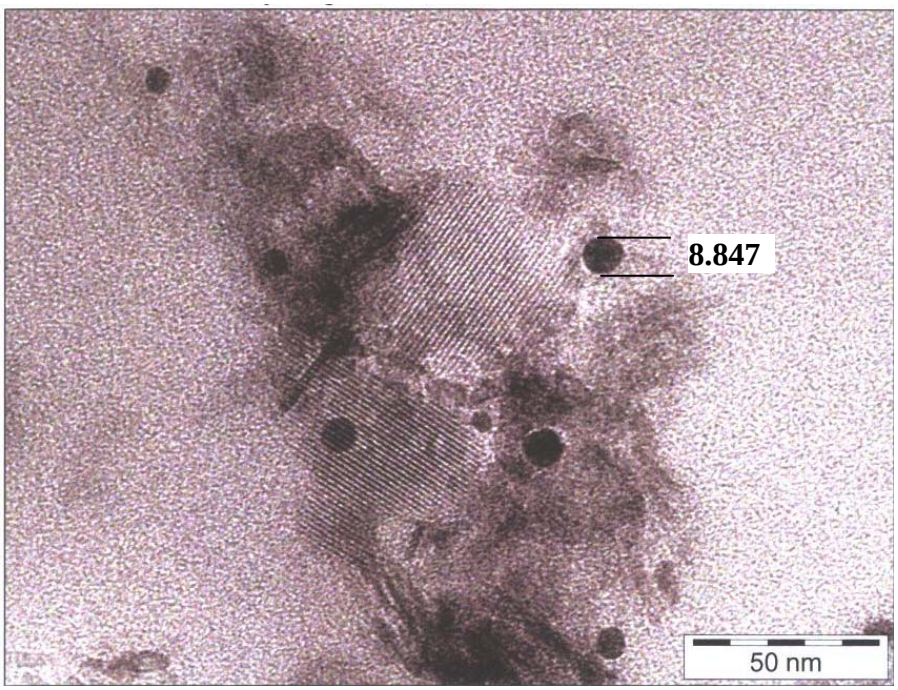

Figure 5-21a: TEM Micrograph for Pt loaded Over HZSM-5 by Impregnation Method

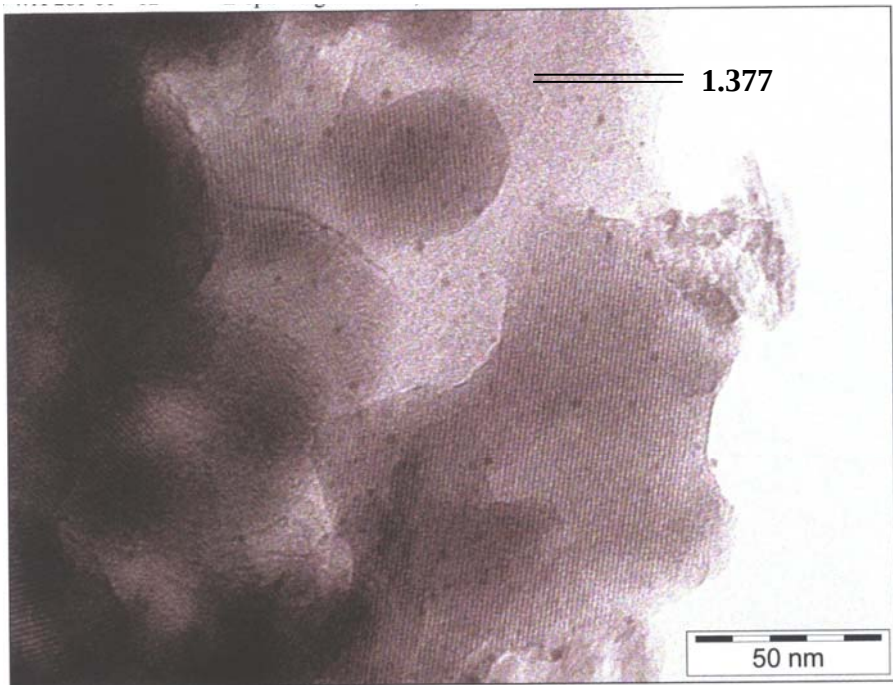

Figure 5-21b: TEM Micrograph for Pt loaded Over HZSM-5 by $scCO_2$ at T=80 ^oC and P=280 bar

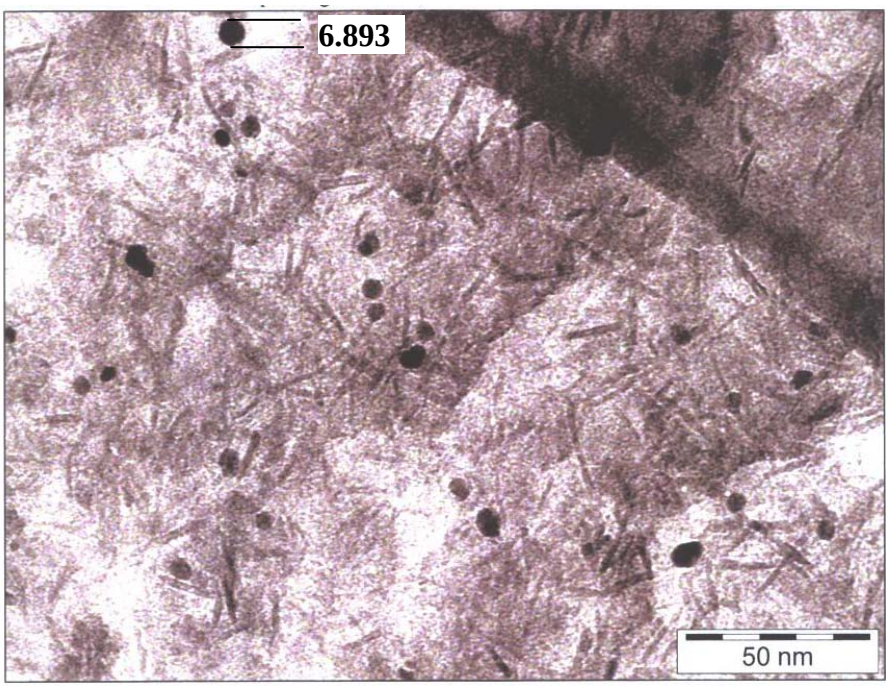

Figure 5-22a: TEM Micrograph for Pt loaded Over HMOR by Impregnation Method

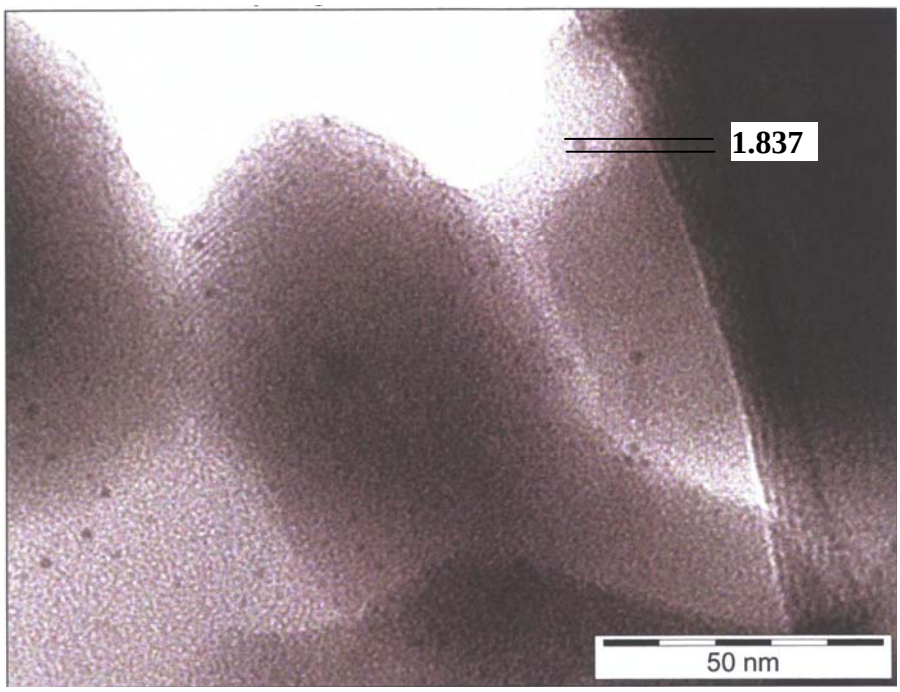

Figure 5-22b: TEM Micrograph for Pt loaded Over HMOR by $scCO_2$ at T=80 ^oC and P=280 bar

5.5 Catalytic Activity for Isomerization Reaction

5.5.1 Introduction

Two types of zeolite catalysts ZSM-5 and Mordenite were used for studying there activity towards isomerization reaction for n-Hexane. These zeolite catalysts contains Hydrogen in the original form. Barium and Strontium were exchanged with hydrogen using Batch wise ion exchange.

Platinum was loaded to the original samples contains hydrogen cation using two methods, one prepared by impregnation method and the other one was prepared by super critical carbon dioxide technique. Platinum, with Ruthenium and Zirconium companied bi and trimetals were loaded to the original and their exchanged catalysts using supercritical carbon dioxide techniques.

The isomerization results of n-Hexane on noble metals/Zeolite supported catalysts included three reaction namely, isomerization, hydrocracking, and cyclization. The cyclization to cyclohexane and Benzene are reactions of little significant on all considered catalysts. These reactions were used to study the catalytic behavior forms by both impregnation and in super critical carbon dioxide as relatively new method.

The results show the effect of temperature in the range of 250-325 ^{o}C and hydrogen to Hexane ratios of 3, 6 and 9 at 5 bar pressure.

The conversion of n-Hexane, selectivity of isomerized hexanes, and the yield of the more desired isomers, namely 2- and 3-methyle pentane in addition to cracked C_1-C_4 fraction were calculated by equations 4-2, 4-3 and 4-4 respectively. The main important comparison between the prepared catalysts was the selectivity and yields towards of desired Hexane isomers.

$$Conversion = (1 - \frac{N_A}{N_{A_o}}) * 100 \qquad (4\text{-}2)$$

$$\%\,Selectivity = \frac{N_i}{N_{Ao} - N_A} * 100 \quad (4\text{-}3)$$

$$Percentage\,Yield = \frac{N_i}{N_{A_o}} * 100 \quad (4\text{-}4)$$

5.5.2 Platinum Loaded H-Zeolites

5.5.2.1 Temperature Effect

The product distribution upon n-hexane isomerization is shown in appendix A-1 to A-12. The fraction of C_1-C_4 cracked product, percent n-Hexane conversion, and catalytic selectivity towards isomerization as well as the isomers yield and aromatics yield were presented in these appendices. The main important comparison between the prepared catalysts was selectivity and yield of desired product.

The effect of temperature on the conversion and the selectivity are summarized in figures 5-23 through 5-28 by using Pt/HZSM-5 and Pt/HMOR catalysts at 5 bar pressure and different H_2/HC ratios.

All figures show that the percentage conversion of n-Hexane is slightly higher on catalysts prepared by impregnation method than those loaded in supercritical carbon dioxide technique. While, the selectivity towards C_6-isomers is significant higher on catalysts prepared in $scCO_2$ than the catalysts loaded by impregnation for all temperatures and H_2/HC ratios studied.

As its expected that the temperature increase leads to conversion increase gradually. While the selectivity decreases with temperature increase. Temperature increase enhances the hydrocracking reactions producing more C_1-C_4 gases product, and decreasing the value of desired product. Therefore at low temperature, such as 250 ^oC, the $scCO_2$ catalysts give about 100 % selectivity at conversion more than 50 % at higher temperatures, the selectivity of impregnated catalysts decrease rapidly, reaching about 20 % at

325 ^{o}C and 3 H_2/HC ratio as shown in figure 5-23. The corresponding selectivity for $scCO_2$ catalysts are about 55 % at the same conditions.

It could be concluded that 290 ^{o}C is the optimum temperature to get selectivity more than 90 % at expectable conversion about 76 % for Pt/HZSM-5. While, the required temperature was about 275 ^{o}C to get a selectivity higher than 90 % at a conversion above 65 %.

Furthermore, the results show that Pt/HZSM-5 catalyst is more active and selective than Pt/HMOR catalyst for the considered temperature range.

5.5.2.2 Hydrogen to n-Hexane Ratio

The effect of hydrogen to hydrocarbon variation for n-Hexane isomerization reactions were carried out on Pt/HZSM-5 and Pt/HMOR catalysts. Both types were prepared by impregnation and in supercritical carbon dioxide as solvent. All experiments were conducted at a constant flow rate of n-Hexane and H_2/HC ratios 3, 6 and 9 by increasing of hydrogen flow rate.

Figures 5-29 to 5-32 show the effect of H_2/HC ratios on the conversion and selectivity of the above mentioned catalysts at temperature 25, 275, 300 and 325 ^{o}C respectively. It is noticed that a slightly increase in the selectivity is observed as H_2/HC ratio increased. This could be attributed to the fact that by increasing the hydrogen partial pressure the rate of cracking reactions is decreased. Furthermore, the catalysts loaded in supercritical carbon dioxide show relatively higher selectivity in the temperature range 250-300 ^{o}C than those loaded by impregnation, as given in figures 5-29 to 5-31. While at temperature 325 ^{o}C, Pt/HZSM-5 prepared in $scCO_2$ gives the lowest selectivity compared with the other catalyst types, as shown in figure 5-32.

It was generally observed, that the conversion of n-Hexane increases gradually with increasing of H_2/HC ratio for all catalysts types and temperatures studied. This effect is noticeable at 325°C as shown in Fig. 5-32

5.5.2.3 Yields

The isomerization reaction of n-Hexane results usually in four isomers. Those are 2-Methylpentane (2MP), 3-Methylpentane (3MP), 2, 2-Dimethylbutane (2, 2 DMB) and 2, 3-Dimethylbutane (2, 3 DMB). 2MP and 3MP are the most required compounds for upgrading of motor gasoline, due to there sufficient volatility and high Octane number. Therefore, it was worthy to investigate the effectiveness of the platinum supported HZSM-5 and Mordenite catalysts towards the yield of these compounds. Special attention was done to the effect of loading method on the performance of catalysts. Furthermore, the hydrocracking of n-Hexane feed to C_1-C_4 hydrocarbons are considered as undesired reactions, producing gaseous components. The yield of C_1-C_4 fraction was also evaluated to study the catalytic behavior of platinum HZSM-5 and HMOR catalysts.

Figure 5-33 to 5-35 and 5-36 to 5-38 show the yield of 2MP and 3MP on Pt/HZSM-5 and Pt/HMOR, respectively at different temperatures and H_2/HC ratios. Both catalysts were loaded by impregnation and in supercritical carbon dioxide. The yields of 2MP and 3MP for catalysts prepared in $scCO_2$ are higher than for those prepared by impregnation method, because the former method gives uniform metal distribution on the support, resulted in more selective catalyst behavior. Furthermore, Pt/HZSM-5 shows more selective towards 2MP and 3MP than Pt/HMOR generally for both loading methods.

Generally, the figures show that, maximum yields for 2MP and 3MP were achieved at 275 ^{o}C within the temperature range 250-325 ^{o}C considered. The decline of yields by increasing the temperature is probably due to hydrocracking of these isomers, 2MP and 3MP to low hydrocarbons, mainly by using impregnated catalysts. The figures also indicate that the decrease of

yield by increasing of temperature is more noticeable for impregnated catalysts than in case of those prepared in $scCO_2$.

Hydrogen to hydrocarbon ratio seems to be having a little effect on the yield of 2MP and 3MP for both catalysts. Generally, a ratio of about 6 shows as an optimum within the range studied, as exhibited in figures 5-34 and 5-37 for 2MP and 3MP respectively.

The selectivity of prepared Pt on HZSM-5 and HMOR zeolite catalysts were studied under different temperatures and H_2/HC ratios in hydrocracking of n-Hexane during the isomerization process. Figures 5-39 through 5-41 are summarized the results. The figures show, that the effect of temperature on the yield of C_1-C_4 hydrocarbons is noticeable for all catalysts studied. At temperature 250 ^oC and H_2/HC ratio of 6 as an example, the yield of C_1-C_4 was only about 4 % but jumped to around 26 % at 300 ^oC and 62 % at 325 ^oC for the catalysts loaded by impregnation. The corresponding data for the catalysts loaded in $scCO_2$, were nearly one percent at 250 ^oC increased to around 11% at 300 ^oC and 33% and 41 % for Pt/HZSM-5 and Pt/HMOR respectively. Therefore the results show clearly, the catalysts of $scCO_2$ are less selective for hydrocarcking reactions than those loaded by impregnation. While Pt/HZSM-5 $scCO_2$ catalysts less selective for C_1-C_4 hydrocarbons formation.

The H_2/HC ratio was influenced the hydrocracking reactions of n-Hexane. Those as the ratio increases, the yield of C_1-C_4 hydrocarbons declines for all catalysts studied.

The results discussed in this section indicate that the loading of Platinum in supercritical carbon dioxide possesses higher selectivity for n-Hexane isomerization, particularly between 275 and 300 ^oC.

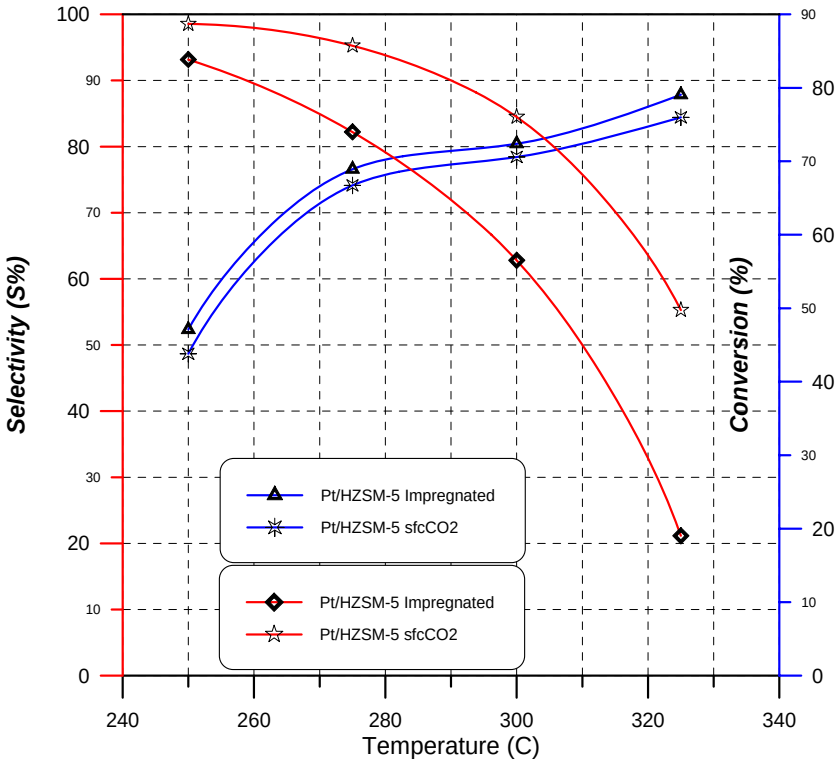

Figure 5-23: Selectivity and Conversion vs.Temperature for Zeolite Pt/HZSM-5 at Pressure 5bar and H/HC=3

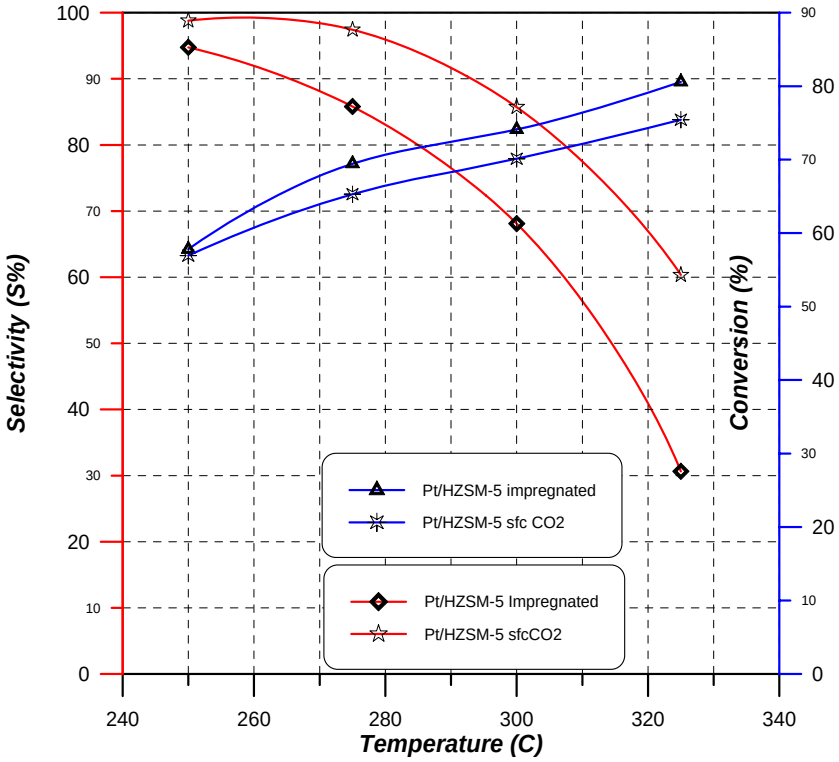

Figure 5-24: Selectivity and Conversion vs.Temperature for Zeolite Pt/HZSM-5 at Pressure 5bar and H/HC=6

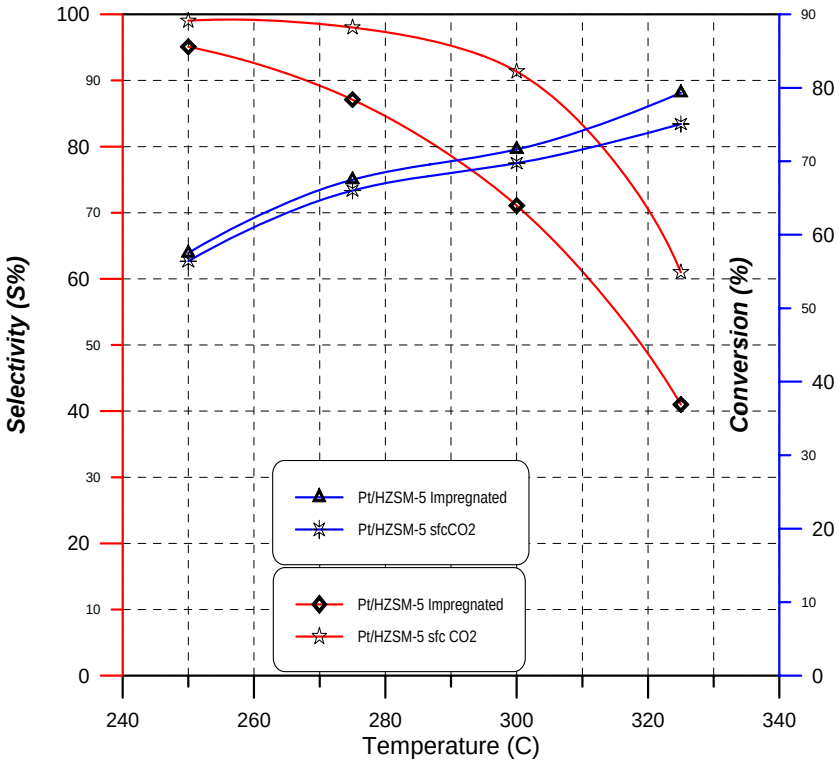

Figure 5-25:Selectivity and Conversion vs.Temperature for Zeolite Pt/HZSM-5 at Pressure 5bar and H/HC=9

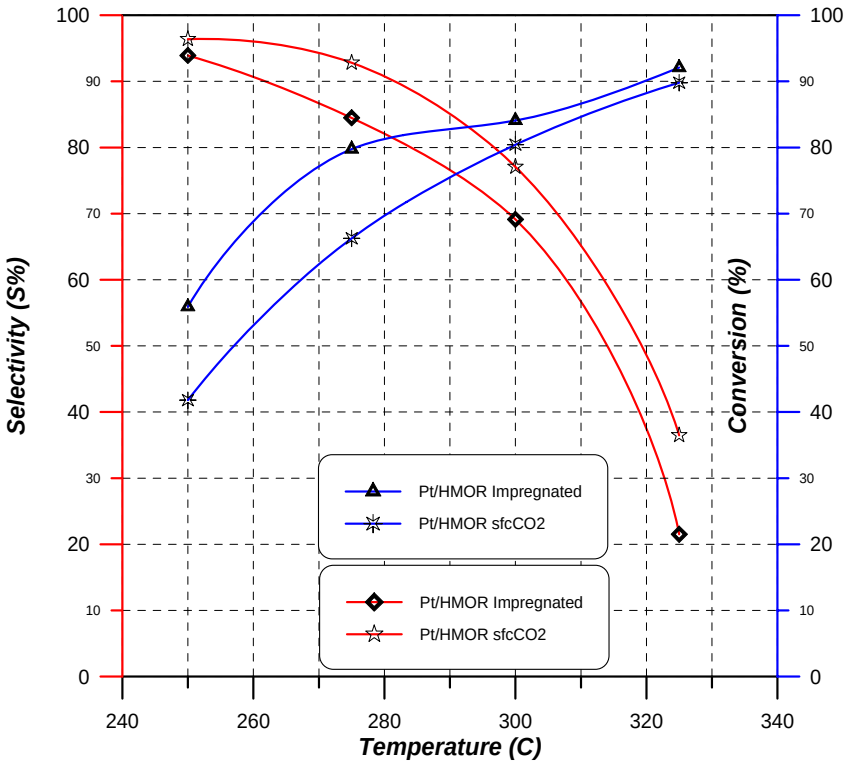

Figure 5-26:Selectivity and Conversion vs.Temperature for Zeolite Pt/HMOR at Pressure 5bar and H/HC=3

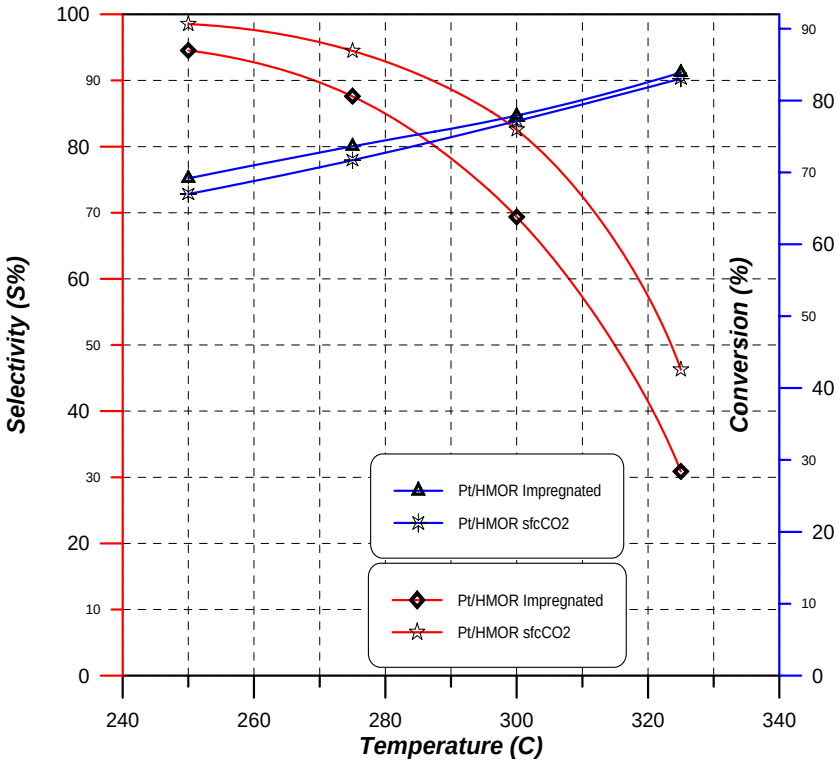

Figure 5-27: Selectivity and Conversion vs.Temperature for Zeolite Pt/HMOR at Pressure 5bar and H/HC=6

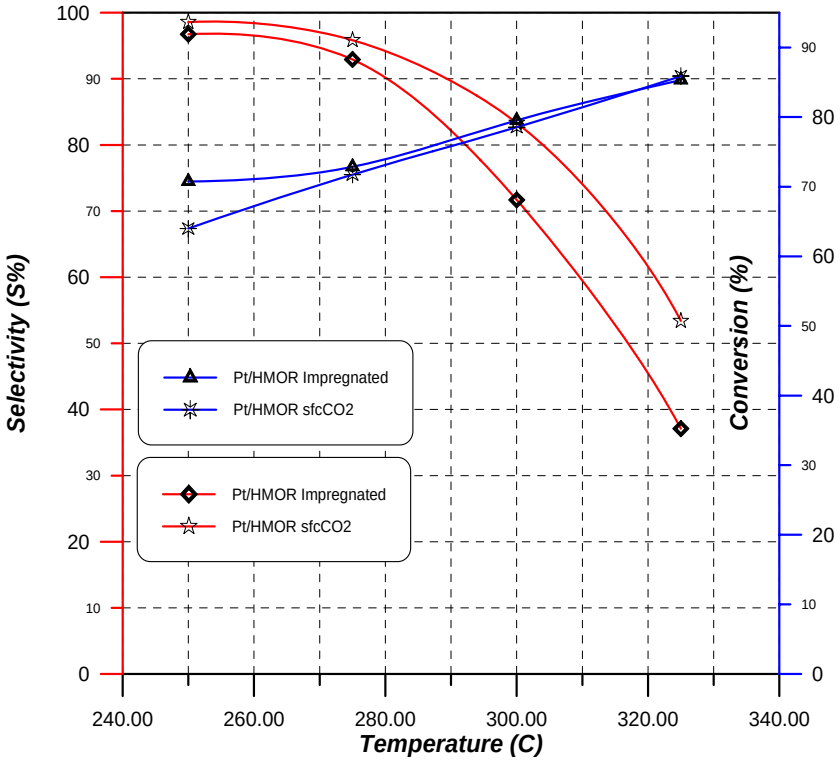

Figure 5-28: Selectivity and Conversion vs.Temperature for Zeolite Pt/HMOR at Pressure 5bar and H/HC=9

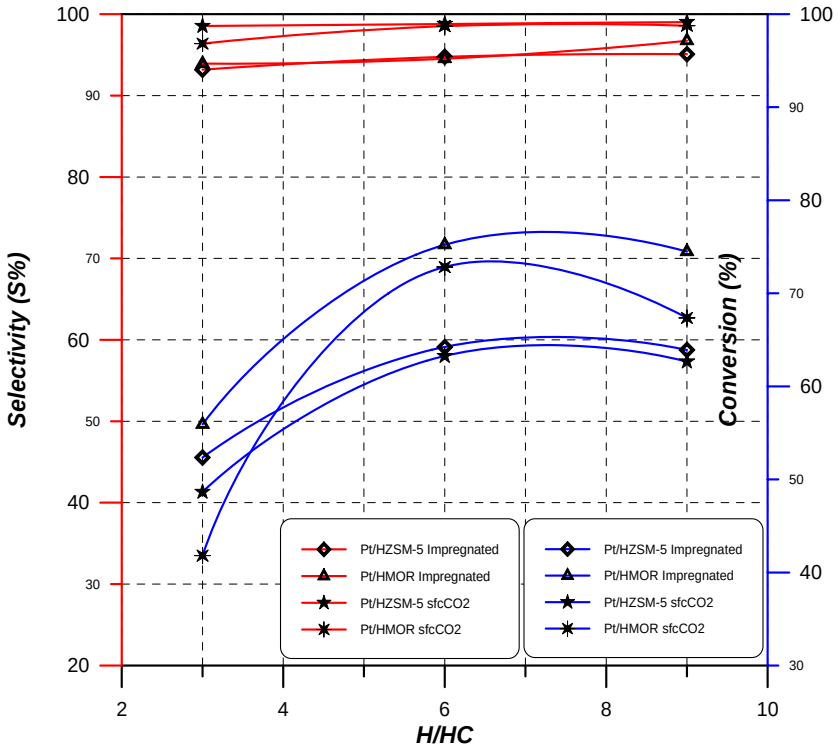

Figure 5-29: Selectivity and Conversion vs. H/HC for Zeolites Pt/HZSM-5 and Pt/HMOR at Pressure 5bar and T=250 ^{o}C

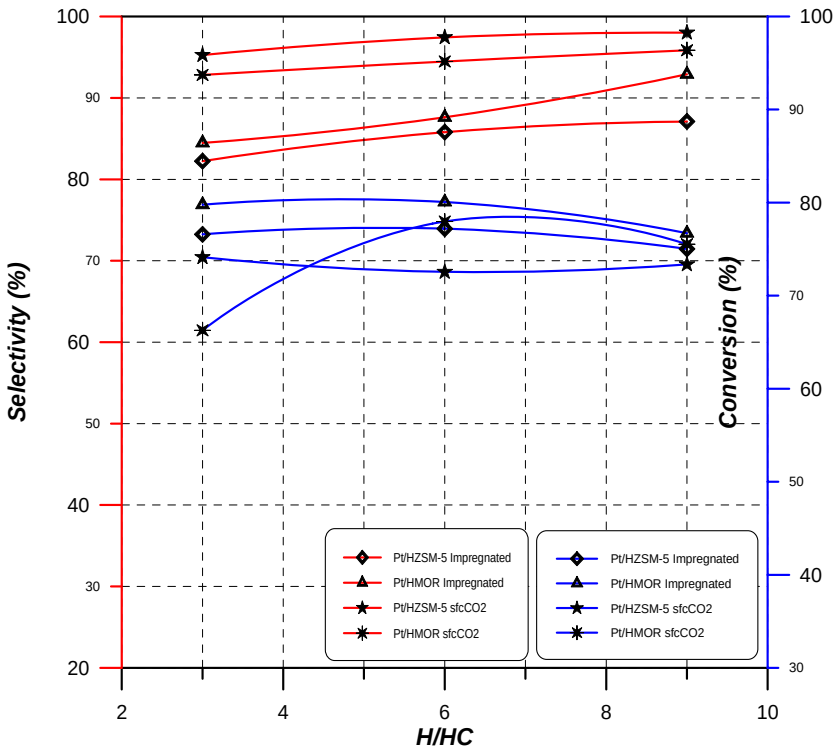

Figure 5-30: Selectivity and Conversion vs. H/HC for Zeolites Pt/HZSM-5 and Pt/HMOR at Pressure 5bar and T=275 ^{o}C

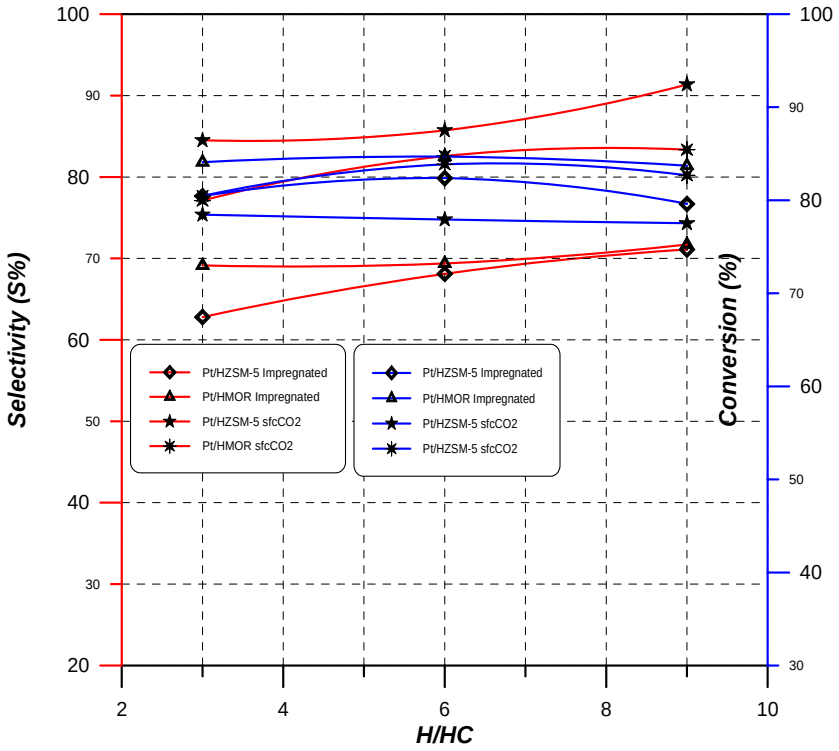

Figure 5-31: Selectivity and Conversion vs. H/HC for Zeolites Pt/HZSM-5 and Pt/HMOR at Pressure 5bar and T=300 ^{o}C

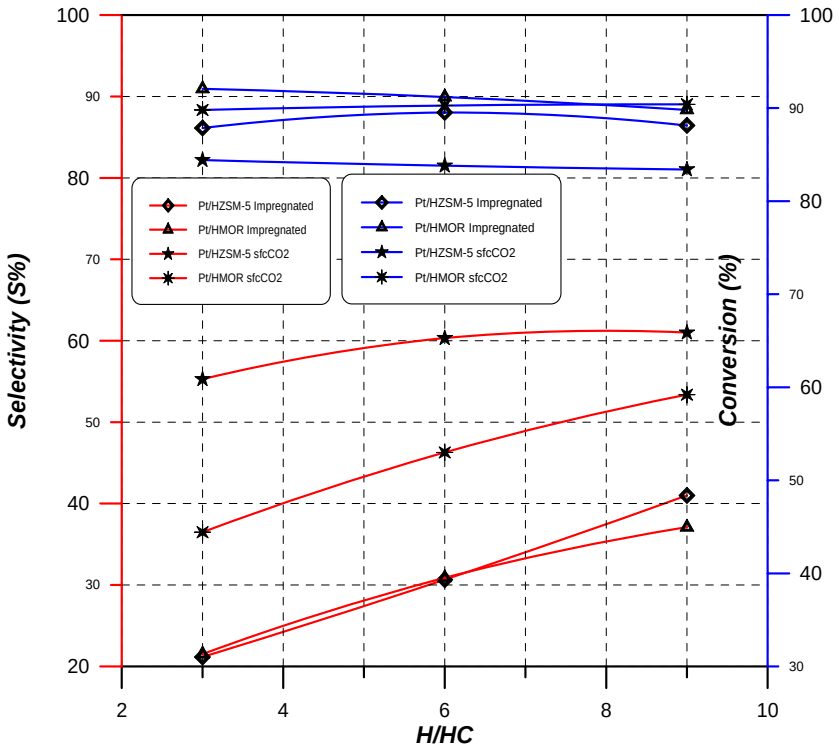

Figure 5-32: Selectivity and Conversion vs. H/HC for Zeolites Pt/HZSM-5 and Pt/HMOR at Pressure 5bar and T=325 ^{o}C

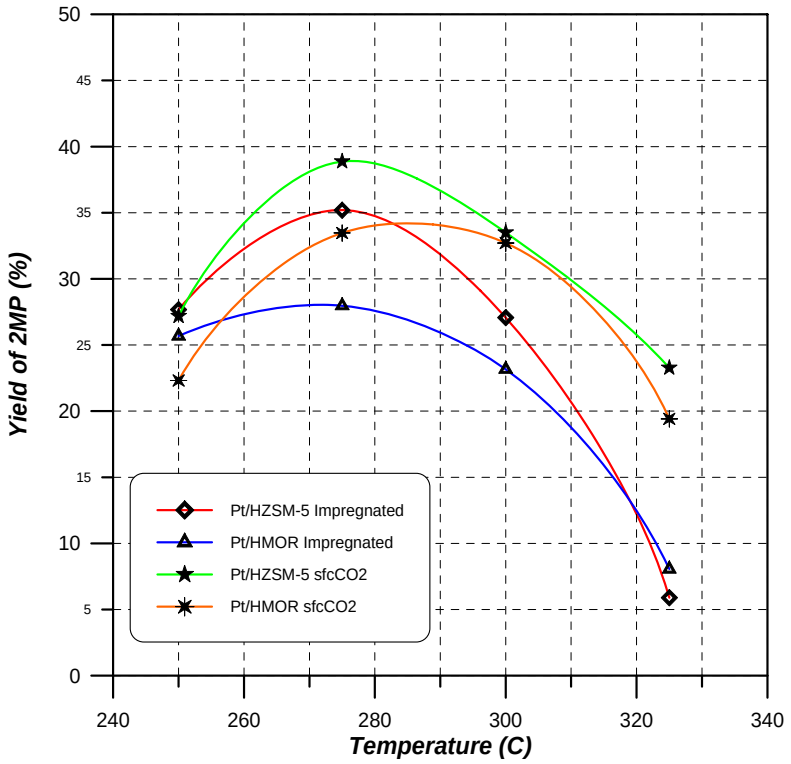

Figure 5-33: Yield of 2MP vs. Temperature for Zeolites Pt/HZSM-5 and Pt/HMOR at Pressure 5bar and H/HC=3

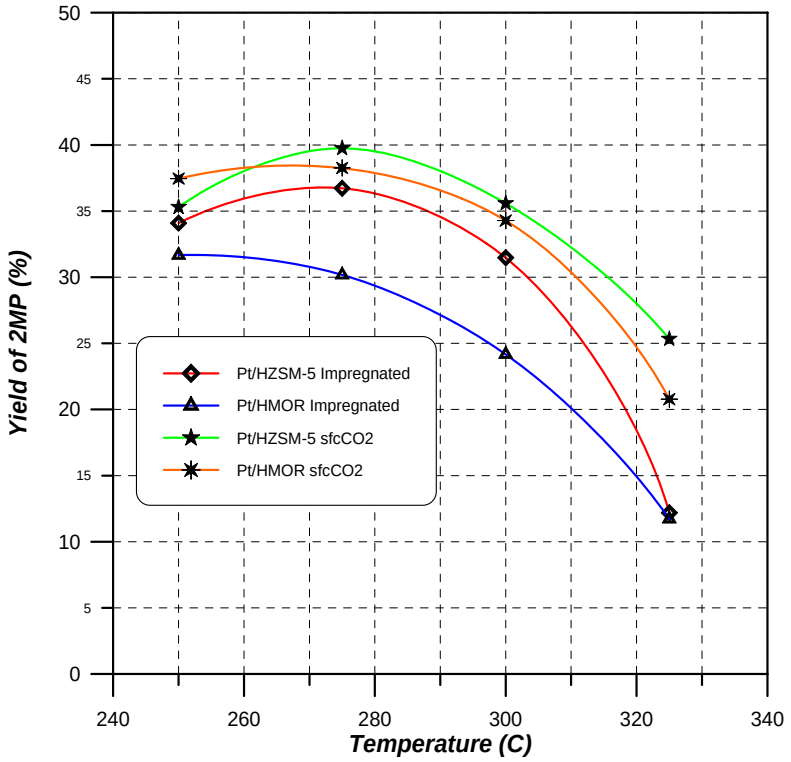

Figure 5-34: Yield of 2MP vs. Temperature for Zeolites Pt/HZSM-5 and Pt/HMOR at Pressure 5bar and H/HC=6

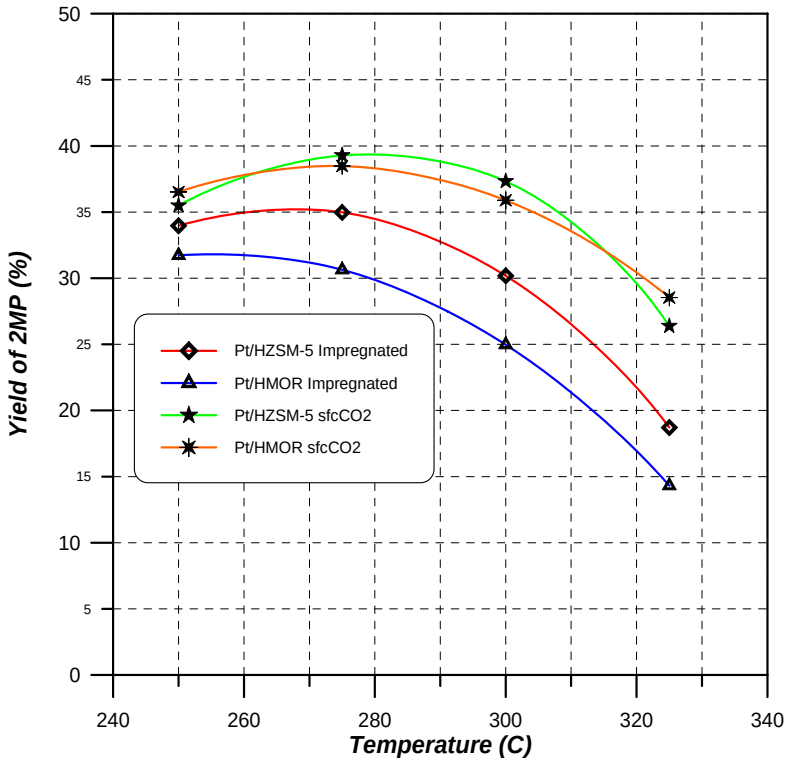

Figure 5-35: Yield of 2MP vs. Temperature for Zeolites Pt/HZSM-5 and Pt/HMOR at Pressure 5bar and H/HC=9

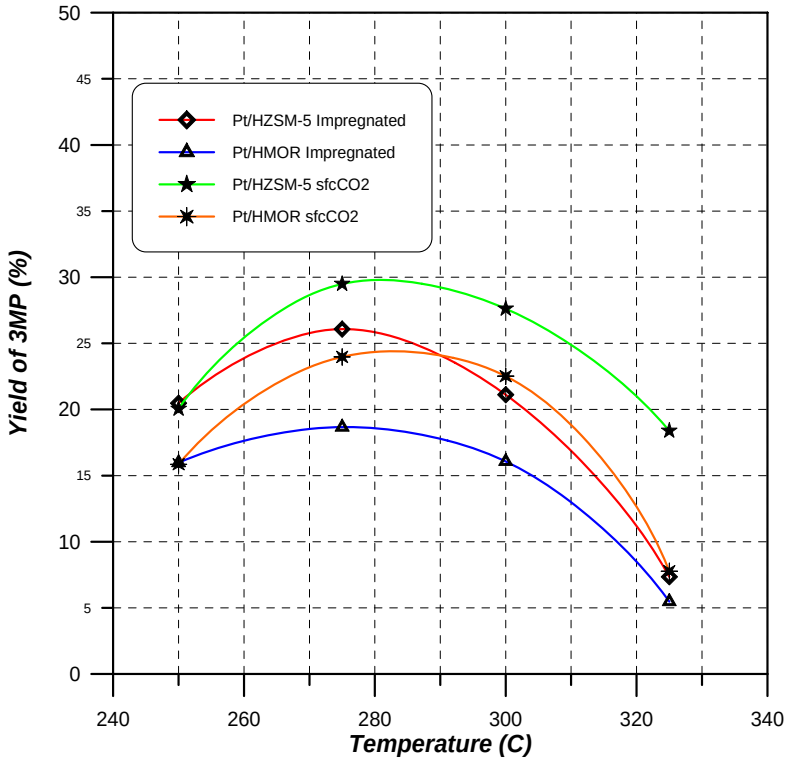

Figure 5-36: Yield of 3MP vs. Temperature for Zeolites Pt/HZSM-5 and Pt/HMOR at Pressure 5bar and H/HC=3

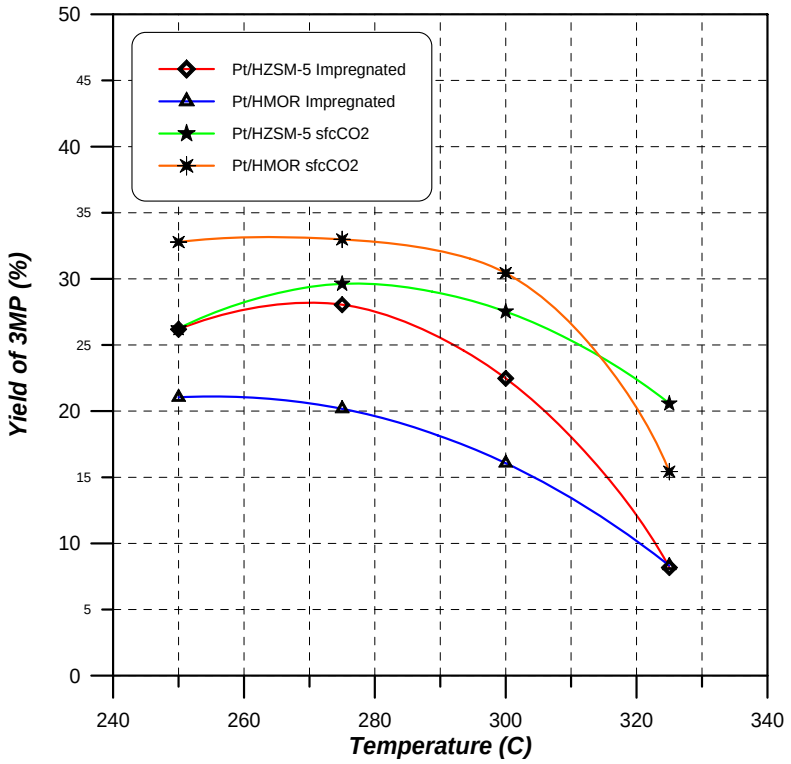

Figure 5-37: Yield of 3MP vs. Temperature for Zeolites Pt/HZSM-5 and Pt/HMOR at Pressure 5bar and H/HC=6

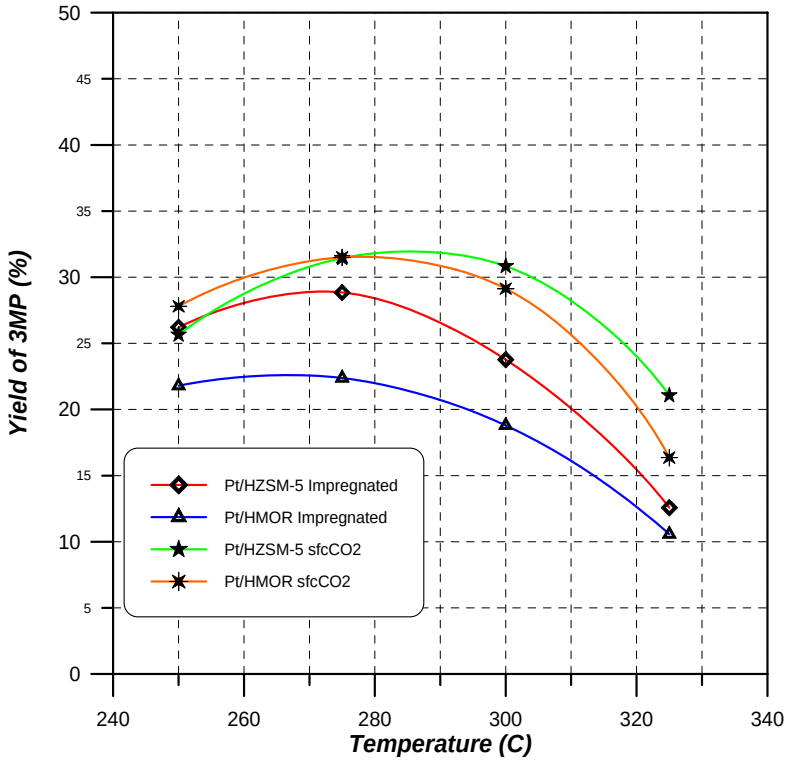

Figure 5-38: Yield of 3MP vs. Temperature for Zeolites Pt/HZSM-5 and Pt/HMOR at Pressure 5bar and H/HC=9

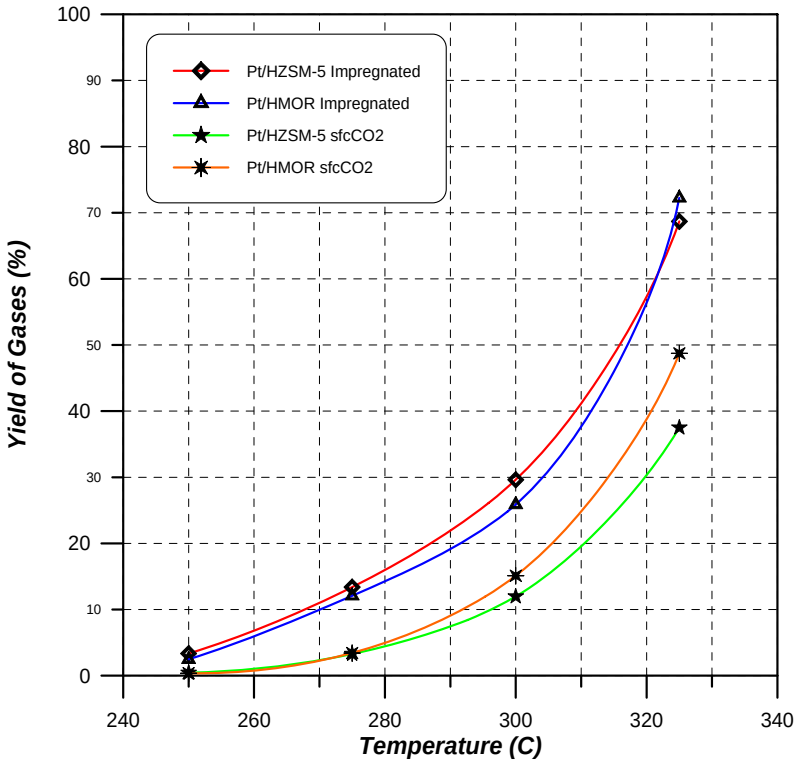

Figure 5-39: Yield of (C_1-C_4) vs. Temperature for Zeolites Pt/HZSM-5 and Pt/HMOR at Pressure 5bar and H/HC=3

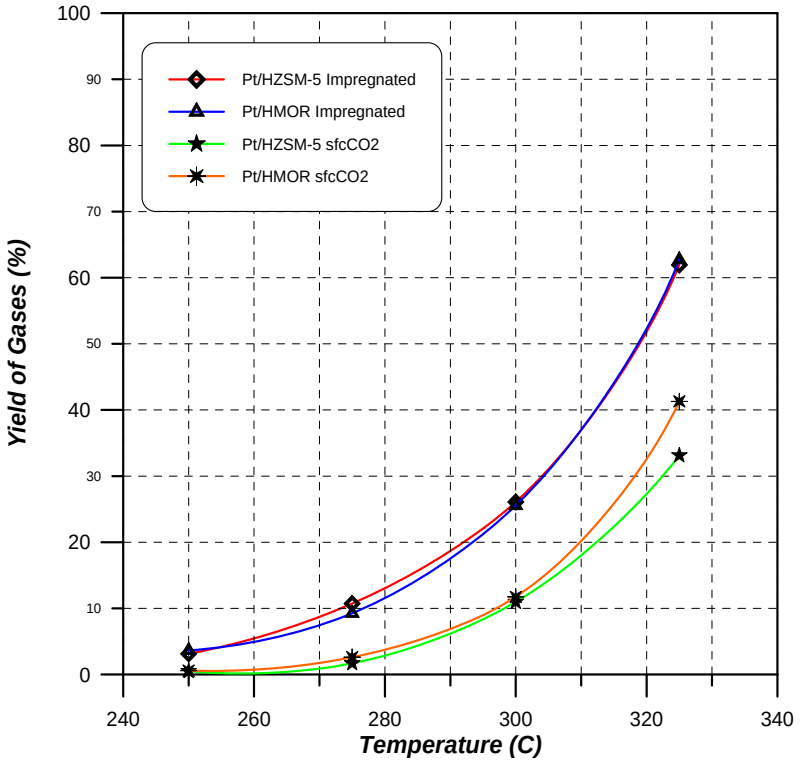

Figure 5-40: Yield of (C_1-C_4) vs. Temperature for Zeolites Pt/HZSM-5 and Pt/HMOR at Pressure 5bar and H/HC=6

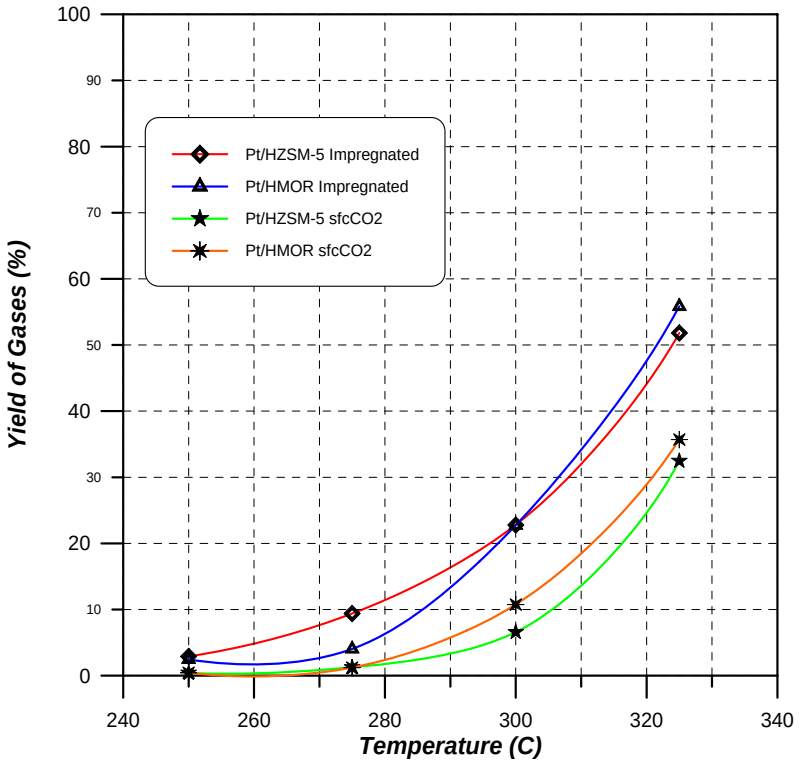

Figure 5-41: Yield of (C_1-C_4) vs. Temperature for Zeolites Pt/HZSM-5 and Pt/HMOR at Pressure 5bar and H/HC=9

5.5.3 Platinum on Cation Modified Zeolites

5.5.3.1 Temperature Effect

The catalytic behavior of Platinum supported on cationic forms, Strontium and Barium of ZSM-5 and Mordenite zeolites were studied on hydroconversion of n-Hexane. The Platinum was loaded in supercritical carbon dioxide in all catalyst types studied. The experimental investigation was aimed to show the effectiveness of Strontium and Barium modified zeolites and whether the loading in $scCO_2$ affected the isomerization reaction.

Figures 5-42 through 5-45 show the conversion and selectivity variations with temperature at a pressure 5 bar for these types of catalysts at different H_2/HC ratios. Platinum loading on ZSM-5 and Mordenite zeolite in supercritical carbon dioxide resulted in active and stable catalysts. The trend

of temperature effect on the percent conversion of n-Hexane and the selectivity of isomerization is approximately similar for all catalyst types studied. That gradual increase of conversion with temperature increase was observed, mainly in the range 250 to 300 ^{o}C. The selectivity was near or above 90 % up to 300 ^{o}C for these catalysts.

It was observed generally, that Ba^{++} and Sr^{++} modified ZSM-5 Platinum catalysts are more active and selective than thus Pt loaded on Ba^{++} and Sr^{++} Mordenite zeolite. Both Pt/SrZSM-5 and Pt/BaZSM-5 show nearly similar catalytic behavior, as shown in figures 5-42 and 5-43 respectively. While, Pt/SrMOR is more active and selective as Pt/BaMOR as illustrated in figure 5-44 and 5-45.

The variation of H_2/HC ratio in the range of 3-9 had a little effect on these catalyst types. In general higher conversions and selectivity's were observed by increasing the hydrogen to partial pressure.

It could be concluded that temperature of 300 ^{o}C is optimum to get about 96- 97 % isomerization selectivity with about 77 % conversion by using Platinum loaded on Sr and Ba-ZSM-5. While about 78- 83 % were achieved with Barium and Strontium Mordenite platinum catalysts.

Figures 5-46 through 5-51 show a comparative study of catalytic behavior of Platinum loaded on ZSM-5 and MOR zeolites of H^{+}, Sr^{++} and Ba^{++} cations on hydroconversion of n-hexane at different temperatures and H_2/HC ratios. The performances of these catalysts are compared in table 5-9 as percentage conversion of n-Hexane, and percentage selectivity towards the isomerized product, at 300 ^{o}C, 5 bar and 3 H_2/HC ratio. This comparison indicates clearly, that Platinum loaded on H- Sr- and Ba- forms of ZSM-5 and Mordenite zeolites gave around 77- 80 % conversion of n-Hexane at 300 ^{o}C and H_2/HC ratio of 3. While, the selectivity's towards the isomerized product were enhanced noticeable on catalysts of Strontium and Barium forms. Table

5-9 also indicates that ZSM-5 catalysts possess higher selectivity, about 96 % compared with MOR catalysts with 90 %.

5.5.3.2 Yield

The yields of desired isomers 2MP and 3MP and undesired crack gases C_1-C_4 were investigated in presence of Strontium and Barium cations modified ZSM-5 and Mordenite Platinum catalysts.

Figure 5-52 and 5-53 show the yields of cracked gases as function of temperature for original H-Forms and by Strontium and Barium modified ZSM-5 and Mordenite loaded with Platinum catalysts respectively. The results show that the yields of cracked gases increases rapidly with increasing temperature on H-Form zeolite support. Thus about 38 and 48 % C_1-C_4 yields were achieved on Pt/HZSM-5 and Pt/HMOR catalysts respectively at 325°C. Those indicating, that these types are active cracking catalysts, at high temperature, such as 325 ^{o}C, particularly Pt/HMOR type.

Furthermore, the Strontium and Barium cations modified Platinum zeolites show noticeable lower tendency toward cracking reactions reaching maximum yield of around 10 % and 21-26 % for ZSM-5 and MOR zeolites. The yields of C_1-C_4 gases were about 5 % and 7- 10 % at 300 ^{o}C for the above mentioned catalysts, which are quite low. Moreover Ba- and Sr-Forms of Pt/ZSM-5 was less selective toward the cracking reactions than the corresponding Mordenite support, as shown in table 5-9.

Table 5-9: Catalytic Performance of Platinum Loaded by $scCO_2$ on Different Cation Forms ZSM-5 and MOR Zeolites by Hydroconversion of n-Hexane at 300 ^oC, 5 bar 3 H_2/HC Ratio.

Catalyst	% Conversion	% Selectivity	% Yield of 2MP and 3MP	% Yield of (C_1-C_4)
Pt/HZSM-5	78.0	84.5	61.0	13.0
Pt/SrZSM-5	77.0	96.0	70.0	5.5
Pt/BaZSM-5	77.0	96.0	70.0	5.0
Pt/HMOR	80.0	78.0	55.5	15.0
Pt/SrMOR	80.0	90.0	54.0	7.5
Pt/BaMOR	78.0	87.0	47.0	10.0

The yields of the more desired C_6–isomers, 2MP and 3 MP are illustrated in figures 5-54 through 5-57 as function of temperature for Platinum supported on the different ZSM-5 and MOR zeolites cationic forms.

The yields of 2MP and 3MP isomers were increased as temperature increase from 250 ^oC up to 300 ^oC, and then decreased at about 325 ^oC on all catalyst types considered in present investigation. Therefore, temperature of 300 ^oC could be considered as an optimum for higher yield of 2MP+3MP. ZSM-5 catalysts were more active for these isomers than MOR catalysts.

Total yields of 2MP and 3MP are 61% for Pt/HZSM-5 and about 70 % for Pt loaded on Sr- and Ba-ZSM-5 zeolites at 300 ^oC. While the corresponding values for Pt loaded on H-Sr- and BaMOR are in the range of 47-55% at 300 ^oC as shown in table 5-9.

Figure 5-58 and 5-59 show the yield of more volatile isomers, Dimethylbutanes for Platinum loaded in all forms of ZSM-5 and MOR zeolites respectively. Zeolite Mordenite was highly selective to DMB's rather than zeolite ZSM-5, the reversion of DMB's selectivity may be attributed to the combined effect of acidity; channel structure including pore size and

dispersion as well as distribution of metallic centers. In addition the acidity of MOR was much higher than that of ZSM-5. At high contact time, the residence time of carbonium ions on acid site would become much larger and thus the structure effect and metal function in zeolite channels appear to play important roles in the formation of DMB's. Therefore the changing of hydrogen cation was affected on the acidity of Pt/MOR from the increasing of DMB's selectivity. The yields of these isomers were significant low for Pt loaded on ZSM-5 zeolite forms around 2.5- 5 % at 300°C. While at the same temperature for zeolite Mordenite this value to vary from 6 to 20 %. The corresponding values for HZSM-5 and HMOR catalyst forms were 5 and 6 % respectively. These indicate that the replacement of H^{+} cation by Sr^{++} and Ba^{++} catios enhances the acid-site and improved the surface characteristics zeolite catalysts.

In Summary, the Sr- and Ba- modified catalysts were high selective even though at high temperature about 325°C as shown in figures 5-46 to 5-49. The selectivity's of H-zeolites decreased dramatically at 325 ^{o}C, reaching around 38-60%. The lowest value (38 %) was achieved with Pt/HMOR catalysts. Increasing of H_2/HC ratio from 3 to 9 gave a slight increase of the selectivity of these catalysts. While the increasing of hydrogen partial pressure reduced the conversion in a little value. The improving of acid site was clearly shown for zeolite Mordenite by increasing the value of DMB's from 6% to 18 % for Ba cation and 20 % for Sr cation, while for zeolite ZSM-5 the value of DMB's decreased from 5% to ~3% for Ba and Sr cations.

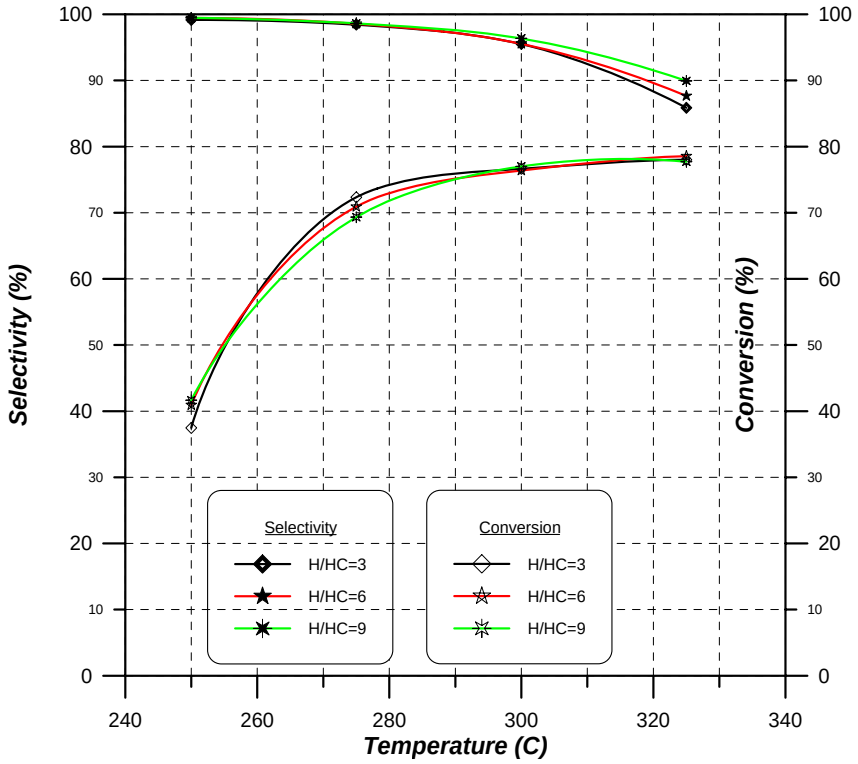

Figure 5-42:Selectivity and Conversion vs. Temperature for Zeolite Pt/SrZSM-5 at P=5bar and H/HC=3, 6 and 9

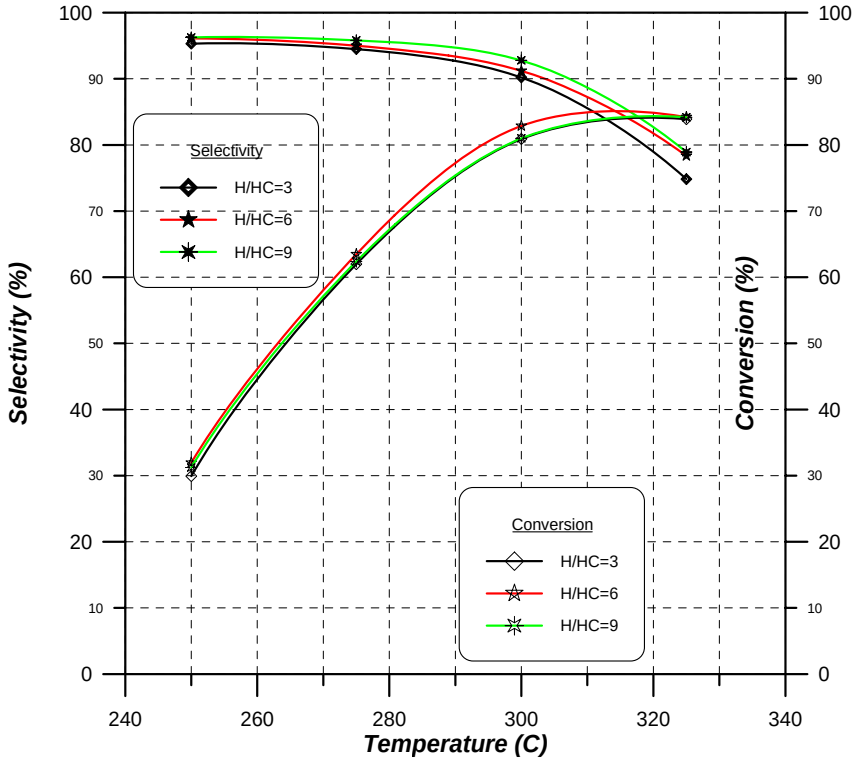

Figure 5-43:Selectivity and Conversion vs. Temperature for Zeolite Pt/SrMOR at P=5bar and H/HC=3, 6 and 9

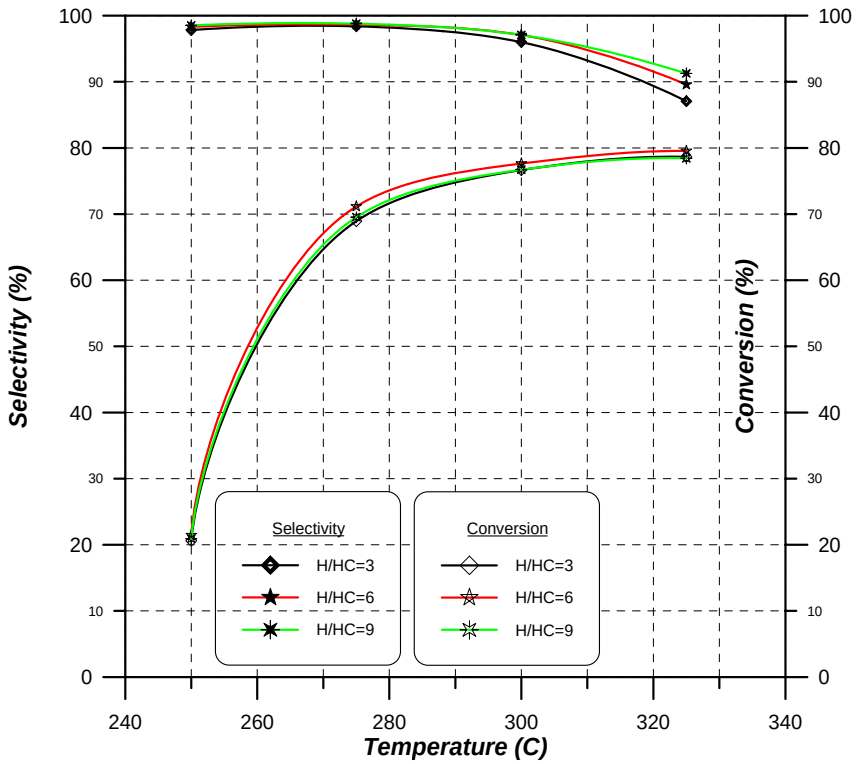

Figure 5-44:Selectivity and Conversion vs. Temperature for Zeolite Pt/BaZSM-5 at P=5bar and H/HC=3, 6 and 9

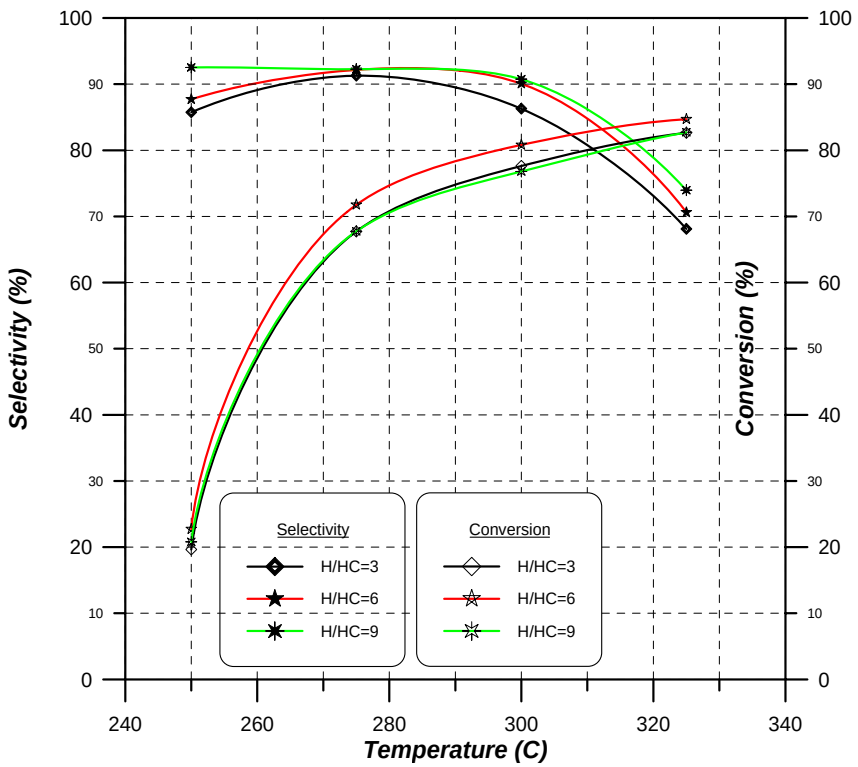

Figure 5-45:Selectivity and Conversion vs. Temperature for Zeolite Pt/BaMOR at P=5bar and H/HC=3, 6 and 9

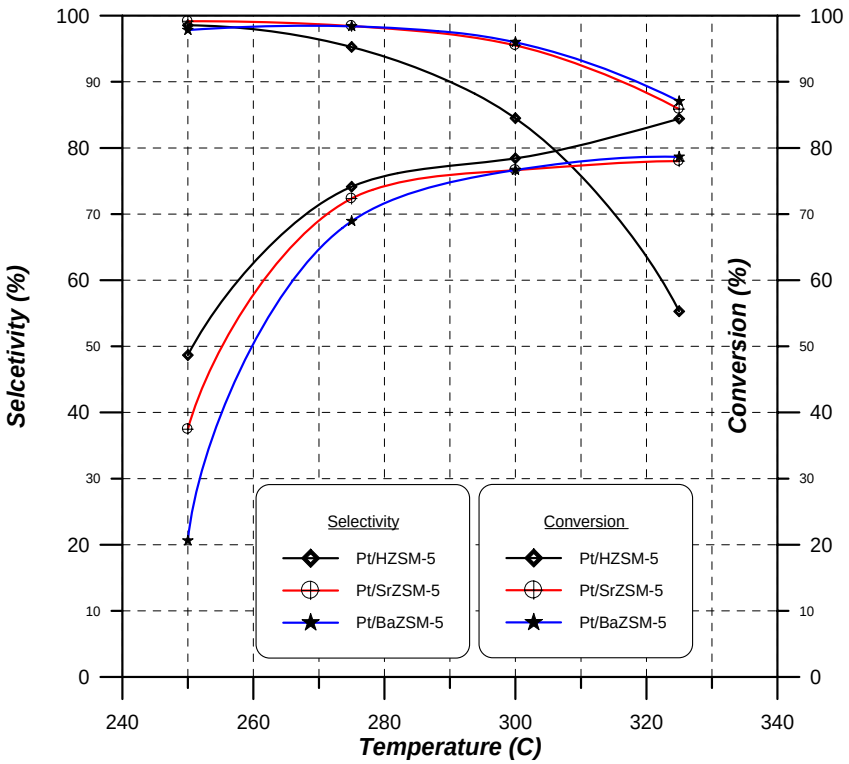

Figure 5-46: Selectivity and Conversions vs. Temperature at H/HC=3 and P=5bar for Pt on H, Sr and BaZSM-5 Zeolite

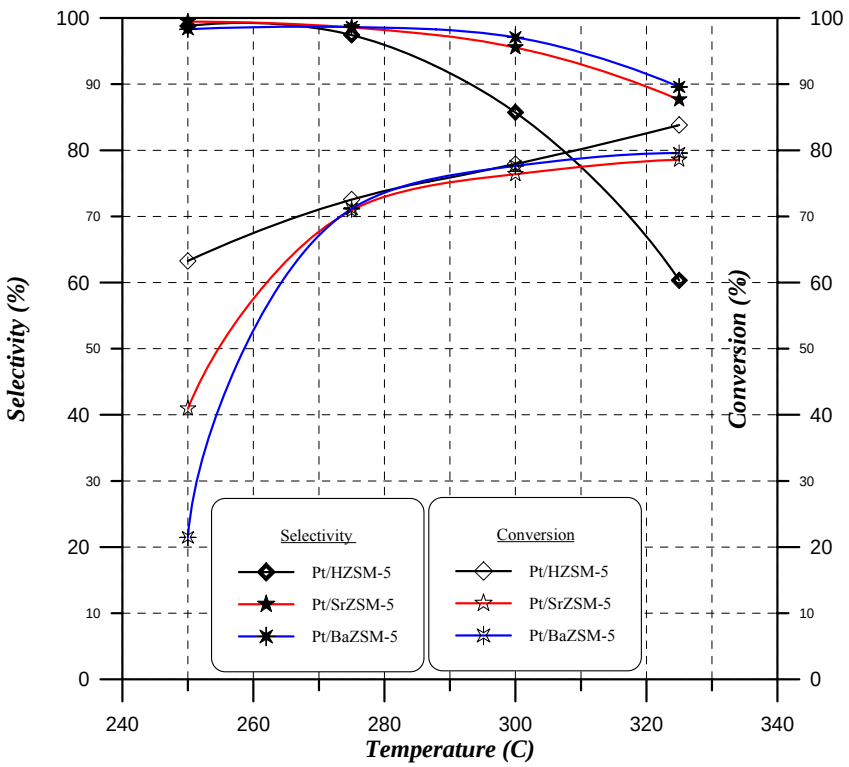

Figure 5-47: Selectivity and Conversions vs. Temperature at H/HC=6 and P=5bar for Pt on H, Sr and BaZSM-5 Zeolite

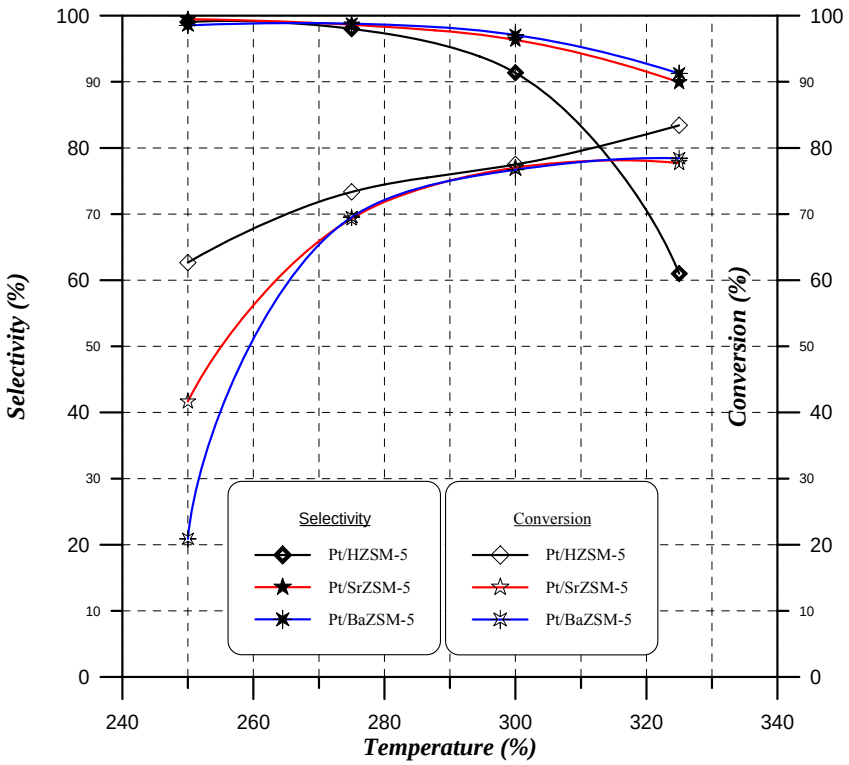

Figure 5-48: Selectivity and Conversions vs. Temperature at H/HC=9 and P=5bar for Pt on H, Sr and BaZSM-5 Zeolite

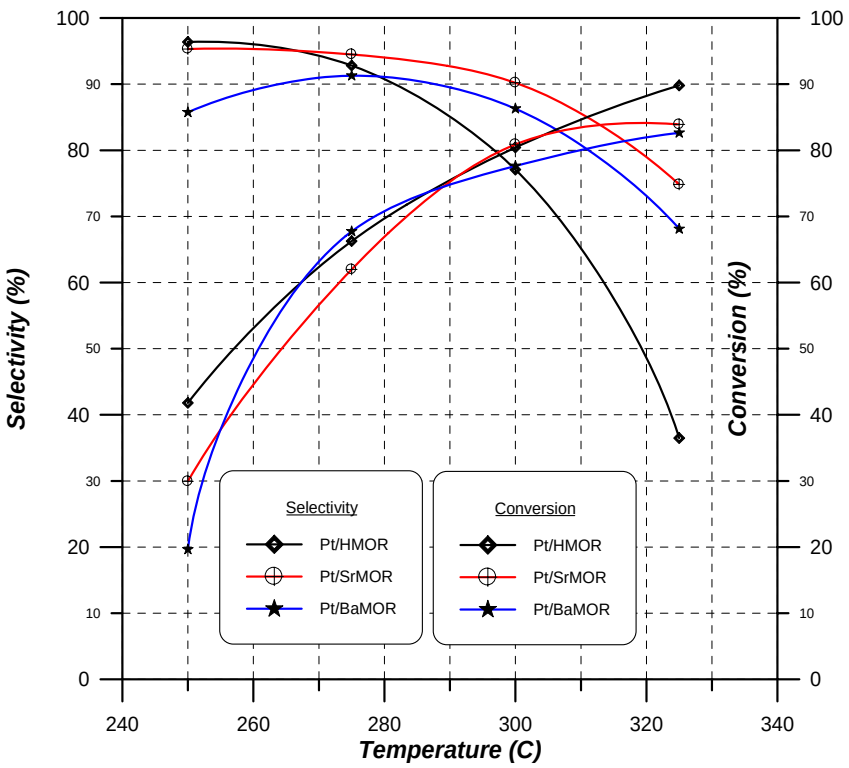

Figure 5-49: Selectivity and Conversions vs. Temperature at H/HC=3 and P=5bar for Pt on H, Sr and BaMOR Zeolite

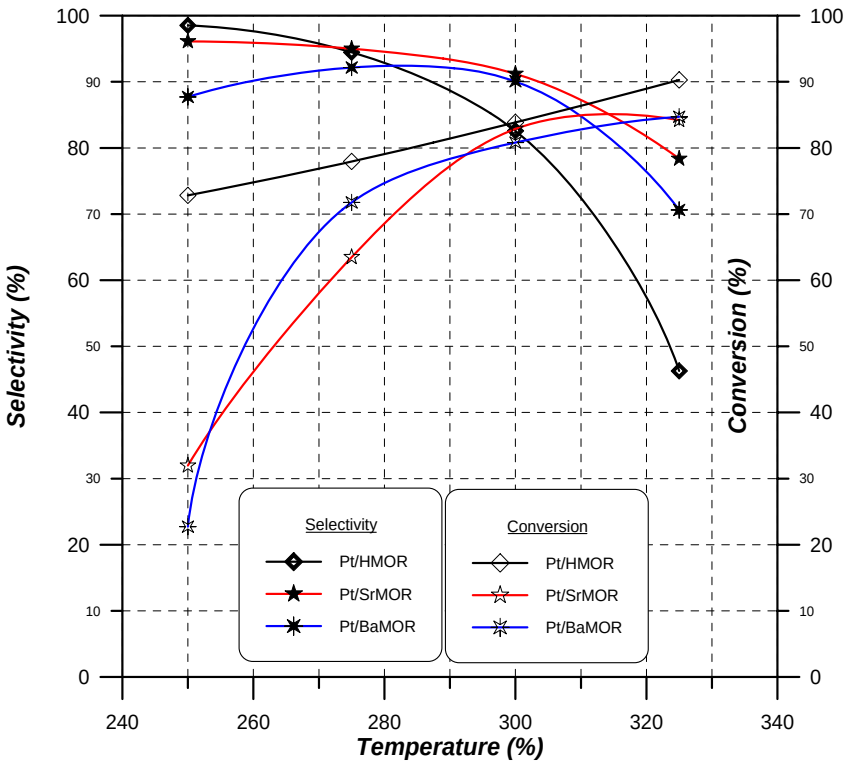

Figure 5-50: Selectivity and Conversions vs. Temperature at H/HC=6 and P=5bar for Pt on H, Sr and BaMOR Zeolite

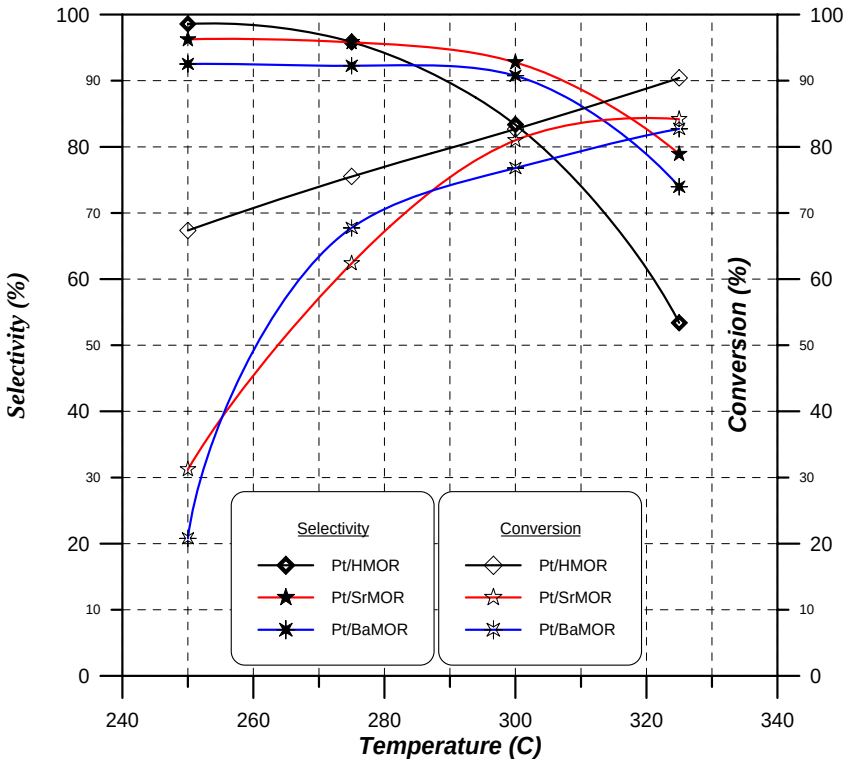

Figure 5-51: Selectivity and Conversions vs. Temperature at H/HC=9 and P=5bar for Pt on H, Sr and BaMOR Zeolite

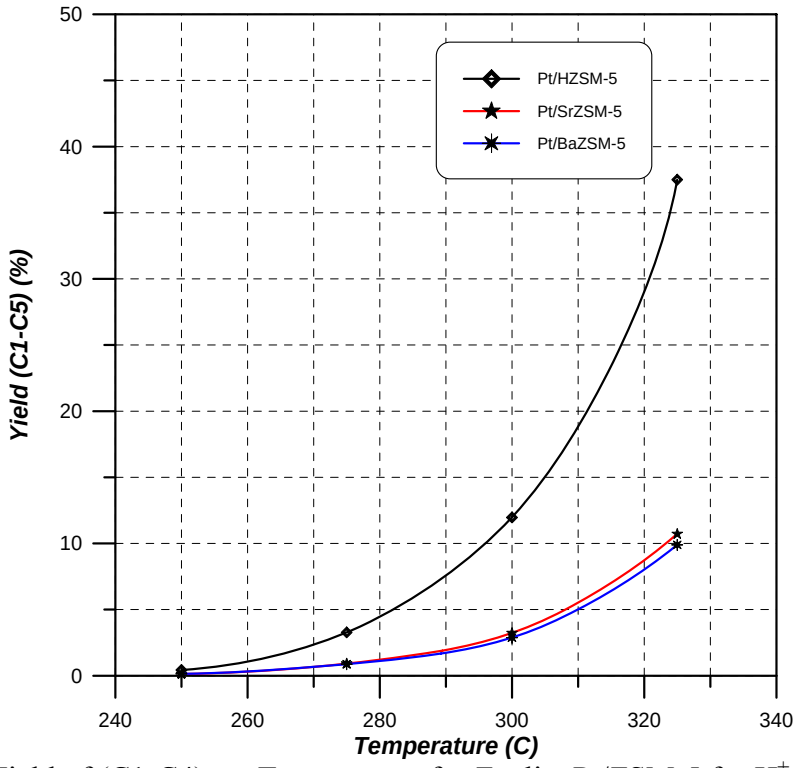

Figure 5-52:Yield of (C1-C4) vs. Temperature for Zeolite Pt/ZSM-5 for H^{+}, Sr^{++} and Ba^{++} catios at P=5bar and H/HC=3

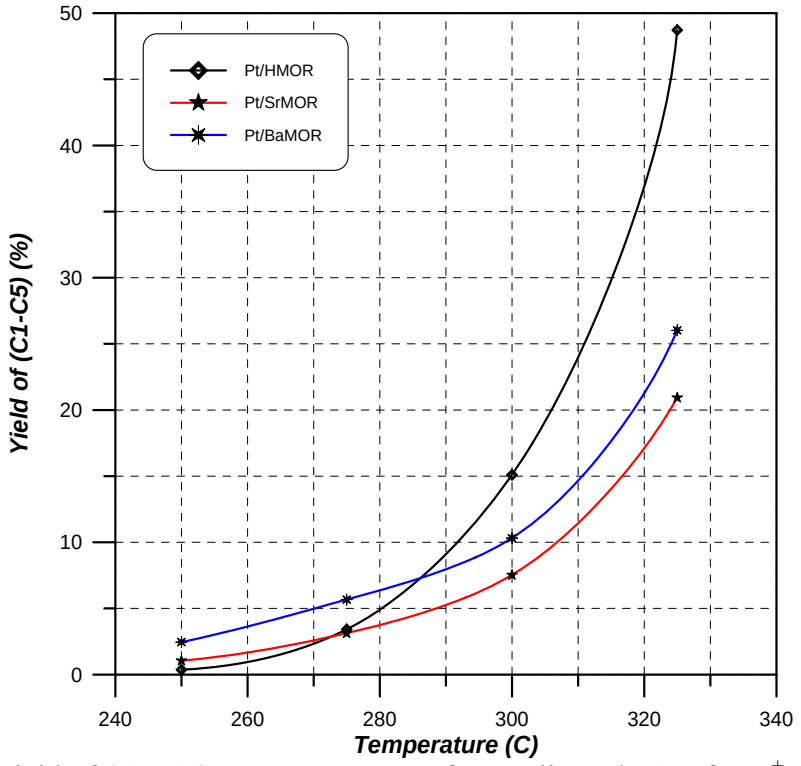

Figure 5-53:Yield of (C1-C4) vs. Temperature for Zeolite Pt/MOR for H^{+}, Sr^{++} and Ba^{++} catios at P=5bar and H/HC=3

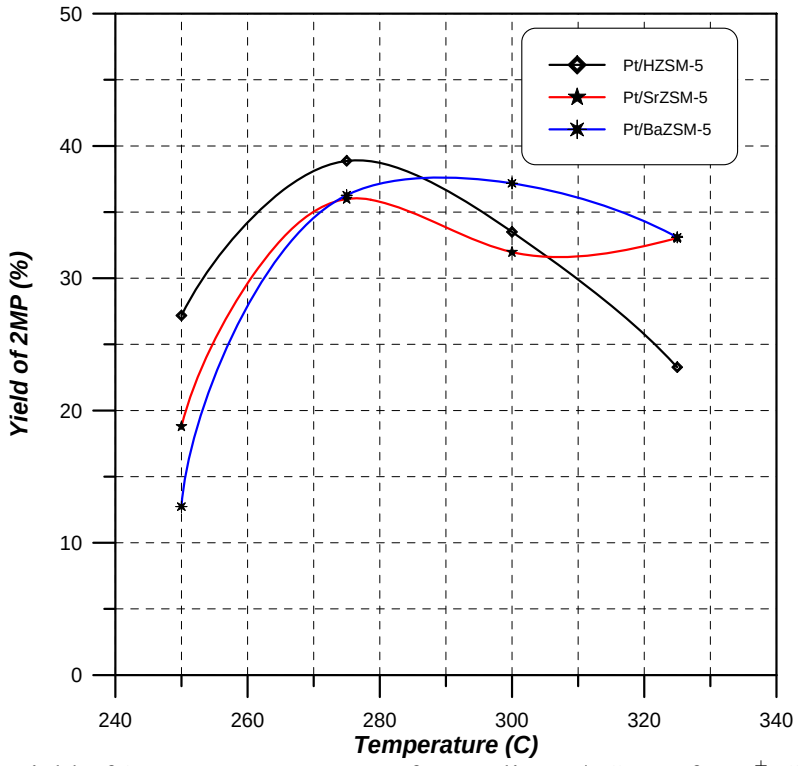

Figure 5-54:Yield of 2MP vs. Temperature for Zeolite Pt/ZSM-5 for H^{+}, Sr^{++} and Ba^{++} catios at P=5bar and H/HC=3

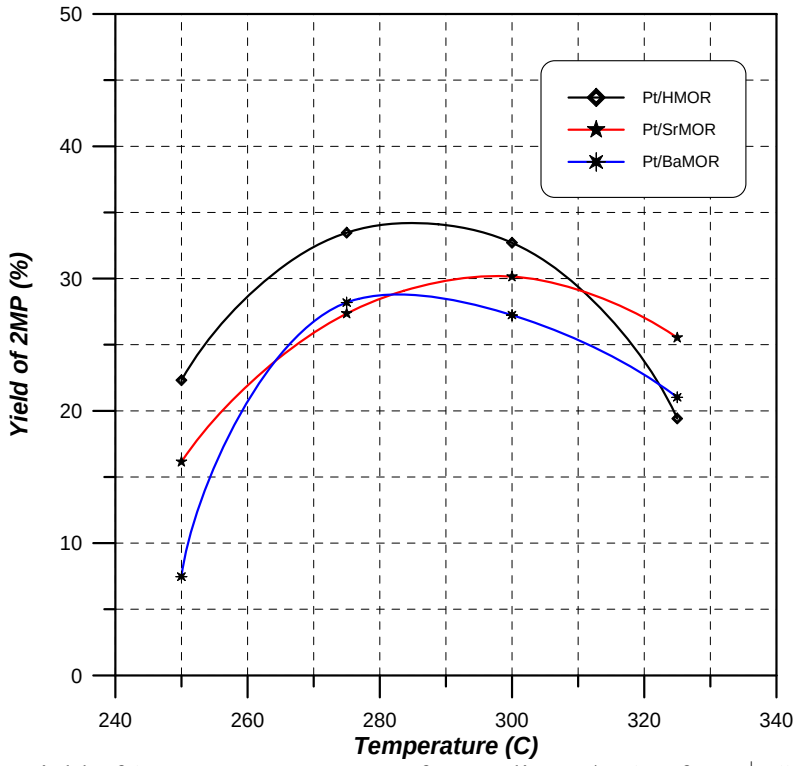

Figure 5-55:Yield of 2MP vs. Temperature for Zeolite Pt/MOR for H^{+}, Sr^{++} and Ba^{++} catios at P=5bar and H/HC=3

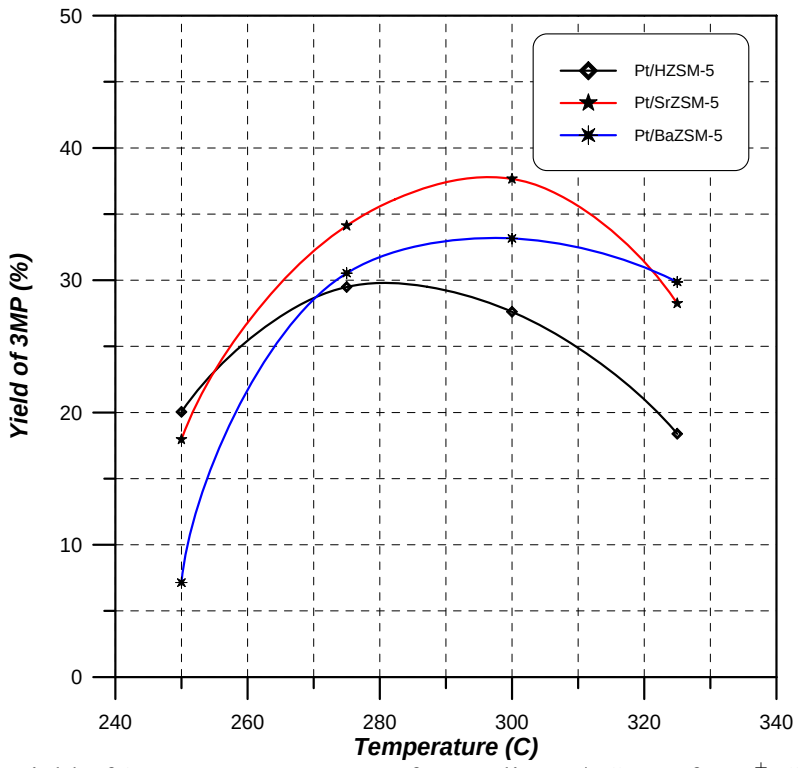

Figure 5-56:Yield of 3MP vs. Temperature for Zeolite Pt/ZSM-5 for H^{+}, Sr^{++} and Ba^{++} catios at P=5bar and H/HC=3

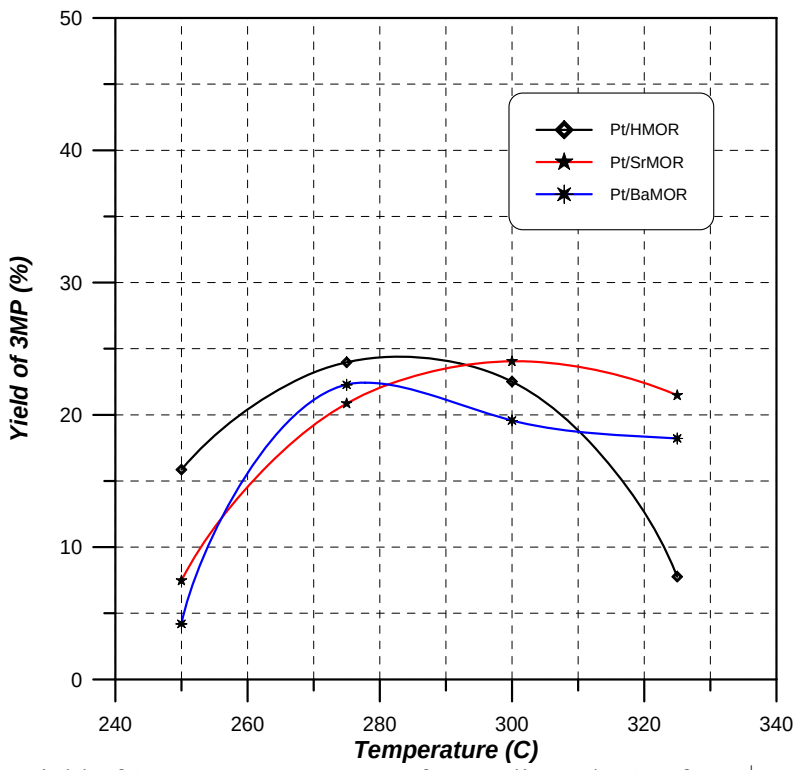

Figure 5-57:Yield of 3MP vs. Temperature for Zeolite Pt/MOR for H^{+}, Sr^{++} and Ba^{++} catios at P=5bar and H/HC=3

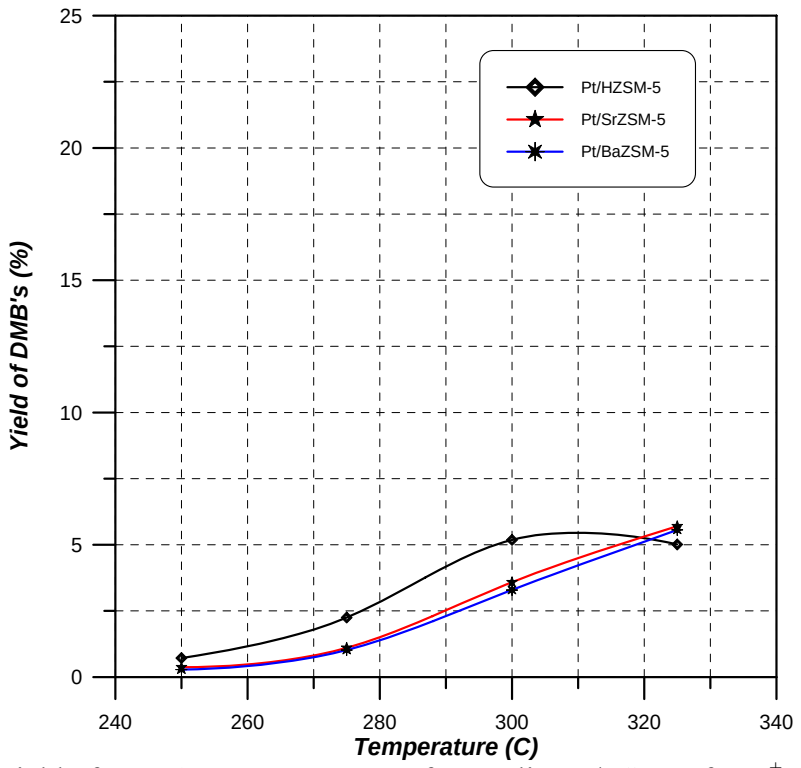

Figure 5-58:Yield of DMB's vs. Temperature for Zeolite Pt/ZSM-5 for H^{+}, Sr^{++} and Ba^{++} catios at P=5bar and H/HC=3

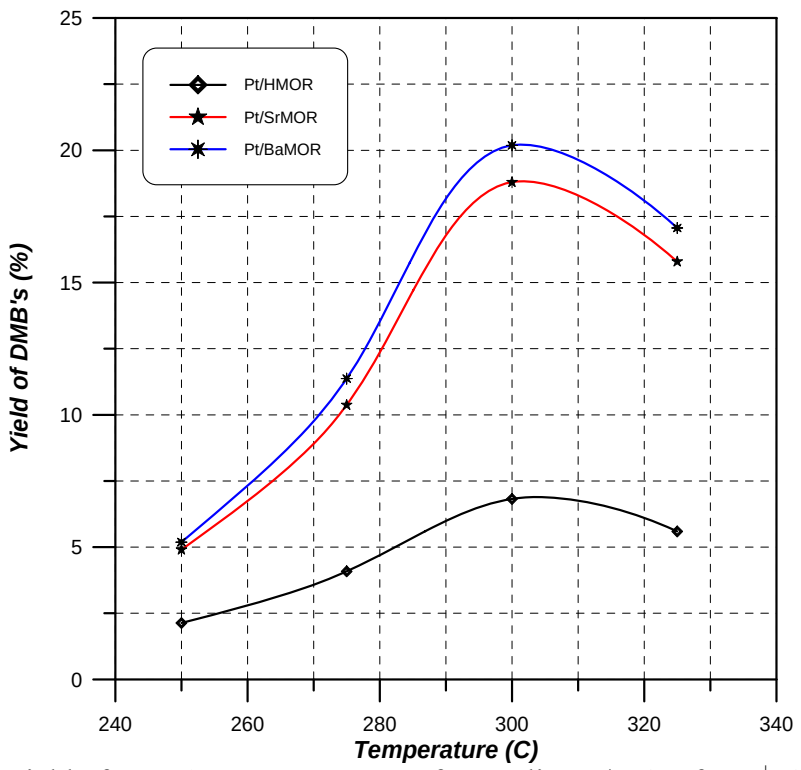

Figure 5-59:Yield of DMB's vs. Temperature for Zeolite Pt/MOR for H^{+}, Sr^{++} and Ba^{++} catios at P=5bar and H/HC=3

5.5.4 Multi Metal over Zeolite Catalysts

It is well known that the addition of a second metal, such as Rhenium, Indium and Tin to the platinum supported catalyst enhances the selectivity and stability in catalytic reforming processes [155]. Therefore Ruthenium and Zirconium were used in addition to Platinum to prepare bi-and trimetallic zeolite catalysts by loading in supercritical carbon dioxide. Since, there are no or little publications were done about these metals. The performance of the multimetal catalysts were studied on hydroconversion of n-Hexane at 5 bar pressure, 250-325 ^{o}C temperature and 3, 6 and 9 H_2/HC ratios. An attention was done on the percent conversion of n-Hexane and on the selectivity of isomerized product, to show however any improvement could be observed by addition of Ru and Zr to Platinum catalysts.

Figures 5-60 and 5-61 show the conversion and selectivity variation with temperature for PtRu/HZSM-5 and PtRu/HMOR catalysts at different H_2/HC ratios. The results show that the presence of Ru in both catalyst types was enhanced the conversion of n-Hexane noticeable. Those above 95 % conversion were achieved, particular at H_2/HC ratio above 3. While, the selectivity's towards the isomerized Hexane were low. It was observed that most of the prepared catalyst possess extremely high C-C bond splitting activity in hydrocarbons. The temperature dependence of the product distribution showed a strong predominance of Ethane and Methane, indicating that the Ruthenium zeolite catalysts are active for hydrocracking reactions rather than for isomerization.

Similar observation was noticed for Sr- and Ba- cations zeolites. The PtRu/SrZSM-5, PtRu/BaZSM-5, PtRu/SrMOR and PtRu/BaMOR catalysts were very active towards the conversion of n-Hexane, but low selective for the isomerization, as show in figures 5-62, 5-63, 5-64 and 5-65 respectively.

The variation of H_2/HC ratio had little effect on performance of Ruthenium contains catalysts. The increases in Hydrogen partial pressure increased the selectivity slightly.

The loading of Zirconium with Platinum on HZSM-5 and HMOR resulted in noticeable increase in the selectivity for both zeolite types compared with PtRu bimetallic, as shown in figures 5-66 and 5-67 respectively. The selectivity towards the isomerized product decreases dramatically at 325 ^{o}C for both catalyst types. This suggest that bimetallic zeolite catalysts with Pt and Zr are active for cracking reactions at temperature 325 ^{o}C and above, particularly for HMordenite type. The later gave high conversion of n-Hexane around 86-92% with more than 50 % selectivity to cracking product. Here again, the increase of H_2/HC ratio decreases the conversion slightly and leading in a little increase of the selectivity for both catalyst types.

Figures 5-68 and 5-69 represent the activity and selectivity of PtZr/SrZSM-5 and PtZr/BaZSM-5 catalysts. The results show that incorporation of metallic cation enhances the selectivity towards the isomerized products particularly at 300 ^{o}C, reaching above 95 % at a conversion above 75 %. Mordenite zeolite bimetallic catalysts have about similar general trend, as shown in figures 5-70 and 5-71 for Strontium and Barium cation forms respectively.

A comparison of Pt and PtZr loaded HZSM-5 and HMOR zeolite catalysts on selectivity of more desired isomers (Methylepentane) are shown in figure 5-72 as function of temperature. The selectivity posses through a maximum at about 275 ^{o}C for all catalyst types. Highest selectivity of MP's was achieved on HZSM-5 zeolite support, where the bimetallic was more active reaching about 73 % at this temperature. While the corresponding selectivity on PtZr/HMOR was about 68%. Furthermore figure 5-73 shows

the effect of incorporation of Zr with Pt on selectivity of Dimethylbutanes isomers on HZSM-5 zeolite. It shows that the presence of Zirconium leads to less formation of DMB's, which enhances the selectivity of MP's formation, as illustrated in figure 5-72.

The performance of trimetallic catalysts, PtRuZr on HZSM-5 and HMOR zeolites were also investigated, as shown in figures 5-74 and 5-75 respectively. Data on these figures show similar behavior to that explained previously for Ruthenium loaded catalysts. Those a noticeable high conversion above 90% was observed for the temperature range studied. While the selectivity towards the isomerized product were very low below 30% and reaching less than 10 % for HZSM-5 supported trimetals at 300-325°C. This behavior can be explained that Ruthenium catalysts are in active for the isomerization reactions and are more suitable for cracking.

The trimetalls catalysts containing Ruthenium loaded on metal cations, Sr^{++} and Ba^{++} ZSM-5 and MOR zeolites were also in active for isomerization of n-Hexane as shown in figures 5-76 through 5-79. It was noticed that PtRuZr/SrZSM-5 has significant high conversion ability, of n-Hexane, (more than 97 %), mainly to cracked gaseous hydrocarbons, with significant low tendency for the isomerization reaction, ranging between about 5 to lower than 20 %, as shown in figure 5-76.

The catalytic behavior mono, di and trimetallic catalysts supported on HZSM-5 and HMOR zeolites are plotted on figures 5-80 to 5-85 at different temperatures and H_2/HC ratios. Moreover, table 5-10 summarized the catalytic behavior of these catalysts at 300 ^{o}C and H_2/HC ratio 3. The results indicate that the mono metallic Pt as well as the bimetallic PtZr loaded on HZSM-5 and HMOR are the most active and selective catalysts for isomerization of n-Hexane. While the Ru containing catalysts exhibit high

activity for hydroconversion of n-Hexane, producing significant amount of cracked gases.

Table 5-10: Hydroconversion of n-Hexane on Mono-Di and Trimetals Zeolite Catalysts at 300 ^{o}C and H_2/HC ratio=3

Catalyst	% X	% S	Catalyst	% X	% S
Pt/HZSM-5	88	86	Pt/HMOR	84	83
PtRu/HZSM-5	98	20	PtRu/HMOR	97	14
PtZr/HZSM-5	88	91	PtZr/HMOR	76	87
PtRuZr/HZSM-5	99	10	PtRuZr/HMOR	96	16

X: Conversion of n-Hexane, S: Selectivity towards isomerized producer

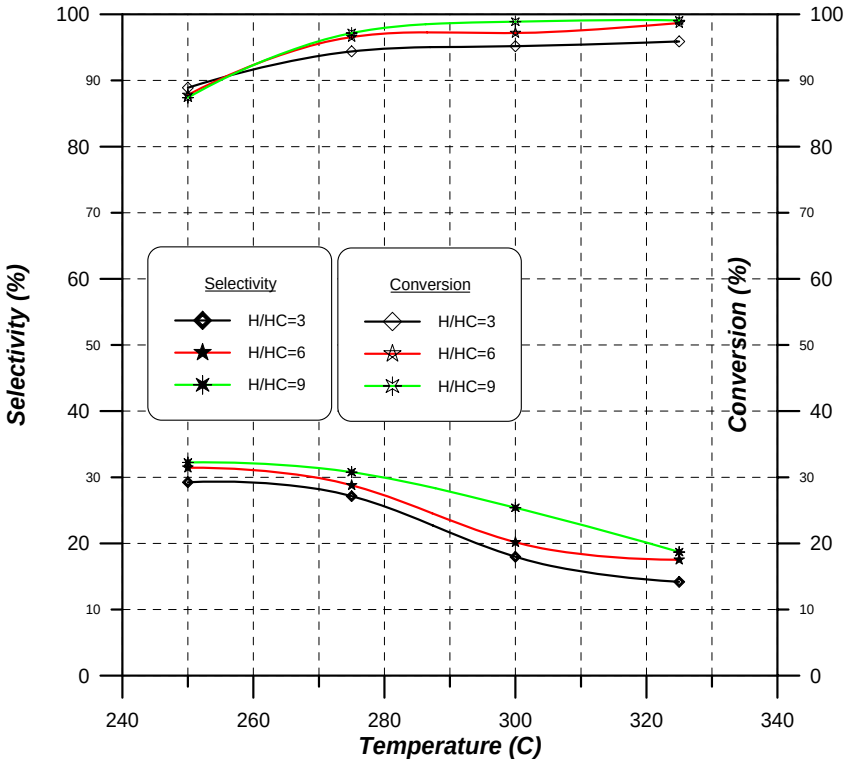

Figure 5-60:Selectivity and Conversion vs. Temperature for Zeolite PtRu/HZSM-5 at P=5bar and H/HC=3, 6 and 9

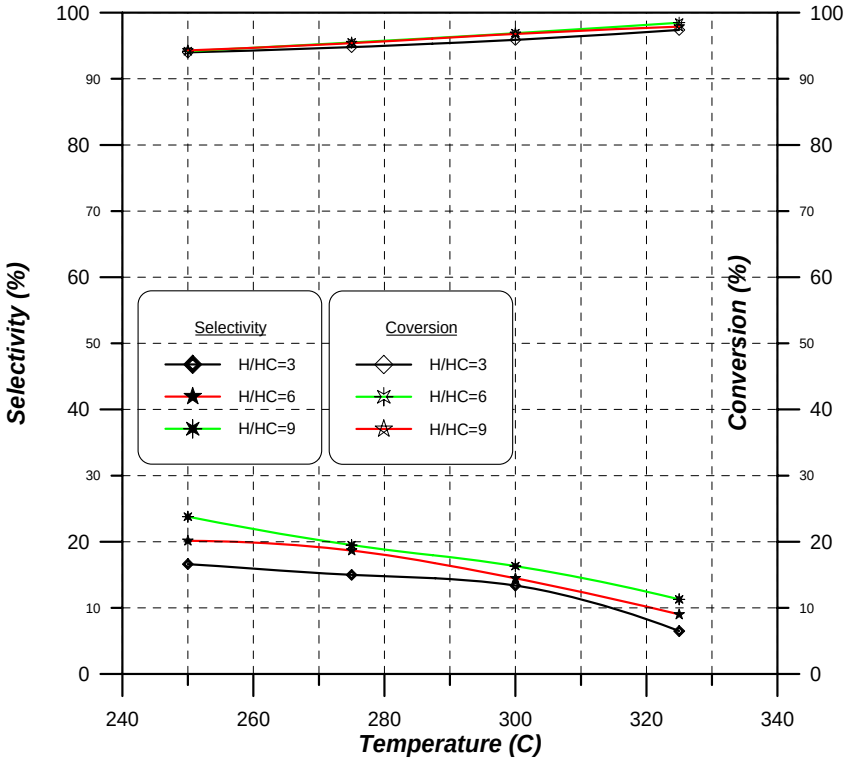

Figure 5-61:Selectivity and Conversion vs. Temperature for Zeolite PtRu/HMOR at P=5bar and H/HC=3, 6 and 9

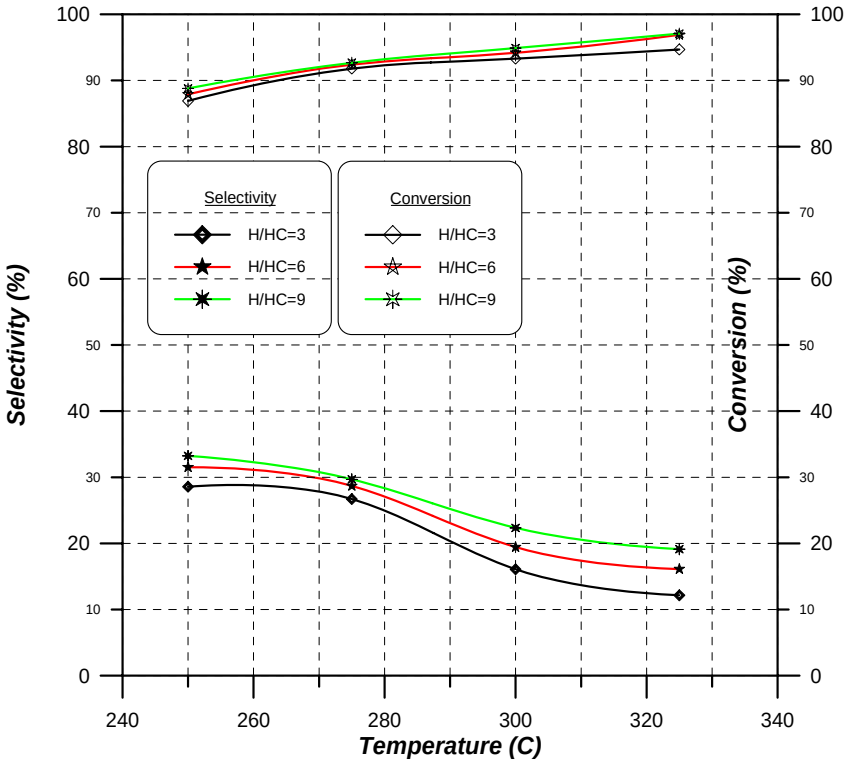

Figure 5-62:Selectivity and Conversion vs. Temperature for Zeolite PtRu/SrZSM-5 at P=5bar and H/HC=3, 6 and 9

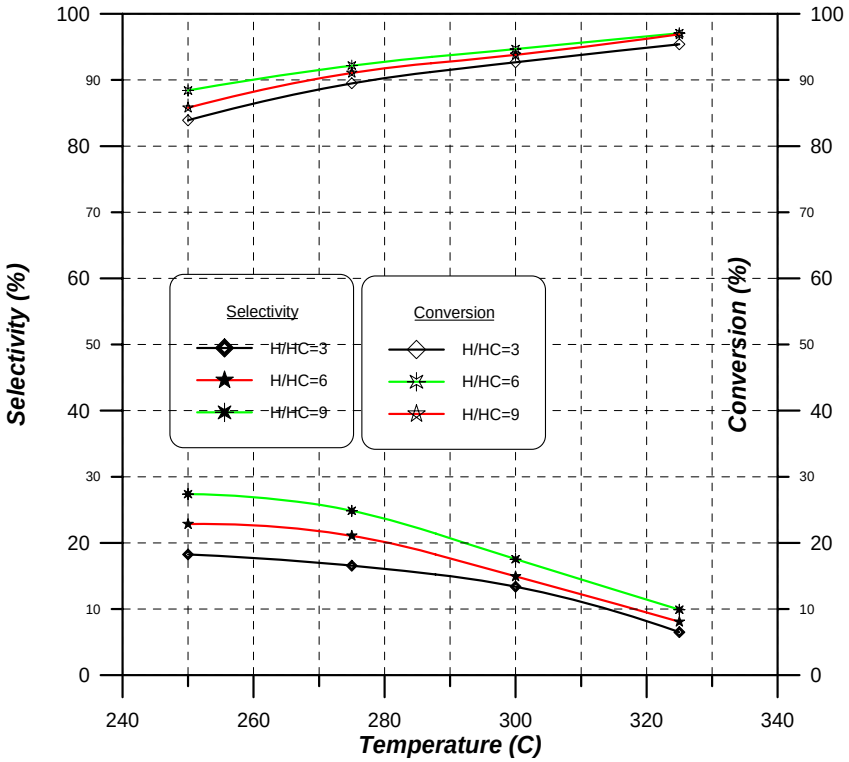

Figure 5-63:Selectivity and Conversion vs. Temperature for Zeolite PtRu/BaZSM-5 at P=5bar and H/HC=3, 6 and 9

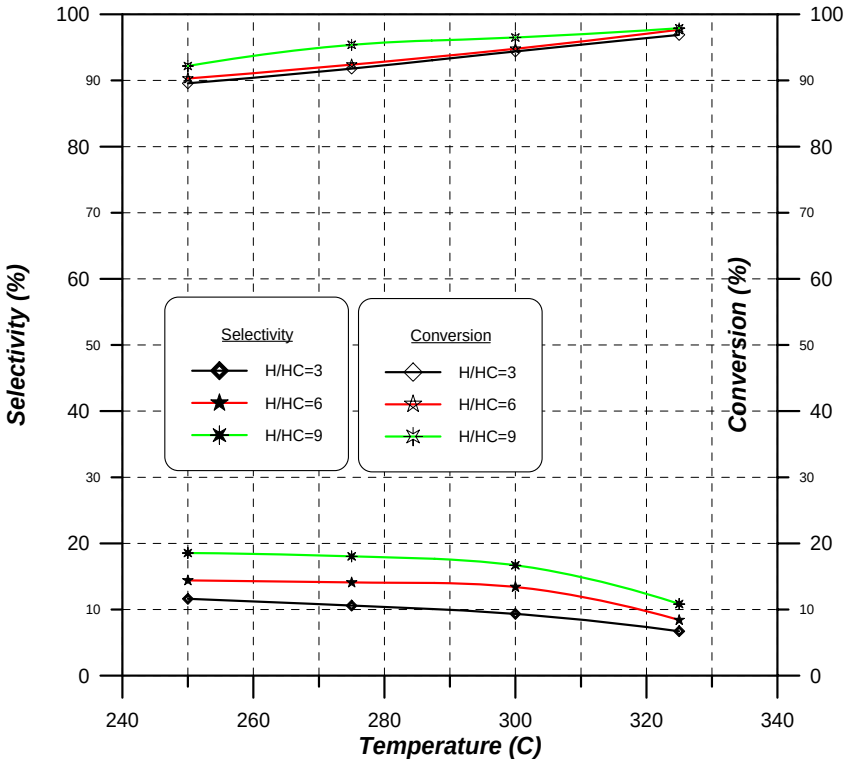

Figure 5-64:Selectivity and Conversion vs. Temperature for Zeolite PtRu/SrMOR at P=5bar and H/HC=3, 6 and 9

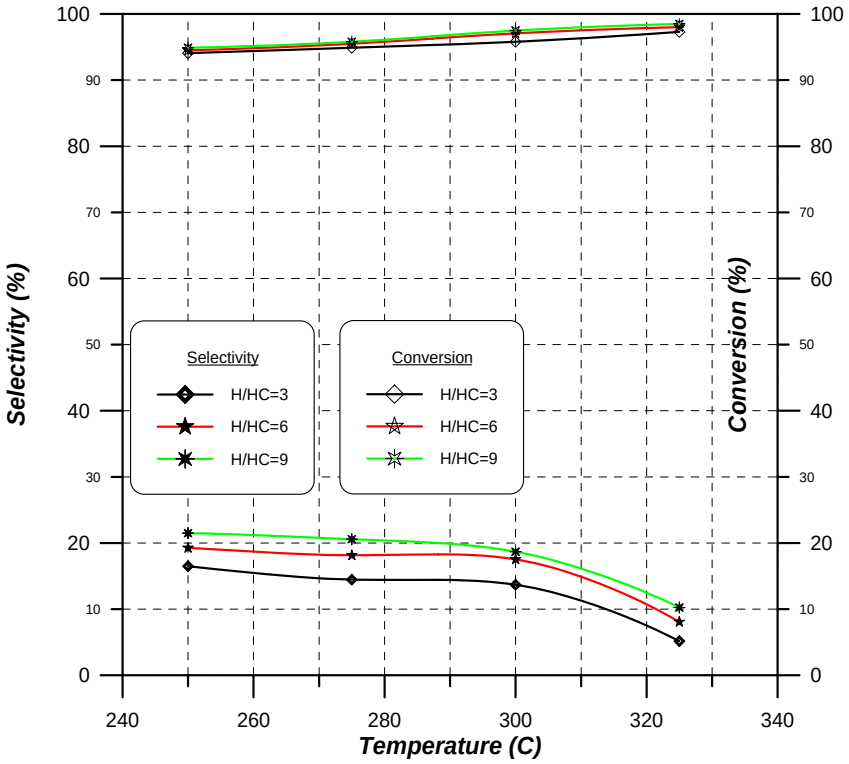

Figure 5-65:Selectivity and Conversion vs. Temperature for Zeolite PtRu/BaMOR at P=5bar and H/HC=3, 6 and 9

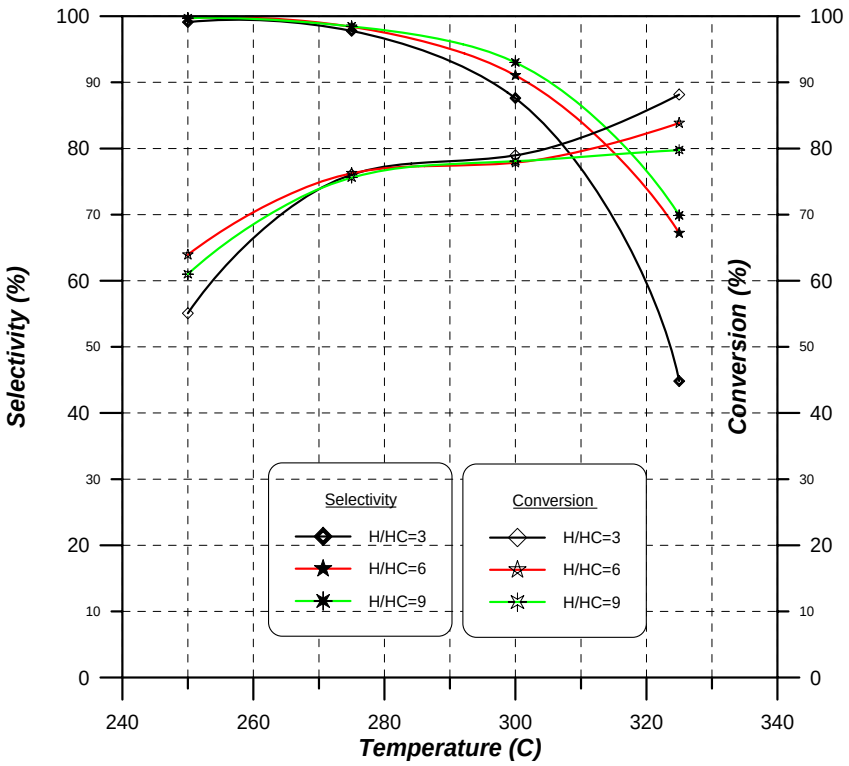

Figure 5-66:Selectivity and Conversion vs. Temperature for Zeolite PtZr/HZSM-5 at P=5bar and H/HC=3, 6 and 9

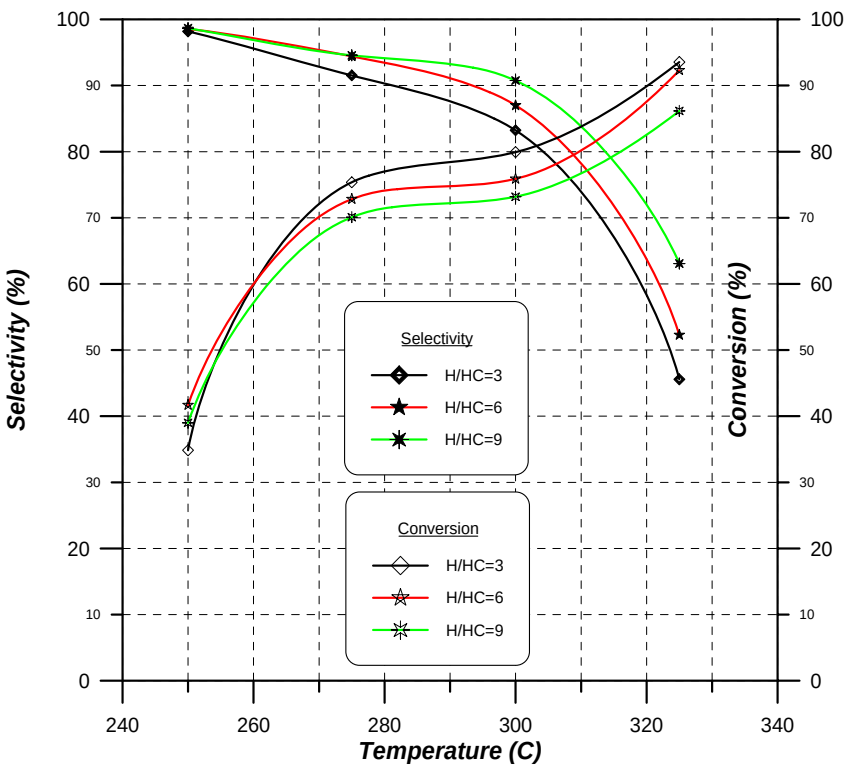

Figure 5-67:Selectivity and Conversion vs. Temperature for Zeolite PtZr/HMOR at P=5bar and H/HC=3, 6 and 9

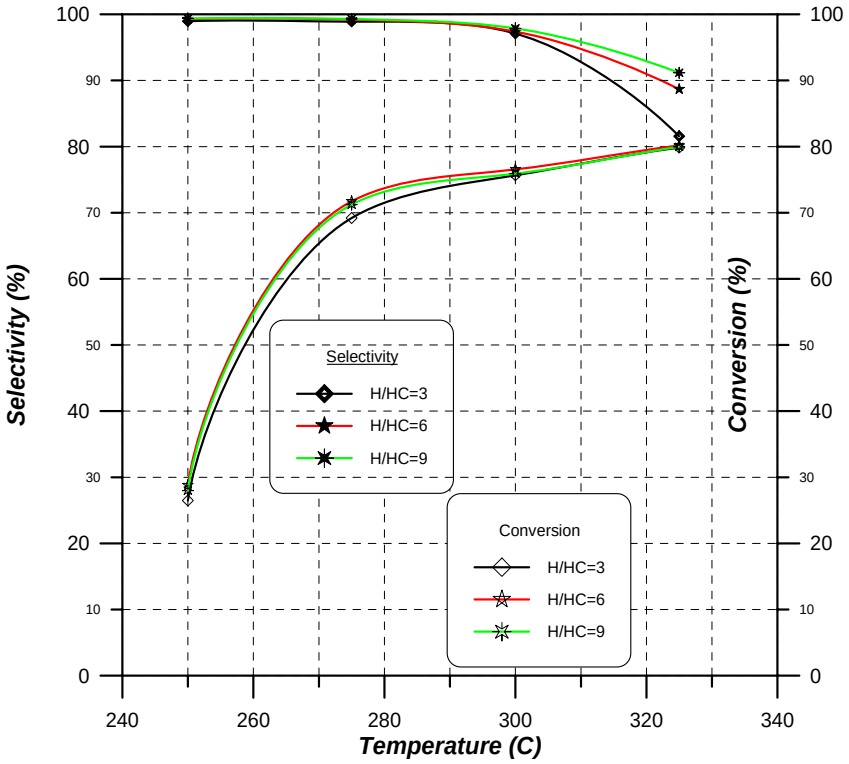

Figure 5-68:Selectivity and Conversion vs. Temperature for Zeolite PtZr/SrZSM-5 at P=5bar and H/HC=3, 6 and 9

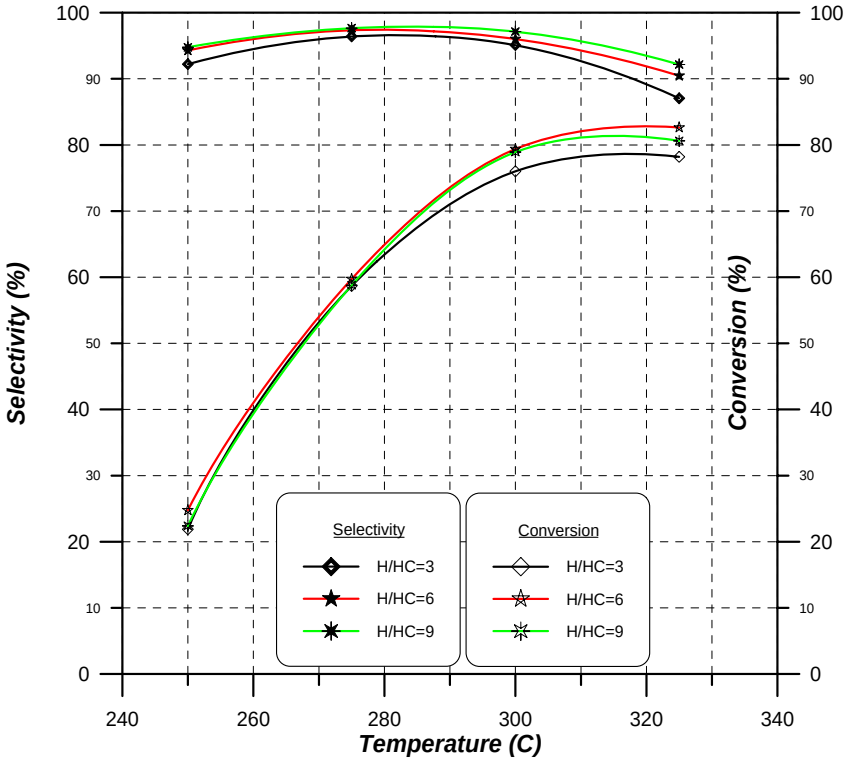

Figure 5-69:Selectivity and Conversion vs. Temperature for Zeolite PtZr/BaZSM-5 at P=5bar and H/HC=3, 6 and 9

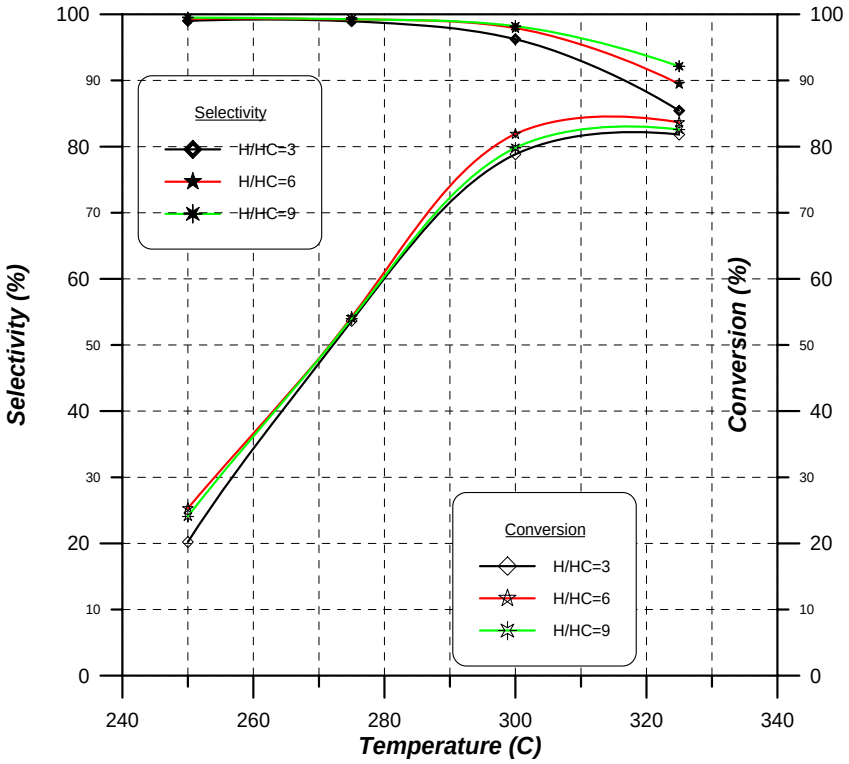

Figure 5-70:Selectivity and Conversion vs. Temperature for Zeolite PtZr/SrMOR at P=5bar and H/HC=3, 6 and 9

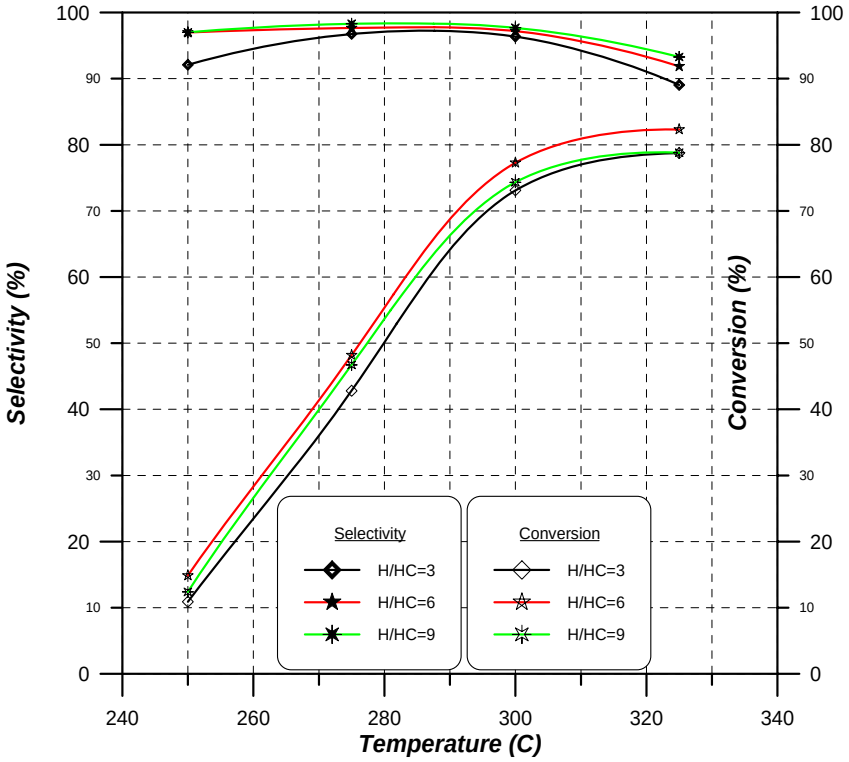

Figure 5-71:Selectivity and Conversion vs. Temperature for Zeolite PtZr/BaMOR at P=5bar and H/HC=3, 6 and 9

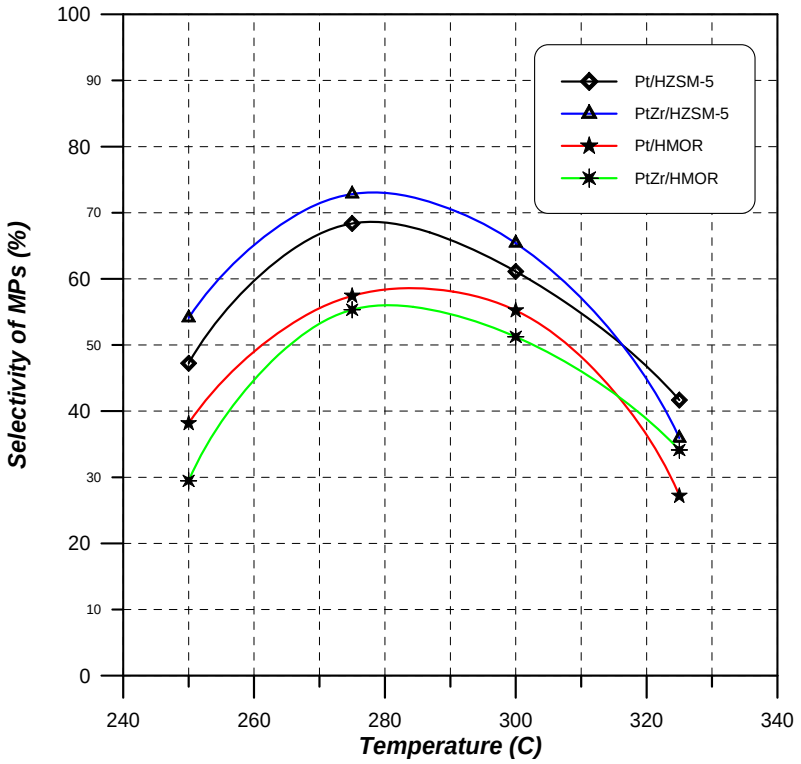

Figure 5-72:Selectivity of MP's vs. Temperature at H/HC=3 and P=5bar for Four Zeolite Pt/HZSM-5, Pt/HMOR and Bimetal with Zr Metal

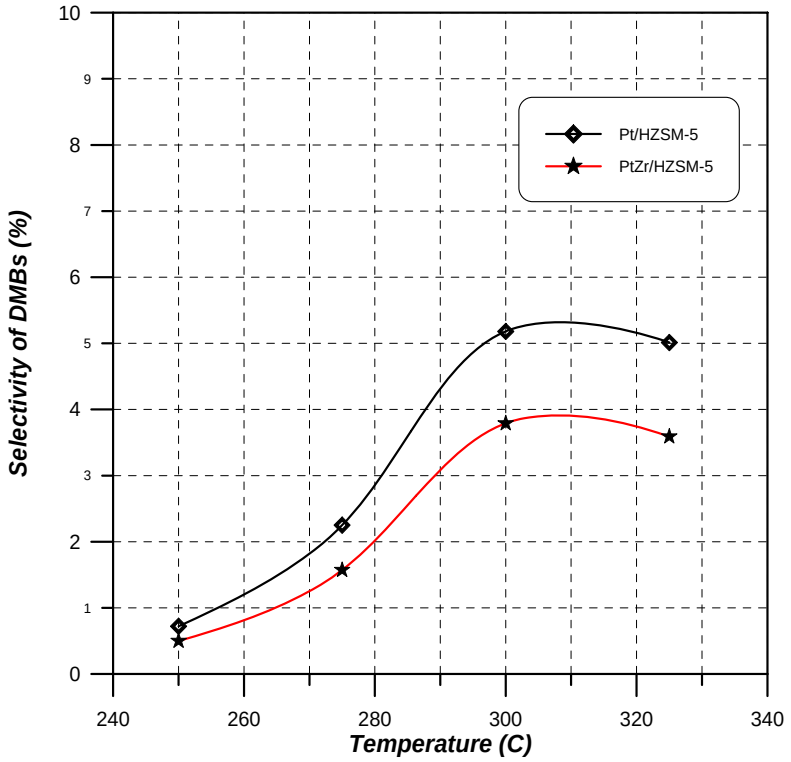

Figure 5-73: Selectivity of DMB's vs. Temperature for Zeolite Pt/HZSM-5 and PtZr/HZSM-5 at P=5bar and H/HC=3

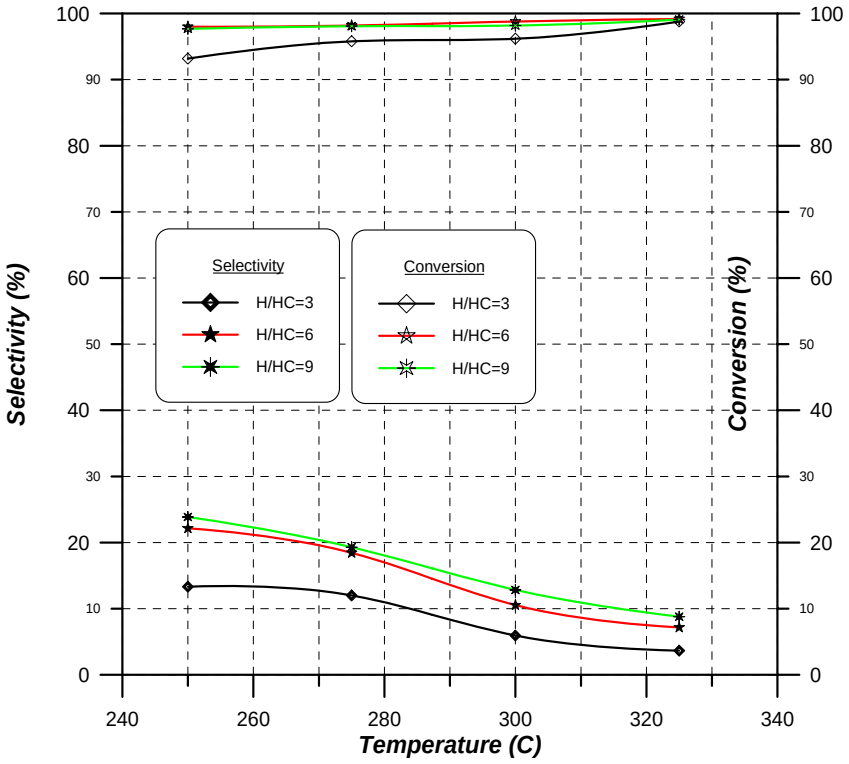

Figure 5-74:Selectivity and Conversion vs. Temperature for Zeolite PtRuZr/HZSM-5 at P=5bar and H/HC=3, 6 and 9

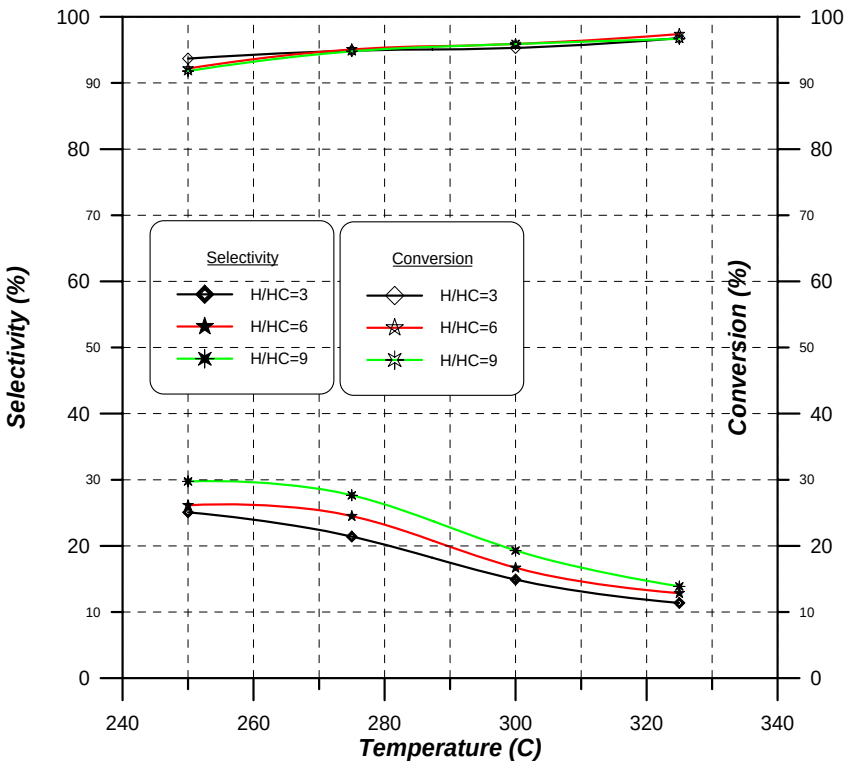

Figure 5-75:Selectivity and Conversion vs. Temperature for Zeolite PtRuZr/HMOR at P=5bar and H/HC=3, 6 and 9

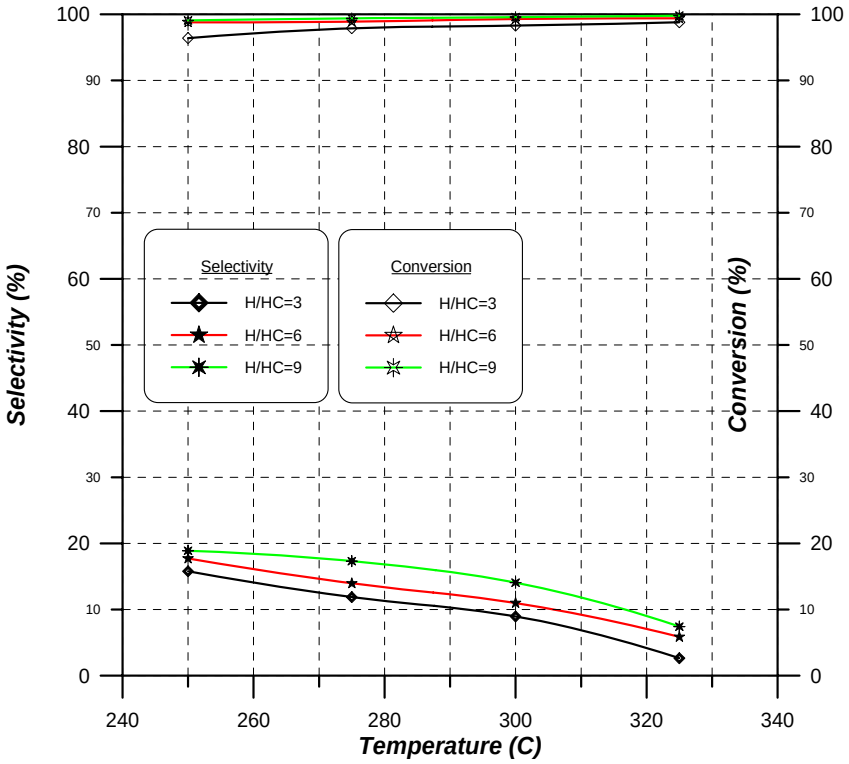

Figure 5-76:Selectivity and Conversion vs. Temperature for Zeolite PtRuZr/SrZSM-5 at P=5bar and H/HC=3, 6 and 9

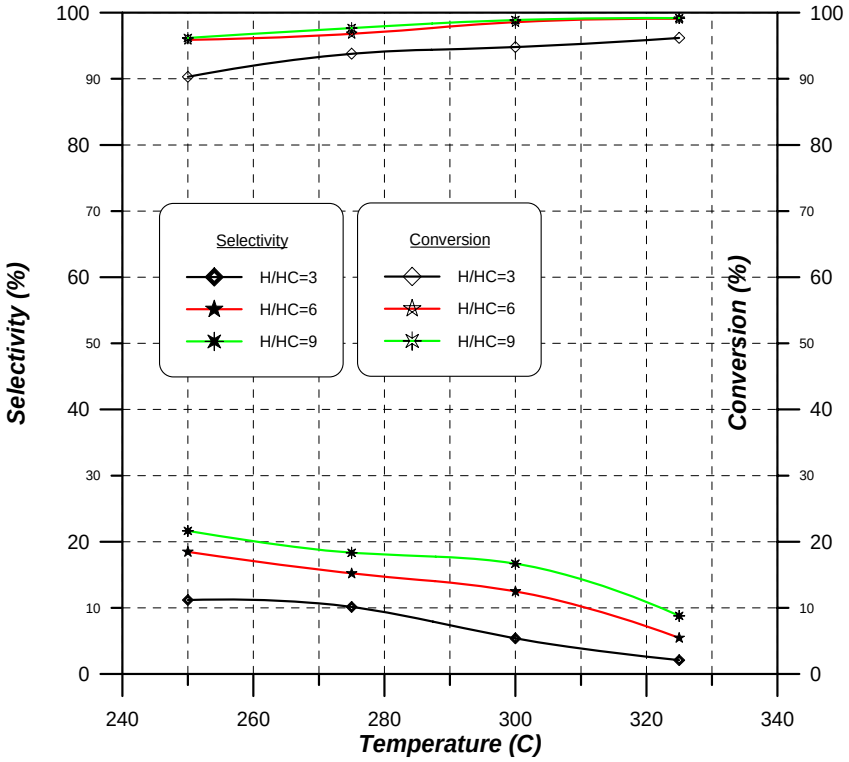

Figure 5-77:Selectivity and Conversion vs. Temperature for Zeolite PtRuZr/BaZSM-5 at P=5bar and H/HC=3, 6 and 9

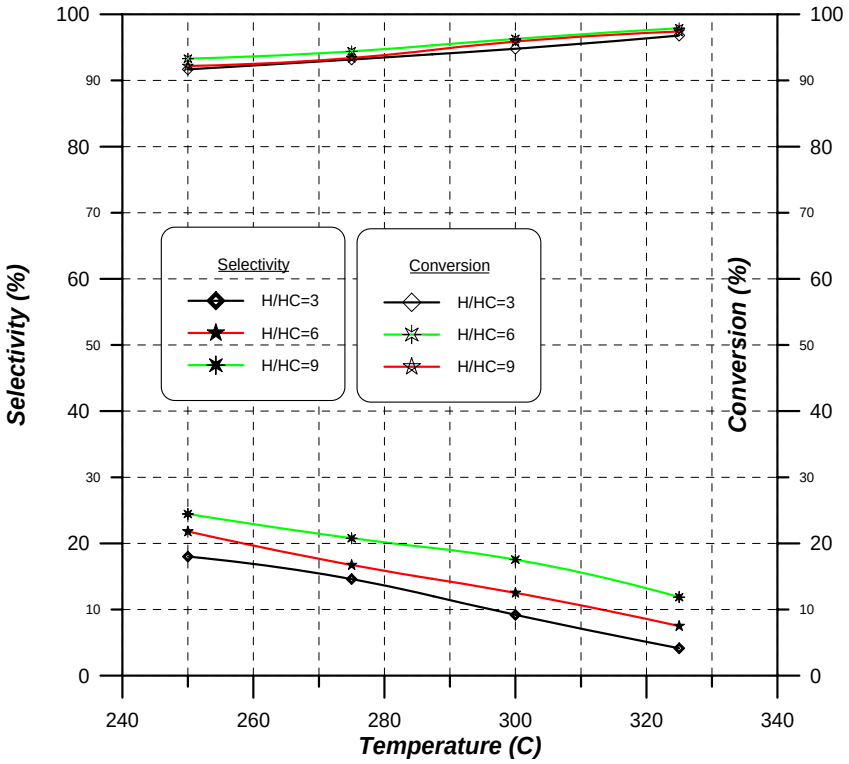

Figure 5-78:Selectivity and Conversion vs. Temperature for Zeolite PtRuZr/SrMOR at P=5bar and H/HC=3, 6 and 9

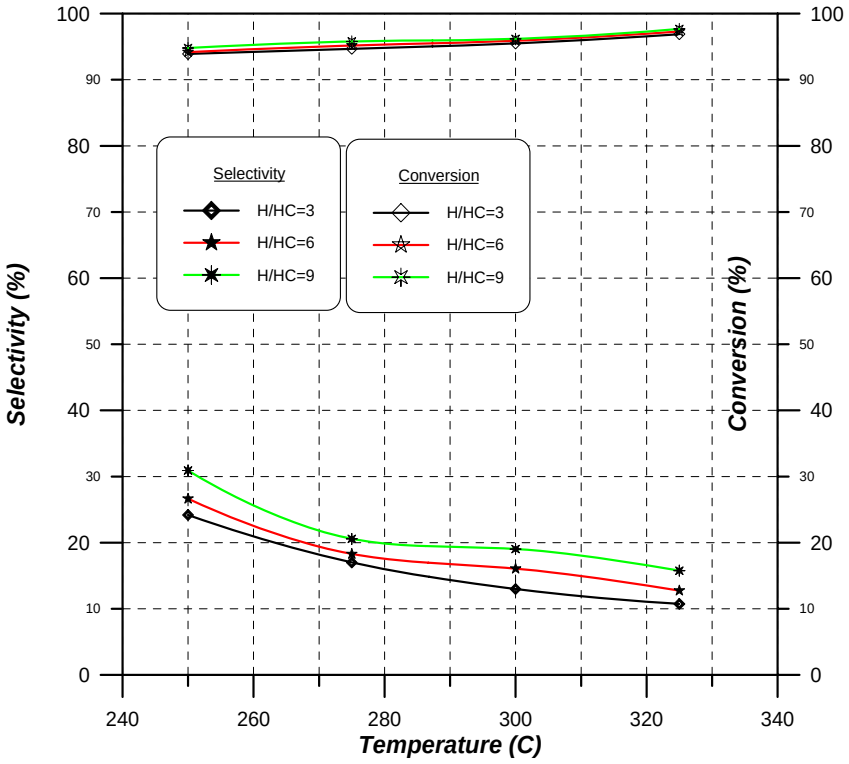

Figure 5-79:Selectivity and Conversion vs. Temperature for Zeolite PtRuZr/BaMOR at P=5bar and H/HC=3, 6 and 9

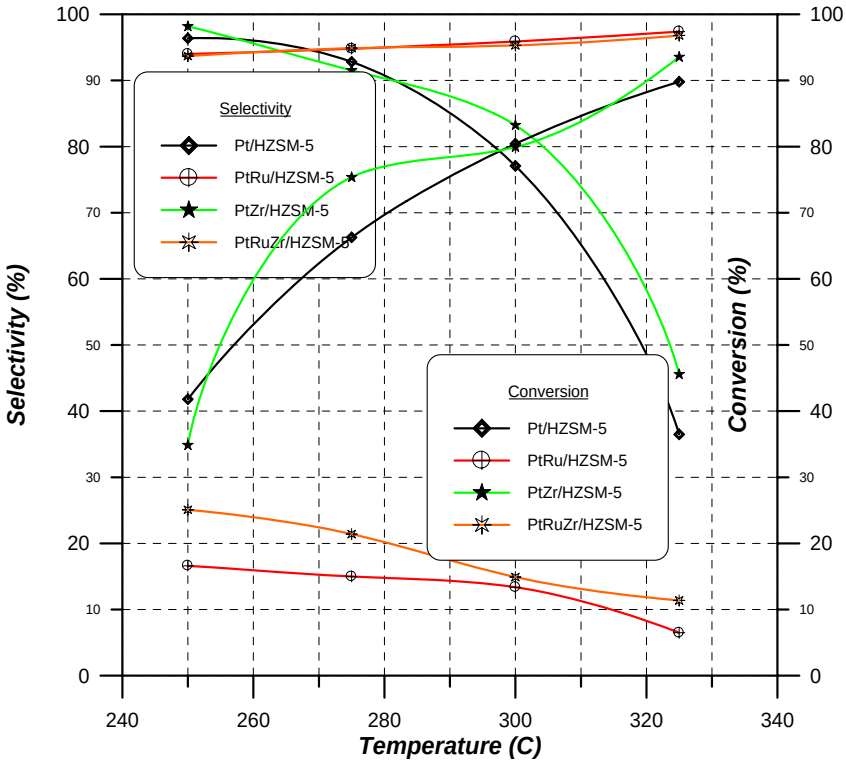

Figure 5-80:Selectivity and Conversions vs. Temperature at H/HC=3 and P=5bar for Four Zeolite Pt, PtRu, PtZr and PtRuZr Over HZSM-5

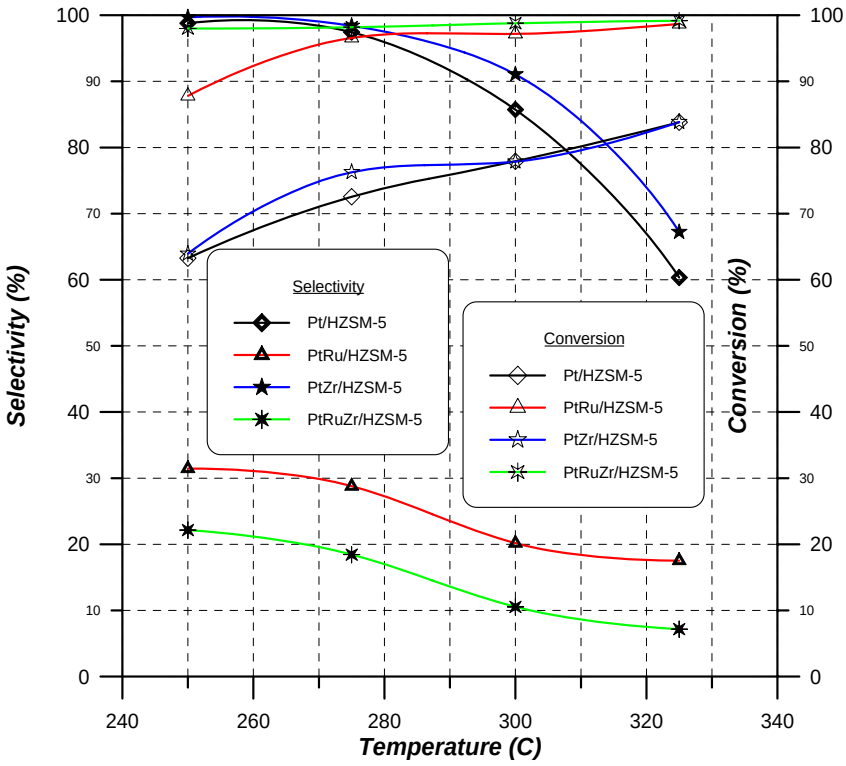

Figure 5-81: Selectivity and Conversions vs. Temperature at H/HC=6 and P=5bar for Four Zeolite Pt, PtRu, PtZr and PtRuZr Over HZSM-5

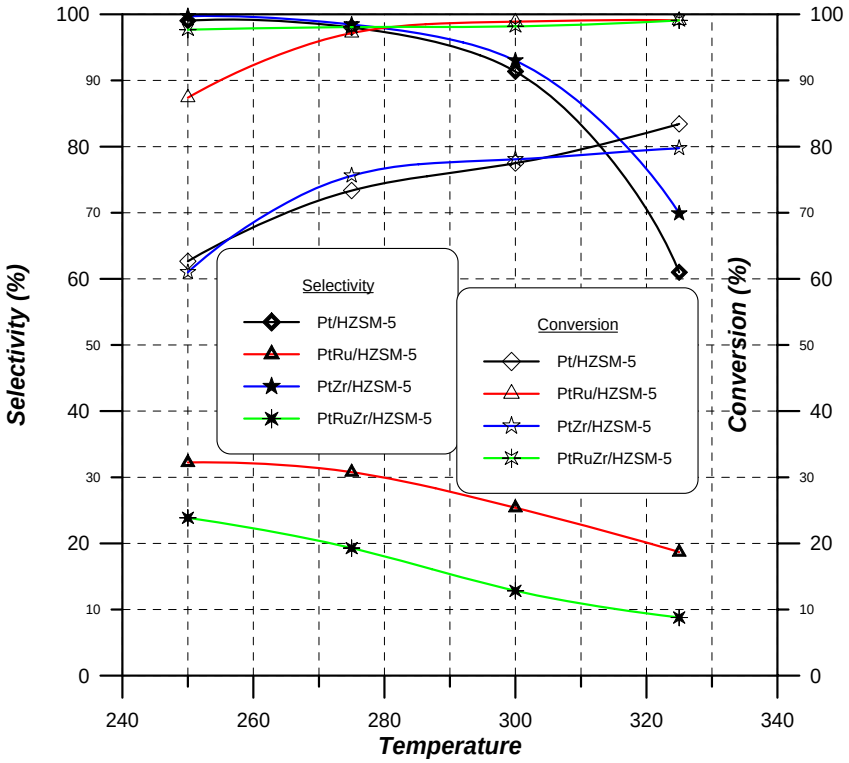

Figure 5-82: Selectivity and Conversions vs. Temperature at H/HC=9 and P=5bar for Four Zeolite Pt, PtRu, PtZr and PtRuZr Over HZSM-5

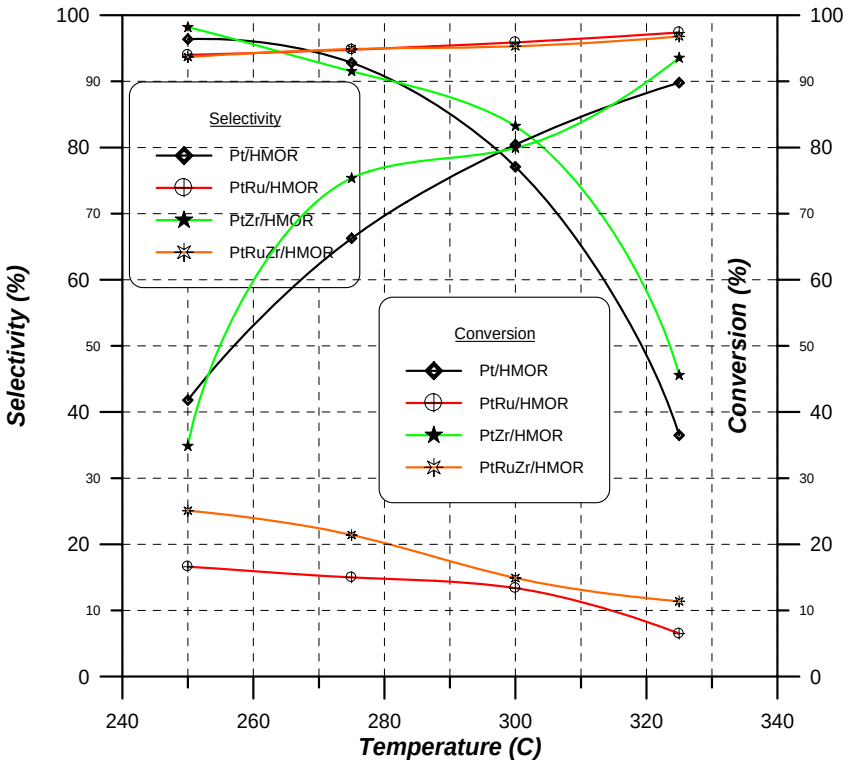

Figure 5-83: Selectivity and Conversions vs. Temperature at H/HC=3 and P=5bar for Four Zeolite Pt, PtRu, PtZr and PtRuZr Over HMOR

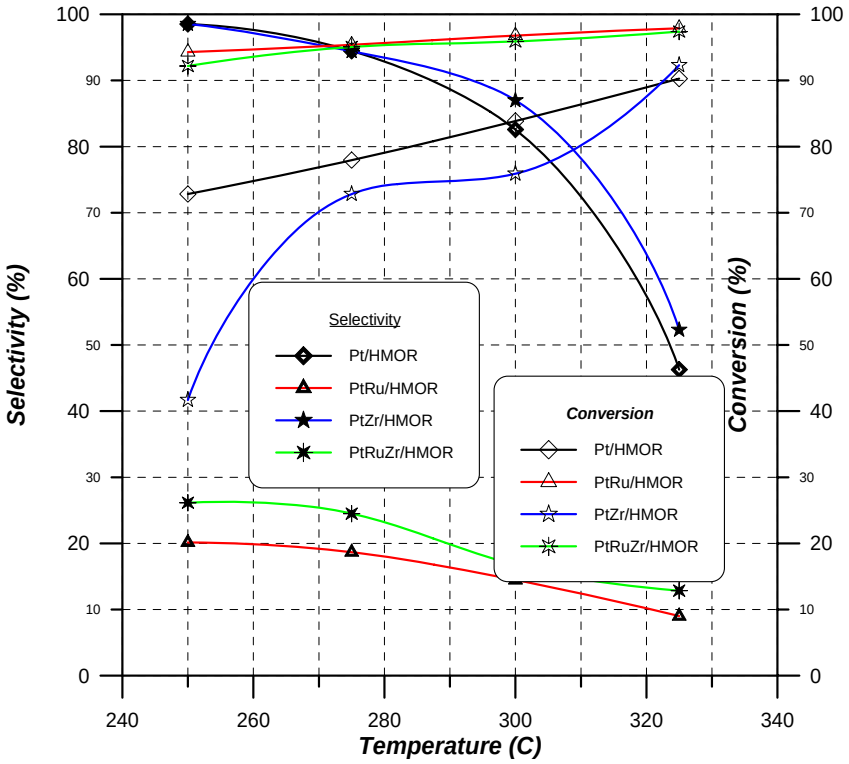

Figure 5-84: Selectivity and Conversions vs. Temperature at H/HC=6 and P=5bar for Four Zeolite Pt, PtRu, PtZr and PtRuZr Over HMOR

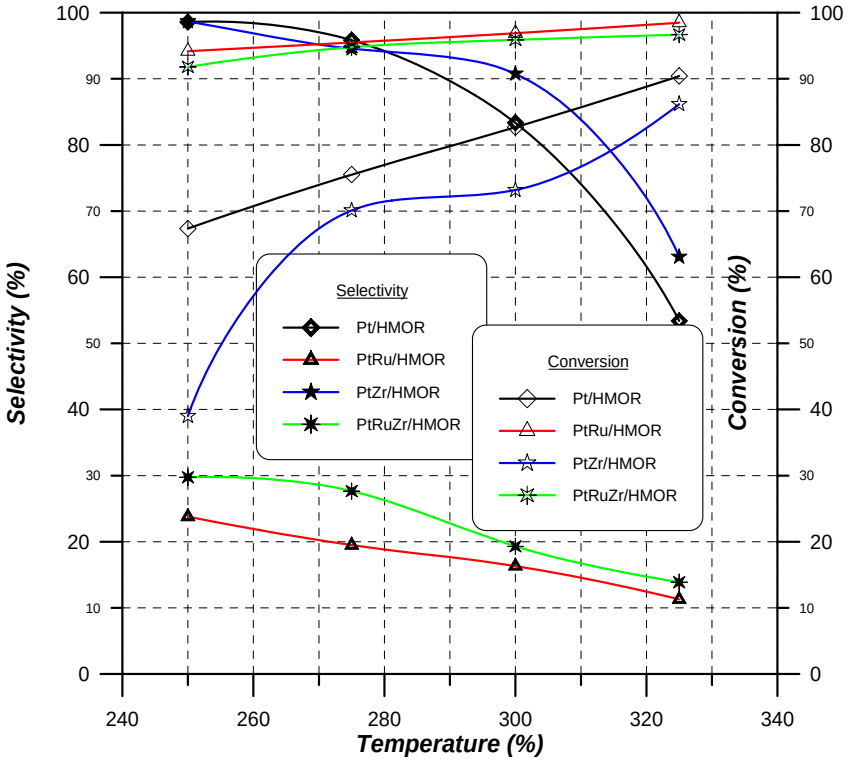

Figure 5-85: Selectivity and Conversions vs. Temperature at H/HC=9 and P=5bar for Four Zeolite Pt, PtRu, PtZr and PtRuZr Over HMOR

5.6 Rate of Reaction and Activation Energy

The rate of reaction for overall conversion, isomerization and cracking reactions were calculated from equation 4-6. The cyclyzation reactions were neglected because there was no or low products for cyclic compounds. The results were listed in appendix B for all zeolite catalysts at different conditions.

Activation Energy and pre-exponential factor was calculated by equation 4-10. The values of activation energy were taken from the slops of plotting $Ln(-r_A)$ vs. $1/T\,(K)$, while the pre-exponential factor were taken from the intercepts of the line with y-axis as shown in figures 5-86 and 5-87. The values of activation energy and pre-exponential factor were listed in table 5-11.

$$-r_A = \frac{F_{A_o}.X}{w} \tag{4-6}$$

$$Ln\,(-r_A) = Ln\,(A) - \left(\frac{E}{R.T}\right) \tag{4-10}$$

The results of activation energy shows high disturbance especially for bi and trimetallic zeolite catalysts. The corresponding values vary from 6 kJ/mole to 64 kJ/mole. This variety is due to variation in conversion and selectivity to desired product. The highest value of E_a, 63.748 kJ/mole is for Pt/Ba-Zeolite catalysts due to there high stability at the temperature range applied, while the activation energy of low values are for reactions that produced more gases compounds.

The effect of improving catalysts by adding bimetallic to the activation energy was showed from the increasing of the value of E_a for catalysts Pt/HMOR from 10.15 to 25.57 kJ/mole for PtZr/HMOR. The later catalyst is more active and selective towards the isomerization reactions.

The low values of activation energy in table 5-11 belong to Ruthenium containing catalysts, which have noticeable low selectivity towards the isomerization.

Table 5-11: Activation Energy (E_a) in (kJ/mole) and pre-exponential factor (A)in (s^{-1}) for Different Noble Metal Loaded Zeolite Catalysts

Zeolite Sample	E_a in kJ/mole	A in s^{-1}
Pt/HZSM-5 (I)	10.696	$4.627 *10^{9}$
Pt/HMOR (I)	6.709	$2.086 *10^{9}$
Pt/HZSM-5	9.576	$3.525 *10^{9}$
Pt/HMOR	10.151	$4.243 *10^{9}$
PtRu/HZSM-5	4.195	$1.433 *10^{9}$
PtRu/HMOR	1.541	$8.163 *10^{8}$
PtZr/HZSM-5	8.886	$3.014 *10^{9}$
PtZr/HMOR	25.573	$0.960 *10^{9}$
PtRuZr/HZSM-5	0.449	$6.590 *10^{8}$
PtRuZr/HMOR	1.766	$8.436 *10^{8}$
Pt/SrZSM-5	21.026	$3.612 *10^{10}$
Pt/SrMOR	34.248	$5.811 *10^{11}$
PtRu/ SrZSM-5	3.048	$1.094 *10^{9}$
PtRu/ SrMOR	2.008	$8.950 *10^{8}$
PtZr/ SrZSM-5	34.245	$5.666 *10^{11}$
PtZr/ SrMOR	43.244	$3.604 *10^{10}$
PtRuZr/ SrZSM5	0.241	$6.378 *10^{8}$
PtRuZr/ SrMOR	1.703	$8.383 *10^{8}$
Pt/BaZSM-5	43.391	$3.738 *10^{10}$
Pt/BaMOR	45.313	$5.084 *10^{10}$
PtRu/ BaZSM-5	3.220	$1.132 *10^{9}$
PtRu/ BaMOR	1.342	$7.855 *10^{8}$
PtZr/ BaZSM-5	43.983	$4.125 *10^{10}$
PtZr/ BaMOR	63.748	$2.351 *10^{14}$
PtRuZr/ BaZSM-5	1.095	$7.551 *10^{8}$
PtRuZr/ BaMOR	0.977	$7.225 *10^{8}$
0.09Pt/HZSM-5	9.009	$3.243 *10^{9}$

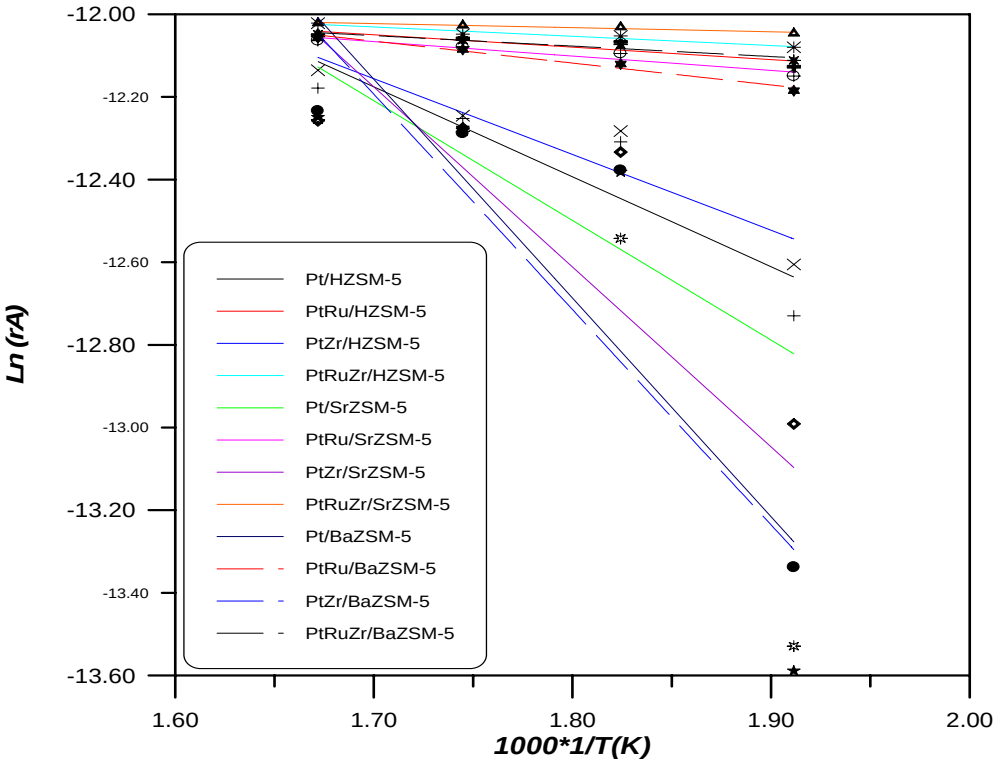

Figure 5-86: $Ln(-r_A)$ vs. 1/T for modified and metal loaded ZSM-5 Zeolite at 5 bar

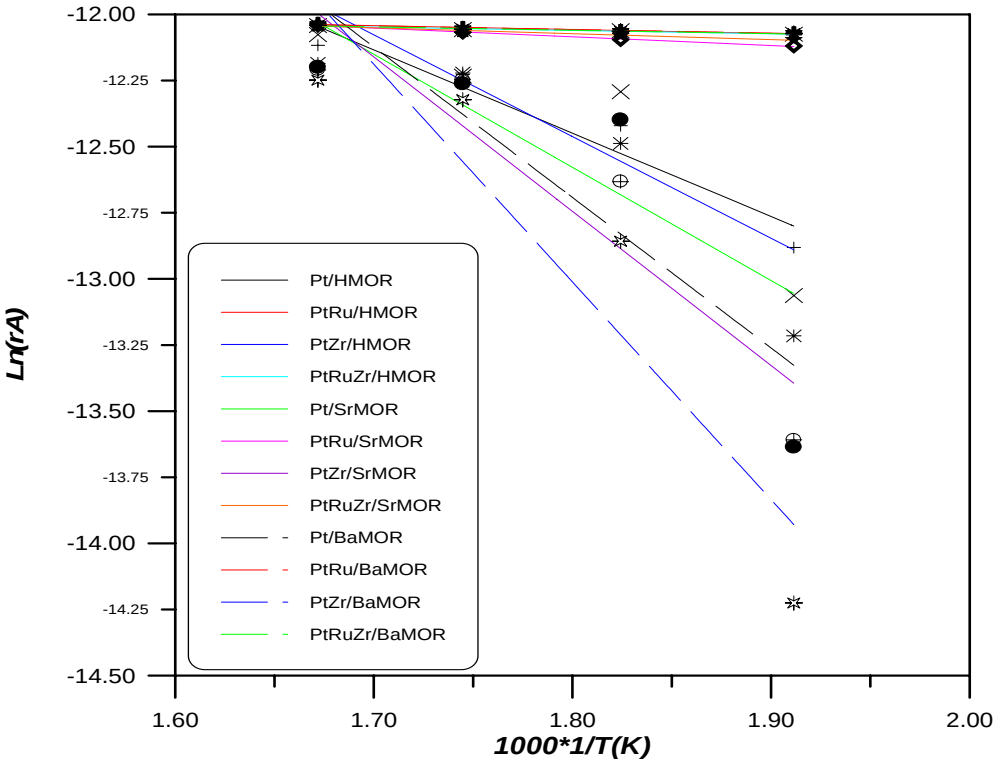

Figure 5-87: $Ln(-r_A)$ vs. 1/T for modified and metal loaded MOR Zeolite at 5 bar

Chapter Six
Kinetic Modeling

6.1 Introduction

An important step of any kinetic study is a mathematical model capable of predicting product yields for given feed rate, feed composition, and reaction conditions. It translates experimental data into parameters used as the basis of commercial reactor design [156].

Kinetic model can be either empirical or theoretical in nature, but is usually a combination of both .A theoretical models is based strictly on reaction mechanisms. Where the database and model fit are quite good. A theoretical model can sometimes be used with care to extrapolate predictions beyond the range of experimental data. While, empirical models are often used to fit kinetic data especially if the data are very complex. In many systems, the number of parameters and nature of the equations prevent usage of a theoretically based model [156].

6.2 Kinetic Modeling Based on Adsorption Desorption Isotherm

6.2.1. Introduction

Reaction mechanisms have been imagined for the heterogeneous catalytic reaction between molecules of the same kind or different molecules; On the basis of these mechanisms kinetic models of the process were developed by various authors [156].

Boreskov [157], showed that for a heterogeneous catalytic process the equation of reaction rate should satisfy the following general scheme:

$$\textit{reaction rate} = \frac{(\textit{kinetics factor}) \times (\textit{driving force})}{(\textit{adsorption factor})^{n}} \qquad (6\text{-}1)$$

which takes account of the mechanism advanced for the process, the rate determining step, and the reaction regression factors. The general model of describing the reaction rate equation suggested by Boreskov fits Langmuir-Hinshelwood theory of surface reactions.

Langmuir-Hinshelwood's theory [158, 159] is one of the most frequently employed kinetic theories of heterogeneous catalysis which gives very good results in many instances. It supplies hypotheses upon the state (adsorbed or in gas phase) of the reactants and products during the advancement of the reaction. Then one has to check if the experimental data fit the mathematical equations of a reaction rate resulted from the assumption of a process mechanism.

Another theory, widely employed in heterogeneous catalysis, was developed by Rideal-Eley [160]; they assumed that, at the time of reaction, only one of the reactants lies in adsorbed state, while the other one is in gas state.

6.2.2 Steps in Catalytic Reaction

The overall process by which hetrogenous catalytic reactions proceed can be broken down into the sequence of individual steps shown in table 6-1 for an isomerization [161]. Therefore the overall rate of reaction is equal to the rate of the slowest step in the mechanism. When the diffusion steps 1, 2, 6, and 7 in Table 6-1 are very fast compared with the reaction steps 3, 4, and 5, the concentrations in the immediate vicinity of the active sites are indistinguishable from those in the bulk fluid. In this situation, the transport or diffusion steps do not affect the overall rate of the reaction. In other situations, if the reaction steps are very fast compared with the diffusion steps, mass transport does affect the reaction rate. With this introduction, we are ready to individually treat the steps involved in catalytic reactions.

Table 6-1: Steps in a Catalytic Reaction

1-	Mass transfer (diffusion) of the reactant(s) (e.g., species A) from the bulk fluid to the external surface of the catalyst pellet.
2-	Diffusion of the reactant from the pore mouth through the catalyst pores to the immediate vicinity of the internal catalytic surface.
3-	Adsorption of reactant A onto the catalyst surface.
4-	Reaction on the surface of the catalyst (e.g., $A \longrightarrow B$)
5-	Desorption of the products (e.g., B) from the surface.
6-	Diffusion of the products from the interior of the pellet to the pore mouth at the external surface.
7-	Mass transfer of the products from the external pellet surface to the bulk fluid.

Any one of the steps listed in table 6-1 can be the slowest and hence the rate-controlling step. Increasing reactor mass velocity and reducing catalyst particle size can eliminate external mass transfer and diffusion limitations. The approach here will be to assume that mass transfer effects are negligible and that the Langmuir-Hinshelwood models for adsorption, reaction, and desorption on active sites will be adequately described this study.

6.2.3 Synthesizing A Rate Law, Mechanism, and Rate Limiting Step

From the first lock to the reaction of isomerization of n-hexane, we should know that only n-hexane was adsorbed to the surface of catalyst and the hydrogen feed are inert gas and the isomers from the reaction was desorbed to the gas phase after the end of reaction. Many researchers investigated the isomerization reaction, described the limiting step within adsorption, surface reaction or desorption [162, 163]. Therefore, we must derive the steps separately and fitting them with experimental data for checking. If the data are straight lines so this is the rate limiting step [161].

The simplified reaction of isomerization of n-hexane is shown below:

$$n-C_6H_{14} \xrightarrow[Pt/Cat]{H_2} i-C_6H_{14} \qquad (6\text{-}2)$$

The following nomenclature will be used to denote the various species in this reaction: $n-C_6H_{14}$=A, H_2=B, $i-C_6H_{14}$=C, S=Vacant Site, Cv= Vacant Site Occupied and Ct=Total Vacant. And subscripts: A=Adsorption, s=Surface Reaction and D=Desorption.

The Reactions sequences for n-hexane conversion to isomers are:

1.$a-Adsorption\ of\ n-hexane$

$$n-C_6H_{14}+S \rightleftharpoons n-C_6H_{14}.S \tag{6-3a}$$

$$A \quad +S \rightleftharpoons A.S \tag{6-3b}$$

$b-Adsorption\ of\ Hydrogen$

$$H_2 \quad +S \rightleftharpoons H_2.S \tag{6-4a}$$

$$B_2 \quad +S \rightleftharpoons B_2.S \tag{6-4b}$$

$The\ corresponding\ rate\ are\ as\ follows$

$$-r_{AA}=k_{AA}\left(p_A Cv-\frac{C_{A.S}}{Ke_{AA}}\right) \tag{6-5}$$

$$-r_{AB_2}=k_{AB_2}\left(p_{B_2}Cv-\frac{C_{B_2.S}}{Ke_{AB_2}}\right) \tag{6-6}$$

Where $-r_{AA}$, $-r_{AB_2}$, k_{AA}, k_{AB_2}, p_A, p_{B_2}, $C_{A.S}$, $C_{B_2.S}$, Ke_{AA} and Ke_{AB_2} are the rate of adsorption, rate constant, partial pressure, concentration in the vacant and the equilibrium constant ($Ke=k_{forword}/k_{backword}$) of n-hexane and hydrogen respectively,

2.$Surface$ Re$action$

$$n-C_6H_{14}.S \rightleftharpoons i-C_6H_{14}.S \tag{6-7}$$

$$A.S \rightleftharpoons C.S$$

$and\ the\ rate\ of\ reaction$

$$-r_{SA}=k_{SA}\left(C_{A.S}-\frac{C_{C.S}}{Ke_S}\right) \tag{6-8}$$

Where $-r_{SA}$, k_{SA}, $C_{C.S}$, Ke_S are the rate of surface reaction, rate constant, concentration on the vacant and the equilibrium constant at the surface reaction.

$$3.\textit{Desorption Reaction of } i-hexane$$

$$i-C_6H_{14}.S \rightleftharpoons i-C_6H_{14}+S \tag{6-9}$$

$$C.S \rightleftharpoons C+S$$

$$\textit{the rate of desorption is}$$

$$-r_{DC}=k_{DC}\left(C_{C.S}-\frac{p_C Cv}{Ke_{DC}}\right) \tag{6-10}$$

Where $-r_{DC}$, k_{DC} , $C_{C.S}$, Ke_{DC} are the rate of desorption reaction, rate constant, concentration on the vacant and the equilibrium constant of the desorption reaction of isomers.

Equations (6-3) through (6-10) represent the proposed mechanism for such isomerization reaction. By writing rate laws for these steps, each step is considered as an elementary reaction. Furthermore the species concentrations in the gas phase are replaced by their respective partial pressure. To determine which step is rate-limiting, firstly one of the steps could assumed as rate-limiting (rate-controlling) and then formulate the reaction rate law in terms of partial pressures of the species present. From this expression, the variation of the initial reaction rate with the initial total pressure could be determined. If the predicted rate varies with pressure in the same manner as the rate observed experimentally, the implication is that the assume mechanism and rate-limiting step is correct.

Case 1) The Adsorption Reaction is Rate Limiting Step.

A assume that the adsorption of n-hexane is indeed rate-limiting, derive the corresponding rate law, and then check to see if it is consistent with experimental observation.

By assuming that the rate of adsorption is rate limiting step rather than surface reaction and desorption, the rate equation is expressed from rate of adsorption.

The rate of adsorption as written in Eq. (6-5)

$$-r_{AA} = k_{AA}\left(p_A Cv - \frac{C_{A.S}}{Ke_{AA}}\right) \tag{6-5}$$

Use equation of surface reaction to getting $C_{A.S}$ after we was assume that at equilibrium the rate of reaction goes to zero $-r_{SA}/k_{SA} \approx 0$, because k_{SA} was very large then:

$$C_{A.S} = \frac{C_{C.S}}{Ke_S} \tag{6-11}$$

Also from desorption reaction we assume that rate of reaction at equilibrium goes to zero $-r_{DC}/k_{DC} \approx 0$, (also k_{DC} was very large) then:

$$C_{C.S} = \frac{p_C Cv}{Ke_D} \tag{6-12}$$

Then substitute Eq. 6-12 in Eq. 6-11 given Eq. 6-13

$$C_{A.S} = \frac{p_C Cv}{Ke_S Ke_D} \tag{6-13}$$

Sub. Eq. 6-13 in Eq. 6-5 gives:

$$-r_{AA} = k_{AA}\left(p_A Cv - \frac{p_C Cv}{Ke_{AA} Ke_S Ke_D}\right) \tag{6-14}$$

Rearranging, by replacing $Ke = Ke_{AA} Ke_S Ke_D$ and taking Cv outside the arguments to obtain:

$$-r_{AA} = k_{AA}\left(p_A - \frac{p_C}{Ke}\right)Cv \tag{6-15}$$

Since Cv cannot be measured, and replaced in the rate equation with measurable quantities for the equation to be meaningful, that can be obtained from the total vacant Ct ;

$$\begin{aligned} Ct &= Cv + concentrations\ of\ compounts\ adsorbed \\ Ct &= Cv + C_{A.S} + C_{C.S} + C_{B_2.S} \end{aligned} \tag{6-16}$$

The concentration of inert gas was taken from Eq. 6-4 as follows:

$$-r_{AB_2} / k_{AB_2} \approx 0 \Rightarrow C_{B_2.S} = (p_{B_2} Ke_{AB_2})Cv \tag{6-17}$$

Sub. Eqs. 6-12, 13 and 17 in Eq. 6-16 gives:

$$Ct = Cv + \frac{p_C}{Ke_D Ke_S}Cv + \frac{p_C}{Ke_D}Cv + (p_{B_2} Ke_{AB_2})Cv \tag{6-18}$$

Taking Cv obtains

$$Cv = \frac{Ct}{1 + \left(\frac{1}{Ke_D Ke_S} - \frac{1}{Ke_D}\right)p_C + (p_{B_2} Ke_{AB_2})} \tag{6-19}$$

Sub. Eq. 6-19 in Eq. 6-5 will give:

$$-r_{AA} = k_{AA}\left(p_A - \frac{p_C}{Ke}\right) * \left(\frac{Ct}{1+\left(\frac{1}{Ke_D Ke_S} - \frac{1}{Ke_D}\right)p_C + (p_{B_2} Ke_{AB_2})}\right) \quad (6\text{-}20)$$

Rearranging Eq. 6-20 gives;

$$-r_{AA} = k\left(\frac{p_A - \frac{p_C}{Ke}}{1+\left(\frac{1}{Ke_D Ke_S} - \frac{1}{Ke_D}\right)p_C + (p_{B_2} Ke_{AB_2})}\right) \quad (6\text{-}21)$$

Where $k = k_{AA}Ct$, Eq. 6-21 represents the final equation of adsorption of n-hexane on the surface of catalyst.

Case 2) The Surface Reaction is Rate Limiting Step.

The same procedure would be used, by assuming the surface reaction is rate limiting step, as in Eq. 6-8

$$-r_{SA} = k_{SA}\left(C_{A.S} - \frac{C_{C.S}}{Ke_S}\right) \quad (6\text{-}8)$$

Sub. Eqs 6-12 and 13 in Eq. 6-8 gives

$$-r_{SA} = k_{SA} Ke_A \left(p_A - \frac{p_C}{Ke_S Ke_A Ke_D}\right) Cv \quad (6\text{-}22)$$

Also the same value of Cv was taken from Eq. 6-19, substitute these equation in equation 6-22 obtain the final form of surface reaction.

$$-r_{SA} = kKe_A \left(\frac{p_A - \frac{p_C}{Ke}}{1 + \left(\frac{1}{Ke_D Ke_S} - \frac{1}{Ke_D} \right) p_C + (p_{B_2} Ke_{AB_2})} \right) \quad (6\text{-}23)$$

Where $k = k_{AS} Ct$ and $Ke = Ke_D Ke_S Ke_A$

Case 3) The Desorption Reaction is Rate Limiting Step.

The rate limiting step for this case is the desorption of product and equation 6-9 is used to derive the rate of desorption from the surface of catalyst as the same steps described previously, the final equation that obtained from the derivation is;

$$-r_{DC} = kKe_A Ke_S \left(\frac{p_A - \frac{p_C}{Ke}}{1 + \left(\frac{1}{Ke_D Ke_S} - \frac{1}{Ke_D} \right) p_C + (p_{B_2} Ke_{AB_2})} \right) \quad (6\text{-}24)$$

6.3 Determine Rate Low Parameter

Before starting of analyzing and determining rate low parameter, some points should be solved and cleared.

All derived equations give a solution to the isomerization reaction but it is dependent on the linearization of rate low because only one of these equations are rate limiting steps, therefore the kinetics of n-hexane isomerization was discussed in the literature and they found that the surface reaction was rate limiting step [164, 165]. The actual partial pressure can be calculated from the experimental data as show below:

From the chemical reaction equation eq. 6-2

$$n - C_6H_{14} \xrightarrow[Pt/Cat]{H_2} i - C_6H_{14} \quad (6\text{-}2)$$

$$P_A = P_A^{\,o} \frac{(1-X)}{(1+\varepsilon X)} \qquad (6\text{-}25)$$

$$Where\ P_A^{\,o} = y * P_t$$

$$y = mole\ fraction\ of\ \ n-Hexane$$

$$P_t = Total\ \mathrm{Pressure}\ of\ \ \mathrm{Reaction} = 5bar$$

$$\varepsilon = Correction\ factor\ for\ Gas\ phase$$

$$= y\,(mole\ of\ \ product - mole\ of\ \ reac\tan t)$$

$$= 0$$

Hydrogen inter to the reactor as inert gas with n-hexane for three different ratios as 3, 6 and 9 mole, therefore the partial pressure of hydrogen should be also calculated as the same above.

$$P_{B_2} = P_A^{\,o} \frac{(\theta_{B_2} - X)}{(1+\varepsilon X)} \qquad (6\text{-}26)$$

where $$\theta_{B_2} = \frac{Mole\ of\ \ Hydrogen}{Mole\ of\ \ n-Hexane} \qquad (6\text{-}27)$$

$$P_C = P_A^{\,o} \frac{(X)}{(1+\varepsilon X)} \qquad (6\text{-}28)$$

The parameters of the rate equation were determined using a statistical program. Thirty of different points were substituted in the equation 6-23, the experimental data was taken depending on the actual conversion that should be given at a certain temperature after the comparison with data that had taken from the literature.

The data was taken at temperature 275 ^{o}C and 300 ^{o}C to show the effect of temperature on the rate of reaction. The data for parameters at these temperatures and the activation energy of these constants were shown in table (6-2)

Table 6-2: The Parameters of eq. 5-23 at Different Temperature and The Activation Energy with There Pre-exponential Factor

Parameter Constant	***275 ^oC***	***300 ^oC***	***Activation Energy in kJ/mole***	***Pre-exponential Factor (A)***
K	0.024274	0.012100	72.700	$2.06*10^5$
Ke	0.512164	0.177379	110.728	$1.84*10^{10}$
Ked	0.00019	0.000123	45.629	4.248
Kes	-1.57371	-.005976	7.848	-8.8107
KeAB	0.101261	0.10022	1.083	0.128

Figures 6-1 to 6-10 show the experimental data and those calculated from equation 6-23 after the parameters had been calculated. The parameters of the derived equation were evaluated using statistical method, with a correlation coefficient of 0.9929. This mode gave very accurate results at different temperatures and different hydrogen to hydrocarbon ratios. This rate equation was applied also for Ruthenium metal in spite of bad results that obtained from it. From the above results concluded the rate equation of surface reaction was rate limiting step and the reaction parameter was applied for the isomerization reaction of n-hexane for high temperature range and different flow rate with high accuracy of results.

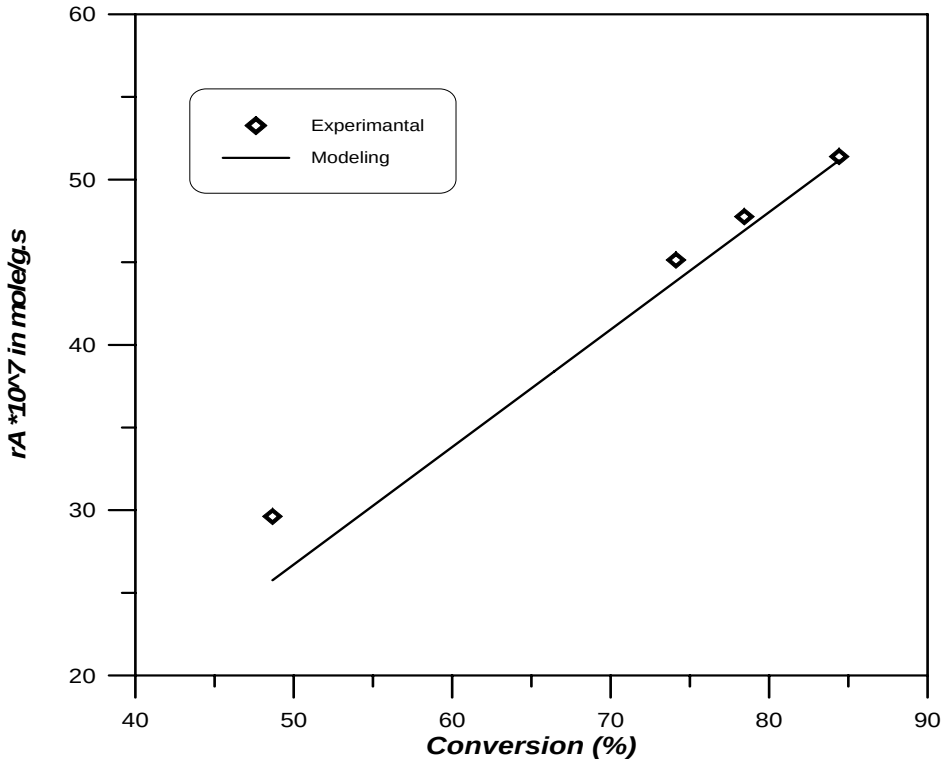

Figure 6-1: Experimental and Modeled Rate of Reaction vs, Conversion for Isomerization of n-Hexane Using Pt/HZSM-5 at 5 bar total Pressure and H/HC=3

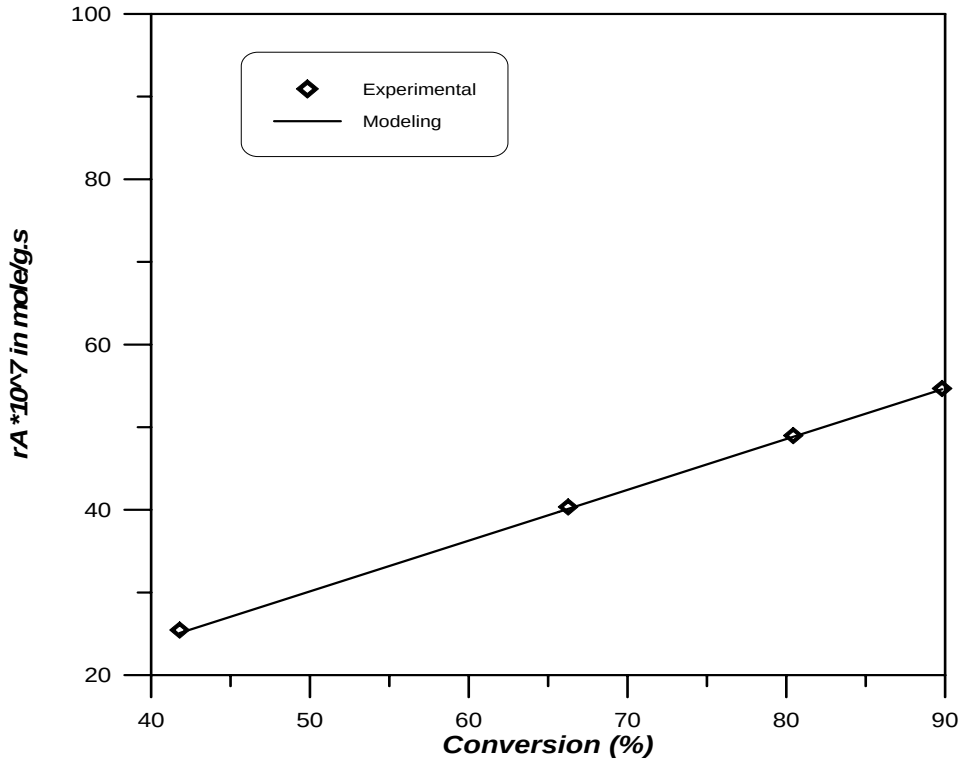

Figure 6-2: Experimental and Modeled Rate of Reaction vs, Conversion for Isomerization of n-Hexane Using Pt/HMOR at 5 bar total Pressure and H/HC=3

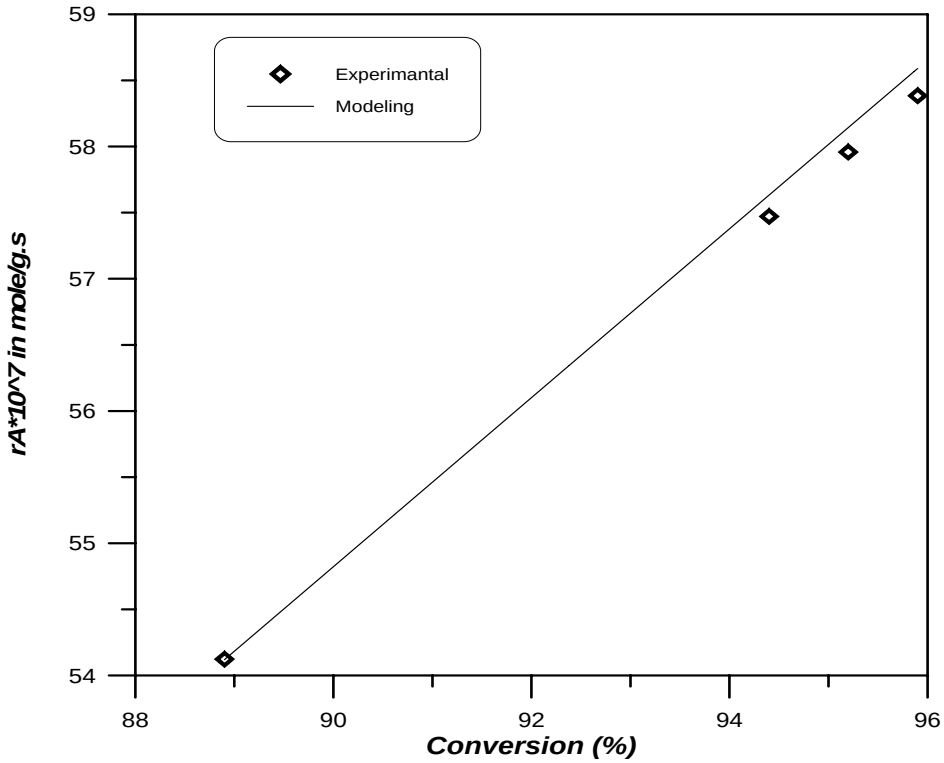

Figure 6-3: Experimental and Modeled Rate of Reaction vs, Conversion for Isomerization of n-Hexane Using PtRu/HZSM-5 at 5 bar total Pressure and H/HC=3

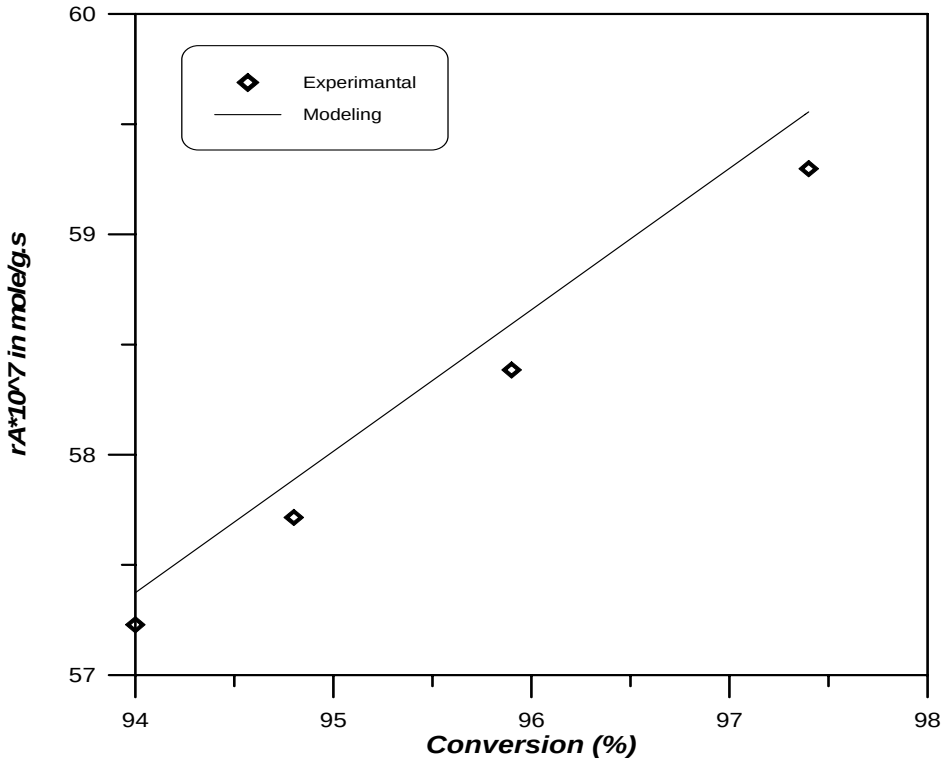

Figure 6-4: Experimental and Modeled Rate of Reaction vs, Conversion for Isomerization of n-Hexane Using PtRu/HMOR at 5 bar total Pressure and H/HC=3

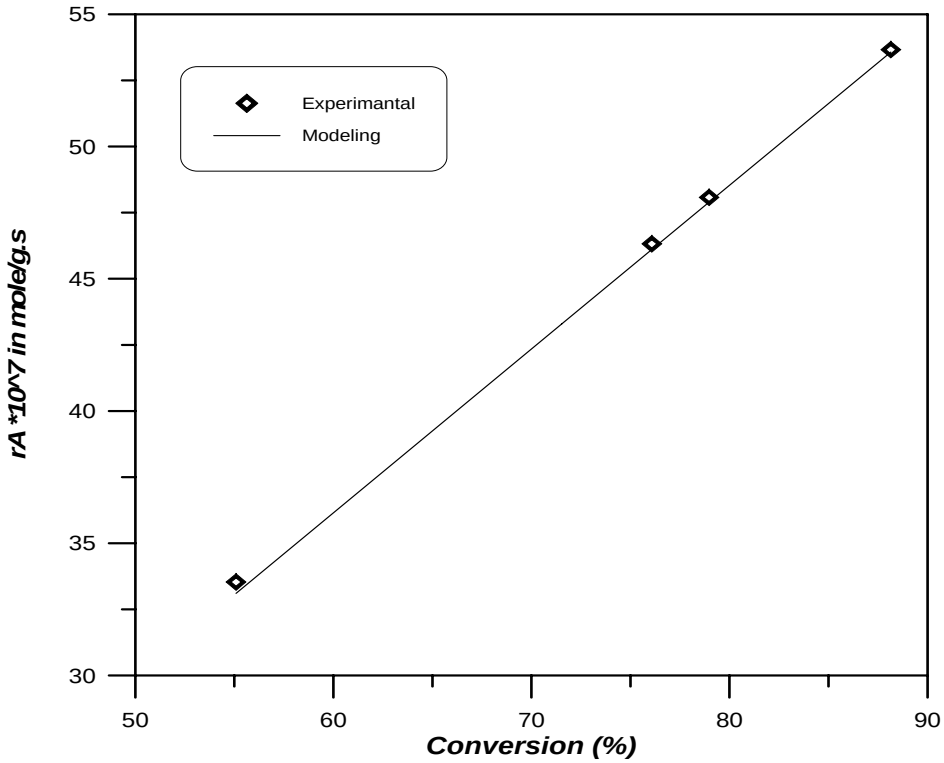

Figure 6-5: Experimental and Modeled Rate of Reaction vs, Conversion for Isomerization of n-Hexane Using PtZr/HZSM-5 at 5 bar total Pressure and H/HC=3

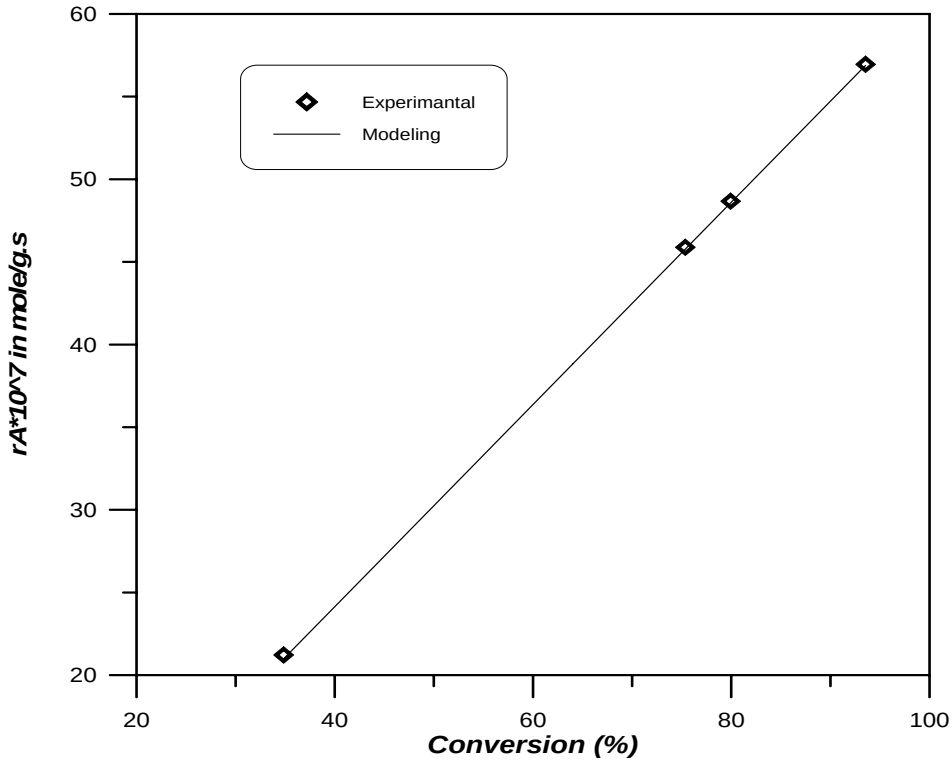

Figure 6-6: Experimental and Modeled Rate of Reaction vs, Conversion for Isomerization of n-Hexane Using PtZr/HMOR at 5 bar total Pressure and H/HC=3

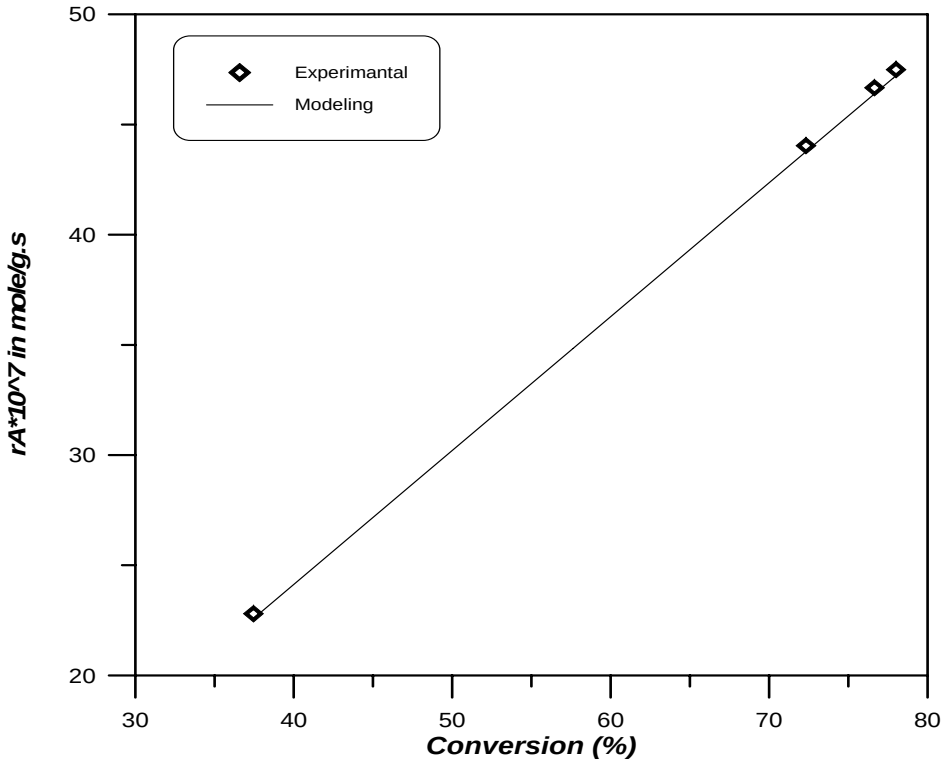

Figure 6-7: Experimental and Modeled Rate of Reaction vs, Conversion for Isomerization of n-Hexane Using Pt/SrZSM-5 at 5 bar total Pressure and H/HC=3

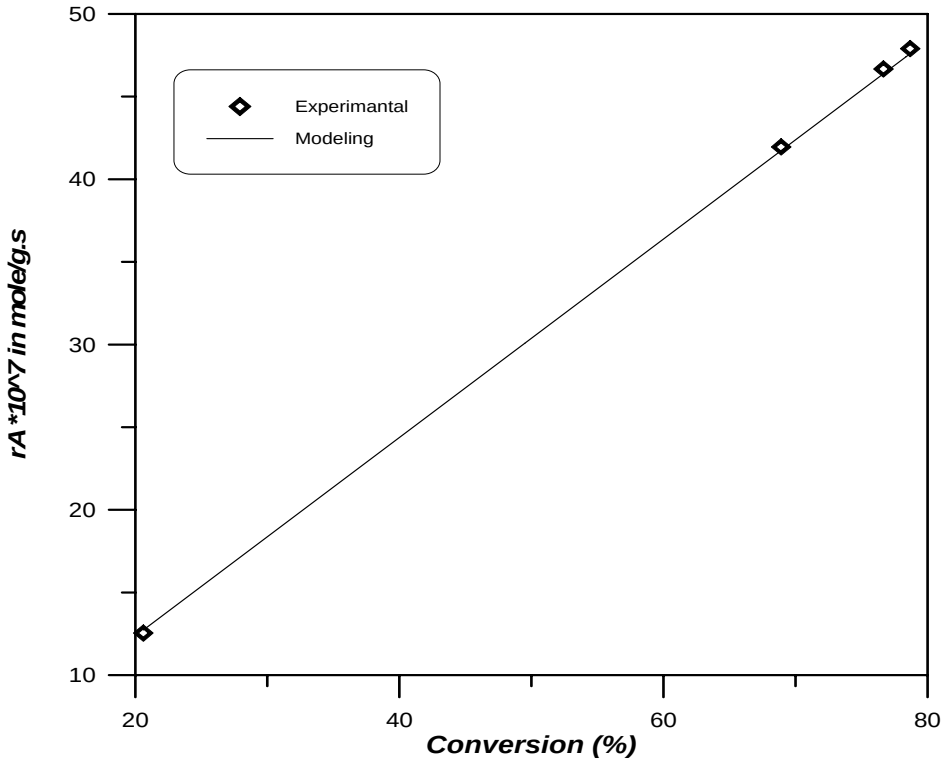

Figure 6-8: Experimental and Modeled Rate of Reaction vs, Conversion for Isomerization of n-Hexane Using Pt/BaZSM-5 at 5 bar total Pressure and H/HC=3

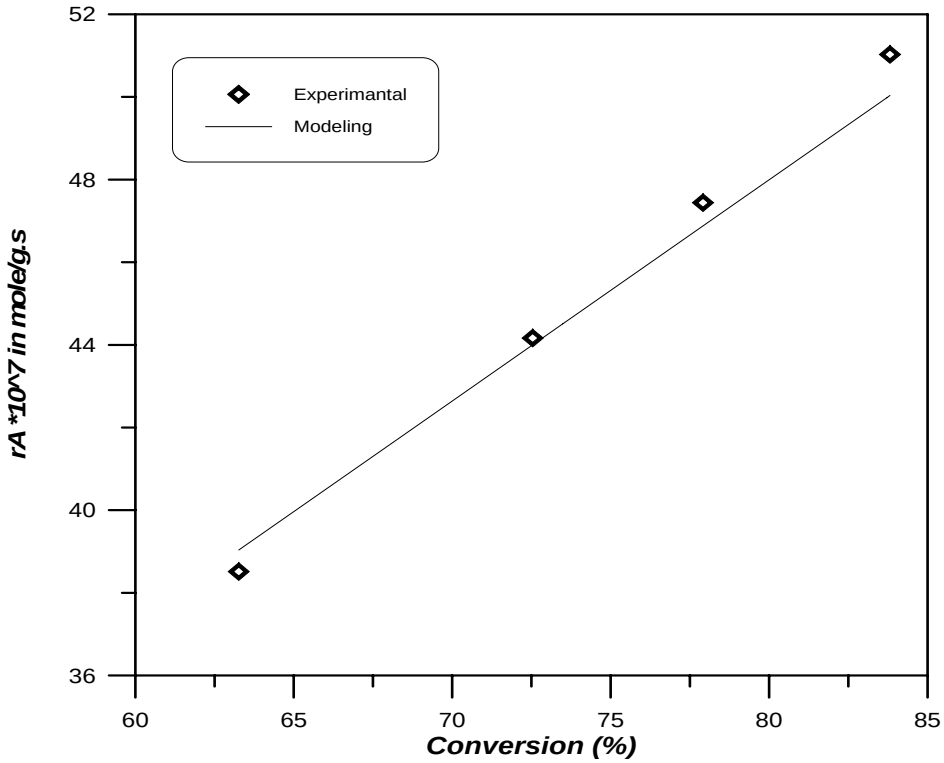

Figure 6-9: Experimental and Modeled Rate of Reaction vs, Conversion for Isomerization of n-Hexane Using Pt/HZSM-5 at 5 bar total Pressure and H/HC=6

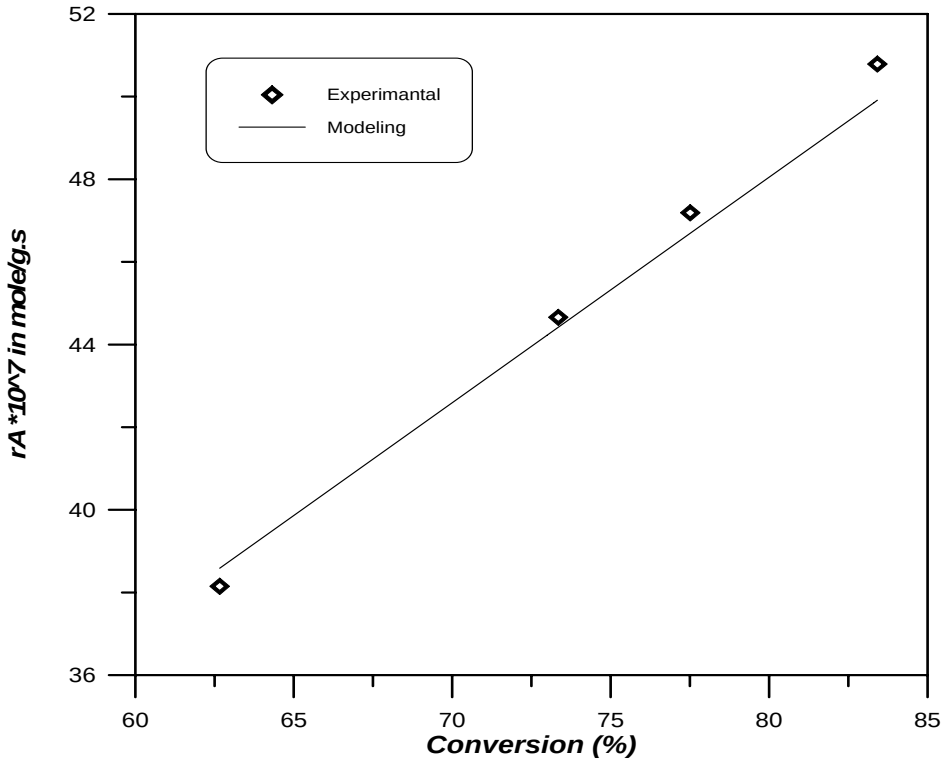

Figure 6-10: Experimental and Modeled Rate of Reaction vs, Conversion for Isomerization of n-Hexane Using Pt/HZSM-5 at 5 bar total Pressure and H/HC=9

Chapter Seven
Conclusions and Future Work

7.1 Conclusions

- Barium and Strontium forms of ZSM-5 and Morenite were prepared from the corresponding hydrogen form (HZSM-5 and HMOR) by batch wise repeated two times ion exchanging with appropriate salt solution. The degree of ion exchange for Strontium had higher exchanging in comparison with Barium for the same zeolite type.
- The noble metal loading by super critical carbon dioxide technique was very efficient. The efficiency of loading was increased with increasing the pressure, while, the temperature has a little effect. The best time for contact of precursor with the substrate was 24 hr.
- The metal particles loaded by $scCO_2$ had good distribution and gave very small nano particles rather than that prepared by impregnation method. The BET surface area increased in spite of the zeolite sample has higher platinum content.
- ZSM-5 catalysts are generally more active and selective than MOR catalysts in isomerization of n-Hexane.
- The Strontium and Barium modified zeolite catalysts are selective for the isomerization than H-Forms, while they have low activity at T=250 ^{o}C.
- The bimetal Pt-Zr loaded catalysts enhanced the isomerization reaction resulted in increasing the selectivity of desired product. While the

catalysts loaded with Ruthenium have low activity for the isomerization and low selectivity due to high yield of undesired cracking.

- Adequate model describing the kinetics of hydroconversion of n-Hexane over Noble-metal/ZSM-5 and MOR catalysts was derived under the assumption that the rate controlling step is the surface reaction of n-hexane on active site. The model was applied for all prepared catalysts at different temperature and three different hydrogen to n-hexane ratio. The results show the accuracy of calculating the rate of reaction. The error of this model did not exceed 2% in comparison with experimental data.

7.2 Recommendations

- Precede the isomerization at longer time to check the activity and stability of prepared Noble-metal zeolite catalyst.
- Studying the effect of platinum content prepared by supercritical carbon dioxide.
- An extension of this work would be comparable study with different zeolite types as support and there effect on catalytic activity.
- An obvious area for future work is by using supercritical carbon dioxide for cation exchange.
- The experimental work can be extended to investigate the effect of dealumination of zeolites support to enhance the activity and selectivity of catalytic isomerization process.

References

1- Stanley Gembiki, Published by the National Academy of Sciences in **(2006)**.

2- BP Amoco Statistical Review of World Energy, report available on the internet **(2007)**.

3- Gates B. C., Katzer J. B. and Schmuit G. C., "*Chemistry of Catalytic Processes"*, Mc Graw-Hill, Tokyo, **(1979).**

4- Patrilyak L. K., Manza I. A., Vypirailenko V. I., and Korovistsyna A. S., "*Theoretical and Experimental Chemistry"*, **39, No. 4, (2003).**

5- Laizet J. B., Soiland A. K., Leglise J. and Duchet J. C., "*Topics in Catalysis"*, **10, 89, (2000).**

6- Thomas, C. L., "*Catalytic Processes and Proven Catalyst"*, Academic Press, New York, **(1979).**

7- Acosta, D. R., Orozco, J., and Ogura, M., "*Studies in Surface Science and Catalysis"*, **49, 1035, (1989).**

8- Hegedus, L. L., Aris R., Bell, A. T., and Boudart, M. "*Catalyst Design Progress and Perspectives"*, John Wiely & Sons, **(1987).**

9- Morley, S. K., Marr, P. C., "*J. Mater. Chem."* **12, 1898 (2002).**

10- Morley, S. K., Marr, P. C., Hyde, J. R., Brown, P. D., "*J. Mater. Chem."* **14, 1212 (2004).**

11- Sterba, H. J., and Haensel, V., *Ind. Eng. Chem. Prod. Res. Dev.*, **15, 2 (1976)**.

12- Ciapetta, F. C., *Petro. Chem. Eng.*, **33, No. 5, C-19 (1961).**

13- Mills, G. A., Heinemann, T. H., and Obald, *Ind. Eng. Chem.*, **45, 134 (1953)**.

14- Esberl, S., *"Catalytic Processing in Refining "*, Pennwell, **(1983).**

15- Weisz, P. B., *Adv. Catal.*, **13, 137 (1962).**

16- Figoli, N. S., Beltramini, J. N., Matinell, E. E., and Parera, J. M. *J. Chem. Biotechnol.*, **32, 445 (1982).**

17- Lackner, K. and Emmrich, G., *Hydrocarbon Processing*, **Oct., 87 (1988).**

18- Murphree, E. V., *Petroleum Refiner*, **30, No. 12, 97 (1951).**

19- Kuchar, A. O., Braun, J. B., Shetton, R. K., and Olson, R. K., *"Platforming Developments For The Energy Conscious Era"*, UOP Technology Conference, **P-2, (1978).**

20- Richard, W., Rice, and Kang, L., *J. Catal.*, **77, 104 (1982).**

21- Michael, J. K., Robert, L. F., and Dennis, G. S., *J. Catal.*, **78,. 445 (1982).**

22- Hughes. T. R., Jacobson, R. L., and Tamm, P, W., *Studies in surface Science and Catalysis*, **38, 317 (1988).**

23- Srivastava, R. D., *"Heterogeneous Catalytic Science"*, CRC Press, Florida **(1988).**

24- Mills, G. A., Weller, S., and Cornelius, E. B., *"Pro. 2nd. Int. Cong. on Catalysis"*, Amsterdam, **Part II, No. 113, 1 (1960).**

25- Sinfelt, J. H., Hurwitz, H., and Rohrer, *J. Catal.*, **1, 481 (1962).**

26- Hettinger, W. P., Keith, C. D., Gring, J. L., and Teter, J. W., *Ind. Eng. Chem.*, **47, No. 4, 719 (1955).**

27- Christoffel, E., Fetting, F., and Vierrath, H., *J. Catal.*, **40, 349 (1975).**

28- Ray, G. C., Myers, J. W., and Ripley, D. L., *Hydrocarbon Processing*, **53, No. 1, 141 (1974).**

29- Weisz, P. B., *"Advances in Catalysis"*, Vol. 13, Academic Press, New York, **(1963).**

30- Kouwenhoven, H. W., and Vanz, L. L., *Chem. Eng. Prog.*, **67, 65 (1971).**

31- Coonradt, H. L., and Garwood, W. E., *Ind. Eng. Chem. Prod. Res. Dev.*, **31, No. 1, 38 (1964).**

32- Brown, Y., Cornet, D., Maire, G., and Gault, F. G., *J. Catal*., **2, 152 (1963).**

33- Weisz, P.B., and Swegler, E. W., *Science*, **31, 126 (1957).**

34- Sinfelt, J. H., Hurwitz, H., and Rohrer, J. C., *Phys. Chem*., **64, 892 (1960).**

35- Haensel, V., *"Advances in Catalysis"*, Vol. 3, Academic Press, New York, **179 (1951).**

36- Schulz, H. F., and Weitkamp, J. H., *Ind. Eng. Chem. Prod. Res. Dev.*, **11, No. 1, 46 (1972).**

37- Schmerling, L., *Ind. Eng. Chem*., **45, 1447 (1953).**

38- El-Kady, F. Y. A., Menoufy, M. F., and Hassan, H. A., *Indian J. of Tech.*, **21, June, 213 (1983).**

39- Ribeiro, F., Mareill, C., and Guisnet, M., *J. Catal*., **78, 267 (1982).**

40- Dartigues, J. M., Chanbellan, A., and Gault, F. G., *J. Am. Chem. Soc*., **98, 856 (1976).**

41- Haensel, V., and Donaldson, G. B., *Ind. Eng. Chem*., **43, No. 9, 2102 (1951).**

42- Sinfelt, J. H., and Rohrer, *J. Chem. Eng. Data*, **8, 109 (1963).**

43- Rohrer, J. C., Hurwitz, H., and Sinfelt, J. H., *J. Phys. Chem.*, **65, 1458 (1961).**

44- Giannetti, i. P., Sebulsky, R. T., *Ind. Eng. Chem. Prod. Res. Dev*., **8, No. 4, 356 (1969).**

45- Orkin, B. A., *Ind. Eng. Chem. Prod. Res. Dev*., **8, No. 2, 145 (1962).**

46- Choudhary, V. R., *Ind. Eng. Chem, Prod. Res. Dev*., **16, No. 1, 12 (1977).**

47- Choudhary, V. R., Doraiswamy, L. K., *J. Catal*., **23, 54 (1971).**

48- Burch, R., *J. Catal*., **58, 220 (1979).**

49- Shanshool, J., Al-Mutawali, F. S., Al-Madfai S. H., and Mansor, E. F., *J. Eng. and Tech., Special Issue*, "Proc. 2nd Iraqi Conf. on Engineering, **36 (1988).**

50- Gerberich, H. R., Lutinski, F. E., and Hall, W. K., *J. Catal*., **6, 209 (1966).**

51- Meier, W.M., and Olsone, D.H., *"In the second international conference on molecular sieves"*, **386 (1970).**

52- Cronstedt, A.F., Akad. Hanki. Stockholm, **18**, (1756) 120. Transl. By Sumelius, I.G., in *"Molecular Sieves"*, Reinhold, New York, **(1992).**

53- Sand, L.B., and Mumpton, F.A., *"Natural Zeolites: Occurrence properties, use"*, Pergamon, Oxford, **(1978).**

54- Barrer, R.M., *J. Chem. Soc*., **21, 58 (1948).**

55- Milton, In *"Molecular Sieves"*, (Soc. Of Chem. Ind. London), **199 (1968).**

56- Hegedus, L.L, Aris, R., and Bell, A.T., *"Catalyst Design Progress and Perspectives"*, John Wiely & Sons, **(1987).**

57- John, D., and Sherman, *Proc. Natt. Acad. Sci*., USA, **96, 3471 (1999).**

58- Buchner, W., Schliebs, R., Winter, G., and Buchel, K.H., *"Industrial Inorganic Chemistry"*, Terrell, Germany, **(1989).**

59- Chen, N.Y., *"Shape Selective Catalysts In Industrial Applications"*, Dekker, New York, **(1989).**

60- Ychen, N., and Degnan, T.F., *"J. of Chemical Engineering Progress"*, 84, 32 (1988).

61- P. Barger (UOP), IZA Pre-Conference School, Poitiers, France, July, **5-7, (2001).**

62- Bankos, I., Valyon, J., Kapustin, G. I., and Kallo, D., *Zeolites*, **8, 189 (1988).**

63- Musa, M., Tarina, V., and Stoica, A.D., *Zeolites*, **7,. 427 (1987).**

64- Bhatia, S., Beltramini, J., and Do, D., *Catal. Rev. Sci. Eng.*, **31, 431 (1990).**

65- Weisz, P.B., and Frilette, V.J., *J. Phys. Chem*., **64, 382 (1960).**

66- Weisz, P.B., *Studies in Surface Science and Catalysis*, **7, 3 (1980).**

67- Bodart, P., and Nagy, J. B., *J. Phys. Chem*., **90, 5183 (1986**).

68- Meier, W. M., *Zeolite Kristallogr*, **115, 439 (1961).**

69- Szostak, R., *Molecular sieves*, Thomson, USA, **(1998).**

70- Breck, D.W., *"Zeolite Molecular sieves"*, John Wiley, New York, **(1974).**

71- Kladnlg, W. F., *Acta. Cient. Venez*., **926, 40 (1975).**

72- Bajpai, P. K., *Zeolites*, **6, 1 (1986).**

73- Jacobs, P., *"Carboniogenic Activity of Zeolites"*, Elsevier, New York, **(1977).**

74- Chem L. F., and Rees U. C., *J. Zeolites*, **8, (1988).**

75- Anderson J. R., *"Structure of Metallic Catalysis"*, Academic Press, New York **(1975).**

76- Kokotailo G. T., Chu P., and Lawton S.L., *J. Nature*, 272, (1978).

77- Gray, J. A., and Cobb, J.T., *J. of Catal*. , **36, 125 (1975).**

78- Elian H. M., *"Study the Activity of Platinum and Palladium Zeolites Supported Catalysts for Hydrocrbon Reaction"*, M.Sc. Thesis, University of Technology **(1998).**

79- Breck, D. W., *"Zeolite Molecular Sieves"*, John Wiley & Sons, New York **(1974).**

80- Leach, B. E., *"Applied Industrial Catalysis"*, Academic Press, New York, **Vol. 3 (1984).**

81- Dwyer, J. 'and Omalley, P. J., *Studies in Surface Science and Catalysis*, **36, 33 (1988).**

82- Breck, D.W., *"Zeolite Molecular sieves"*, John Wiley, New York, **(1974).**

83- Chester, A. W., *J. Catal.*, **86, 16 (1984).**

84- Shanshool, J., A. Mohammed and, S. R. Rauf, *"Modification of Zeolites as Support for Platinum Catalysts"*, **Eng. and Tech. Baghdad, Vol. 15 No. 7 (1996).**

85- Montes, A., Perot, G., and Guisnet, M., *React. Kinet. Catal. Lett*., **29, 7 (1985).**

86- Rabo, J. A., Pickert, P. E., Stamires, D. N., and Bayle, J. E., *"Proc. 2nd. Int. Cong. on Catalysis"*, Paris, **2055 (1960).**

87- Sherman, J.D., Danner, R.P., Dranoff, J.S., and Sweed, N.H., *AIChE*, **74, 179 (1978).**

88- Dwyer, J., and Omally, P.J., *Studies in Surface Science and Catalysis*, **35, 33 (1988).**

89- Moss, R. L., Gibbens, H. R., and Thomas, D. H., *J. Catal.* **16, 117 (1970).**

90- Swift, H. P., Lutinski, F. E. and Tobin, H. H., *J. Catal*. **5, 285 (1966).**

91- Anderson, J. R., and Boudart, M., *"Catalysis Science and Technology"*, Springer-Verlag, Berlin, **Vol. 6, 248 (1984).**

92- Vanden, G. H., and Rijnten, H., *Studies in Surface Science and Catalysis*, **3, 265 (1979).**

93- Anderson, J. R., *"Structure of Metallic Catalysis"*, Academic Press, New York, **(1975).**

94- Richardson, J. T., *"Principles of Catalyst Development"*, Plenum Press, New York **(1989).**

95- Namba, S., Inaka, A., and Yashima, T., *Zeolites*, **6, 107 (1986).**

96- Ciapetta, F. G., *Oil and Gas J*., **Oct. 16 (1967).**

97- Ghosh, A. K., and Kydd, R. A., *Catal. Rev. Sci. Eng*., **27, 539 (1985).**

98- Ali, J. K., *Iraqi Eng. Soc*., **March, 2 (1978).**

99- Scherzer, J., *J. Catal*., **54, 285 (1978).**

100- Halasz, I., Horvath, J., Nandy, T., and Tasnadi, E., *Studies in Surface Science and Catalysis*, **24, 393 (1985).**

101- Tan, G., Rangwala, H. A., Szymura, J. A., Otto, F. D., and Wanke, S. E., *Studies in Surface Science and Catalysis*, **19, 123 (1984).**

102- Ward, J. W., *J. Catal*., **9, 225 (1967).**

103- Wendlandt, W. W., *"Thermal Methods of Analysis"*, John Wiley & Sons, New York **(1974).**

104- Sibilia, J., *"A Guide to Characterization and Chemical Analysis"*, VCH Publishers **(1988).**

105- Daniels,"*Thermal Analysis* ", VNR Comp., London, **45 (1973).**

106- Tolovski, I., Minchev, C., Senderov, E. E., and Penchev, V., *Studies in Surface Science and Catalysis*, **24, 337 (1985).**

107- Shanshool J., and AL-Sammerrai, D., *Thermochimica Acta*, **127, 217-222 (1988).**

108- Bremer, H., Morke, W., and Vogt, F., "*Influence of Cations on the Thermal Stability of Modified Y Zeolites"*, (Molecular Sieve, Edited by Meiar, W. M.), D. C., Washington, **249 (1973).**

109- Kustov, L. M., Borovkov, V., and Kazanskii, V. B., *Kint. Catal*., **25, 2 (1984).**

110- Bolton, A. P., and Bujalski, R. L., *J. Catal*., **23, 331 (1971).**

111- Tsuneji, S., Hideo, O., Hiroshi, S., and Haruo, T., *Bull. Chem. Soc. of Japan*, **63, 1555 (1990).**

112- Tempere, J. F., and Dela, F. D., *J. Catal*., **39, 1 (1975).**

113- Hearle, J. W., Sparrow, J. T., and Cross, P. M. *"The use of the SEM'*, Pergamon Press, Oxford, **6 (1972).**

114- Smith, D. J., White, D., Baird, T., and Fryer, J. R., *J. Catal*., **81, 107 (1983).**

115- Tzou, N. S., and Schtler, W. M., *Studies in Surface Science and Catalysis*, **38, 233 (1988).**

116- Baker, R. T., Baker, M. A., and White, R. J., *J. Catal*., **26, 51 (1972).**

117- Aiello, R., Nastro, A., and Pellegrino, C., *Studies in Surface science and Catalysis*, **29, 255 (1986).**

118- Ginnetto, G., Perot, G., and Guisnet, M., *Studies in Surface Science and Catalysis*, **24, 63 (1985).**

119- Taylor, L. T. *"Supercritical Fluid Extraction"* John Wiley & Sons: New York, **(1996).**

120- McHugh, M. A. and Krukonis, V. J. *"Supercritical Fluid Extraction –Principles and Practice"* 2nd ed. Butterworth-Heinemann: Boston, **(1994).**

121- Brennecke, J. F. and Eckert, C. A. *AIChE J*. **35, 1409, (1989).**

122- McHugh, M. and Paulaitis, M. E. *J. Chem. Eng. Data*, **25, 326, (1980).**

123- Tester, J. W., Holgate, H. R., Armellini, F. J.; Webley, P. A.; Killilea, W. R. ; Hong, G. T. and Barner, H. E. *American Chemical Society*: Washington, **DC, Vol. 3, (1993).**

124- Subramaniam, B. and McHugh, M. A. *Ind. Eng. Chem. Process Des. Dev.* **25, 1, (1986).**

125- Tiltscher, H. and Hofmann, H. *Chem. Eng. Sci*. **42, 959, (1987).**

126- Bruno, T. J. and Ely, J. F. *"In Supercritical Fluid Technology: Review in Modern Theory and Applications";* CRC Press: Boca Raton **(1991).**

127- Reid, R. C., Prausnitz, J. M. and Poling, B. E. *"The Properties of gases and Liquids*"; 4th ed., McGraw-Hill: New York, **(1988).**

128- Peters, C. J. *"In Supercritical Fluids - Fundamentals for Application"* Kluwer Academic Publishers: Dordrecht, **(1994)**.

129- Petsche, I. B. and Debenedetti, P. G., *J. Phys. Chem*., **95, 386, (1991).**

130- Lucien, F. P., Foster, N. R., Jessop, P. G., and Leitner, W., *"In Chemical Synthesis Using Supercritical Fluids"*, Willy-VCH:Weinheim, **(1999).**

131- Ekart, M. P.; Bennett, K. L.; Ekart, S. M.; Gurdial, G. S.; Liotta, C. L. and Eckert, C. A. *AIChE J.* **39, 235, (1993).**

132- Brennecke, J. F.; Debenedetti, P. G.; Eckert, C. A. and Johnston, K. P. *AIChE J.* **36, 1972, (1990).**

133- Eckert, C. A. and Knutson, B. L. *Fluid Phase Equil***., 83, 93, (1993).**

134- Eckert, C. A. and Chandler, K. *"The 4th International Symposium on Supercritical Fluids"*, Sendai, Japan, **799-806, (1997).**

135- Roland W. and Aflons B. *"Supercritical Fluids, Opportunities in Hetrogenous Catalysis"* **Vol. 4, No. 1, (2000).**

136- Dillow, A. K.; Brown, J. S.; Liotta, C. L. and Eckert, C. A. *J. Phys. Chem.* **102, 7609, (1998).**

137- Dillow, A. K.; Hafner, K. P.; Yun, S. L. J.; Deng, F.; Kazarian, S. G.; Liotta, C. L. and Eckert, C. A. *AIChE J***. 43, 515, (1997).**

138- Tiltscher, H.; Wolf, H.; Schelchshorn, J. and Dialer, K. *United States Patent* **4605811, 1986.**

139- Subramaniam, B. and McCoy, B. *J. Ind. Eng. Chem. Res***., 33, 504, (1994).**

140-Pickel, K. H. and Steiner, K. *"3rd International Symposium on Supercritical Fluids"*, Strasbourg, France, **pp 7-12, (1994).**

141-Hoffmann-La Roche Ltd. In Roche Magazin, **(1992).**

142-Stinson, S. C. *Chem. Eng. News***, 75, 37, (1997).**

143-Schneider, M. and Baiker, A. *Catal. Rev. Sci. Eng***., 37, 515, (1995).**

144-Huesing, N. and Schubert, U. *Angew. Chem. Int. Ed. Engl***. 37, 22, (1998).**

145- M. Chatterjee, Y. Ikushima, Y. Hakutta and H. Kawanami, *Adv. Synth. Catal*. **348, 1580, (2006).**

146- Y. J. Han. J. M. Kim, and G. D. Stucky, *Chem. Mater.,* **12, 2068, (2000).**

147- Z. Konya, V. F. Puntes, I. Kiricsi and J. W. Ager, *Chem. Mater.,* **15, 1242, (2002).**

148- W. Yan, B. Chen, S. M. Mahurian and E. W. Hagaman, *J. Phys. Chem.,* **108, 2793, (2004).**

149- S. R. Hall, S. A. Davis, and S. Mann, *Langmuir,* **16, 1454, (2000).**

150- Y. Zhang, D. Kang, C. Saquing, M. Aindow and C. Erkey, *Ind. Eng. Chem. Res.,* **44, 4161, (2005).**

151- D. Carl, T. Tsui, M. Aindow and C. Erkey, *J. Phys. Chem. B.,* **108, 7716, (2004).**

152- A. Bayrakceken, U. Kitkamthorn, M. Aindow and C. Erkey, *Scripta Materialia,* **56, 101, (2007).**

153- Y. Zhang, D. Kang, M. Anidow and C. Erkey, *J. Phys. Chem. B.,* **109, 2617, (2005).**

154- Griffth, R. H., and Marsh, J. D. F.,"Contact Catalysis", Third Edition, Oxford University Press, Amen Houst, London E. G. 4, (1957).

155- A. G. Muller, P. A. Engehard and J. E. Weisang, *J. Catal.,* **56, 65 (1979).**

156- Weller, S. W., *Adv. Chem. Ser*., **148**, **26 (1975).**

157- Boreskov, G., *"Conference Nationale Sur Les Reacteur Chemiques"*, **4**, **(1966).**

158- Langmuir, I., *J. Amer. Chem. Soc*., **37**, **1139 (1915).**

159- Hinshelwood, C. N., *"Kinetics of Chemical Change"*, Clanderon Press, Oxford, **(1926).**

160- Clark, A., *"The Theory of Adsorption and Catalysis"*, Academic Press, New York and London, **(1970)**.

161- Fogler, H. S., *"Elements of chemical Reaction Engineering"*, 2nd ed., Printice-Hall of India Private Limited, New Delhi, **248 (1997).**

162- Ribero, F., Marcilly, C. and Guisnet, M. "*Hydroisomerization of n-Hexane on Platinum Zeolites"* **J. of Catalysis 78, 267-274 (1982).**

163- Guisnet, M., Garcia, J. J., Chevalier, F., and Maurel, R., **Bull. Soc. Chim. 1657 (1976).**

164- J. F. Allain, et. all. "*Hydroisomerization of n-hexane over platinum mazzite and platinum mordenite catalysts, Kinetics and Mechanism*" Applied Catalysis, 152, 221-235 (1997).

165- A. Van De Runstraat, J. Van Grondelle and R. Van Santen " *Microkinetics Modeling of the Hydroisomerization of n-Hexane*" Ind. Eng. Chem. Res., **36, 3116-3125 (1997)**

Appendix A

Table A-1*:** Experimental Results for Isomerization of n-Hexane using Pt/HZSM-5 (I) Zeolite catalyst at ***5 bar and H/HC=3

Temp.	(C1-C5)	2.2DMB	2.3DMB	2MP	3MP	n-C6	Aromatics	Conv. X%	Selec. S%
250	3.35	0.42	0.22	27.67	20.47	47.65	0.22	52.35	93.18
275	13.38	0.07	1.65	35.19	26.07	23.41	0.23	76.59	82.23
300	29.61	0.23	2.11	27.06	21.11	19.56	0.32	80.44	62.79
325	68.67	0.91	4.43	5.89	7.35	12.14	0.61	87.86	21.15

Table A-2*:** Experimental Results for Isomerization of n-Hexane using Pt/HZSM-5 (I) Zeolite catalyst at ***5 bar and H/HC=6

Temp.	(C1-C5)	2.2DMB	2.3DMB	2MP	3MP	n-C6	Aromatics	Conv. X%	Selec. S%
250	3.12	0.31	0.28	34.09	26.18	35.78	0.24	64.22	94.76
275	10.71	0.42	1.05	36.72	28.04	22.82	0.24	77.18	85.81
300	26.08	0.99	1.16	31.47	22.47	17.64	0.19	82.36	68.10
325	61.92	1.27	5.81	12.19	8.17	10.46	0.18	89.54	30.65

Table A-3*:** Experimental Results for Isomerization of n-Hexane using Pt/HZSM-5 (I) Zeolite catalyst at ***5 bar and H/HC=9

Temp.	(C1-C5)	2.2DMB	2.3DMB	2MP	3MP	n-C6	Aromatics	Conv. X%	Selec. S%
250	2.89	0.31	0.29	33.96	26.21	36.09	0.25	63.91	95.09
275	9.37	0.41	1.12	34.97	28.84	24.99	0.30	75.01	87.11
300	22.78	0.67	1.97	30.18	23.76	20.40	0.24	79.60	71.08
325	51.81	0.77	4.10	18.70	12.57	11.86	0.19	88.14	41.00

Table A-4*:** Experimental Results for Isomerization of n-Hexane using Pt/HMOR (I) Zeolite catalyst at ***5 bar and H/HC=3

Temp.	(C1-C5)	2.2DMB	2.3DMB	2MP	3MP	n-C6	Aromatics	Conv. X%	Selec. S%
250	2.45	5.35	5.36	25.67	15.97	44.09	1.11	55.91	93.93
275	12.05	13.41	7.38	27.96	18.66	20.22	0.32	79.78	84.49
300	25.85	12.58	6.32	23.16	16.07	15.90	0.12	84.10	69.12
325	72.22	4.14	2.15	8.05	5.47	7.91	0.06	92.09	21.51

Table A-5*:** Experimental Results for Isomerization of n-Hexane using Pt/HMOR (I) Zeolite catalyst at ***5 bar and H/HC=6

Temp.	(C1-C5)	2.2DMB	2.3DMB	2MP	3MP	n-C6	Aromatics	Conv. X%	Selec. S%
250	3.63	10.42	7.97	31.66	21.05	24.79	0.48	75.21	94.54
275	9.25	12.59	7.21	30.17	20.18	19.95	0.65	80.05	87.63
300	25.54	12.31	6.42	24.16	16.07	15.30	0.20	84.70	69.36
325	62.71	5.25	2.89	11.72	8.31	8.79	0.33	91.21	30.88

Table A-6*:** Experimental Results for Isomerization of n-Hexane using Pt/HMOR (I) Zeolite catalyst at ***5 bar and H/HC=9

Temp.	(C1-C5)	2.2DMB	2.3DMB	2MP	3MP	n-C6	Aromatics	Conv. X%	Selec. S%
250	2.44	10.68	7.86	31.72	21.79	24.52	0.99	74.48	96.74
275	4.03	10.98	7.30	30.63	22.37	23.29	1.40	76.71	92.92
300	22.73	10.37	5.89	24.97	18.80	16.28	0.96	83.72	71.70
325	55.83	5.26	3.20	14.30	10.56	10.18	0.67	89.82	37.09

Table A-7*:** Experimental Results for Isomerization of n-Hexane using Pt/HZSM-5 Zeolite catalyst at ***5 bar and H/HC=3

Temp.	(C1-C5)	2.2DMB	2.3DMB	2MP	3MP	n-C6	Aromatics	Conv. X%	Selec. S%
250	0.43	0.16	0.56	27.18	20.05	51.35	0.27	48.65	98.56
275	3.27	0.13	2.12	38.88	29.49	25.87	0.24	74.13	95.27
300	11.96	0.63	4.55	33.50	27.61	21.56	0.19	78.44	84.51
325	37.50	1.47	3.54	23.27	18.39	15.58	0.25	84.42	55.28

Table A-8*:** Experimental Results for Isomerization of n-Hexane using Pt/HZSM-5 Zeolite catalyst at ***5 bar and H/HC=6

Temp.	(C1-C5)	2.2DMB	2.3DMB	2MP	3MP	n-C6	Aromatics	Conv. X%	Selec. S%
250	0.49	0.44	0.51	35.30	26.25	36.74	0.27	63.26	98.80
275	1.68	0.17	1.15	39.75	29.62	27.46	0.17	72.54	97.45
300	10.96	0.25	3.46	35.58	27.52	22.08	0.15	77.92	85.74
325	33.11	1.99	2.68	25.33	20.56	16.18	0.15	83.82	60.32

Table A-9*:** Experimental Results for Isomerization of n-Hexane using Pt/HZSM-5 Zeolite catalyst at ***5 bar and H/HC=9

Temp.	(C1-C5)	2.2DMB	2.3DMB	2MP	3MP	n-C6	Aromatics	Conv. X%	Selec. S%
250	0.41	0.18	0.74	35.49	25.65	37.34	0.19	62.66	99.04
275	1.25	0.04	1.13	39.29	31.44	26.65	0.20	73.35	98.02
300	6.58	0.13	2.54	37.32	30.83	22.49	0.11	77.51	91.37
325	32.46	0.19	3.26	26.38	21.06	16.58	0.07	83.42	61.00

Table A-10*:** Experimental Results for Isomerization of n-Hexane using Pt/HMOR Zeolite catalyst at ***5 bar and H/HC=3

Temp.	(C1-C5)	2.2DMB	2.3DMB	2MP	3MP	n-C6	Aromatics	Conv. X%	Selec. S%
250	0.36	0.52	1.61	22.31	15.85	58.2	1.15	41.80	96.39
275	3.41	0.23	3.85	33.46	23.97	33.74	1.34	66.26	92.83
300	15.09	2.81	4.01	32.70	22.51	19.55	3.33	80.45	77.10
325	48.73	0.92	4.67	19.41	7.76	10.19	8.32	89.81	36.48

Table A-11*:** Experimental Results for Isomerization of n-Hexane using Pt/HMOR Zeolite catalyst at ***5 bar and H/HC=6

Temp.	(C1-C5)	2.2DMB	2.3DMB	2MP	3MP	n-C6	Aromatics	Conv. X%	Selec. S%
250	0.58	0.46	1.07	37.45	32.78	27.18	0.48	72.82	98.54
275	2.61	0.31	2.11	38.26	32.98	22.04	1.69	77.96	94.48
300	11.72	1.89	2.68	34.28	30.43	16.13	2.87	83.87	82.60
325	41.30	2.06	3.53	20.77	15.42	9.71	7.21	90.29	46.27

Table A-12*:** Experimental Results for Isomerization of n-Hexane using Pt/HMOR Zeolite catalyst at ***5 bar and H/HC=9

Temp.	(C1-C5)	2.2DMB	2.3DMB	2MP	3MP	n-C6	Aromatics	Conv. X%	Selec. S%
250	0.43	0.42	1.67	36.51	27.80	32.65	0.52	67.35	98.59
275	1.21	0.06	2.34	38.49	31.50	24.48	1.92	75.52	95.86
300	10.75	1.16	2.75	35.89	29.13	17.31	3.01	82.69	83.36
325	35.69	0.21	3.17	28.53	16.35	9.58	6.47	90.42	53.37

Table A-13*:** Experimental Results for Isomerization of n-Hexane using PtRu/HZSM-5 Zeolite catalyst at ***5 bar and H/HC=3

Temp.	(C1-C5)	2.2DMB	2.3DMB	2MP	3MP	n-C6	Aromatics	Conv. X%	Selec. S%
250	62.7	----	0.1	11.2	14.7	11.1	----	88.90	29.25
275	68.8	0.2	0.1	10.5	14.8	5.6	----	94.40	27.12
300	78.1	0.1	0.1	6.6	10.3	4.8	----	95.20	17.96
325	82.3	0.1	0.1	5.2	8.2	4.1	----	95.90	14.18

Table A-14*:** Experimental Results for Isomerization of n-Hexane using PtRu/HZSM-5 Zeolite catalyst at ***5 bar and H/HC=6

Temp.	(C1-C5)	2.2DMB	2.3DMB	2MP	3MP	n-C6	Aromatics	Conv. X%	Selec. S%
250	60.2	----	0.1	11.4	16.1	12.2	----	87.80	31.44
275	68.8	0.2	1.8	10.6	15.2	3.4	----	96.60	28.78
300	77.6	0.1	0.8	7.1	11.6	2.8	----	97.20	20.16
325	81.4	0.1	0.4	6.3	10.5	1.3	----	98.70	17.53

Table A-15*:** Experimental Results for Isomerization of n-Hexane using PtRu/HZSM-5 Zeolite catalyst at ***5 bar and H/HC=9

Temp.	(C1-C5)	2.2DMB	2.3DMB	2MP	3MP	n-C6	Aromatics	Conv. X%	Selec. S%
250	59.2	0.1	----	10.5	17.6	12.6	----	87.40	32.23
275	67.3	0.4	0.3	11.5	17.7	2.8	----	97.20	30.76
300	73.8	0.2	0.1	10.1	14.7	1.1	----	98.90	25.38
325	80.6	0.1	0.1	7.1	11.2	0.9	----	99.10	18.67

Table A-16*:** Experimental Results for Isomerization of n-Hexane using PtRu/HMOR Zeolite catalyst at ***5 bar and H/HC=3

Temp.	(C1-C5)	2.2DMB	2.3DMB	2MP	3MP	n-C6	Aromatics	Conv. X%	Selec. S%
250	78.4	2.9	7.9	4.6	0.2	6	----	94.00	16.60
275	80.6	1.4	6.2	5.8	0.8	5.2	----	94.80	14.98
300	83.1	4.2	4.3	3.7	0.6	4.1	----	95.90	13.35
325	91.1	2.3	2.1	1.6	0.3	2.6	----	97.40	6.47

Table A-17*:** Experimental Results for Isomerization of n-Hexane using PtRu/HMOR Zeolite catalyst at ***5 bar and H/HC=6

Temp.	(C1-C5)	2.2DMB	2.3DMB	2MP	3MP	n-C6	Aromatics	Conv. X%	Selec. S%
250	75.3	3.8	8.6	5.9	0.7	5.7	----	94.30	20.15
275	77.6	1.6	7.1	7.6	1.5	4.6	----	95.40	18.66
300	82.8	4.7	3.6	5.1	0.6	3.2	----	96.80	14.46
325	89.1	2.9	2.1	3.4	0.4	2.1	----	97.90	8.99

Table A-18*:** Experimental Results for Isomerization of n-Hexane using PtRu/HMOR Zeolite catalyst at ***5 bar and H/HC=9

Temp.	(C1-C5)	2.2DMB	2.3DMB	2MP	3MP	n-C6	Aromatics	Conv. X%	Selec. S%
250	71.5	5.2	8.3	7.4	1.5	5.8	----	94.20	23.78
275	76.9	2.3	6.5	7.7	2.1	4.5	----	95.50	19.48
300	81.1	4.8	3.7	5.9	1.4	3.1	----	96.90	16.31
325	87.4	3.5	2.6	4.3	0.7	1.5	----	98.50	11.27

Table A-19*:** Experimental Results for Isomerization of n-Hexane using PtZr/HZSM-5 Zeolite catalyst at ***5 bar and H/HC=3

Temp.	(C1-C5)	2.2DMB	2.3DMB	2MP	3MP	n-C6	Aromatics	Conv. X%	Selec. S%
250	0.28	0.14	0.36	30.91	23.19	44.92	0.20	55.08	99.13
275	1.54	0.03	1.54	37.05	35.78	23.92	0.14	76.08	97.79
300	9.63	0.23	3.56	34.56	30.85	21.03	0.14	78.97	87.63
325	47.92	0.22	3.37	19.45	16.46	11.85	0.73	88.15	44.81

Table A-20*:** Experimental Results for Isomerization of n-Hexane using PtZr/HZSM-5 Zeolite catalyst at ***5 bar and H/HC=6

Temp.	(C1-C5)	2.2DMB	2.3DMB	2MP	3MP	n-C6	Aromatics	Conv. X%	Selec. S%
250	0.07	0.21	0.23	34.31	28.98	36.08	0.12	63.92	99.70
275	1.03	0.02	1.26	38.5	35.28	23.73	0.13	76.27	98.41
300	6.81	0.15	2.95	36.65	31.18	22.12	0.14	77.88	91.08
325	26.9	0.22	2.91	28.47	24.76	16.14	0.60	83.86	67.21

Table A-21*:** Experimental Results for Isomerization of n-Hexane using PtZr/HZSM-5 Zeolite catalyst at ***5 bar and H/HC=9

Temp.	(C1-C5)	2.2DMB	2.3DMB	2MP	3MP	n-C6	Aromatics	Conv. X%	Selec. S%
250	0.04	0.24	0.23	34.79	25.56	39.01	0.13	60.99	99.72
275	1.02	0.01	1.11	39.56	33.79	24.38	0.13	75.62	98.48
300	5.35	0.63	1.38	37.48	33.16	21.91	0.09	78.09	93.03
325	23.48	0.31	2.85	28.42	24.16	20.23	0.55	79.77	69.88

Table A-22*:** Experimental Results for Isomerization of n-Hexane using PtZr/HMOR Zeolite catalyst at ***5 bar and H/HC=3

Temp.	(C1-C5)	2.2DMB	2.3DMB	2MP	3MP	n-C6	Aromatics	Conv. X%	Selec. S%
250	0.41	2.36	2.42	17.96	11.48	65.15	0.22	34.85	98.19
275	6.13	4.02	9.64	30.78	24.55	24.63	0.25	75.37	91.54
300	13.30	5.98	9.33	29.65	21.58	20.06	0.10	79.94	83.24
325	50.81	0.67	7.84	21.62	12.49	6.45	0.12	93.55	45.56

Table A-23*:** Experimental Results for Isomerization of n-Hexane using PtZr/HMOR Zeolite catalyst at ***5 bar and H/HC=6

Temp.	(C1-C5)	2.2DMB	2.3DMB	2MP	3MP	n-C6	Aromatics	Conv. X%	Selec. S%
250	0.39	2.75	2.32	21.98	14.03	58.32	0.21	41.68	98.56
275	3.78	2.17	8.64	32.68	25.28	27.17	0.28	72.83	94.43
300	9.76	5.93	7.31	30.77	22.02	24.10	0.11	75.90	87.00
325	43.91	4.41	7.29	20.58	15.98	7.67	0.16	92.33	52.27

Table A-24*:** Experimental Results for Isomerization of n-Hexane using PtZr/HMOR Zeolite catalyst at ***5 bar and H/HC=9

Temp.	(C1-C5)	2.2DMB	2.3DMB	2MP	3MP	n-C6	Aromatics	Conv. X%	Selec. S%
250	0.35	2.30	1.70	21.36	13.12	61.01	0.16	38.99	98.69
275	3.69	6.61	2.53	33.28	23.87	29.91	0.11	70.09	94.58
300	6.67	8.07	7.27	30.81	20.27	26.83	0.08	73.17	90.77
325	31.69	5.37	7.46	23.96	17.57	13.83	0.12	86.17	63.08

Table A-25*:** Experimental Results for Isomerization of n-Hexane using PtRuZr/HZSM-5 Zeolite catalyst at ***5 bar and H/HC=3

Temp.	(C1-C5)	2.2DMB	2.3DMB	2MP	3MP	n-C6	Aromatics	Conv. X%	Selec. S%
250	80.8	0.1	0.1	6.9	5.3	6.8	----	93.20	13.30
275	84.3	0.1	0.1	6.2	5.1	4.2	----	95.80	12.00
300	90.5	0.1	0.1	3.4	2.1	3.8	----	96.20	5.93
325	95.2	0.1	0.1	2.1	1.3	1.2	----	98.80	3.64

Table A-26*:** Experimental Results for Isomerization of n-Hexane using PtRuZr/HZSM-5 Zeolite catalyst at ***5 bar and H/HC=6

Temp.	(C1-C5)	2.2DMB	2.3DMB	2MP	3MP	n-C6	Aromatics	Conv. X%	Selec. S%
250	76.3	0.1	0.1	12.3	9.2	2.0	----	98.00	22.14
275	80.1	0.1	0.1	11.5	6.4	1.8	----	98.20	18.43
300	88.4	0.1	0.1	7.1	3.1	1.2	----	98.80	10.53
325	92.1	0.1	0.1	4.6	2.3	0.8	----	99.20	7.16

Table A-27*:** Experimental Results for Isomerization of n-Hexane using PtRuZr/HZSM-5 Zeolite catalyst at ***5 bar and H/HC=9

Temp.	(C1-C5)	2.2DMB	2.3DMB	2MP	3MP	n-C6	Aromatics	Conv. X%	Selec. S%
250	74.4	0.1	0.1	13.6	9.5	2.3	----	97.70	23.85
275	79.2	0.1	0.1	12.1	6.6	1.9	----	98.10	19.27
300	85.6	0.1	0.1	7.9	4.5	1.8	----	98.20	12.83
325	90.4	0.1	0.1	5.4	3.1	0.9	----	99.10	8.78

Table A-28*:** Experimental Results for Isomerization of n-Hexane using PtRuZr/HMOR Zeolite catalyst at ***5 bar and H/HC=3

Temp.	(C1-C5)	2.2DMB	2.3DMB	2MP	3MP	n-C6	Aromatics	Conv. X%	Selec. S%
250	70.2	3.3	9.1	8.6	0.5	6.3	----	93.70	25.08
275	74.6	3.2	9.3	7.3	0.5	5.1	----	94.90	21.39
300	81.1	2.1	7.1	4.6	0.4	4.7	----	95.30	14.90
325	85.8	1.2	5.1	4.3	0.4	3.2	----	96.80	11.36

Table A-29*:** Experimental Results for Isomerization of n-Hexane using PtRuZr/HMOR Zeolite catalyst at ***5 bar and H/HC=6

Temp.	(C1-C5)	2.2DMB	2.3DMB	2MP	3MP	n-C6	Aromatics	Conv. X%	Selec. S%
250	68.1	3.4	11.1	9.0	0.6	7.8	----	92.20	26.14
275	71.8	2.2	11.1	9.5	0.5	4.9	----	95.10	24.50
300	79.9	2.1	7.1	6.3	0.5	4.1	----	95.90	16.68
325	84.9	1.3	6.1	4.7	0.4	2.6	----	97.40	12.84

Table A-30*:** Experimental Results for Isomerization of n-Hexane using PtRuZr/HMOR Zeolite catalyst at ***5 bar and H/HC=9

Temp.	(C1-C5)	2.2DMB	2.3DMB	2MP	3MP	n-C6	Aromatics	Conv. X%	Selec. S%
250	64.5	4.3	12.4	9.7	0.9	8.2	----	91.80	29.74
275	68.6	4.2	12.1	9.1	0.8	5.2	----	94.80	27.64
300	77.4	1.6	9.8	6.4	0.7	4.1	----	95.90	19.29
325	83.3	1.1	7.1	4.6	0.6	3.3	----	96.70	13.86

Table A-31*:** Experimental Results for Isomerization of n-Hexane using Pt/SrZSM-5 Zeolite catalyst at ***5 bar and H/HC=3

Temp.	(C1-C5)	2.2DMB	2.3DMB	2MP	3MP	n-C6	Aromatics	Conv. X%	Selec. S%
250	0.12	0.3	0.07	18.80	17.96	62.55	0.2	37.45	99.15
275	0.91	0.05	1.05	35.99	34.12	27.67	0.21	72.33	98.45
300	3.22	0.12	3.46	31.97	37.67	23.35	0.21	76.65	95.53
325	10.71	0.62	5.08	33.04	28.25	21.99	0.31	78.01	85.87

Table A-32: Experimental Results for Isomerization of n-Hexane using Pt/SrZSM-5 Zeolite catalyst at ***5 bar and H/HC=6***

Temp.	(C1-C5)	2.2DMB	2.3DMB	2MP	3MP	n-C6	Aromatics	Conv. X%	Selec. S%
250	0.03	0.17	0.05	21.22	19.26	59.08	0.19	40.92	99.46
275	0.83	0.03	0.78	36.09	33.02	29.09	0.16	70.91	98.60
300	3.24	0.04	3.69	32.21	37.09	23.59	0.14	76.41	95.58
325	9.47	0.27	3.76	35.84	29.02	21.43	0.21	78.57	87.68

Table A-33: Experimental Results for Isomerization of n-Hexane using Pt/SrZSM-5 Zeolite catalyst at ***5 bar and H/HC=9***

Temp.	(C1-C5)	2.2DMB	2.3DMB	2MP	3MP	n-C6	Aromatics	Conv. X%	Selec. S%
250	0.02	0.19	0.04	22.83	18.36	58.36	0.20	41.64	99.47
275	0.76	0.21	0.49	36.96	30.72	30.68	0.18	69.32	98.64
300	2.38	0.3	1.75	39.66	32.52	22.98	0.41	77.02	96.38
325	7.62	0.92	2.67	37.51	28.82	22.27	0.19	77.73	89.95

Table A-34*:** Experimental Results for Isomerization of n-Hexane using Pt/SrMOR Zeolite catalyst at ***5 bar and H/HC=3

Temp.	(C1-C5)	2.2DMB	2.3DMB	2MP	3MP	n-C6	Aromatics	Conv. X%	Selec. S%
250	1.05	3.48	1.42	16.15	7.47	70.08	0.35	29.92	95.32
275	3.12	7.58	2.79	27.35	20.85	38.03	0.28	61.97	94.51
300	7.52	15.19	3.61	30.15	24.05	19.09	0.40	80.91	90.22
325	20.93	12.91	2.88	25.53	21.47	16.09	0.19	83.91	74.83

Table A-35*:** Experimental Results for Isomerization of n-Hexane using Pt/SrMOR Zeolite catalyst at ***5 bar and H/HC=6

Temp.	(C1-C5)	2.2DMB	2.3DMB	2MP	3MP	n-C6	Aromatics	Conv. X%	Selec. S%
250	0.95	3.57	1.37	18.21	7.57	68.04	0.29	31.96	96.12
275	2.95	7.25	2.04	28.52	22.49	36.53	0.22	63.47	95.01
300	6.57	14.88	3.02	32.56	25.15	17.11	0.22	82.89	91.22
325	18.06	11.87	2.69	28.58	22.87	15.77	0.16	84.23	78.37

Table A-36*:** Experimental Results for Isomerization of n-Hexane using Pt/SrMOR Zeolite catalyst at ***5 bar and H/HC=9

Temp.	(C1-C5)	2.2DMB	2.3DMB	2MP	3MP	n-C6	Aromatics	Conv. X%	Selec. S%
250	0.91	3.69	1.42	18.08	6.87	68.77	0.26	31.23	96.25
275	2.42	7.46	1.90	28.83	21.59	37.62	0.18	62.38	95.83
300	5.73	14.79	1.97	32.69	25.72	18.99	0.11	81.01	92.79
325	17.56	13.46	1.30	28.99	22.70	15.81	0.18	84.19	78.93

Table A-37*:** Experimental Results for Isomerization of n-Hexane using PtRu/SrZSM-5 Zeolite catalyst at ***5 bar and H/HC=3

Temp.	(C1-C5)	2.2DMB	2.3DMB	2MP	3MP	n-C6	Aromatics	Conv. X%	Selec. S%
250	62.0	----	0.1	11.6	13.2	13.1	----	86.90	28.56
275	67.3	0.2	0.1	10.4	13.8	8.2	----	91.80	26.69
300	78.3	0.1	0.1	5.6	9.2	6.7	----	93.30	16.08
325	83.2	0.1	0.1	4.1	7.2	5.3	----	94.70	12.14

Table A-38*:** Experimental Results for Isomerization of n-Hexane using PtRu/SrZSM-5 Zeolite catalyst at ***5 bar and H/HC=6

Temp.	(C1-C5)	2.2DMB	2.3DMB	2MP	3MP	n-C6	Aromatics	Conv. X%	Selec. S%
250	60.2	----	0.1	11.2	16.4	12.1	----	87.90	31.51
275	66.1	0.2	0.8	10.6	14.9	7.4	----	92.40	28.68
300	75.9	0.1	0.8	6.9	10.5	5.8	----	94.20	19.43
325	81.3	0.1	0.4	6.2	8.9	3.1	----	96.90	16.10

Table A-39*:** Experimental Results for Isomerization of n-Hexane using PtRu/SrZSM-5 Zeolite catalyst at ***5 bar and H/HC=9

Temp.	(C1-C5)	2.2DMB	2.3DMB	2MP	3MP	n-C6	Aromatics	Conv. X%	Selec. S%
250	59.3	0.1	----	10.9	18.5	11.2	----	88.80	33.22
275	65.2	0.4	0.3	10.1	16.7	7.3	----	92.70	29.67
300	73.7	0.2	0.1	7.7	13.2	5.1	----	94.90	22.34
325	80.5	0.1	0.1	6.2	10.2	2.9	----	97.10	19.10

Table A-40*:** Experimental Results for Isomerization of n-Hexane using PtRu/SrMOR Zeolite catalyst at ***5 bar and H/HC=3

Temp.	(C1-C5)	2.2DMB	2.3DMB	2MP	3MP	n-C6	Aromatics	Conv. X%	Selec. S%
250	79.2	1.9	4.6	3.6	0.3	10.4	----	89.60	11.61
275	82.1	1.4	4.2	3.2	0.9	8.2	----	91.80	10.57
300	85.6	2.2	3.4	2.7	0.5	5.6	----	94.40	9.32
325	90.4	2.1	2.2	1.9	0.3	3.1	----	96.90	6.71

Table A-41*:** Experimental Results for Isomerization of n-Hexane using PtRu/SrMOR Zeolite catalyst at ***5 bar and H/HC=6

Temp.	(C1-C5)	2.2DMB	2.3DMB	2MP	3MP	n-C6	Aromatics	Conv. X%	Selec. S%
250	77.3	2.2	5.5	4.5	0.8	9.7	----	90.30	14.40
275	79.4	2.6	6.1	3.6	0.7	7.6	----	92.40	14.07
300	82.1	3.4	4.6	4.1	0.6	5.2	----	94.80	13.39
325	89.5	2.5	2.1	3.2	0.4	2.3	----	97.70	8.39

Table A-42*:** Experimental Results for Isomerization of n-Hexane using PtRu/SrMOR Zeolite catalyst at ***5 bar and H/HC=9

Temp.	(C1-C5)	2.2DMB	2.3DMB	2MP	3MP	n-C6	Aromatics	Conv. X%	Selec. S%
250	75.1	3.2	7.3	5.1	1.5	7.8	----	92.20	18.55
275	78.2	3.3	7.5	4.7	1.7	4.6	----	95.40	18.03
300	80.4	4.8	6.1	3.8	1.4	3.5	----	96.50	16.68
325	87.2	3.4	4.1	2.3	0.8	2.1	----	97.90	10.83

Table A-43*:** Experimental Results for Isomerization of n-Hexane using PtZr/SrZSM-5 Zeolite catalyst at ***5 bar and H/HC=3

Temp.	(C1-C5)	2.2DMB	2.3DMB	2MP	3MP	n-C6	Aromatics	Conv. X%	Selec. S%
250	----	0.23	0.15	16.05	9.77	73.53	0.27	26.47	98.98
275	0.41	----	1.21	35.63	31.62	30.80	0.33	69.20	98.93
300	1.90	0.12	3.48	37.00	32.90	24.33	0.27	75.67	97.13
325	14.43	0.43	4.71	32.15	27.85	20.14	0.29	79.86	81.57

Table A-44*:** Experimental Results for Isomerization of n-Hexane using PtZr/SrZSM-5 Zeolite catalyst at ***5 bar and H/HC=6

Temp.	(C1-C5)	2.2DMB	2.3DMB	2MP	3MP	n-C6	Aromatics	Conv. X%	Selec. S%
250	----	0.29	0.11	17.80	10.39	71.20	0.21	28.80	99.27
275	0.31	----	0.98	36.91	33.27	28.28	0.25	71.72	99.22
300	1.81	0.04	1.95	37.72	34.88	23.43	0.17	76.57	97.41
325	8.88	0.2	3.21	35.77	31.93	19.83	0.18	80.17	88.70

Table A-45*:** Experimental Results for Isomerization of n-Hexane using PtZr/SrZSM-5 Zeolite catalyst at ***5 bar and H/HC=9

Temp.	(C1-C5)	2.2DMB	2.3DMB	2MP	3MP	n-C6	Aromatics	Conv. X%	Selec. S%
250	----	0.34	0.13	17.12	10.22	72.02	0.17	27.98	99.39
275	0.20	0.33	0.59	38.38	31.42	28.78	0.30	71.22	99.30
300	1.45	0.40	1.21	40.15	32.56	24.08	0.15	75.92	97.89
325	6.87	0.33	2.91	38.14	31.54	20.03	0.18	79.97	91.18

Table A-46*:** Experimental Results for Isomerization of n-Hexane using PtZr/SrMOR Zeolite catalyst at ***5 bar and H/HC=3

Temp.	(C1-C5)	2.2DMB	2.3DMB	2MP	3MP	n-C6	Aromatics	Conv. X%	Selec. S%
250	----	1.42	1.34	11.01	6.22	79.81	0.20	20.19	99.00
275	0.23	3.95	3.08	26.42	19.62	46.37	0.33	53.63	98.96
300	2.74	9.39	6.38	32.53	27.60	21.15	0.21	78.85	96.26
325	12.29	9.88	6.77	28.98	23.72	18.17	0.19	81.83	85.44

Table A-47*:** Experimental Results for Isomerization of n-Hexane using PtZr/SrMOR Zeolite catalyst at ***5 bar and H/HC=6

Temp.	(C1-C5)	2.2DMB	2.3DMB	2MP	3MP	n-C6	Aromatics	Conv. X%	Selec. S%
250	----	1.73	1.50	13.35	8.55	74.70	0.17	25.30	99.33
275	0.16	3.66	2.52	27.63	19.97	45.81	0.25	54.19	99.24
300	1.52	9.43	6.36	35.36	29.07	18.10	0.16	81.90	97.95
325	8.62	9.46	6.51	32.15	26.74	16.35	0.17	83.65	89.49

Table A-48*:** Experimental Results for Isomerization of n-Hexane using PtZr/SrMOR Zeolite catalyst at ***5 bar and H/HC=9

Temp.	(C1-C5)	2.2DMB	2.3DMB	2MP	3MP	n-C6	Aromatics	Conv. X%	Selec. S%
250	----	1.51	1.39	12.65	8.39	75.94	0.12	24.06	99.50
275	0.15	3.18	2.35	28.80	19.25	46.03	0.24	53.97	99.28
300	1.25	8.11	5.77	35.57	28.96	20.18	0.16	79.82	98.23
325	6.37	9.75	6.64	33.40	26.32	17.41	0.11	82.59	92.15

Table A-49*:** Experimental Results for Isomerization of n-Hexane using PtRuZr/SrZSM-5 Zeolite catalyst at ***5 bar and H/HC=3

Temp.	(C1-C5)	2.2DMB	2.3DMB	2MP	3MP	n-C6	Aromatics	Conv. X%	Selec. S%
250	84.8	0.1	0.1	6.9	4.5	3.6	----	96.40	15.77
275	86.3	0.1	0.1	7.2	4.2	2.1	----	97.90	11.85
300	89.5	0.1	0.1	4.9	3.7	1.7	----	98.30	8.95
325	96.2	0.1	0.1	1.6	0.8	1.2	----	98.80	2.63

Table A-50*:** Experimental Results for Isomerization of n-Hexane using PtRuZr/SrZSM-5 Zeolite catalyst at ***5 bar and H/HC=6

Temp.	(C1-C5)	2.2DMB	2.3DMB	2MP	3MP	n-C6	Aromatics	Conv. X%	Selec. S%
250	81.3	0.1	0.1	10.1	7.2	1.2	----	98.80	17.71
275	85.1	0.1	0.1	8.5	5.1	1.1	----	98.90	13.95
300	88.4	0.1	0.1	7.1	3.6	0.7	----	99.30	10.98
325	93.6	0.1	0.1	3.3	2.3	0.6	----	99.40	5.84

Table A-51*:** Experimental Results for Isomerization of n-Hexane using PtRuZr/SrZSM-5 Zeolite catalyst at ***5 bar and H/HC=9

Temp.	(C1-C5)	2.2DMB	2.3DMB	2MP	3MP	n-C6	Aromatics	Conv. X%	Selec. S%
250	80.4	0.1	0.1	10.0	8.5	0.9	----	99.10	18.87
275	82.2	0.1	0.1	9.4	7.6	0.6	----	99.40	17.31
300	85.6	0.1	0.1	8.5	5.3	0.4	----	99.60	14.06
325	92.4	0.1	0.1	4.4	2.8	0.2	----	99.80	7.41

Table A-52: Experimental Results for Isomerization of n-Hexane using PtRuZr/SrMOR Zeolite catalyst at ***5 bar and H/HC=3***

Temp.	(C1-C5)	2.2DMB	2.3DMB	2MP	3MP	n-C6	Aromatics	Conv. X%	Selec. S%
250	75.2	2.3	8.1	5.6	0.5	8.3	----	91.70	17.99
275	79.6	2.2	7.1	3.9	0.4	6.8	----	93.20	14.59
300	86.1	2.1	4.1	2.1	0.4	5.2	----	94.80	9.18
325	92.8	1.2	1.6	0.9	0.3	3.2	----	96.80	4.13

Table A-53**:** Experimental Results for Isomerization of n-Hexane using PtRuZr/SrMOR Zeolite catalyst at ***5 bar and H/HC=6***

Temp.	(C1-C5)	2.2DMB	2.3DMB	2MP	3MP	n-C6	Aromatics	Conv. X%	Selec. S%
250	72.1	2.4	10.1	6.9	0.7	7.8	----	92.20	21.80
275	77.8	2.2	7.1	5.6	0.7	6.6	----	93.40	16.70
300	83.9	2.1	6.1	3.3	0.5	4.1	----	95.90	12.51
325	90.1	1.2	3.1	2.6	0.4	2.6	----	97.40	7.49

Table A-54**:** Experimental Results for Isomerization of n-Hexane using PtRuZr/SrMOR Zeolite catalyst at ***5 bar and H/HC=9***

Temp.	(C1-C5)	2.2DMB	2.3DMB	2MP	3MP	n-C6	Aromatics	Conv. X%	Selec. S%
250	70.5	4.1	10.1	7.8	0.8	6.7	----	93.30	24.44
275	74.8	3.4	8.4	7.1	0.7	5.6	----	94.40	20.76
300	79.4	2.2	7.2	6.8	0.7	3.7	----	96.30	17.55
325	86.3	1.3	5.3	4.4	0.6	2.1	----	97.90	11.85

Table A-55*:** Experimental Results for Isomerization of n-Hexane using Pt/BaZSM-5 Zeolite catalyst at ***5 bar and H/HC=3

Temp.	(C1-C5)	2.2DMB	2.3DMB	2MP	3MP	n-C6	Aromatics	Conv. X%	Selec. S%
250	0.14	0.23	0.05	12.73	7.14	79.4	0.31	20.60	97.82
275	0.87	0.16	0.86	36.27	30.53	31.08	0.23	68.92	98.40
300	2.87	0.09	3.2	37.17	33.15	23.33	0.19	76.67	96.01
325	9.89	0.52	5.04	33.09	29.86	21.32	0.28	78.68	87.07

Table A-56*:** Experimental Results for Isomerization of n-Hexane using Pt/BaZSM-5Zeolite catalyst at ***5 bar and H/HC=6

Temp.	(C1-C5)	2.2DMB	2.3DMB	2MP	3MP	n-C6	Aromatics	Conv. X%	Selec. S%
250	0.05	0.29	0.05	13.35	7.40	78.55	0.31	21.45	98.32
275	0.77	0.16	0.62	36.57	32.84	28.86	0.18	71.14	98.66
300	2.11	0.04	2.16	38.23	34.97	22.34	0.15	77.66	97.09
325	8.07	0.11	3.89	36.54	30.75	20.43	0.21	79.57	89.59

Table A-57*:** Experimental Results for Isomerization of n-Hexane using Pt/BaZSM-5Zeolite catalyst at ***5 bar and H/HC=9

Temp.	(C1-C5)	2.2DMB	2.3DMB	2MP	3MP	n-C6	Aromatics	Conv. X%	Selec. S%
250	0.04	0.35	0.03	13.15	7.05	79.11	0.27	20.89	98.52
275	0.64	0.15	0.54	36.38	31.63	30.47	0.19	69.53	98.81
300	2.07	0.10	1.74	38.63	34.03	23.28	0.15	76.72	97.11
325	6.66	0.20	3.70	36.94	30.76	21.55	0.19	78.45	91.27

Table A-58*:** Experimental Results for Isomerization of n-Hexane using Pt/BaMOR Zeolite catalyst at ***5 bar and H/HC=3

Temp.	(C1-C5)	2.2DMB	2.3DMB	2MP	3MP	n-C6	Aromatics	Conv. X%	Selec. S%
250	2.45	3.81	1.38	7.46	4.20	80.35	0.35	19.65	85.75
275	5.66	8.76	2.61	28.18	22.27	32.28	0.24	67.72	91.29
300	10.31	16.45	3.74	27.24	19.57	22.36	0.33	77.64	86.30
325	26.02	14.26	2.80	21.02	18.21	17.35	0.34	82.65	68.11

Table A-59*:** Experimental Results for Isomerization of n-Hexane using Pt/BaMOR Zeolite catalyst at ***5 bar and H/HC=6

Temp.	(C1-C5)	2.2DMB	2.3DMB	2MP	3MP	n-C6	Aromatics	Conv. X%	Selec. S%
250	1.50	2.98	1.21	11.31	5.43	77.28	0.29	22.72	87.72
275	5.41	7.65	2.16	30.69	25.64	28.24	0.21	71.76	92.17
300	7.81	15.41	3.57	29.47	24.37	19.18	0.19	80.82	90.10
325	24.68	13.10	2.71	24.75	19.29	15.27	0.20	84.73	70.61

Table A-60*:** Experimental Results for Isomerization of n-Hexane using Pt/BaMOR Zeolite catalyst at ***5 bar and H/HC=9

Temp.	(C1-C5)	2.2DMB	2.3DMB	2MP	3MP	n-C6	Aromatics	Conv. X%	Selec. S%
250	1.35	3.01	0.96	10.08	5.19	79.21	0.20	20.79	92.54
275	5.02	8.17	1.49	29.74	23.11	32.26	0.21	67.74	92.27
300	6.92	16.56	2.78	28.51	21.86	23.19	0.18	76.81	90.76
325	21.36	13.69	1.65	26.26	19.58	17.28	0.18	82.72	73.96

Table A-61*:** Experimental Results for Isomerization of n-Hexane using PtRu/BaZSM-5 Zeolite catalyst at ***5 bar and H/HC=3

Temp.	(C1-C5)	2.2DMB	2.3DMB	2MP	3MP	n-C6	Aromatics	Conv. X%	Selec. S%
250	68.6	----	0.1	6.9	8.3	16.1	----	83.90	18.24
275	74.7	0.2	0.1	6.4	8.1	10.5	----	89.50	16.54
300	80.3	0.1	0.1	5.0	7.2	7.3	----	92.70	13.38
325	89.2	0.1	0.1	2.7	3.3	4.6	----	95.40	6.50

Table A-62*:** Experimental Results for Isomerization of n-Hexane using PtRu/BaZSM-5 Zeolite catalyst at ***5 bar and H/HC=6

Temp.	(C1-C5)	2.2DMB	2.3DMB	2MP	3MP	n-C6	Aromatics	Conv. X%	Selec. S%
250	66.2	----	0.1	9.4	10.1	14.2	----	85.80	22.84
275	71.9	0.2	0.5	8.6	9.9	8.9	----	91.10	21.08
300	79.8	0.1	0.6	4.7	8.6	6.2	----	93.80	14.93
325	89.1	0.1	0.3	2.4	5.0	3.1	----	96.90	8.05

Table A-63*:** Experimental Results for Isomerization of n-Hexane using PtRu/BaZSM-5 Zeolite catalyst at ***5 bar and H/HC=9

Temp.	(C1-C5)	2.2DMB	2.3DMB	2MP	3MP	n-C6	Aromatics	Conv. X%	Selec. S%
250	64.2	0.1	----	9.5	14.6	11.6	----	88.40	27.38
275	69.3	0.4	0.3	8.5	13.7	7.8	----	92.20	24.84
300	78.1	0.2	0.1	7.1	9.2	5.3	----	94.70	17.53
325	87.5	0.1	0.1	3.2	6.2	2.9	----	97.10	9.89

Table A-64*:** Experimental Results for Isomerization of n-Hexane using PtRu/BaMOR Zeolite catalyst at ***5 bar and H/HC=3

Temp.	(C1-C5)	2.2DMB	2.3DMB	2MP	3MP	n-C6	Aromatics	Conv. X%	Selec. S%
250	78.6	2.8	7.6	4.8	0.3	5.9	----	94.10	16.47
275	81.2	1.4	6.2	5.5	0.6	5.1	----	94.90	14.44
300	82.7	4.3	4.6	3.7	0.5	4.2	----	95.80	13.67
325	92.3	1.5	2.3	0.8	0.4	2.7	----	97.30	5.14

Table A-65*:** Experimental Results for Isomerization of n-Hexane using PtRu/BaMOR Zeolite catalyst at ***5 bar and H/HC=6

Temp.	(C1-C5)	2.2DMB	2.3DMB	2MP	3MP	n-C6	Aromatics	Conv. X%	Selec. S%
250	76.3	3.6	8.4	5.7	0.5	5.5	----	94.50	19.26
275	78.2	2.5	7.2	6.9	0.7	4.5	----	95.50	18.12
300	80.1	4.6	6.6	5.1	0.7	2.9	----	97.10	17.51
325	90.1	2.5	2.8	2.1	0.5	2.0	----	98.00	8.06

Table A-66*:** Experimental Results for Isomerization of n-Hexane using PtRu/BaMOR Zeolite catalyst at ***5 bar and H/HC=9

Temp.	(C1-C5)	2.2DMB	2.3DMB	2MP	3MP	n-C6	Aromatics	Conv. X%	Selec. S%
250	74.5	5.4	7.3	6.4	1.3	5.1	----	94.90	21.50
275	76.1	2.9	7.5	7.1	2.2	4.2	----	95.80	20.56
300	79.3	4.9	6.1	5.7	1.5	2.5	----	97.50	18.67
325	88.4	3.4	3.6	2.3	0.8	1.5	----	98.50	10.25

Table A-67*:** Experimental Results for Isomerization of n-Hexane using PtZr/BaZSM-5 Zeolite catalyst at ***5 bar and H/HC=3

Temp.	(C1-C5)	2.2DMB	2.3DMB	2MP	3MP	n-C6	Aromatics	Conv. X%	Selec. S%
250	1.37	0.07	0.38	12.27	7.45	78.13	0.33	21.87	92.22
275	1.67	0.12	0.92	30.48	25.05	41.33	0.23	58.67	96.42
300	3.49	0.20	3.68	36.23	32.20	23.97	0.23	76.03	95.11
325	9.80	0.50	4.91	34.19	28.49	21.79	0.32	78.21	87.06

Table A-68*:** Experimental Results for Isomerization of n-Hexane using PtZr/BaZSM-5 Zeolite catalyst at ***5 bar and H/HC=6

Temp.	(C1-C5)	2.2DMB	2.3DMB	2MP	3MP	n-C6	Aromatics	Conv. X%	Selec. S%
250	1.13	0.07	0.39	13.57	9.30	75.26	0.28	24.74	94.30
275	1.39	0.18	0.69	31.84	25.44	40.28	0.18	59.72	97.37
300	2.97	0.24	2.83	39.74	33.44	20.61	0.17	79.39	96.04
325	7.65	0.36	4.62	38.84	30.95	17.36	0.22	82.64	90.48

Table A-69*:** Experimental Results for Isomerization of n-Hexane using PtZr/BaZSM-5 Zeolite catalyst at ***5 bar and H/HC=9

Temp.	(C1-C5)	2.2DMB	2.3DMB	2MP	3MP	n-C6	Aromatics	Conv. X%	Selec. S%
250	0.97	0.06	0.40	13.43	7.33	77.61	0.20	22.39	94.77
275	1.20	0.17	0.50	31.40	25.33	41.23	0.17	58.77	97.67
300	2.06	0.23	2.69	40.58	33.19	21.07	0.18	78.93	97.16
325	6.10	0.30	4.07	39.41	30.53	19.38	0.21	80.62	92.17

Table A-70*:** Experimental Results for Isomerization of n-Hexane using PtZr/BaMOR Zeolite catalyst at ***5 bar and H/HC=3

Temp.	(C1-C5)	2.2DMB	2.3DMB	2MP	3MP	n-C6	Aromatics	Conv. X%	Selec. S%
250	0.15	0.33	0.32	6.41	2.98	89.1	0.44	10.90	92.11
275	0.97	2.66	2.33	21.30	15.13	57.20	0.41	42.80	96.78
300	2.19	6.8	5.87	32.27	25.52	26.89	0.28	73.11	96.38
325	8.33	8.65	6.25	30.56	24.68	21.24	0.29	78.76	89.06

Table A-71*:** Experimental Results for Isomerization of n-Hexane using PtZr/BaMOR Zeolite catalyst at ***5 bar and H/HC=6

Temp.	(C1-C5)	2.2DMB	2.3DMB	2MP	3MP	n-C6	Aromatics	Conv. X%	Selec. S%
250	0.13	0.29	0.33	8.64	5.15	85.14	0.32	14.86	96.97
275	0.83	2.27	2.15	23.70	18.93	51.83	0.29	48.17	97.67
300	1.96	6.46	5.12	36.27	27.28	22.71	0.20	77.29	97.21
325	6.51	7.89	6.03	35.42	26.29	17.68	0.18	82.32	91.87

Table A-72*:** Experimental Results for Isomerization of n-Hexane using PtZr/BaMOR Zeolite catalyst at ***5 bar and H/HC=9

Temp.	(C1-C5)	2.2DMB	2.3DMB	2MP	3MP	n-C6	Aromatics	Conv. X%	Selec. S%
250	0.09	0.30	0.31	7.52	3.87	87.63	0.28	12.37	97.01
275	0.57	1.98	2.06	23.76	18.12	53.29	0.22	46.71	98.31
300	1.52	6.20	5.20	35.21	26.01	25.68	0.18	74.32	97.71
325	5.12	7.13	5.80	34.81	25.77	21.20	0.17	78.80	93.29

Table A-73*:** Experimental Results for Isomerization of n-Hexane using PtRuZr/BaZSM-5 Zeolite catalyst at ***5 bar and H/HC=3

Temp.	(C1-C5)	2.2DMB	2.3DMB	2MP	3MP	n-C6	Aromatics	Conv. X%	Selec. S%
250	80.2	0.1	0.1	5.6	4.3	9.7	----	90.30	11.18
275	84.3	0.1	0.1	5.2	4.1	6.2	----	93.80	10.13
300	89.7	0.1	0.1	2.8	2.1	5.2	----	94.80	5.38
325	94.2	0.1	0.1	1.1	0.7	3.8	----	96.20	2.08

Table A-74*:** Experimental Results for Isomerization of n-Hexane using PtRuZr/BaZSM-5 Zeolite catalyst at ***5 bar and H/HC=6

Temp.	(C1-C5)	2.2DMB	2.3DMB	2MP	3MP	n-C6	Aromatics	Conv. X%	Selec. S%
250	78.2	0.1	0.1	9.3	8.2	4.1	----	95.90	18.46
275	82.1	0.1	0.1	8.1	6.4	3.2	----	96.80	15.19
300	86.3	0.1	0.1	7.1	5.0	1.4	----	98.60	12.47
325	93.7	0.1	0.1	3.0	2.2	0.9	----	99.10	5.45

Table A-75*:** Experimental Results for Isomerization of n-Hexane using PtRuZr/BaZSM-5 Zeolite catalyst at ***5 bar and H/HC=9

Temp.	(C1-C5)	2.2DMB	2.3DMB	2MP	3MP	n-C6	Aromatics	Conv. X%	Selec. S%
250	75.4	0.1	0.1	11.5	9.1	3.8	----	96.20	21.62
275	79.8	0.1	0.1	10.1	7.6	2.3	----	97.70	18.32
300	82.4	0.1	0.1	9.8	6.5	1.1	----	98.90	16.68
325	90.5	0.1	0.1	5.4	3.1	0.8	----	99.20	8.77

Table A-76*:** Experimental Results for Isomerization of n-Hexane using PtRuZr/BaMOR Zeolite catalyst at ***5 bar and H/HC=3

Temp.	(C1-C5)	2.2DMB	2.3DMB	2MP	3MP	n-C6	Aromatics	Conv. X%	Selec. S%
250	71.2	3.3	10.1	8.8	0.5	6.1	----	93.90	24.17
275	78.6	3.2	7.1	5.2	0.6	5.3	----	94.70	17.00
300	83.1	2.1	5.6	4.2	0.5	4.5	----	95.50	12.98
325	86.8	1.2	4.9	3.6	0.4	3.1	----	96.90	10.73

Table A-77*:** Experimental Results for Isomerization of n-Hexane using PtRuZr/BaMOR Zeolite catalyst at ***5 bar and H/HC=6

Temp.	(C1-C5)	2.2DMB	2.3DMB	2MP	3MP	n-C6	Aromatics	Conv. X%	Selec. S%
250	69.1	4.4	11.1	8.9	0.7	5.8	----	94.20	26.65
275	77.8	4.3	7.1	5.4	0.6	4.8	----	95.20	18.28
300	80.5	3.6	6.6	4.6	0.6	4.1	----	95.90	16.06
325	84.9	3.1	5.1	3.7	0.5	2.7	----	97.30	12.74

Table A-78*:** Experimental Results for Isomerization of n-Hexane using PtRuZr/BaMOR Zeolite catalyst at ***5 bar and H/HC=9

Temp.	(C1-C5)	2.2DMB	2.3DMB	2MP	3MP	n-C6	Aromatics	Conv. X%	Selec. S%
250	65.5	4.5	14.1	9.8	0.9	5.2	----	94.80	30.91
275	76.1	4.2	9.1	5.6	0.8	4.2	----	95.80	20.56
300	77.9	3.7	8.7	5.2	0.7	3.8	----	96.20	19.02
325	82.3	2.1	8.1	4.6	0.6	2.3	----	97.70	15.76

Appendix B

Table B-1: Rate of Reaction in (10^{-7} mole/g.s) for Zeolite Pt/HZSM-5 (I) at P=5 bar and *H/HC=3*

Temperature	Rate of Overall Conversion	Rate of Isomerization	Rate for Cracking
250	31.8712	29.83169	2.039513
275	46.62876	38.48288	8.145878
300	48.97268	30.94581	18.02687
325	53.49005	11.68307	41.80698

Table B-2: Rate of Reaction in (10^{-7} mole/g.s) for Zeolite Pt/HZSM-5 (I) at P=5 bar and *H/HC=6*

Temperature	Rate of Overall Conversion	Rate of Isomerization	Rate for Cracking
250	39.09778	37.19829	1.899487
275	46.98796	40.46761	6.520355
300	50.14159	34.26383	15.87776
325	54.51285	16.81534	37.69751

Table B-3: Rate of Reaction in (10^{-7} mole/g.s) for Zeolite Pt/HZSM-5 (I) at P=5 bar and *H/HC=9*

Temperature	Rate of Overall Conversion	Rate of Isomerization	Rate for Cracking
250	38.90905	37.14959	1.759461
275	45.66684	39.96229	5.70455
300	48.46127	34.59258	13.86869
325	53.66051	22.11806	31.54245

Table B-4: Rate of Reaction in (10^{-7} mole/g.s) for Zeolite Pt/HMOR(I) at P=5 bar and *H/HC=3*

Temperature	Rate of Overall Conversion	Rate of Isomerization	Rate for Cracking
250	34.03857	32.54699	1.491585
275	48.57086	41.2347	7.336161
300	51.20092	35.46318	15.73774
325	56.06531	12.09705	43.96826

Table B-5: Rate of Reaction in (10^{-7} mole/g.s) for Zeolite Pt/ HMOR (I) at P=5 bar and *H/HC=6*

Temperature	Rate of Overall Conversion	Rate of Isomerization	Rate for Cracking
250	45.7886	43.57862	2.20998
275	48.73524	43.10375	5.631493
300	51.5662	36.01719	15.54901
325	55.52956	17.35109	38.17847

Table B-6: Rate of Reaction in (10^{-7} mole/g.s) for Zeolite Pt/ HMOR (I) at P=5 bar and *H/HC=9*

Temperature	Rate of Overall Conversion	Rate of Isomerization	Rate for Cracking
250	45.34417	43.85867	1.485496
275	46.70181	44.24831	2.453504
300	50.96957	37.13132	13.83825
325	54.68332	20.69346	33.98986

Table B-7: Rate of Reaction in (10^{-7} mole/g.s) for Zeolite Pt/HZSM-5 at P=5 bar and *H/HC=3*

Temperature	Rate of Overall Conversion	Rate of Isomerization	Rate for Cracking
250	29.61861	29.35682	0.2617883
275	45.13108	43.14027	1.990809
300	47.75506	40.47369	7.281368
325	51.39574	28.56536	22.83038

Table B-8: Rate of Reaction in (10^{-7} mole/g.s) for Zeolite Pt/HZSM-5 at P=5 bar and *H/HC=6*

Temperature	Rate of Overall Conversion	Rate of Isomerization	Rate for Cracking
250	38.51332	38.215	0.2983169
275	44.16308	43.14028	1.022801
300	47.43847	40.76591	6.672558
325	51.03045	30.87275	20.1577

Table B-9: Rate of Reaction in (10^{-7} mole/g.s) for Zeolite Pt/HZSM-5 at P=5 bar and *H/HC=9*

Temperature	Rate of Overall Conversion	Rate of Isomerization	Rate for Cracking
250	38.14803	37.89842	0.2496121
275	44.65621	43.8952	0.7610125
300	47.18887	43.1829	4.00597
325	50.78693	31.02496	19.76197

Table B-10: Rate of Reaction in (10^{-7} mole/g.s) for Zeolite Pt/HMOR at P=5 bar and *H/HC=3*

Temperature	Rate of Overall Conversion	Rate of Isomerization	Rate for Cracking
250	25.44826	25.22909	0.2191716
275	40.33975	38.26371	2.076042
300	48.97876	39.79182	9.186943
325	54.67722	25.00991	29.66731

Table B-11: Rate of Reaction in (10^{-7} mole/g.s) for Zeolite Pt/ HMOR at P=5 bar and *H/HC=6*

Temperature	Rate of Overall Conversion	Rate of Isomerization	Rate for Cracking
250	44.33355	43.98044	0.3531098
275	47.46283	45.87384	1.588994
300	51.0609	43.92565	7.135253
325	54.96946	29.82561	25.14385

Table B-12: Rate of Reaction in (10^{-7} mole/g.s) for Zeolite Pt/ HMOR at P=5 bar and *H/HC=9*

Temperature	Rate of Overall Conversion	Rate of Isomerization	Rate for Cracking
250	41.00335	40.74156	0.2617883
275	45.97733	45.24067	0.7366601
300	50.3425	43.79779	6.544707
325	55.0486	33.32017	21.72843

Table B-13: Rate of Reaction in (10^{-7} mole/g.s) for Zeolite PtRu/HZSM-5 at P=5 bar and *H/HC=3*

Temperature	Rate of Overall Conversion	Rate of Isomerization	Rate for Cracking
250	54.12321	15.95082	38.17239
275	57.47166	15.58553	41.88613
300	57.95871	10.41065	47.54806
325	58.38488	8.27982	50.10506

Table B-14: Rate of Reaction in (10^{-7} mole/g.s) for Zeolite PtRu/HZSM-5 at P=5 bar and *H/HC=6*

Temperature	Rate of Overall Conversion	Rate of Isomerization	Rate for Cracking
250	53.45352	16.80316	36.65036
275	58.81105	16.92492	41.88613
300	59.17633	11.93267	47.24366
325	60.08955	10.53241	49.55714

Table B-15: Rate of Reaction in (10^{-7} mole/g.s) for Zeolite PtRu/HZSM-5 at P=5 bar and *H/HC=9*

Temperature	Rate of Overall Conversion	Rate of Isomerization	Rate for Cracking
250	53.21	17.16845	36.04155
275	59.17633	18.20341	40.97292
300	60.21131	15.28113	44.93018
325	60.33307	11.26299	49.07008

Table B-16: Rate of Reaction in (10^{-7} mole/g.s) for Zeolite PtRu/HMOR at P=5 bar and *H/HC=3*

Temperature	Rate of Overall Conversion	Rate of Isomerization	Rate for Cracking
250	57.22814	9.49743	47.73071
275	57.71519	8.64511	49.07008
300	58.38488	7.79277	50.59211
325	59.2981	3.83551	55.46259

Table B-17: Rate of Reaction in (10^{-7} mole/g.s) for Zeolite PtRu/ HMOR at P=5 bar and *H/HC=6*

Temperature	Rate of Overall Conversion	Rate of Isomerization	Rate for Cracking
250	57.41079	11.56739	45.8434
275	58.08047	10.83681	47.24366
300	58.93281	8.52334	50.40947
325	59.6025	5.35753	54.24497

Table B-18: Rate of Reaction in (10^{-7} mole/g.s) for Zeolite PtRu/ HMOR at P=5 bar and *H/HC=9*

Temperature	Rate of Overall Conversion	Rate of Isomerization	Rate for Cracking
250	57.3499	13.81999	43.52991
275	58.14135	11.32386	46.81749
300	58.99369	9.6192	49.37449
325	59.96778	6.75778	53.21

Table B-19: Rate of Reaction in (10^{-7} mole/g.s) for Zeolite PtZr/HZSM-5 at P=5 bar and *H/HC=3*

Temperature	Rate of Overall Conversion	Rate of Isomerization	Rate for Cracking
250	33.53326	33.36279	0.1704668
275	46.31826	45.38069	0.9375674
300	48.07773	42.21489	5.86284
325	53.6666	24.49243	29.17417

Table B-20: Rate of Reaction in (10^{-7} mole/g.s) for Zeolite PtZr/HZSM-5at P=5 bar and *H/HC=6*

Temperature	Rate of Overall Conversion	Rate of Isomerization	Rate for Cracking
250	38.91513	38.87251	0.0426167
275	46.43394	45.80687	0.6270743
300	47.41412	43.26812	4.145996
325	51.05481	34.67782	16.37699

Table B-21: Rate of Reaction in (10^{-7} mole/g.s) for Zeolite PtZr/HZSM-5at P=5 bar and *H/HC=9*

Temperature	Rate of Overall Conversion	Rate of Isomerization	Rate for Cracking
250	37.13132	37.10697	0.0243524
275	46.03822	45.41723	0.6209862
300	47.54197	44.28484	3.257133
325	48.56477	34.26991	14.29486

Table B-22: Rate of Reaction in (10^{-7} mole/g.s) for Zeolite PtZr/HMOR at P=5 bar and *H/HC=3*

Temperature	Rate of Overall Conversion	Rate of Isomerization	Rate for Cracking
250	21.21703	20.96742	0.2496121
275	45.88601	42.15401	3.732005
300	48.66827	40.5711	8.097173
325	56.95418	26.02054	30.93364

Table B-23: Rate of Reaction in (10^{-7} mole/g.s) for Zeolite PtZr/HMOR at P=5 bar and *H/HC=6*

Temperature	Rate of Overall Conversion	Rate of Isomerization	Rate for Cracking
250	25.3752	25.13776	0.2374359
275	44.33963	42.03833	2.301302
300	46.20868	40.26669	5.941986
325	56.21143	29.47858	26.73285

Table B-24: Rate of Reaction in (10^{-7} mole/g.s) for Zeolite PtZr/HMOR at P=5 bar and *H/HC=9*

Temperature	Rate of Overall Conversion	Rate of Isomerization	Rate for Cracking
250	23.7375	23.52442	0.2130835
275	42.67149	40.42498	2.246509
300	44.54663	40.48587	4.060763
325	52.46115	33.16796	19.29319

Table B-25: Rate of Reaction in (10^{-7} mole/g.s) for Zeolite PtRuZr/HZSM-5 at P=5 bar and *H/HC=3*

Temperature	Rate of Overall Conversion	Rate of Isomerization	Rate for Cracking
250	56.74109	7.54924	49.19185
275	58.324	7.00131	51.32269
300	58.56752	3.47021	55.09731
325	60.15043	2.19172	57.95871

Table B-26: Rate of Reaction in (10^{-7} mole/g.s) for Zeolite PtRuZr/HZSM-5at P=5 bar and *H/HC=6*

Temperature	Rate of Overall Conversion	Rate of Isomerization	Rate for Cracking
250	59.66338	13.21117	46.45221
275	59.78514	11.01946	48.76568
300	60.15043	6.33162	53.81881
325	60.39395	4.32255	56.0714

Table B-27: Rate of Reaction in (10^{-7} mole/g.s) for Zeolite PtRuZr/HZSM-5at P=5 bar and *H/HC=9*

Temperature	Rate of Overall Conversion	Rate of Isomerization	Rate for Cracking
250	59.48074	14.18528	45.29546
275	59.72426	11.50651	48.21775
300	59.78514	7.671	52.11414
325	60.33307	5.29664	55.03643

Table B-28: Rate of Reaction in (10^{-7} mole/g.s) for Zeolite PtRuZr/HMOR at P=5 bar and *H/HC=3*

Temperature	Rate of Overall Conversion	Rate of Isomerization	Rate for Cracking
250	57.04549	14.30703	42.73846
275	57.77607	12.35885	45.41722
300	58.0196	8.64511	49.37449
325	58.93281	6.69691	52.2359

Table B-29: Rate of Reaction in (10^{-7} mole/g.s) for Zeolite PtRuZr/ HMOR at P=5 bar and *H/HC=6*

Temperature	Rate of Overall Conversion	Rate of Isomerization	Rate for Cracking
250	56.13228	14.67232	41.45996
275	57.89783	14.18527	43.71256
300	58.38488	9.74096	48.64392
325	59.2981	7.61013	51.68797

Table B-30: Rate of Reaction in (10^{-7} mole/g.s) for Zeolite PtRuZr/ HMOR at P=5 bar and *H/HC=9*

Temperature	Rate of Overall Conversion	Rate of Isomerization	Rate for Cracking
250	55.88876	16.62051	39.26825
275	57.71519	15.95082	41.76437
300	58.38488	11.26299	47.12189
325	58.87193	8.15806	50.71387

Table B-31: Rate of Reaction in (10^{-7} mole/g.s) for Zeolite Pt/SrZSM-5 at P=5 bar and *H/HC=3*

Temperature	Rate of Overall Conversion	Rate of Isomerization	Rate for Cracking
250	22.79993	22.72687	0.0730572
275	44.03523	43.48121	0.5540171
300	46.66529	44.70492	1.960368
325	47.49327	40.97292	6.520355

Table B-32: Rate of Reaction in (10^{-7} mole/g.s) for Zeolite Pt/SrZSM-5at P=5 bar and *H/HC=6*

Temperature	Rate of Overall Conversion	Rate of Isomerization	Rate for Cracking
250	24.9125	24.89424	0.0182643
275	43.17072	42.66541	0.5053123
300	46.51917	44.54663	1.972544
325	47.8342	42.06877	5.765431

Table B-33: Rate of Reaction in (10^{-7} mole/g.s) for Zeolite Pt/SrZSM-5at P=5 bar and *H/HC=9*

Temperature	Rate of Overall Conversion	Rate of Isomerization	Rate for Cracking
250	25.35085	25.33867	0.0121762
275	42.20271	41.74001	0.4626956
300	46.89054	45.44157	1.448968
325	47.3228	42.68367	4.639132

Table B-34: Rate of Reaction in (10^{-7} mole/g.s) for Zeolite Pt/SrMOR at P=5 bar and *H/HC=3*

Temperature	Rate of Overall Conversion	Rate of Isomerization	Rate for Cracking
250	18.2156	17.57635	0.6392505
275	37.72795	35.82846	1.899487
300	49.25882	44.68057	4.578251
325	51.08525	38.34286	12.74239

Table B-35: Rate of Reaction in (10^{-7} mole/g.s) for Zeolite Pt/SrMOR at P=5 bar and *H/HC=6*

Temperature	Rate of Overall Conversion	Rate of Isomerization	Rate for Cracking
250	19.45757	18.8792	0.5783695
275	38.64117	36.84518	1.79599
300	50.46426	46.46438	3.999882
325	51.28007	40.28496	10.99511

Table B-36: Rate of Reaction in (10^{-7} mole/g.s) for Zeolite Pt/SrMOR at P=5 bar and *H/HC=9*

Temperature	Rate of Overall Conversion	Rate of Isomerization	Rate for Cracking
250	19.01314	18.45912	0.5540171
275	37.97757	36.50425	1.47332
300	49.3197	45.83122	3.488481
325	51.25571	40.56501	10.6907

Table B-37: Rate of Reaction in (10^{-7} mole/g.s) for Zeolite PtRu/SrZSM-5 at P=5 bar and *H/HC=3*

Temperature	Rate of Overall Conversion	Rate of Isomerization	Rate for Cracking
250	52.90559	15.15937	37.74622
275	55.88876	14.91584	40.97292
300	56.80198	9.13215	47.66983
325	57.6543	7.00131	50.65299

Table B-38: Rate of Reaction in (10^{-7} mole/g.s) for Zeolite PtRu/SrZSM-5at P=5 bar and *H/HC=6*

Temperature	Rate of Overall Conversion	Rate of Isomerization	Rate for Cracking
250	53.5144	16.86404	36.65036
275	56.25404	16.0117	40.24234
300	57.3499	11.14122	46.20868
325	58.99369	9.49744	49.49625

Table B-39: Rate of Reaction in (10^{-7} mole/g.s) for Zeolite PtRu/SrZSM-5at P=5 bar and *H/HC=9*

Temperature	Rate of Overall Conversion	Rate of Isomerization	Rate for Cracking
250	54.06233	17.9599	36.10243
275	56.43668	16.74227	39.69441
300	57.77607	12.90677	44.8693
325	59.11545	10.10625	49.0092

Table B-40: Rate of Reaction in (10^{-7} mole/g.s) for Zeolite PtRu/SrMOR at P=5 bar and *H/HC=3*

Temperature	Rate of Overall Conversion	Rate of Isomerization	Rate for Cracking
250	54.54937	6.33162	48.21775
275	55.88876	5.90546	49.9833
300	57.47166	5.35752	52.11414
325	58.99369	3.95726	55.03643

Table B-41: Rate of Reaction in (10^{-7} mole/g.s) for Zeolite PtRu/SrMOR at P=5 bar and *H/HC=6*

Temperature	Rate of Overall Conversion	Rate of Isomerization	Rate for Cracking
250	54.97554	7.91452	47.06102
275	56.25404	7.91452	48.33952
300	57.71519	7.73189	49.9833
325	59.48074	4.99225	54.48849

Table B-42: Rate of Reaction in (10^{-7} mole/g.s) for Zeolite PtRu/SrMOR at P=5 bar and *H/HC=9*

Temperature	Rate of Overall Conversion	Rate of Isomerization	Rate for Cracking
250	56.13228	10.41065	45.72163
275	58.08047	10.47153	47.60894
300	58.75016	9.80183	48.94833
325	59.6025	6.51427	53.08823

Table B-43: Rate of Reaction in (10^{-7} mole/g.s) for Zeolite PtZr/SrZSM-5 at P=5 bar and *H/HC=3*

Temperature	Rate of Overall Conversion	Rate of Isomerization	Rate for Cracking
250	16.1152	16.1152	0
275	42.12965	41.88004	0.2496121
300	46.06865	44.91191	1.156739
325	48.61957	39.83444	8.785129

Table B-44: Rate of Reaction in (10^{-7} mole/g.s) for Zeolite PtZr/SrZSM-5at P=5 bar and *H/HC=6*

Temperature	Rate of Overall Conversion	Rate of Isomerization	Rate for Cracking
250	17.53373	17.53373	0
275	43.66385	43.47512	0.1887311
300	46.61658	45.51463	1.101946
325	48.8083	43.40207	5.406233

Table B-45: Rate of Reaction in (10^{-7} mole/g.s) for Zeolite PtZr/SrZSM-5at P=5 bar and *H/HC=9*

Temperature	Rate of Overall Conversion	Rate of Isomerization	Rate for Cracking
250	17.0345	17.0345	0
275	43.35945	43.23769	0.121762
300	46.22086	45.33809	0.8827745
325	48.68653	44.50401	4.182525

Table B-46: Rate of Reaction in (10^{-7} mole/g.s) for Zeolite PtZr/SrMOR at P=5 bar and *H/HC=3*

Temperature	Rate of Overall Conversion	Rate of Isomerization	Rate for Cracking
250	12.29187	12.29187	0
275	32.65048	32.51045	0.1400263
300	48.00467	46.33653	1.668139
325	49.81892	42.33665	7.482275

Table B-47: Rate of Reaction in (10^{-7} mole/g.s) for Zeolite PtZr/SrMOR at P=5 bar and *H/HC=6*

Temperature	Rate of Overall Conversion	Rate of Isomerization	Rate for Cracking
250	15.40289	15.40289	0
275	32.99141	32.894	0.0974096
300	49.86154	48.93615	0.9253912
325	50.92696	45.67902	5.247942

Table B-48: Rate of Reaction in (10^{-7} mole/g.s) for Zeolite PtZr/SrMOR at P=5 bar and *H/HC=9*

Temperature	Rate of Overall Conversion	Rate of Isomerization	Rate for Cracking
250	14.64797	14.64797	0
275	32.85748	32.76616	0.0913215
300	48.59521	47.8342	0.7610125
325	50.28162	46.4035	3.87812

Table B-49: Rate of Reaction in (10^{-7} mole/g.s) for Zeolite PtRuZr/SrZSM-5 at P=5 bar and *H/HC=3*

Temperature	Rate of Overall Conversion	Rate of Isomerization	Rate for Cracking
250	58.68929	7.0622	51.62709
275	59.6025	7.06219	52.54031
300	59.84602	5.35753	54.48849
325	60.15043	1.58291	58.56752

Table B-50: Rate of Reaction in (10^{-7} mole/g.s) for Zeolite PtRuZr/SrZSM-5 at P=5 bar and *H/HC=6*

Temperature	Rate of Overall Conversion	Rate of Isomerization	Rate for Cracking
250	60.15043	10.65418	49.49625
275	60.21131	8.40158	51.80973
300	60.45483	6.63602	53.81881
325	60.51572	3.5311	56.98462

Table B-51: Rate of Reaction in (10^{-7} mole/g.s) for Zeolite PtRuZr/SrZSM-5 at P=5 bar and *H/HC=9*

Temperature	Rate of Overall Conversion	Rate of Isomerization	Rate for Cracking
250	60.33307	11.38474	48.94833
275	60.51572	10.47154	50.04418
300	60.63747	8.52333	52.11414
325	60.75924	4.5052	56.25404

Table B-52: Rate of Reaction in (10^{-7} mole/g.s) for Zeolite PtRuZr/SrMOR at P=5 bar and *H/HC=3*

Temperature	Rate of Overall Conversion	Rate of Isomerization	Rate for Cracking
250	55.82788	10.04537	45.78251
275	56.74109	8.27982	48.46127
300	57.71519	5.29665	52.41854
325	58.93281	2.43524	56.49757

Table B-53: Rate of Reaction in (10^{-7} mole/g.s) for Zeolite PtRuZr/SrMOR at P=5 bar and *H/HC=6*

Temperature	Rate of Overall Conversion	Rate of Isomerization	Rate for Cracking
250	56.13228	12.23708	43.8952
275	56.86285	9.49743	47.36542
300	58.38488	7.30572	51.07916
325	59.2981	4.44432	54.85378

Table B-54: Rate of Reaction in (10^{-7} mole/g.s) for Zeolite PtRuZr/SrMOR at P=5 bar and *H/HC=9*

Temperature	Rate of Overall Conversion	Rate of Isomerization	Rate for Cracking
250	56.80198	13.88088	42.9211
275	57.47166	11.93267	45.53899
300	58.62841	10.28889	48.33952
325	59.6025	7.06219	52.54031

Table B-55: Rate of Reaction in (10^{-7} mole/g.s) for Zeolite Pt/BaZSM-5 at P=5 bar and *H/HC=3*

Temperature	Rate of Overall Conversion	Rate of Isomerization	Rate for Cracking
250	12.54149	12.45626	0.0852334
275	41.95918	41.42952	0.5296647
300	46.67746	44.93018	1.747285
325	47.90117	41.88004	6.021131

Table B-56: Rate of Reaction in (10^{-7} mole/g.s) for Zeolite Pt/BaZSM-5at P=5 bar and *H/HC=6*

Temperature	Rate of Overall Conversion	Rate of Isomerization	Rate for Cracking
250	13.05898	13.02854	0.0304405
275	43.31074	42.84196	0.4687837
300	47.28019	45.9956	1.284589
325	48.44301	43.52991	4.913096

Table B-57: Rate of Reaction in (10^{-7} mole/g.s) for Zeolite Pt/BaZSM-5at P=5 bar and *H/HC=9*

Temperature	Rate of Overall Conversion	Rate of Isomerization	Rate for Cracking
250	12.71804	12.69369	0.0243524
275	42.33056	41.94092	0.3896384
300	46.7079	45.44766	1.260237
325	47.76114	43.70647	4.054675

Table B-58: Rate of Reaction in (10^{-7} mole/g.s) for Zeolite Pt/BaMOR at P=5 bar and *H/HC=3*

Temperature	Rate of Overall Conversion	Rate of Isomerization	Rate for Cracking
250	11.96312	10.47154	1.491585
275	41.22861	37.78275	3.445864
300	47.26801	40.99118	6.276831
325	50.31815	34.47691	15.84124

Table B-59: Rate of Reaction in (10^{-7} mole/g.s) for Zeolite Pt/BaMOR at P=5 bar and *H/HC=6*

Temperature	Rate of Overall Conversion	Rate of Isomerization	Rate for Cracking
250	13.83216	12.91895	0.913215
275	43.68821	40.39455	3.293662
300	49.20403	44.44922	4.754806
325	51.58447	36.55904	15.02543

Table B-60: Rate of Reaction in (10^{-7} mole/g.s) for Zeolite Pt/BaMOR at P=5 bar and *H/HC=9*

Temperature	Rate of Overall Conversion	Rate of Isomerization	Rate for Cracking
250	12.65716	11.83527	0.8218935
275	41.24079	38.18456	3.056226
300	46.7627	42.54974	4.212965
325	50.36076	37.35658	13.00418

Table B-61: Rate of Reaction in (10^{-7} mole/g.s) for Zeolite PtRu/BaZSM-5 at P=5 bar and *H/HC=3*

Temperature	Rate of Overall Conversion	Rate of Isomerization	Rate for Cracking
250	51.07916	9.31479	41.76437
275	54.48849	9.01039	45.4781
300	56.43668	7.54924	48.88744
325	58.08047	3.77462	54.30585

Table B-62: Rate of Reaction in (10^{-7} mole/g.s) for Zeolite PtRu/BaZSM-5at P=5 bar and *H/HC=6*

Temperature	Rate of Overall Conversion	Rate of Isomerization	Rate for Cracking
250	52.2359	11.93268	40.30322
275	55.46259	11.68915	43.77344
300	57.10638	8.52334	48.58304
325	58.99369	4.74872	54.24497

Table B-63: Rate of Reaction in (10^{-7} mole/g.s) for Zeolite PtRu/BaZSM-5at P=5 bar and *H/HC=9*

Temperature	Rate of Overall Conversion	Rate of Isomerization	Rate for Cracking
250	53.81881	14.73321	39.0856
275	56.13228	13.94174	42.19054
300	57.6543	10.10624	47.54806
325	59.11545	5.84458	53.27087

Table B-64: Rate of Reaction in (10^{-7} mole/g.s) for Zeolite PtRu/BaMOR at P=5 bar and *H/HC=3*

Temperature	Rate of Overall Conversion	Rate of Isomerization	Rate for Cracking
250	57.28902	9.43655	47.85247
275	57.77607	8.3407	49.43537
300	58.324	7.97541	50.34859
325	59.23721	3.04405	56.19316

Table B-65: Rate of Reaction in (10^{-7} mole/g.s) for Zeolite PtRu/BaMOR at P=5 bar and *H/HC=6*

Temperature	Rate of Overall Conversion	Rate of Isomerization	Rate for Cracking
250	57.53254	11.08033	46.45221
275	58.14135	10.53241	47.60894
300	59.11545	10.34977	48.76568
325	59.66338	4.8096	54.85378

Table B-66: Rate of Reaction in (10^{-7} mole/g.s) for Zeolite PtRu/BaMOR at P=5 bar and *H/HC=9*

Temperature	Rate of Overall Conversion	Rate of Isomerization	Rate for Cracking
250	57.77607	12.41972	45.35635
275	58.324	11.99356	46.33044
300	59.35897	11.08034	48.27863
325	59.96778	6.14897	53.81881

Table B-67: Rate of Reaction in (10^{-7} mole/g.s) for Zeolite PtZr/BaZSM-5 at P=5 bar and *H/HC=3*

Temperature	Rate of Overall Conversion	Rate of Isomerization	Rate for Cracking
250	13.31468	12.48061	0.8340697
275	35.71888	34.70217	1.016713
300	46.28782	44.16307	2.124747
325	47.61503	41.64869	5.966338

Table B-68: Rate of Reaction in (10^{-7} mole/g.s) for Zeolite PtZr/BaZSM-5at P=5 bar and *H/HC=6*

Temperature	Rate of Overall Conversion	Rate of Isomerization	Rate for Cracking
250	15.06196	14.374	0.6879553
275	36.35814	35.51189	0.8462459
300	48.33343	46.52526	1.808166
325	50.31206	45.65466	4.657397

Table B-69: Rate of Reaction in (10^{-7} mole/g.s) for Zeolite PtZr/BaZSM-5at P=5 bar and *H/HC=9*

Temperature	Rate of Overall Conversion	Rate of Isomerization	Rate for Cracking
250	13.63126	13.04071	0.5905457
275	35.77976	35.04919	0.730572
300	48.05338	46.79923	1.254149
325	49.08226	45.36852	3.713741

Table B-70: Rate of Reaction in (10^{-7} mole/g.s) for Zeolite PtZr/BaMOR at P=5 bar and *H/HC=3*

Temperature	Rate of Overall Conversion	Rate of Isomerization	Rate for Cracking
250	6.636029	6.544707	0.09132151
275	26.05707	25.46652	0.5905457
300	44.5101	43.17681	1.333294
325	47.94988	42.87849	5.071387

Table B-71: Rate of Reaction in (10^{-7} mole/g.s) for Zeolite PtZr/BaMOR at P=5 bar and *H/HC=6*

Temperature	Rate of Overall Conversion	Rate of Isomerization	Rate for Cracking
250	9.046916	8.967771	0.0791453
275	29.32638	28.82107	0.5053123
300	47.05492	45.86165	1.193268
325	50.11724	46.15389	3.963353

Table B-72: Rate of Reaction in (10^{-7} mole/g.s) for Zeolite PtZr/BaMOR at P=5 bar and *H/HC=9*

Temperature	Rate of Overall Conversion	Rate of Isomerization	Rate for Cracking
250	7.53098	7.476187	0.0547929
275	28.43752	28.0905	0.3470217
300	45.24676	44.32137	0.9253912
325	47.97423	44.85712	3.117107

Table B-73: Rate of Reaction in (10^{-7} mole/g.s) for Zeolite PtRuZr/BaZSM-5 at P=5 bar and *H/HC=3*

Temperature	Rate of Overall Conversion	Rate of Isomerization	Rate for Cracking
250	54.97554	6.14898	48.82656
275	57.10638	5.78369	51.32269
300	57.71519	3.10493	54.61026
325	58.56752	1.21762	57.3499

Table B-74: Rate of Reaction in (10^{-7} mole/g.s) for Zeolite PtRuZr/BaZSM-5at P=5 bar and *H/HC=6*

Temperature	Rate of Overall Conversion	Rate of Isomerization	Rate for Cracking
250	58.38488	10.77594	47.60894
275	58.93281	8.94951	49.9833
300	60.02866	7.48835	52.54031
325	60.33307	3.28758	57.04549

Table B-75: Rate of Reaction in (10^{-7} mole/g.s) for Zeolite PtRuZr/BaZSM-5 at P=5 bar and *H/HC=9*

Temperature	Rate of Overall Conversion	Rate of Isomerization	Rate for Cracking
250	58.56752	12.66325	45.90427
275	59.48074	10.8977	48.58304
300	60.21131	10.04537	50.16594
325	60.39395	5.29664	55.09731

Table B-76: Rate of Reaction in (10^{-7} mole/g.s) for Zeolite PtRuZr/BaMOR at P=5 bar and *H/HC=3*

Temperature	Rate of Overall Conversion	Rate of Isomerization	Rate for Cracking
250	57.16726	13.81999	43.34727
275	57.6543	9.80183	47.85247
300	58.14135	7.54924	50.59211
325	58.99369	6.14898	52.84471

Table B-77: Rate of Reaction in (10^{-7} mole/g.s) for Zeolite PtRuZr/BaMOR at P=5 bar and *H/HC=6*

Temperature	Rate of Overall Conversion	Rate of Isomerization	Rate for Cracking
250	57.3499	15.28113	42.06877
275	57.95871	10.59329	47.36542
300	58.38488	9.37568	49.0092
325	59.23721	7.54924	51.68797

Table B-78: Rate of Reaction in (10^{-7} mole/g.s) for Zeolite PtRuZr/BaMOR at P=5 bar and *H/HC=9*

Temperature	Rate of Overall Conversion	Rate of Isomerization	Rate for Cracking
250	57.71519	17.83813	39.87706
275	58.324	11.99356	46.33044
300	58.56752	11.14122	47.4263
325	59.48074	9.37568	50.10506

Appendix C

Method of Calculation:

Bulk density of Pt/HZSM-5 =0.6113 g/cm^3

Space Veolsity hr^{-1} (LHSV)=$\frac{Volumetric\ Flow\ Rate\ (cm^3/\min)}{Volume\ of\ Catalyst\ (cm^3)}$

Wc=7 gr of catalyst

Volume = $\frac{w_C(g)}{Bulk\ Density\ (g/cm^3)} = \frac{7}{0.6113} = 11.45 cm^3 \simeq 12 cm^3$

As for example chose LHSV=2.5 hr^{-1}=$\frac{Flow\ Rate}{11.45}$

Flow rate =28.627 cm^3/hr
=0.477 cm^3/min

M. wt. of n-hexane=86.18 g/gmole
Sp. gr. =0.659 g/cm^3

Mass flow rate =0.477 * 0.659
=0.3144 g/min

Molar flow rate = $\frac{0.3144}{86.18} = 0.00364\, mole/\min$

For example use H/HC =3

Hydrogen flow rate =0.00364*3=0.01092 mole/min

Hydrogen flow rate =0.01092*22.4=0.244608 liter/min

Then substitute this value in graph down to find the value of mass flow meter voltage.

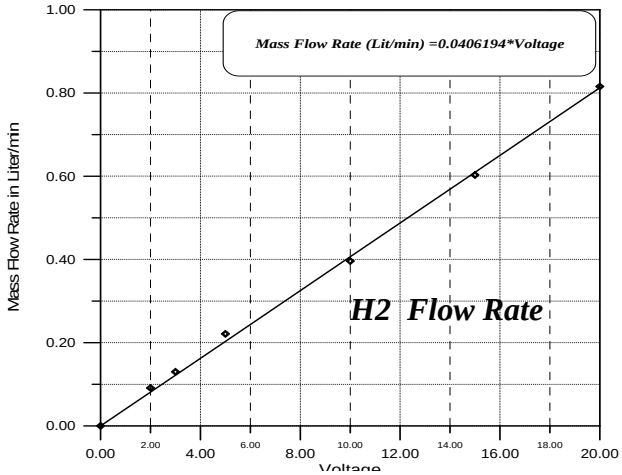

Figure C-1: Mass Flow Meter in Liter/min against Voltage for Hydrogen

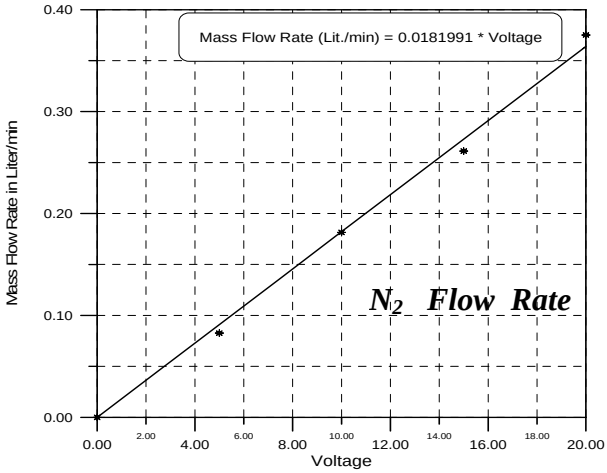

Figure C-2: Mass Flow Rate as function of Voltage in Liter/ min for Nitrogen Flow Rate

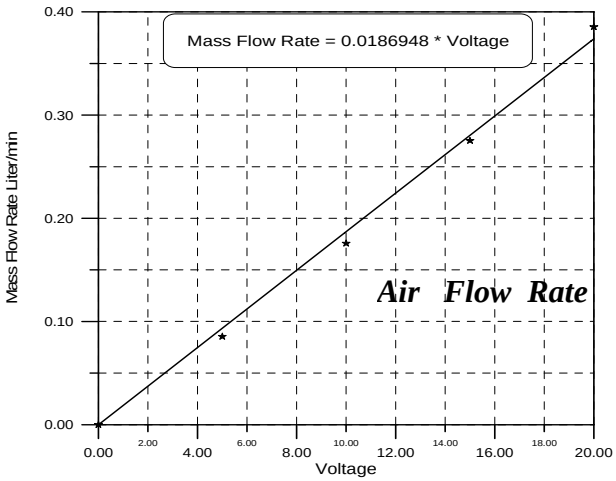

***Figure C-3*:** Mass Flow Rate as function of Voltage in Liter/ min for Air Flow Rate

Appendix D

Table D-1: Samples of Full Gas Chromatography Analysis for isomerization of n-Hexane at T=275 ^{o}C , P=5bar and H/HC=3 for Three samples of Catalysts

Component	Pt/HZSM-5	Pt/SrZSM-5	Pt/BaZSM-5
Methane	0.38	0.04	0.13
Ethane	0.28	0.05	0.10
Propane	1.17	0.25	0.25
Iso-Butane	0.32	0.05	0.05
n-Butane	0.46	0.14	0.10
Iso-Pentane	0	0	0
2MB	0.39	0.15	0.10
n-Pentane	0.27	0.23	0.14
2,2DMB	0.13	0.05	0.16
2,3DMB	2.12	1.05	0.86
2MP	38.88	35.99	36.27
3MP	29.49	34.12	30.53
n-Hexane	25.87	27.67	31.08
Benzene	0.18	0.17	0.19
Toluene	0.06	0.04	0.04
Conversion	74.13	72.33	68.92
Selectivity	95.27	98.45	98.40

الخلاصة

تم استخدام نو عين من الاطيان المصنعة بلوريا كعوامل مساعد محملة بالمعادن النبيلة H-ZSM-5 وH-Mordenite، اللذين يملكان نسبة السيلكون الى الالمنيوم (SiO_2/Al_2O_3)٩٠ و٤٠ على التوالي. أستخدمت عملية التبادل الايوني لتبديل ايون الهايدروجين الموجب بأيونين موجبين اخرين هما عنصري السترونتيوم (Sr^{++}) والباريوم (Ba^{++})، حيث ان عملية التبادل جرت مع محاليلهما الملحية بتركيز ٣ (3N) ومقياس حامضية بحوالي ٧,٢ (pH=7.2) عند درجة حرارة ٥٠ م، تمت اعادت التجربة لكلا العنصرين مرتين للتأكد من تبادل اكثر. بعد عملية التبادل تم غسل هذه الاطيان جيدا بالماء المنزوع الايون للتأكد من خلوها من ايون الكلور السالب ثم تجفيفها عند درجة حرارة ١١٠ م لمدة ٢٤ ساعة وكلست عند درجة حرارة ٤٥٠ م بأستخدام زيادة منظمة في درجة الحرارة. عند الفحص شوهد ان ايون السترونتيوم اكثر فعالية من ايون الباريوم الموجب وان قابلية التبادل لايون الهايدروجين بالنسبة للاطيان Mordenite اكثر فعالية من الاطيان ZSM-5.

عملية التحميل للمعادنِ النبيلةِ على كُلّ أشكال الاطيان المُعتَبَرةِ نُفّذتْ بوجود المذيب ثاني أكسيد الكاربونِ المسال فوق الظروف الحرجة ($scCO_2$). حضرت الاطيان المحملة باحادي وثنائي وثلاثي المعدن باستخدام عناصر البلاتين والروتينيوم والزركونيوم كمعقد اسيتيل اسيتونيت (acetylacetonate)، حمل عنصر البلاتين باستخدام ($PtMe_2COD$) لتحميل أطيان ذات احادي المعدن، حيث ان هذا المُركّبِ قابل للذوبان جيداً في ثاني أكسيد الكاربونِ، بالنسبة الى التحميل الثنائي والثلاثي استخدمت المركبات المعدنية المعقدة التي تمتلك قابليةُ ذوبان منخفضةُ في ($scCO_2$)، لذلك تم اضافة ١٠% من الميثانول (Methanol) لزيَادَة القطبية. هذه التقنية العصريةِ نسبياً استعملت في العملِ الحاليِ للمرة الأولى في تحميل المعادنِ النبيلةِ على محفّزاتِ الاطيان واستخدامها في تفاعلات التحول الهايدروكاربوني (Hydroconversion).

أن نسبة التحميل للمعادن النبيلة تأثرت بزيادة الضغط، حيث ان هذه النسبة وصلت الى ٨٧% عند ضغط ٣٠٠ بار ودرجة حرارة ١٠٠م، ان زيادة الضغط ادى الى زيادة في درجة القطبية والكثافة لثاني اكسيد الكاربون اعطته قابلية اعلى في اذابة المركبات العضوية وقابلية اكبر على النفاذية من خلال المسامات الموجودة في الاطيان. من جهة اخرى لوحظ ان درجة الحرارة لها تأثير طفيف على عملية التحميل حيث انه ليس هناك زيادة ملحوظة خلال ٢٤ ساعة من وقت التحميل.

العديد من الفحوصات اجريت للتأكد من نجاح عملية التحميل والتأكد من جهازية واستقرار العوامل المساعدة والتي تتضمن الاشعة السنية (X-Ray diffraction)، (FTIR spectroscopy)، قياس المساحة السطحية (BET surface area)، التحلل الحراري (TGA)، الصور الاليكترونية المجهرية (TEM)، ان جميع الفحوصات اعطت نتائج مذهلة خصوصا تلك اللتي وضحت الصورة من خلال تصوير سطح الزولايت في دقة متناهية بأستخدام المجهر الاليكتروني حيث شوهد الفرق بين الطريقة الحديثة المتمثلة باستخدام ($scCO_2$) وطريقة التشريب (Impregnation). من الواضح ان زيادة الضغط وخصوصا من ٢٨٠بار الى ٣٠٠بار سبب زيادة اكبر في الانتشار وزيادة في المساحة السطحية بالاضافة الى صغر حجم حبيبات المعدن على السطح وداخل المسامات بالمقارنة مع طريقة التشريب أضافة الى زيادة الفعالية لهذه الاطيان.

تم دراست سلوك العامل المساعد المحمل باحادي وثناي وثلاثي المعدن على اطيان (ZSM-5) و (MOR) ذات ايون الهايدروجين وعلى الاطيان المحسنة ذات ايونات السترونتيوم والباريوم في تفاعل التحول الهايدروجيني المتشعب للهكسان الطبيعي باستخدام وحدة تفاعل تحتوي على مفاعل انبوبي مصغر تم حشوه بالعوامل المساعدة المحضرة. حيث تم تحليل الغازات الناتجة بعد تبريدها وفصلها الى سوائل وغازات خفيفة باستخدام جهازين للتحليل الطيفي للغازات (Gas Chromatography) احدهما مربوط بشكل مباشر مع مجرى الغازات والاخر منفصل يتم حقنه يدويا. تم دراست فعالية العوامل المساعدة المذكورة سابقا لعملية التشعب للهكسان (Isomerization) وعملية التكسير (Cracking) المصاحبة لها في درجات حرارة تتراوح من ٢٥٠م الى ٣٢٥م عند ضغط الهايدروجين ٥بار ونسبة الجريان للهايدروجين الى الهكسان (H_2/HC) تتراوح من ٣، ٦ و ٩ بينما اهملت النواتج للمركبات الحلقية (Cyclization) بسبب كميتها القليلة.

أن كفاءة العوامل المساعدة المحملة بطريقة ($scCO_2$) عادة اكبر من كفاءة العوامل المساعدة المحملة بطريقة التشريب في نفس الوقت علما ان المعادن المحملة بالطريقتين تحملان تقريبا نفس الكمية.

أن فعالية العامل المساعد (ZSM-5) الذي يمتلك مسامات داخلية صغيرة اكثر فعالية من العامل المساعد (MOR) الذي يمتلك مسامات اكبر بالاضافة الى ان عنصر الباريوم والسترونتيوم اكثر

فعالية من عنصر الهايدروجين في كل حالات الاطيان اضافة الى ان كفاءة الاطيـــان ذات عنـــصر الباريوم اكثر من مثيلاتها بعد وقبل التبادل الايوني.

لقد اظهرا معدني البلاتين والزركونيوم المحملين على الاطيـــان (ZSM-5) و (MOR) فـــي كـــل اشكالها بعد وقبل التحسين فعالية اكبر لعملية ازمرة الهكسان بالمقارنة مع معدن الروتينيـــوم الـــذي بدوره اعطى مستوى منخفض جداً للازمرة مقارنة بكمية اكبر من النواتج المتكـــسرة فـــي جميـــع الظروف المستخدمة. أن اكبر انتاج يصل الى ٩٠% في ازمرة الهسان بالتوازي مع نـــسبة تحـــول تصل الى ٨٠% تم الحصول عليها في ظروف ٢٧٥م و ٣٠٠م ونسبة الهايدروجين الى الهكسان ٦ و ٩ مع معدني البلاتين والزركونيوم المحملين بواسطة ($scCO_2$).

تم حساب معدل التفاعل للازمرة ومعدل التكسير للهكسان الطبيعي في كل الحالات التي جرى فيها استخدام العامل المساعد فيها، ومن خلالها تم حساب طاقة التنشيط ومعاملها.

ان معدل التفاعل لعملية الازمرة تم نمذجته باستخدام نظرية الامتـــزاز والانفـــصال (adsorption desorption isotherm). حيث تم اعتبار التفاعل السطحي هو الخطوة المحددة للتفاعل بعد ذالـــك تم حساب معاملات النموذج باستخدام الطرق الاحصائية مع معامل تصحيح يصل الـــى ٠,٩٩٢٩. اعطى هذا النموذج الرياضي نتائج دقيقة في مختلف درجات الحرارة وفي مختلف نـــسب الجريـــان للهايدروجين والهايدروكاربون. حيث ان الثوابت المتعلقة بهذه المعاملات تم حـــسابها مـــن معادلـــة Arrhenius، تم ايجاد نسبة الخطأ بالمقارنة مع النتائج العملية لاتتجاوز ٢%.

الشكر والتقدير

اتقدم بخالص الشكر والتقدير للاستاذ المشرف الدكتور جابر شنشول جمالي المحترم الذي ساعدني منذ البداية في نصائحه وارشاداته القيمة النابعة من خبرته الطويلة في هذا المجال وكذلك اتصالاته ومتابعته المستمرة مع الاساتذة في خارج القطر والتي اتاحت لي الفرصة لاكمال هذا البحث في المانيا.

كما اود ان اشكر وزارة التعليم العالي والبحث العلمي لمنحي فرصة اكمال هذه الرسالة في خارج القطر وتوفير النفقات الضرورية لذلك.

ولا يسعني الا ان اقدم امتناني العميق وشكري الجزيل الى الاستاذ الدكتور قاسم جبار سليمان رئيس قسم الهندسة الكيمياوية في جامعة النهرين لمساعدته وارشاداته القيمة.

كما اود ان ابعث خالص شكري وتقديري الى البروفيسور فالتر لايتنر رئيس معهد تكنلوجيا الكيمياء في جامعة RWTH في مدينة آخن في المانيا لاستقباله لي وتوفيره كافة المستلزمات لاكمال هذا البحث.

كما اود ان اشكر عميد كلية الهندسة لسماعدته على منحي الفترة اللازمة لاكمال متطلبات البحث.

واخيرا اود ان اشكر جميع اساتذتي وزملائي الذين اعانوني في انجاز هذا المشروع.

أسامة الراوي

التحول الهايدروجيني للهكسان الطبيعي بوجود الاطيان المحملة بالبلاتين كعامل مساعد والمحضرة باستخدام تقنية الغاز المسال فوق الظروف الحرجة

أطروحة

مقدمة الى كلية الهندسة في جامعة النهرين وهي جزء من متطلبات نيل درجة دكتوراه فلسفة في الهندسة الكيمياوية

من قبل

أسامة أكرم سعيد الراوي

بكالوريوس علوم في الهندسة الكيمياوية ٢٠٠٠

ماجستير علوم في الهندسة الكيمياوية ٢٠٠٣

جمادى الاخر ١٤٢٩

حزيران ٢٠٠٨